Structure-function analysis of an autoactive derivative of the tomato Cf-9 disease resistance protein

Choon Yang (Kevin) Tee

June 2016

A thesis submitted for the degree of Doctor of Philosophy

of the Australian National University

DECLARATION

I declare that this thesis is my own work and has not been submitted in any form for another degree or diploma at any university or other institution of higher education. Information derived from the published or unpublished work of others has been acknowledged in the text and a list of references is given. Materials obtained for use in this study that were generated by others have been acknowledged accordingly in the text.

Choon Yang (Kevin) Tee
6 June 2016

ACKNOWLEDGEMENTS

This work would not have been possible without the support from the following people to whom I express my thanks:

To my principal supervisor Assoc. Prof. Dr David Jones, for his continuous guidance, patience and input in this thesis, although there have been great challenges especially in the writing phase. My PhD advisors Assoc. Prof. Adrienne Hardham and Assoc. Prof. Peter Solomon for their previous advice, Dr Claire Anderson for her initiation of the M205 project and helpful discussions, and Dr Ming-Bo Wang for allowing access to the multiwell fluorescence platereader facility in CSIRO for MUG assay experiments.

To the past and present members of Jones lab for the stimulating research environment, including Dr Ginny Lim, Dr Neil Horner, Dr Maryam Rafiqi, Cahya Prihatna, Thilaga Vellusamy, Ursula Hurley, Dr Ann-Maree Cantanzariti, Dr Yvonne Gonzalez-Cendales, Huong Do, Laura Rolston, Nadya Farah and Jaime Simbaqueba. Special thanks to the plant culture service team Christine Larsen, Jenny Rath and Steve Dempsy for their excellent horticultural assistance.

Finally, to my family and friends: Yileen Lim, Nadia Mohd Radzman, Jason Ng, Wil Hee, Tiffany Loh and Jimmy Chan for the wonderful journey studying in Australia and my parents for their unwavering support and unconditional love.

ABSTRACT

An autoactive chimera of the tomato extracellular leucine-rich repeat receptor-like protein Cf-9, designated Hcr9-M205 has been characterized previously as exhibiting characteristics of constitutive defence activation (Barker *et al.*, 2006b). The initial work of this thesis (Chapter 3) involved generation and assessment of transgenic tobacco containing an *E22 (PR-5)* promoter: *gusA* reporter construct as a quantitative reporter for Hcr9-M205 autoactivity in *Agrobacterium*-mediated transient expression (agroinfiltration) assays. Time course analysis showed that the induction of *E22* promoter preceded the necrotic response induced by Hcr9-M205, providing an early indication of defence activation. Further characterization of the *E22* promoter (Chapter 4) by incubating the *E22*: *gusA* tobacco leaf disks in different defence-inducing compounds using a multi-well plate set-up indicated the defence-inducible nature of *E22* promoter including antagonistic regulation by salicylic acid and jasmonic acid, activation by ethylene and synergistic activation by salicylic acid and cytokinin; demonstrating the applicability of the leaf disks assays in screening potential plant defence activators.

Chapter 5 presents the structure-function analysis of the Hcr9-M205 protein. Previously, domain swapping analysis identified key regions involved in the control of Hcr9-M205 autoactivity namely a mismatch between LRRs 10-17 of Hcr9-9A (an upstream Cf-9 paralogue) and Cf-9 LRR 18 required for basal level of autoactivity and an additional Cf-9 C-terminal region comprising the loop-out domain and LRRs 24-26 for complete level of autoactivity (Anderson *et al.* in preparation). This thesis focuses on the proposed signalling repression domain in LRRs 10-17. Domain swapping analysis showed that an Hcr9-9A substitution in Cf-9 LRRs 15-17 was sufficient to cause autoactivity, suggesting that LRRs 15-17 and LRR 18 normally interacts for Cf-9 autoinhibition. The specificity-determining residues located at the solvent-exposed positions in the concave β-sheet surface of Cf-9 LRRs 13-16 required for Avr9 recognition (Wulff *et al.*, 2009b) lie in the signalling repression domain and overlap the polymorphic positions involved in autoactivity, providing a basis for site-directed mutagenesis analysis. Introduction of these residues into the corresponding positions in Hcr9-M205 via site-directed mutagenesis revealed that those located the closest to LRR

18 had the greatest effects in signalling repression: Y389 of LRR 13 and E411 of LRR 14 did not significantly affect autoactivity, A433 of LRR 15 marginally repressed autoactivity whereas L457 of LRR 16 completely abolished autoactivity, similar to L481 of LRR 17 shown by Anderson *et al.* (in preparation). These findings were consistent with the notion that Cf-9 is autoinhibited by interactions between LRRs 15-17 and LRR 18. Unexpectedly, introduction of C387 of LRR 13 into Hcr9-M205 enhanced autoactivity. Sequence analysis comparing the Hcr9-M205(L389C) mutant containing C387 in Hcr9-M205, the CLB103V(14) domain swap that exhibited enhanced autoactivity and domain swaps that did not indicated that this phenomenon only occurred with an additional Hcr9-9A substitution spanning LRRs 14-17, suggesting that C387 may enhance signal activation upon Avr9-induced derepression and a possible role of E411 of LRR 14 in signalling repression. The data revealing some of the specificity-determining residues in signalling repression suggest that Avr9 recognition may directly compete with the autoinhibitory interactions mediated by these residues for Cf-9 activation.

LIST OF FIGURES

CHAPTER 4

CHAPTER 5

LIST OF TABLES

LIST OF ABBREVIATIONS

ABA	abscisic acid
ANOVA	Analysis of Variance
BAP	6-Benzylaminopurine
bp	base pairs
BS	Bluescript
BSA	Bovine Serum Albumin
Rubisco	ribulose-1,5-bis-phosphate carboxylase/oxygenase
CaMV	cauliflower mosaic virus
CK	cytokinin
CTAB	cetyl trimethyl ammonium bromide
DNA	deoxyribonucleic acid
d	day(s)
dNTP	deoxynucleoside triphosphate
DTT	dithiothreitol
EDTA	ethyelenediaminetetraacetic acid
ETH	ethylene
ETI	effector-triggered immunity
GUS	β-glucuronidase
x g	gravitational force
h	hour(s)
Hcr	Homologues of *Cladosporium fulvum* resistance gene
HR	hypersensitive response
JA	jasmonic acid
kb	kilobase
kDa	kilodalton
LB	Luria-Bertani
LRR	leucine-rich repeat
M	molar
MAMP/PAMP	microbe/pathogen-associated molecular pattern
MCS	multiple cloning site
MES	2-(*N*-morpholino)ethanesulfonic acid
min	minute(s)

mM	millimolar
MS	Murashige and Skoog
MTI/PTI	MAMP/PAMP-triggered immunity
MUG	4-Methylumbelliferyl-β-D-glucuronide
NAA	1-Naphthaleneacetic acid
OD	optical density
PAGE	polyacrylamide gel electrophoresis
PCR	polymerase chain reaction
PRR	pattern recognition receptor
PR	pathogenesis-related
RNA	ribonucleic acid
rpm	rotation per minute
RT	reverse transcription
s	second(s)
SA	salicylic acid
SAR	systemic acquired resistance
SDS	sodium dodecyl sulphate
TAE	Tris-Acetate-EDTA buffer
T-DNA	transfer DNA
TMV	tobacco mosaic virus
UTR	untranslated region
X-gluc	5-bromo-4-chloro-3-indolyl-β-D-glucuronic acid

TABLE OF CONTENTS

CHAPTER 1:

Literature Review

In the natural environment, plants are constantly exposed to various biotic and abiotic stresses. Although plants are sessile organisms, they are able to make appropriate adjustments and respond at the cellular level to counter these stresses. The responses of plants to biotic stress have been of major interest to many researchers because plant diseases cause significant losses to agriculture worldwide. In developing countries, an estimated 30-40% of crop production is lost to pests and diseases (Flood, 2010). Furthermore, the increasing human population imposes a higher demand on global food supply. Therefore, it is important to tackle plant diseases affecting crop plants. Understanding the mechanisms underlying plant defence has given rise to applications that enable intervention against plant diseases such as the genetic engineering of crop plants for improved resistance traits (Lusser *et al.*, 2012). The ultimate goal of studying plant defence systems is to develop durable disease resistance.

1.1 The plant immune system

Plant diseases are caused by a diverse array of pathogens ranging from bacteria, fungi, oomycetes, viruses, nematodes to piercing-sucking insects. Like animals and insects, plants possess an innate immune system that effectively precludes infection by most potential pathogens. However, plants lack an adaptive immune system consisting of a blood circulatory system that delivers specialized immune cells to the sites of infection as found in animals but rather they rely on an evolutionarily ancient innate immune system that operates at a single-cell level (Ausubel, 2005). To circumvent pathogen infections, plant defence occurs at the non-host and host-specific levels (Hammond-Kosack and Parker, 2003; Jones and Takemoto, 2004).

1.1.1 Non-host resistance

Non-host resistance is a broad-spectrum defence mechanism that provides a basal state of immunity against pathogens (Ellis, 2006; Fan and Doerner, 2012; Senthil-Kumar and Mysore, 2013). These include preformed defence barriers such as plant cell walls, thick layers of cuticular wax and trichomes present on the leaf surface. For instance, the leaf cuticle is an important barrier providing resistance to a variety of pathogens ranging from the bacterial pathogen *Pseudomanas syringae* to the fungal pathogen *Botrytis*

cinerea in Arabidopsis (Reina-Pinto and Yephremov, 2009). In addition to these physical barriers, plants also possess constitutive chemical barriers present on the leaf surface. These include phytoanticipins, which represent a diverse group of antimicrobial compounds constitutively present on host surfaces prior to pathogen infection (van Etten *et al.*, 1994; González-Lamothe *et al.*, 2009). At the attempted infection sites, plant cells undergo rapid cytoskeletal reorganization, local callose deposition and accumulation of antimicrobial compounds to prevent pathogen entry (Hardham *et al.*, 2007). However, if pathogens breach these primary barriers e.g. through stomata or wounding, plants rely on the inducible innate immune system to counter these attacks. Pattern recognition receptors (PRRs) constitute the front line of the plant innate immune system by recognizing conserved microbial structures essential for the function and survival of pathogens called microbe/pathogen-associated molecular patterns (MAMPs/PAMPs) (Segonzac and Zipfel, 2011). Typically, PRRs are cell surface localized extracellular leucine-rich repeat (eLRR) receptor-like kinases (RLKs) or receptor-like proteins (RLPs) (Monaghan and Zipfel, 2012; Zhang and Thomma, 2013). Examples of MAMPs include bacterial flagellin, lipopolysaccharides of Gram-negative bacteria and fungal chitin (Newman *et al.*, 2013). The result of this recognition is the activation of a series of immune responses inside the cells including changes in cellular ion fluxes, induction of the mitogen-activated protein kinases (MAPK) cascades, production of reactive oxygen species (ROS) and accumulation of pathogenesis-related (PR) proteins, leading to antimicrobial effects (Asai *et al.*, 2002; Boller and Felix, 2009). Such non-specific defence responses, which constitute non-host resistance are referred to as MAMP-triggered immunity (MTI).

1.1.2 Host-specific resistance

Specific races of pathogens have evolved to infect plants by acquiring effector proteins that suppress MTI. Depending on the genotype of the host, these virulent pathogens can cause disease in plant cultivars lacking disease resistance (*R*) genes, resulting in disease susceptibility (Boller and He, 2009). Pathogen effectors can be secreted into the apoplastic space or translocated into plant cells to suppress plant innate immunity (van der Hoorn and Kamoun, 2008; Dodds and Rathjen, 2010). Gram-negative bacteria often use a type III secretion system (T3SS) for translocation of effector molecules into the

cytoplasm of an infected cell (Alfano and Collmer, 2004). Many fungi and oomycetes invade plant tissues by producing infection hyphae and establishing specialized feeding structures called haustoria, which appear to be the main route of translocation for pathogen effectors (Panstruga and Dodds, 2009). Specific plant cultivars expressing *R* genes can recognize these effector proteins as avirulence (Avr) factors to mount an effective immune response. This host-/race-specific resistance response involving a plant *R* gene product and a pathogen avirulence (*Avr*) gene product occurs in a 'gene-for-gene' manner (Flor, 1971) and is referred to as effector-triggered immunity (ETI) (Hammond-Kosack and Jones, 1996; Dangl and Jones, 2001). ETI is thought as a heightened activation of the same defence mechanisms induced by MTI and is hallmarked by the hypersensitive response (HR), a form of localized cell death that limits pathogen infection (Jones and Dangl, 2006). Subsequently, the local immune response can trigger systemic acquired resistance (SAR) which is often accompanied by a substantial accumulation of pathogenesis-related (PR) proteins, resulting in a protective state of the entire plant to prevent future infections (Hammond-Kosack and Jones, 1996; Durrant and Dong, 2004). In general, most *R* genes involved in race-specific resistance encode intracellular nucleotide-binding leucine-rich repeat (NB-LRR) receptors (Marone *et al.*, 2013) but some *R* genes encode extracellular leucine-rich repeat receptor-like proteins (eLRR RLPs). The arms race between plants and pathogens proceeds continuously through the evolution of new *R* genes and new or modified effector genes, respectively, to overcome one another as illustrated by the so-called 'zig-zag' model proposed by Jones and Dangl (2006). The overview of plant immune system is depicted in Figure 1.1.

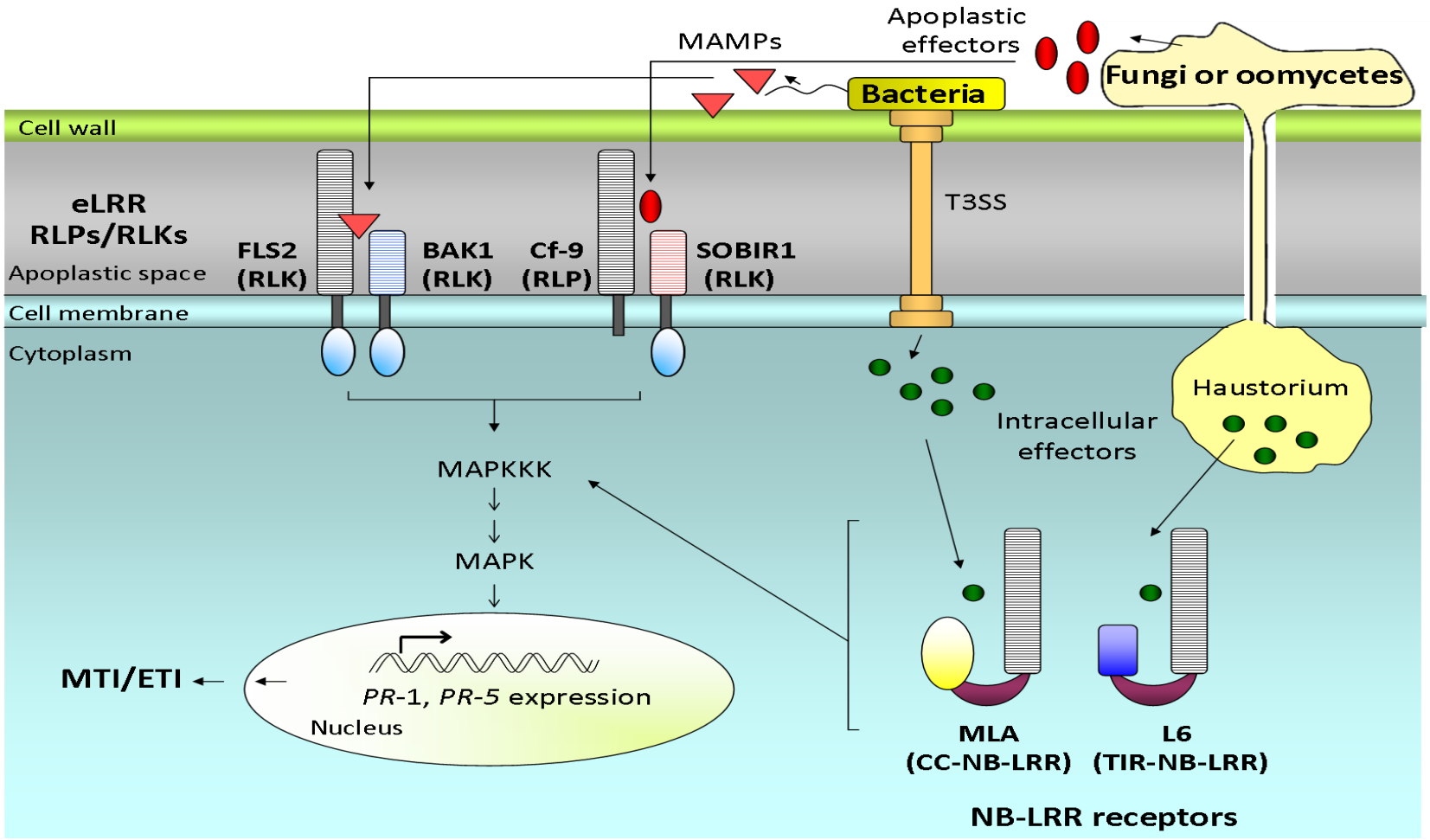
MAMPs
Apoplastic effectors
Bacteria
Fungi or oomycetes
Cell wall
eLRR RLPs/RLKs
Apoplastic space
FLS2 (RLK)
BAK1 (RLK)
Cf-9 (RLP)
SOBIR1 (RLK)
T3SS
Cell membrane
Cytoplasm
Haustorium
Intracellular effectors
MAPKKK
MAPK
MTI/ETI
PR-1, PR-5 expression
Nucleus
MLA (CC-NB-LRR)
L6 (TIR-NB-LRR)
NB-LRR receptors

Figure 1.1 Overview of the plant immune system. The plant immune system consists of two tiers of receptors, one located at the cell surface predominantly consisting of extracellular leucine-rich repeat (eLRR) receptors and the other comprising nucleotide-binding leucine-rich repeat (NB-LRR) receptors found inside the cells. The eLRR receptor-like kinases (RLKs) and receptor-like proteins (RLPs) recognize extracellular pathogen molecules such as the conserved microbe-associated molecular patterns (MAMPs) and/or apoplastic effector proteins. The cytoplasmic NB-LRR receptors, such as MLA10 (a CC-NB-LRR) and L6 (a TIR-NB-LRR) proteins recognize intracellular pathogen effectors, which are delivered by the type III secretion system (T3SS) of Gram-negative bacteria or via the haustorium formed by fungal or oomycete pathogens. The cell surface eLRR receptors recruit additional signalling partner(s) for their function, for instance, the eLRR RLKs BRI1-Associated Receptor Kinase 1 (BAK1) and SUPPRESSOR OF BIR1-1 (SOBIR1) are required for the function of FLS2 (an RLK) and Cf-9 (an RLP), respectively. These surveillance receptors act as molecular switches that govern plant defence activation upon detection of pathogen molecules, leading to MAMP-triggered immunity (MTI) or effector-triggered immunity (ETI) via activation of mitogen-activated protein kinases (MAPKs). Figure adapted from Wirthmueller *et al.* (2013).

1.2 Plant resistance proteins

1.2.1 The NB-LRR receptors

The NB-LRR receptors constitute the majority of *R* genes with approximately 150 and 600 encoding genes identified in Arabidopsis and rice, respectively (Marone *et al.*, 2013). These NB-LRR receptors consist of a C-terminal LRR domain, a central nucleotide binding (NB) domain and an N-terminal domain composed of a coiled-coil (CC) or a Toll/interleukin-1 receptor (TIR) cytoplasmic-domain-like structure that define the two broad groups of these receptors. This class of resistance proteins is very similar to the mammalian intracellular nucleotide-binding oligomerization domain (NOD)–like receptors (NLRs) (Maekawa *et al.*, 2011b). In general, the C-terminal LRR domain of the NB-LRR receptors is more commonly involved in pathogen recognition (Takken and Goverse, 2012) (Section 1.3). However, some exceptions exist in which other domains have also been implicated in pathogen recognition. For instance, some alleles of the flax L resistance protein (a TIR-NB-LRR receptor) that confer different pathogen specificity contain identical LRR domains, suggesting that regions outside the LRR domain can also determine ligand specificity (Luck *et al.*, 2000). Furthermore, Ravensdale *et al.* (2012) showed that co-operative interactions between the TIR, NB and LRR domains of the flax L5 and L6 receptors influence the binding of their corresponding AvrL567 ligands and the resulting HR. By contrast, the N-terminal CC or TIR domain is more commonly involved in signal transduction. This can be observed when the expression of the CC and TIR domains alone of the barley mildew A (MLA) and flax L6 proteins, respectively, was sufficient to trigger an effector-independent HR via domain homodimerization (Bernoux *et al.*, 2011; Maekawa *et al.*, 2011a).

Recently, the Arabidopsis TIR-NB-LRR receptors RPS4 (RESISTANCE TO *PSEUDOMONAS SYRINGAE* 4) and RRS1 (RESISTANCE TO *RALSTONIA SOLANACEARUM* 1) were shown to function as a pair wherein both are required for the recognition of three different pathogens i.e. the bacterial pathogens *P. syringae* pv. *pisi* that secretes AvrRps4 effector and *R. solanacearum* expressing PopP2 effector, and the fungal pathogen *Colletotrichum higginsianum* (Williams *et al.*, 2014). The TIR domains of these receptors were demonstrated to physically associate with one another to form a functional RPS4/RRS1 effector recognition complex. How RPS4 and RRS1

are activated following recognition of the corresponding effectors from these pathogens remains to be elucidated. As this dissertation focuses on an autoactive plant disease resistance protein, Section 1.5 will further discuss NB-LRR receptors involved in autoactivity.

1.2.2 The eLRR RLKs and RLPs

The eLRR RLKs (receptor-like kinases) and RLPs interact with extracellular signals including secreted pathogen-derived molecules and self-derived molecules such as signalling hormones. These receptors are composed of a large extracellular leucine-rich repeat domain, a transmembrane domain and an intracellular domain containing a serine/threonine kinase (for RLKs) or a domain that lacks an obvious signalling function (for RLPs) (Zhang and Thomma, 2013). There are approximately 600 RLKs and 57 RLPs identified in the Arabidopsis genome, and those with known function are involved in plant growth/development and plant defence (Shiu *et al.*, 2004; Wang *et al.*, 2008a). In addition, there are 90 eLRR RLP genes in the rice genome with at least 73 candidate genes predicted to play a role in plant defence (Fritz-Laylin *et al.*, 2005). The eLRR receptors involved in plant growth and development include BRASSINOSTEROID INSENSITIVE 1 (BRI1) (from the RLK class) which mediates brassinosteroid signalling (Hothorn *et al.*, 2011; She *et al.*, 2011), and Arabidopsis CLAVATA1 (CLV1) and CLAVATA2 (CLV2) (an RLK and an RLP, respectively), which regulate shoot-apical meristem development (Clark *et al.*, 1997; Kayes and Clark, 1998). The eLRR RLKs involved in plant defence include some of the best studied PRRs such as the Arabidopsis FLAGELLIN SENSING 2 (FLS2) receptor and EF-Tu receptor (EFR), which play a pivotal role in plant innate immunity by recognizing bacterial flagellin and the bacterial elongation factor EF-Tu, respectively (Gomez-Gomez and Boller, 2000; Zipfel *et al.*, 2006). The eLRR RLK Xa21 from rice, which confers broad-spectrum resistance to the bacterial blight pathogen *Xanthomonas oryzae* pv. *oryzae* (Xoo), has also been classified as a PRR (Song *et al.*, 1995). These receptors are both structurally and functionally analogous to the mammalian Toll-like receptors (TLRs) containing an extracellular LRR domain, a transmembrane domain and an intracellular TIR domain required for signal transduction (Kawai and Akira, 2010).

The eLRR RLP class of resistance proteins is represented by the tomato Cf proteins, which confer resistance to different races of the leaf mould fungus *Cladosporium fulvum* and includes the Cf-9 protein encoded by one of the first isolated *R* genes (Jones *et al.*, 1994; Rivas and Thomas, 2005); the tomato Ve1 protein, which confers resistance to *Verticillium* wilt disease caused by race 1 of *Verticillium dahliae* and strains of *Verticillium albo-atrum* (Kawchuk *et al.*, 2001; Fradin *et al.*, 2009); and the apple HcrVf proteins, which confers resistance to the scab fungus *Venturia inaequalis* (Belfanti *et al.*, 2004). In addition, the tomato eLRR RLPs Eix1 and Eix2, which detect fungal xylanase, are considered PRRs. Xylanase is a potent elicitor of plant defence responses typical of MAMP-induced responses in specific cultivars of tomato and tobacco, including induction of ethylene biosynthesis (Ron and Avni, 2004). Among all the classes of plant resistance proteins, little is known about the molecular activation of the eLRR RLPs because the cytosolic domain lacks an obvious signalling function. While this class of resistance proteins has received less attention to date, there is an increasing number of RLPs that have been shown to play a role in plant immunity and mediate disease resistance to various pathogens (Table 1.1). These include the rapeseed *Brassica napus* LepR3 (*Leptosphaeria maculans* Resistance 3) protein, which confers resistance to races of the fungal pathogen *Leptosphaeria maculans* that secrete the AvrLM1 effector (Larkan *et al.*, 2013); the wheat RLP1.1 protein involved in resistance against stripe rust *Puccinia striiformis* f. sp. *tritici* (Jiang *et al.*, 2013b) and the *Arabidopsis* RFO2 (Resistance to *Fusarium oxysporum* 2) protein that mediates quantitative resistance to vascular wilt disease caused by *F. oxysporum* f. sp. *matthioli* (Shen and Diener, 2013).

The tomato Ve1 and Eix receptors have been more extensively studied than most other eLRR RLPs and are therefore discussed further in the following subsections. The Cf receptors are discussed in detail in Section 1.4.

Table 1.1 eLRR RLPs with demonstrated function in plant immunity. Pathogen-derived molecules marked with asterisks are MAMPs.

eLRR RLPs	Plant species	Pathogen effectors/ *MAMPs	Pathogen	Disease	Reference
Cf- and Cf-ECP proteins	Tomato	Avr proteins and ECPs	*Cladosporium fulvum*	Tomato leaf mold disease	Wulff *et al.* (2009a) (Section 1.4)
Ve1	Tomato	Ave1*	*Verticillium dahliae* and *Verticillium albo-atrum* race1	Vascular wilt disease	de Jong *et al.* (2012)
Hcr-Vf2/ Rvi6 (Resistance to *Venturia inaequalis* 6)	Apple	AvrRvi6	*Venturia inaequalis*	Apple scab disease	Belfanti *et al.* (2004) & Bowen *et al.* (2011)
LepR3 (*Leptosphaeria maculans* Resistance 3)	*Brassica napus*	AvrLM1	*Leptosphaeria maculans*	Blackleg disease	Larkan *et al.* (2013)
TaRLP1.1	Wheat	not identified	*Puccinia striiformis* f. sp. *tritici*	Stripe rust	Jiang *et al.* (2013b)
RFO2 (Resistance to *Fusarium oxysporum* 2)	Arabidopsis	not identified	*F. oxysporum* f. sp. *matthioli*	Vascular wilt disease	Shen & Diener (2013)
Eix1 and Eix2	Tomato	Ethylene-inducing xylanase (Eix)*	*Trichoderma viride*	Non-host resistance	Ron & Avni (2004)

EILP (Elicitor inducible LRR protein)	Tobacco	not identified	*Pseudomonas syringae* pv. *glycinea* and *P. syringae* pv. *tabaci*	Non-host resistance	Takemoto *et al.* (2000)
ReMax (Receptor for eMax	Arabidopsis	eMax*	*Xanthomonas*	Non-host resistance	Jehle *et al.* (2013)
RPBG1 (Responsiveness to Botrytis Polygalacturonases 1)	Arabidopsis	Endopolygalacturo-nases (PGs)*	*Botrytis cinerea* (a necrotroph)	Non-host resistance	Zhang *et al.* (2014a)
RLP30	Arabidopsis	Sclerotinia Culture Filtrate Elicitor 1 (SCFE1)*	*Sclerotinia sclerotiorum* (a necrotroph)	Non-host resistance	Zhang *et al.* (2013)
RLP52	Arabidopsis	Fungal chitin*	*Erysiphe cichoracearum* (a powdery mildew pathogen)	Non-host resistance	Ramonell *et al.* (2005)

1.2.2.1 Tomato Ve1 receptor

The tomato *Ve* locus mediates resistance against race 1 strains of *Verticillium dahliae* and *Verticillium albo-atrum*. The two genes *Ve1* and *Ve2* at this locus encode eLRR RLPs containing 37 LRRs with 84 % amino acid identity but only *Ve1* mediates resistance against race 1 *Verticillium* strains in tomato (Fradin *et al.*, 2009; Fradin *et al.*, 2014). It has been shown that Ve1 remains functional upon interfamily transfer to Arabidopsis and that Ve1-mediated resistance involves similar downstream signalling components to that in tomato (Fradin *et al.*, 2011), indicating conservation of defence signalling mediated by this RLP between different plant species. Recently, the corresponding Ave1 effector protein from race 1 strains of *V. dahliae* and *V. albo-atrum*, which activates Ve1-mediated resistance, was identified via a comparative genomic approach using RNA sequencing technology (de Jonge *et al.*, 2012). Domain swapping between Ve1 and the non-functional homologue Ve2 demonstrated that the first 30 LRRs are required for Ve1/Ave1-mediated HR induction and disease resistance (Fradin *et al.*, 2014).

1.2.2.2 Tomato Eix dual receptor system

The tomato *Eix1* and *Eix2* genes, which confer resistance to the fungal elicitor ethylene-inducing xylanase (Eix) from *Trichoderma viride*, both encode eLRR RLPs containing 31 LRRs. Both Eix1 and Eix2 receptors were shown to bind Eix independently, but only Eix2 is involved in Eix-induced signalling and HR induction (Ron and Avni, 2004). A mutation of the tyrosine residue to alanine in the putative endocytosis motif YxxΦ (where x = any amino acid, Φ = any amino acid with a bulky hydrophobic side chain) present in the cytosolic tail of Eix2 abolished Eix-induced HR, suggesting that endocytosis is required for defence signalling mediated by this RLP (Ron and Avni, 2004). Consistently, binding of Eix was shown to trigger endocytosis of Eix2 and this process can be attenuated by overexpression of the plant endocytic inhibitor protein EHD2 (Bar and Avni, 2009).

1.2.2.3 The requirement for signalling partners in eLRR RLP function

The recent identification of the tomato homologue of the Arabidopsis eLRR RLK SUPPRESSOR OF BIR1-1 (SOBIR1), also known as EVERSHED (EVR) (Gao *et al.*, 2009; Leslie *et al.*, 2010), which interacts with several eLRR RLPs involved in immunity to fungal pathogens including Cf-2, Cf-4, Cf-9, Ve1 and Eix2 (Liebrand *et al.*, 2013), has resolved the search for the long anticipated signalling partner required for the function of the eLRR RLPs (Jones *et al.*, 1994; Rivas and Thomas, 2005). SOBIR1 and its homologue SOBIR1-like protein were shown to be required for Cf-2, Cf-4 and Ve1-mediated resistance by virus-induced gene silencing (VIGS). Likewise, VIGS of SOBIR1 and SOBIR1-like protein also compromised Cf-4/Avr4- and Ve1/Ave1-induced necrosis, demonstrating a role for SOBIR1 and SOBIR-like protein in Cf- and Ve1-mediated immune responses (Liebrand *et al.*, 2013). Of note, the involvement of SOBIR1 appeared to be exclusive to the function of the eLRR RLPs, including that of CLV2 but not for the eLRR RLKs such as FLS2 and CLV1 (Liebrand *et al.*, 2013; Liebrand *et al.*, 2014). By contrast, the SOMATIC EMBRYOGENESIS RECEPTOR KINASES (SERKs), another class of 'short eLRR RLKs' similar to SOBIR1, are required for the function of both RLPs and RLKs (Liebrand *et al.*, 2014). For instance, through VIGS analysis, SERK1 was demonstrated to be involved in both Cf-4- and Ve1-mediated disease resistance whereas SERK3/BRI1-associated kinase 1 (BAK1) was only essential for Ve1-mediated resistance (Fradin *et al.*, 2009). Furthermore, BAK1 has been shown to act as a co-receptor for BRI1 and FLS2 function in the recognition of brassinosteroid and flagellin, respectively (Santiago *et al.*, 2013; Sun *et al.*, 2013).

1.2.2.4 Effector-trigerred defence (ETD) – a new concept in plant defence

Although some eLRR RLPs mediate race-specific resistance, Ve1 mediates resistance based on recognition of the Ave1 avirulence protein, which is also found in the plant pathogenic bacterium *Xanthomonas axonopodis* pv. *citri* and several other fungal pathogens including *Fusarium oxysporum* f. sp. *lycopersici* (de Jonge *et al.*, 2012). Similarly, homologues of several *C. fulvum* effectors recognized by Cf proteins have

also been identified in other Dothideomycete species (Section 1.4). The presence of conserved effector homologues across fungal species has led to the proposition to reclassify the eLRR RLPs including Ve1 as a PRR involved in MTI instead of an R protein that mediates ETI (Thomma *et al.*, 2011; de Jonge *et al.*, 2012). One current view about eLRR RLPs is that this class of resistance proteins is involved in 'effector-triggered defence' (ETD), a newly introduced concept of plant defence involving apoplastic fungal pathogens (Stotz *et al.*, 2014). The blurred definition of some eLRR RLPs based on their involvement in both race-specific resistance (and so these receptors should be classified as R proteins involved in ETI) and recognition of conserved effector molecules (and therefore should be classified as PRRs involved in MTI) has led the introduction of this new concept of plant defence as distinct from 'effector-triggered immunity' (ETI) involving the NB-LRR receptors that recognize intracellular pathogen effectors.

ETD is characterized by a cell death reaction in response to infection by apoplastic fungal pathogens that is slower and weaker than that typically observed during ETI (from no cell death to development of cell death 21 days after infection for ETD versus the rapid cell death that occurs in less than 2 days for ETI) (Stotz *et al.*, 2014). As the response is weaker than 'immunity', the term 'defence' is used. However, while the concept of ETD has been invoked to explain the weaker nature of apoplastic defence responses differing from ETI, it should be noted that an increasing number of eLRR RLPs has been identified with a role in MAMP perception (Table 1.1). Whether or not the eLRR RLPs should be classified as PRRs involved in MTI or in the newly defined ETD remains debatable. The plant immune system, should perhaps be viewed as a continuum of non-host to host-specific resistance involving both the cell surface eLRR and the intracellular NB-LRR receptors that co-operate in activating appropriate immune responses to counteract different types of pathogens (Jones and Takemoto, 2004; Thomma *et al.*, 2011; Senthil-Kumar and Mysore, 2013).

1.3 Pathogen recognition – direct and indirect recognition

1.3.1 The LRR domain

In contrast to the diversity of the pathogen effectors, the plant resistance proteins share striking structural similarities notably in the LRR domain. The LRR motif is found in a wide range of prokaryotic and eukaryotic proteins and provides a versatile platform for interactions with a variety of molecules including proteins, nucleic acids, lipids and small molecule hormones (Kobe and Kajava, 2001; Bella *et al.*, 2008). Typically, each LRR consists of a consensus sequence of 20–30 amino acids containing the characteristic LxxLxLxxNxL motif (with x being any amino acid) (Kobe and Kajava, 2001; Bella *et al.*, 2008). The first crystal structure solved for an LRR containing protein, the porcine ribonuclease inhibitor (RI) revealed that each LRR unit stacks together to form an extended spring-like solenoid in the LRR domain. The β-strands, which contain the putative solvent-exposed residues that determine the recognition specificity of the protein, form a β-sheet occupying the concave (interior) side of the LRR domain. α-helices provide the outer convex surface of the protein and act as wedges that allow curvature of the LRR domain (Kobe and Deisenhofer, 1993). The spring-like structure of the LRR domain allows flexible changes in the curvature of the solenoid and exposure of residues in the β–sheet upon ligand binding as shown by the LRR domain of RI upon binding of ribonuclease A (Kobe and Deisenhofer, 1996). Consistent with its role in protein-protein interactions, the LRR domain serves as the major determinant for pathogen recognitional specificity (Padmanabhan *et al.*, 2009). Sequence comparisons between close homologues of specific resistance proteins often show high variability in the LRR domain particularly in the putative solvent-exposed positions in the β-sheet of the protein, with a higher rate of non-synonymous substitution (nucleotide substitution that results in a change of the encoded amino acid) than synonymous substitution (nucleotide substitution that does not change the encoded amino acid), suggesting that a positive diversifying selection occurs in the LRR domain (Parniske *et al.*, 1997; Ellis *et al.*, 2000; McDowell and Simon, 2008). For instance, flax P1 and P2 specific resistance to flax rust was found to be determined by the solvent-exposed residues in the β-sheet of the LRR domain in these R proteins (Dodds *et al.*, 2001).

Studies on the eLRR RLKs i.e. FLS2 and BRI1 have been at the forefront in understanding the structural basis of plant cell surface receptors with recent X-ray crystallography data elucidating the eLRR domain of these receptors interacting with their corresponding ligands (Hothorn *et al.*, 2011; She *et al.*, 2011; Sun *et al.*, 2013). The solved crystal structure of FLS2 revealed that its eLRR domain adopts a superhelical structure (Figure 1.2) (Sun *et al.*, 2013), similar to that of BRI1 (Hothorn *et al.*, 2011; She *et al.*, 2011) and the antifungal bean polygalacturonase-inhibiting protein (PGIP) (Di Matteo *et al.*, 2003). This differs from the horseshoe-like structure formed by the LRR domains of the porcine ribonuclease inhibitors (RI) and the mammalian Toll-like receptors (Bell *et al.*, 2003), owing to the β1-β2-3_{10} helix LRR structure encoded by a 23- to 25-amino acid consensus plant-specific eLRR motif LxxLxxLxxLxLxxNxLxGxIPxx typical of plant cell surface eLRR receptors (Jones and Jones, 1997).

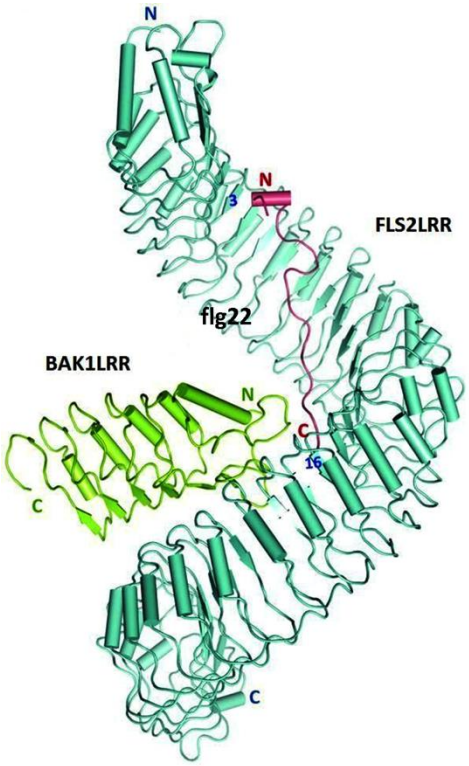

Figure 1.2 Crystal structure of the FLS2-BAK1-flg22 complex. FLS2 adopts a superhelical structure. The positions of LRR3 and LRR16 are indicated. 'N' and 'C' represent the N and C terminus, respectively. FLS2 LRR, BAK1 LRR and flg22 structures are indicated in blue, green and red, respectively. Figure adapted from Sun *et al.* (2013).

It is thought that the eLRR domain of the cell surface receptors provides a platform for receptor complex assembly (Jaillais *et al.*, 2011; Li, 2011). Upon perception of the flg22 epitope from bacterial flagellin, FLS2 undergoes a rapid heterodimerization with BAK1 (BRI1-associated Kinase 1) to form a signalling active FLS2-BAK1 complex, followed by reciprocal phosphorylation to activate plant defence (Chinchilla *et al.*, 2007; Heese *et al.*, 2007; Schulze *et al.*, 2010; Sun *et al.*, 2013). As shown in Figure 1.2, FLS2 and BAK1 form a monomeric heterodimer, whereby the BAK1 LRR domain interacts directly with the C-terminal portion of FLS2 LRR domain in an orientation resulting in both transmembrane domains being located in close proximity to one another (Sun *et al.*, 2013). While the crystal structure of FLS2 did not show that the receptor undergoes homodimerization, FLS2 homodimerization remains possible (Sun *et al.*, 2012). Apart from its interaction with the LRR domain of FLS2, BAK1 also interacts with the C-terminus of flg22, demonstrating its role as a co-receptor in flg22 perception. The flg22 epitope binds to the concave surface of FLS2 from LRR 3 to LRR 16 with its C terminus sandwiched between the LRR domain of FLS2 and the N-terminal cap domain of BAK. The crystal structures of the free and flg22-bound LRR domain of FLS2 are nearly identical, suggesting that conformational changes may not be necessary for FLS2 activation. By contrast, a comparison of the crystal structures of BRI1 on its own or in the presence of its brassinolide ligand showed that the receptor undergoes local structural rearrangements at the loop-out region and the two flanking LRR domains upon binding of the hormone molecule in an 'induced-fit' manner (She *et al.*, 2011). This subsequently forms a docking platform for the co-receptor BAK1 to bind and allow signal transduction (Santiago *et al.*, 2013).

1.3.2 Direct recognition by R proteins

Several studies have demonstrated a direct interaction between the LRR domains for some R proteins with their corresponding pathogen effector proteins. For instance, by using yeast two-hybrid assays, the LRR domain of rice Pi-ta protein was shown to interact with its cognate effector protein AvrPita from the rice blast fungus *Magnaporthe grisea*. Likewise, the LRR domain of the *Arabidopsis* RPP1 (Recognition of *Peronospora parasitica* 1) has been shown to interact with the *Hyaloperonospora arabidopsidis* ATR1 effector *in planta* by co-immumoprecipitation analysis (Krasileva

et al., 2010). Additionally, the flax L6 and M proteins have been shown by yeast two-hybrid assays to interact directly with their corresponding *Melampsora lini* fungal effectors AvrL567 and AvrM (Dodds *et al.*, 2006; Ellis *et al.*, 2007; Catanzariti *et al.*, 2010).

1.3.3 Indirect recognition by R proteins

While some R/Avr interactions have been shown to be direct, most other cases are not. These R/Avr interactions appeared to be mediated by a host protein, which can be envisioned as an adaptor protein that mediates Avr protein recognition by the corresponding R protein. To account for indirect R/Avr interactions, van der Biezen and Jones, (1998) proposed the 'guard model' wherein R proteins act as guards of effector targets (guardees) by sensing modifications of a guardee by a pathogen effector, resulting in activation of plant defence. This model was originally formulated to explain the recognition of *P. syringae* effector AvrPto by the two tomato proteins Pto and Prf (an NB-LRR protein)(van der Biezen and Jones, 1998). In this case, Prf acts as the guard that detects structural changes in Pto (the guardee) caused by AvrPto and then activates defence.

The interaction between RPS2 and the corresponding *P. syringae* effector AvrRpt2 mediated by the Arabidopsis RIN4 (RPM1-INTERACTING PROTEIN 4) also complies with the guard model (Axtell and Staskawicz, 2003; Takemoto and Jones, 2005). AvrRpt2 was found to target RIN4 for degradation and the corresponding RPS2 resistance protein recognizes RIN4 degradation and then activates plant defence. Additionally, RIN4 also mediates the recognition of two other *P. syringae* effectors AvrRpm1 and AvrB by the R protein RPM1 (RESISTANCE TO *P. SYRINGAE* PV. *MACULICOLA* 1). However, this occurs in a slightly different manner wherein these effectors target RIN4 for phosphorylation and RPM1 detects RIN4 phosphorylation and then activates plant defence (Belkhadir *et al.*, 2004). Regardless of the mode of recognition in the two systems described, the example of the recognition of two different pathogen effectors by RPM1 via RIN4 demonstrates how multiple pathogen effectors can be perceived by a single R protein and how individual host proteins can be

targeted by multiple effectors and guarded by multiple *R* genes. An indirect R/Avr recognition enables a limited *R* gene repertoire to recognize diverse pathogens because the same host proteins are often targets for effectors produced by different pathogens (Dangl and Jones, 2001).

1.4 The tomato-*Cladosporium fulvum* pathosystem

Cladosporium fulvum (also known as *Passalora fulva*) is a Dothideomycete fungus that causes tomato leaf mould disease (de Wit *et al.*, 2012). It is a biotrophic pathogen that only colonizes the apoplastic space of tomato leaves without penetrating host cells (Thomma *et al.*, 2005). The tomato leaf mould disease likely originated from South America, the place of origin of tomato and where the disease was first reported in the late 1800s (Cooke, 1883). This disease affects greenhouse-grown tomatoes under conditions of high humidity and warm temperatures but is less common on outdoor crops. Resistance to the disease has been achieved through introgression of *Cf* genes from wild tomato species via breeding (de Wit, 1992), although recent outbreaks have been found in regions that employ these resistance genes extensively (Enya *et al.*, 2009). With a wealth of *Cf* genes and corresponding avirulence genes that have been cloned and studied (Table 1.2 and references therein), the tomato-*C. fulvum* pathosystem is an excellent model system to study the genetic and molecular basis of gene-for-gene interaction involving eLRR RLPs (Joosten and de Wit, 1999; Wulff *et al.*, 2009a).

Table 1.2 ***Dramatis personæ*** **in tomato-*Cladosporium fulvum* interaction.** Proteins indicated in brackets are encoded by genes that have not yet been cloned. Proteins indicated with a question mark are either hypothetical in the case of the Cf-ECP6 or Cf-ECP7 proteins or their role as an effector or effector target is not determined in the case of PhiA, the high-affinity binding site (HABS) and the *Nicotiana benthamiana* necrosis-inducing protein (NbNIP). *Proteins shown to contribute to pathogenicity. *Mycosphaerella fijiensis* Avr4, MfAvr4. Table adapted from Wulff *et al.* (2009a).

Cf proteins	*C. fulvum* effectors (or indicated otherwise)	Structure/ function	Effector target(s)	Reference
Cf-2	Avr2*	Secreted cysteine protease inhibitor	Rcr3 and Pip1 (Secreted cysteine proteases)	Dixon *et al.* (1996) (Cf-2) Luderer *et al.* (2002) and van't Klooster *et al.* (2011) (Avr2) Dixon *et al.* (2000) ($Rcr3^{pimp}$) Shabab *et al.*, (2008) and van Esse *et al.* (2008) (Pip1)
	Nematode VAP1 protein*	Secreted venom allergen-like protein	Rcr3	Lozano-Torres *et al.* (2012) (VAP1)
Cf-4	Avr4*	Secreted chitin-binding protein		Thomas *et al.* (1997) (Cf-4) Joosten *et al.* (1994) (Avr4)
	MfAvr4*	Secreted chitin-binding protein		Stergiopoulos *et al.* (2010) (MfAvr4)
Cf-4E	Avr4E	Secreted cysteine-rich protein		Takken *et al.* (1999) (Cf-4E) Westerink *et al.* (2004) (Avr4E)
Cf-5	Avr5*	Secreted cysteine-rich protein		Dixon *et al.* (1998) (Cf-5) Mesarich *et al.* (2014) (Avr5)
Cf-9	Avr9*	Secreted cystine-knot protein	HABS?	Jones *et al.* (1994) (Cf-9) van den Ackerveken *et al.* (1992) (Avr9) Kooman-Gersmann *et al.* (1996) (HABS)

Cf-9B	(Avr9B)	Unknown	NbNIP orthologue?	Panter *et al.* (2002) (Cf-9B) Chakrabarti *et al.* (2009) (NbNIP)
(Cf-ECP1)	AvrECP1*	Secreted cysteine-rich protein		Soumpourou *et al.* (2007) (Cf-ECP1) van den Ackerveken *et al.* (1993) (ECP1)
(Cf-ECP2)	AvrECP2*	Secreted disulphide-bonded (?) protein		Laugé *et al.* (1998) and Haanstra *et al.* (1999) (Cf-ECP2) van den Ackerveken *et al.* (1993), Stergiopoulos *et al.* (2010) and de Wit *et al.* (2012) (ECP2)
(Cf-ECP4)	AvrECP4	Secreted cysteine-rich protein		Soumpourou *et al.* 2007 (Cf-ECP4) Laugé *et al.* (2000) (ECP4)
(Cf-ECP5)	AvrECP5	Secreted cysteine-rich protein		Haanstra *et al.* (2000) (Cf-ECP5) Laugé *et al.* (2000) (ECP5)
(Cf-ECP6?)	ECP6*	Secreted LysM domain protein, possible chitin-binding protein	None?	Bolton *et al.* (2008) (ECP6)
(Cf-ECP7?)	ECP7	Secreted cysteine-rich protein		Bolton *et al.* (2008) (ECP7)
?	PhiA?	Phialide protein homologue	None?	Bolton *et al.* (2008) (PhiA)

1.4.1 The tomato-*C. fulvum* compatible and incompatible interactions

In a susceptible tomato genotype lacking *Cf* resistance genes, *C. fulvum* can successfully infect and establish a compatible interaction with the host. This fungus infects the abaxial surface of the tomato leaves, starting with conidia that germinate on the leaf surface. At approximately 3 days post-infection, the conidia produce runner hyphae that enter the host leaf through open stomata and colonize the apoplastic space between mesophyll cells. Ten to 14 days later, conidiophores re-emerge from the stomata to release massive amounts of conidia and spread the disease. This results in stomatal clogging and impaired gas exchange, leading to wilting of leaves, defoliation and in the case of severe infections, host death occurs (Bond, 1938; Thomma *et al.*, 2005; de Wit *et al.*, 2012). While *C. fulvum* does not form feeding structures such as the haustoria, the fungal hyphae form close contact with the host cells by appressing the walls of mesophyll cells, perhaps as a way to obtain nutrients from the host (Bond, 1938; Lazarovits and Higgins, 1976).

Infection in incompatible interactions between specific races of *C. fulvum* and tomato cultivars carrying the corresponding *Cf* genes is similar to compatible interactions with respect to the initial stages of infection i.e. conidial germination, runner hyphae formation and stomatal penetration, but the majority of the hyphae do not grow out of the stomata as a consequence of reduced hyphal development in the apoplast and there is little or no conidia formation. Host defence responses such as callose deposition and rapid accumulation of pathogenesis-related proteins including PR-2 (β-1,3-glucanases) and PR-3 (chitinases) occur in the apoplastic space, resulting in an arrest of fungal growth 1 or 2 days after penetration (Lazarovits and Higgins, 1976; de Wit, 1977). Eventually, the mesophyll cells adjacent to the intracellular hyphae and occasionally, some guard cells and epidermal cells collapse, which also results in release of antimicrobial compounds from the cells (Joosten and de Wit, 1999).

1.4.2 The *C. fulvum* effectors

C. fulvum effector proteins can function as virulence factors to promote the infection of susceptible tomato plants but can also act as avirulence factors that trigger host defence in tomato carrying the corresponding *Cf* resistance genes (Thomma *et al.*, 2005; Wulff

et al., 2009a). To date, 13 *C. fulvum* effector genes that encode Avr (avirulence) proteins or ECPs (extracellular proteins) have been cloned (Table 1.2 and references therein). Ten of these effector genes i.e. *Avr2, Avr4, Avr4E, Avr5, Avr9, Ecp1, Ecp2-1, Ecp4, Ecp5* and *Ecp6*, known to function as avirulence genes, are able to elicit a plant defence response in plants carrying the corresponding *Cf* genes *Cf-2, Cf-4, Cf-4E, Cf-5, Cf-9, Cf-Ecp1, Cf-Ecp2, Cf-Ecp4, Cf-Ecp5* and *Cf-Ecp6*, respectively (Stergiopoulos and de Wit, 2009; Wulff *et al.*, 2009a; Mesarich *et al.*, 2014). Most of these effectors, including those encoded by avirulence genes i.e. Avr2, Avr4, Avr4E, Avr5 and Avr9, are small, secreted cysteine-rich proteins with no sequence similarity to one another.

The recent use of RNA-Seq transcriptome sequencing technology has proven a powerful method in the identification of effector genes from the fungal genome (de Jonge *et al.*, 2012), including the *Avr5* gene (Mesarich *et al.*, 2014). Genetic complementation of the newly isolated *Avr5* gene into a *C. fulvum* race 5 strain (that does not elicit an HR in *Cf-5* tomato) triggered resistance in *Cf-5* tomato and resulted in increased fungal biomass in susceptible tomato, demonstrating a role for Avr5 as both an avirulence and a virulence factor (Mesarich *et al.*, 2014). The *C. fulvum* effectors employ different strategies to promote pathogenicity in tomato. Avr2 was found to bind and inhibit the activity of extracellular tomato cysteine proteases Rcr3 (required for *C. fulvum* resistance 3) and Pip1 (*Phytophtora*-inhibited protease 1) (Tian *et al.*, 2007; Shabab *et al.*, 2008; van Esse *et al.*, 2008). The role of Avr2 as a virulence factor is evident wherein transgenic tomato and Arabidopsis expressing Avr2 showed enhanced susceptibility to several fungal pathogens such as *Botrytis cinerea* and *Verticillium dahliae* (van Esse *et al.*, 2008). Avr4 is a chitin-binding protein that protects fungal cell walls against hydrolysis by plant chitinases (van den Burg *et al.*, 2006; van Esse *et al.*, 2007). Therefore, rather than actively suppressing plant defence like Avr2, Avr4 is considered as a defensive virulence factor. Furthermore, the LysM domain-containing Ecp6 effector binds chitin oligomers with high affinity so preventing their detection by PRRs and ultimately contributing to the avoidance of MTI (de Jonge *et al.*, 2010). By contrast, the pathogenic role of Avr9, a small secreted cysteine rich protein structurally related to carboxypeptidase inhibitors, is not known (Vervoort *et al.*, 1997). Disruption of the *Avr9* gene did not affect the virulence of *C. fulvum*, suggesting that Avr9 may not be required for full virulence of the pathogen (Marmeisse *et al.*, 1993).

The *ECP* genes are more conserved across the various races of *C. fulvum* in comparison to the *Avr* genes (Stergiopoulos *et al.*, 2007; Bolton *et al.*, 2008). This is probably due to commercial deployment of *Cf* genes which has imposed selection pressure against the corresponding *Avr* genes (Stergiopoulos *et al.*, 2007). As a result, the *Avr* genes have evolved to escape recognition through a number of mechanisms that shape the polymorphism observed in these genes today. These include gene deletions (which occurs in the case of *Avr4E* and *Avr9*), transposon insertions (*Avr2*) and point mutations either involving single nucleotide polymorphisms (SNPs) that result in nonsynonymous amino acid substitutions (*Avr4* and *Avr4E*) or indels (insertions or deletions) of nucleotides that result in a frame-shift mutation (*Avr4*)(Joosten *et al.*, 1997; Luderer *et al.*, 2002; van den Burg *et al.*, 2003; Westerink *et al.*, 2004; Stergiopoulos *et al.*, 2007; Wulff *et al.*, 2009a). For instance, natural variants of *C. fulvum* strains virulent on *Cf-4* tomato contain point mutations in *Avr4* that destabilize the effector, thereby avoiding recognition by Cf-4 (van den Ackerveken *et al.*, 1992; Joosten *et al.*, 1997; van den Burg *et al.*, 2003) whereas, some *C. fulvum* strains circumvent Cf-2-mediated resistance via alleles of Avr2 truncated by transposon insertion (Luderer *et al.*, 2002).

Recently, a number of *C. fulvum* effector homologues have been identified in other Dothideomycete species including *Mycosphaerella fijiensis*, which causes black Sigatoka disease of banana, and *Dothistroma septosporum*, an economically important hemibiotrophic pathogen that affects pine trees (Stergiopoulos *et al.*, 2010; de Wit *et al.*, 2012). Some of the tomato Cf proteins recognize some of the *C. fulvum* effector homologues from these fungal species. For instance, the *M. fijiensis* Avr4 effector homologue and *M. fijiensis* and *D. septosporum* Ecp2 effector homologues trigger a necrotic response when expressed in tomato lines carrying the corresponding *Cf-4* and *Cf-ECP2* genes, respectively (Stergiopoulos *et al.*, 2010; de Wit *et al.*, 2012). Additionally, numerous *C. fulvum* effector homologues including *Avr4, Ecp2-1, Ecp2-2, Ecp2-3, Ecp4, Ecp5* and *Ecp6* were identified in the *D. septosporum* genome (Stergiopoulos *et al.*, 2010; de Wit *et al.*, 2012).

1.4.3 The tomato *Cf* genes

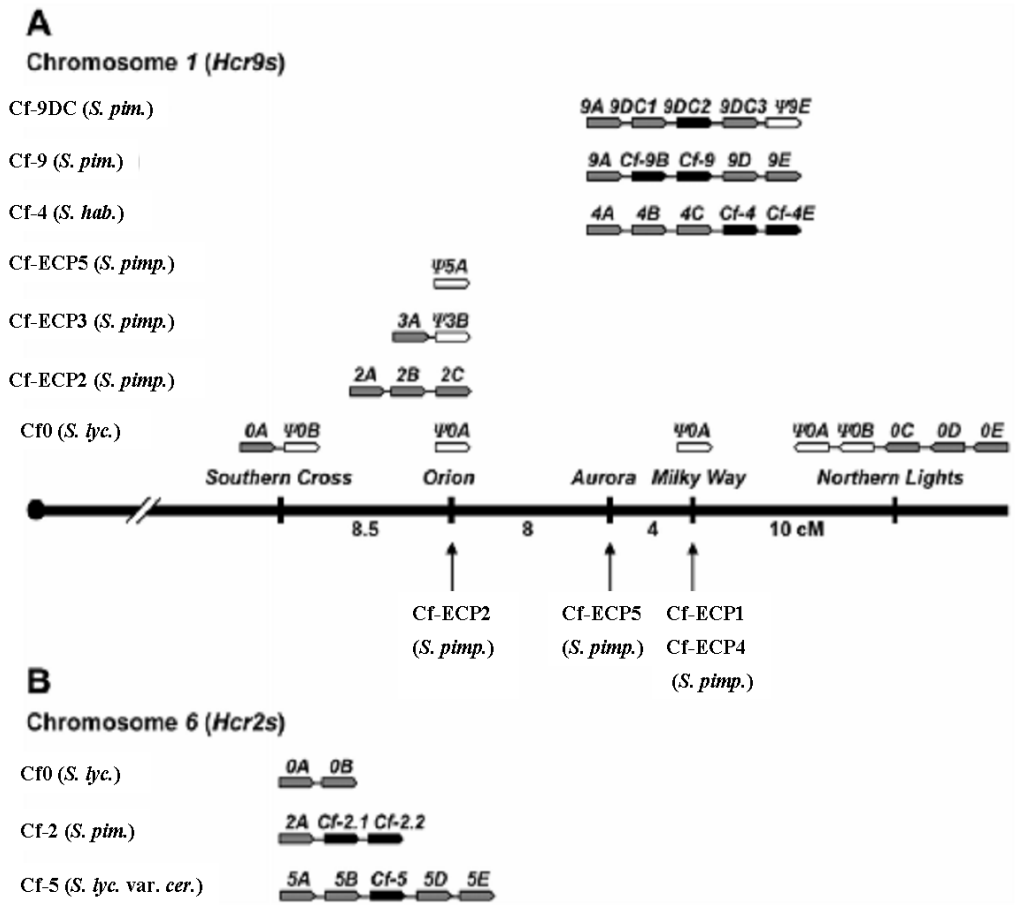

Figure 1.3 Structural organization of *Hcr9* and *Hcr2* gene clusters in the tomato genome. Different *Cf* gene haplotypes have been identified in various tomato species such as *S. lycopersicum, S. habrochaites S. pimpinellifolium* and *S. lycopersicum* var. *cerasiforme*. *Hcr9* genes are mapped to the *Southern Cross*, *Orion*, *Aurora*, *Milky Way* and *Northern Lights* loci in chromosome 1 whereas *Hcr2* genes are located in chromosome 6. The orientation of *Hcr9* genes relative to each other and the centromere (indicated by filled black circle) is shown by arrowed boxes. Genetic distances are indicated in cM. Genes with known resistance specificities are shown in black whereas white denotes non-functional genes. Genes with no known function are indicated in grey. The location of *Cf-ECP1*, *Cf-ECP2*, *Cf-ECP4* and *Cf-ECP5* genes are indicated by arrows although their identity as *Hcr9* genes has not been shown. Figure adapted from Wulff *et al.* (2009a).

Resistance to *C. fulvum* has been achieved by introgression of *Cf* resistance genes from wild tomato species into tomato (*S. lycopersicum*) e.g. the cultivar MoneyMaker (MM), which is also known as Cf0 tomato because it does not carry any known functional *Cf* genes. For instance, *Cf-9* and *Cf-4* genes were introgressed from *S. pimpinellifolium* and *S. harbrochaites*, respectively. Over the last two decades, many *Cf* resistance genes have been isolated (Table 1.2 and references therein). These include *Cf-9* and *Cf-2* which were isolated by transposon tagging and positional cloning, respectively (Jones *et al.*, 1994; Dixon *et al.*, 1996). Functional analysis of *Cf* genes was carried out in near-isogenic line (NILs) generated by crosses between wild tomato species or tomato cultivars carrying resistance genes and susceptible Cf0 tomato. Through genetic mapping of cloned *Cf* genes and their homologues, the locations of *Cf* resistance genes in the tomato genome have been identified (Figure 1.3). In particular, *Cf-9* and *Cf-4* genes were mapped to the *Hcr9* gene cluster in Chromosome 1 whereas *Cf-2* and *Cf-5* genes reside in the *Hcr*2 gene cluster in Chromosome 6 (Parniske *et al.*, 1997; Thomas *et al.*, 1997; Dixon *et al.*, 1998; Parniske and Jones, 1999). *Cf-9* is the central gene among five paralogous genes designated *Hcr9-9A* to *Hcr9-9E* located in the *Milky Way* locus in Cf-9-MM tomato plants. *Cf-9* confers resistance in seedlings and mature plants whereas its paralogue *Cf-9B* only imparts mature plant resistance (Parniske *et al.*, 1997; Panter *et al.*, 2002). Promoter swapping analysis between *Cf-9* and *Cf-9B* showed that this developmental difference is not due to a difference in resistance gene expression but may be associated with delayed expression of a host protein that mediates elicitor recognition by Cf-9B at a later stage of development (Panter *et al.*, 2002). *Cf-4* is the fourth member of a class of five paralogous genes denoted *Hcr9-4A* to *Hcr9-4E* (including the functional *Cf-4E* resistance gene) located at the *Milky Way* locus in Cf-4-MM tomato plants (Parniske *et al.*, 1997; Takken *et al.*, 1999). In the susceptible Cf0 tomato line, there is a single homologous pseudogene denoted *Hcr9-ψ0A* (Parniske *et al.*, 1997). The *Cf-ECP* genes, which confer ECP-dependent resistance, have been mapped to several loci in the short arm of Chromosome 1 in *S. pimpinellifolium* (Figure 1.3) (Haanstra *et al.*, 1999; Haanstra *et al.*, 2000; Laugé *et al.*, 2000; Yuan *et al.*, 2002; de Kock *et al.*, 2005). Sequence comparison among *Cf* genes and analysis of their genomic organization revealed evidence of sequence exchange by inter- and/or intralocus crossing over, gene duplication and diversifying selection favouring point mutations resulting in amino acid substitutions affecting the LRR interaction surface,

thereby contributing to the diversity of recognitional specificity encoded by these genes (Parniske *et al.*, 1997; Wulff *et al.*, 2009a).

1.4.4 Molecular and genetic basis of Cf-/Avr interactions

1.4.4.1 How does Cf-9 recognize Avr9?

Despite the use of various biochemical approaches to investigate the interaction between Cf-9 and Avr9, no interaction has been detected between these proteins (Luderer *et al.*, 2001). By contrast, Avr9 was found to interact with a high affinity binding site (HABS) present in plasma membranes of tomato and other Solanaceous plants independent of the presence of Cf-9 (Kooman-Gersmann *et al.*, 1996). Interestingly, the binding affinity of Avr9 to the HABS positively correlates with its ability to induce a Cf-9-dependent HR, suggesting that Cf-9 recognizes Avr9 indirectly by sensing the interaction of Avr9 with the HABS to then activate defence (Kooman-Gersmann *et al.*, 1998; de Jong *et al.*, 2002). Consistently, co-expression of Cf-9 and Avr9 proteins in tobacco and potato was sufficient to induce an HR. This correlates with the presence of a HABS in these plant species (Hammond-Kosack *et al.*, 1998).

1.4.4.2 The Cf-2-Rcr3-Avr2 interaction

The recognition of the Avr2 effector by the Cf-2 resistance protein requires the presence of $Rcr3^{pimp}$, a cysteine protease originating from *S. pimpinellifolium* (Krüger *et al.*, 2002; Rooney *et al.*, 2005). A positive correlation between the binding affinity of Avr2 to Rcr3 and its ability to trigger Cf-2-mediated necrosis was reported (van't Klooster *et al.*, 2011), suggesting that the recognition of Avr2 by Cf-2 is mediated by Rcr3. The Cf-9-HABS-Avr9 and Cf-2-Rcr3-Avr2 interactions are consistent with the 'guard' hypothesis (van der Biezen and Jones, 1998; Dangl and Jones, 2001), wherein the Cf proteins 'guard' the virulence target of their corresponding *C. fulvum* effector proteins and in these cases, the HABS and Rcr3 are pathogen virulence targets. In fact, the Avr2 effector behaves as a virulence factor of *C. fulvum* by inhibiting Rcr3. However, the inhibition of Rcr3 *per se*, such as that by the *Phytophtora infestans* effector proteins EPIC1 and EPIC2B does not result in Cf-2-dependent cell death (Rooney *et al.*, 2005; Song *et al.*, 2009). These observations indicate that the induction of Cf-2-mediated cell

death requires specific structural modifications of Rcr3. The $Rcr3^{pimp}$ homologue from *S. lycopersicum*, $Rcr3^{lyc}$ was found to trigger an Avr2-independent necrosis among F2 segregants when a tomato line carrying *$Rcr3^{lyc}$* was crossed to a line carrying *Cf-2* (Krüger *et al.*, 2002). The $Rcr3^{lyc}$ protein differs from its *S. pimpinellifolium* homologue by six amino acid substitutions and one amino acid deletion, supporting the model of Cf-2 activation that involves conformational changes of Rcr3. Interestingly, Cf-2 was found to mediate resistance to the root parasitic nematode *Globodera rostochiensis* that secretes a venom allergen-like protein designated VAP1 that has no sequence similarity to Avr2 (Lozano-Torres *et al.*, 2012), demonstrating the ability of Cf-2 to recognize two independently evolved pathogen effectors. Similar to Avr2, VAP1 was also found to bind and inhibit the active site of Rcr3 which in turn allowed its recognition by Cf-2. In addition, tomato plants lacking Cf-2 but carrying Rcr3 showed increased susceptibility to *G. rostochiensis* infection, indicating that VAP1 is involved in pathogenicity and Rcr3 is a virulence target of VAP1 (Lozano-Torres *et al.*, 2012).

1.4.4.3 The interaction between Cf-4 and Avr4

There is no evidence of a direct interaction between the Cf-4 and Avr4 proteins and no HABS has been shown to exist for Avr4 (Luderer *et al.*, 2001; Westerink *et al.*, 2002). While Avr4 is known to bind to fungal chitin (van den Burg *et al.*, 2006), this activity appears to be unnecessary for its recognition by Cf-4 as expression of Avr4 by itself is sufficient to trigger Cf-4-dependent necrosis in tobacco (Thomas *et al.*, 2000). It has been speculated that there is a direct interaction between Cf-4 and Avr4 based on the observations that: 1) perturbation of a host target is normally involved in an indirect R/Avr interaction but instead Avr4 acts as a defensive virulence factor rather than inhibiting any host proteins, 2) expression of Avr4 in tomato lacking Cf-4 did not significantly induce transcription of host genes (van Esse *et al.*, 2007) (which is in contrast to the *PR* gene-like induction of Rcr3 by Avr2, Krüger *et al.*, (2002)) and 3) a rapid and stronger defence response mediated by Cf-4/Avr4 interaction than that of Cf-9/Avr9 interaction (Thomas *et al.*, 2000; van der Hoorn *et al.*, 2000), which suggests that the recognition of Avr4 by Cf-4 may not involve a third party to mediate the interaction.

1.4.5 Structure and function of Cf proteins

The tomato *Cf* resistance genes (i.e. the *Hcr9* and *Hcr2* genes) encode eLRR RLPs, consistent with their proposed role as receptors that recognize *C. fulvum* effectors in the apoplast (Kruijt *et al.*, 2005; Rivas and Thomas, 2005). These resistance proteins adopt a typical eLRR RLP structure as illustrated by the schematic representation of the Cf-9 protein in Figure 1.4.

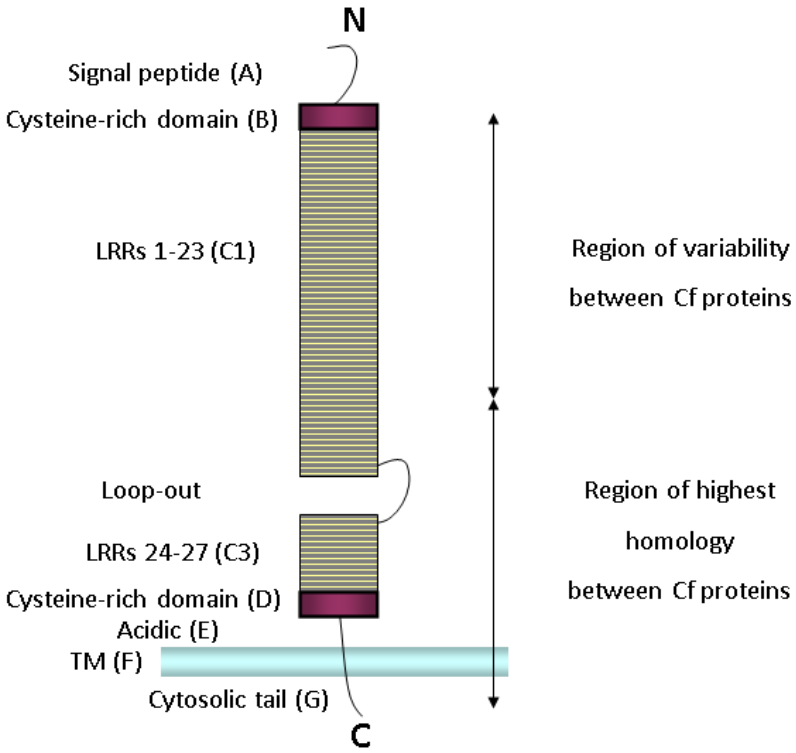

Figure 1.4 Structural domains of the tomato Cf-9 resistance protein. Domain A is a cleavable signal peptide, B and D are cysteine-containing LRR flanking domains, C is the LRR domain containing 27 leucine-rich repeat (LRR) motifs divided into two blocks (C1 and C3) by a non-LRR loop-out region (C2), E is an acidic domain, F is a transmembrane (TM) domain and G is a highly basic cytosolic tail. The N- and C-termini of the protein are denoted by N and C, respectively. Figure adapted from (Barker, 2002)

As a type I transmembrane glycoprotein (Benghezal *et al.*, 2000; Piedras *et al.*, 2000), Cf-9 is heavily glycosylated and most of the putative glycosylation sites particularly those in the helical region were shown to be essential for its function (van der Hoorn *et*

al., 2005). Furthermore, Cf-9 and Cf-4 were shown to interact *in vivo* with several endoplasmic reticulum-resident chaperone proteins, which were thought to be required for proper folding of these eLRR receptors before being transported to the plasma membrane as functional receptor proteins (Liebrand *et al.*, 2012). The N-terminal and C-terminal cysteine-containing LRR-flanking domain (domains B and D) are proposed to function as 'caps' that stabilize the eLRR domain. However, only the conserved cysteine-rich motifs in domain B but not domain D were shown to be essential for Cf-9 function, possibly by maintaining the overall protein structure through intramolecular interactions via the formation of disulphide bridges (van der Hoorn *et al.*, 2005).

Sequence comparison among 39 Hcr9 proteins revealed that domain C1, particularly in LRRs 4-18, is highly variable (Parniske *et al.*, 1997; Wulff *et al.*, 2009b). In this region, a higher rate of non-synonymous amino acid substitutions to synonymous amino acid substitutions was found notably at the interstitial solvent-exposed positions in the central LRRs (Parniske *et al.*, 1997). By contrast, the C-terminal portion of Hcr9 proteins is more conserved and this sequence conservation can be also found in the more distantly related Hcr2 proteins (Dixon *et al.*, 1996; Parniske *et al.*, 1997). These observations suggest a role of the variable N-terminus in ligand recognition whereas the conserved C-terminus is more likely to be involved in the interaction with a common signalling partner(s) in signal transduction (Jones and Jones, 1997; Parniske *et al.*, 1997). For instance, Cf-9 and Cf-4 proteins are completely identical in their C-termini (from LRR 17 to the C-terminus of Cf-9) and yet these proteins recognize the sequence unrelated Avr9 (28 amino acids) and Avr4 (86 amino acids) elicitors (Thomas *et al.*, 1997; Joosten and de Wit, 1999). This indicates that the recognition of Avr9 and Avr4 effectors by Cf-9 and Cf-4, respectively, is likely to be mediated by the differing N-termini of these proteins.

The molecular basis of recognitional specificity for Cf-2, Cf-4, Cf-5, Cf-9 and Cf-9B has been functionally dissected by domain swapping, gene shuffling and site-directed mutagenesis. For instance, domain swapping between Cf-4 and Cf-9 revealed that Cf-4 specificity is determined by differences in LRR copy number, domain B and three putative solvent exposed residues residing in LRRs 13-16 whereas Cf-9 specificity is distributed over several LRRs (van der Hoorn *et al.*, 2001a). In fact, LRR copy number

may be an important determinant of ligand recognitional specificity as it determines the spacing between solvent-exposed residues in contact with ligand (Jones and Jones, 1997). Domain swapping between Cf-9 and its close homologue, Cf-9B led to greater resolution in the identification of Cf-9 specificity-determining residues located at the solvent-exposed positions in the β-strand/ β-turn motif in the central LRRs of the protein (Chakrabarti *et al.*, 2009, Wulff *et al.*, 2009b). An advantage of using Cf-9B as a domain-swapping template is the greater similarity between Cf-9 and Cf-9B compared to the similarity between Cf-9 and Cf-4 in their proposed recognition domains (84 % identity versus 72 % identity from the N-terminus to LRR 15 of these proteins). Furthermore, Cf-4 also lacks two LRRs that correspond to LRRs 11 and 12 of Cf-9 whereas both Cf-9 and Cf-9B contain 27 LRRs. Collectively, the aforementioned studies have pinpointed five key amino acid residues i.e. C387 and Y389 in LRR 13, E411 in LRR 14, A433 in LRR 15 and L457 in LRR 16 as the major specificity determinants of Cf-9. In addition, through Cf-9/Cf-9B domain swaps, Chakrabarti *et al.* (2009) showed via agroinfiltrations in *Avr9*-expressing tobacco that LRRs 10-12 located upstream of the major specificity-determining region (LRRs 13-16) contributed to the strength of HR induction in wild type Cf-9,

By generating transgenic tomato containing Cf-9/Cf-9B domain swaps to test for *C. fulvum* resistance, the N-terminus to LRR 15 was found to be required for Cf-9B-mediated resistance in flowering tomato plants (Chakrabarti *et al.*, 2009). Similarly, transgenic tomato plants transformed with domain swaps between Cf-2 and Cf-5 showed that LRRs 3-27 and LRRs 3-21 are involved in Cf-2- and Cf-5-mediated disease resistance, respectively (Seear and Dixon, 2003). As shown in Table 1.3, the specificity-determining regions of the Cf resistance proteins broadly overlap in the central LRRs of these proteins, suggesting this region may be involved in ligand recognition.

Cf proteins	Number of LRRs	Specificity-determining region	References
Cf-2	38	LRRs 3-27	Seear and Dixon (2003)
Cf-4	25	LRRs 13-16	van der Hoorn *et al.* (2001a)
Cf-5	32	LRRs 3-21	Seear and Dixon (2003)
Cf-9	27	LRRs 10-16	Chakrabarti *et al.* (2009) Wulff *et al.* (2009b)
Cf-9B	27	N-terminus to LRR 15	Panter *et al.* (2002) Chakrabarti *et al.* (2009)

Table 1.3 Specificity-determining region of Cf resistance proteins.

The loop-out region of Cf-9 has no demonstrated function as yet. This region has been proposed to act as a molecular hinge between domain C1 and C3, which may allow the protein to take on a conformational change during ligand interaction (van der Hoorn *et al.*, 2005). Not much is known about the cytosolic tail (domain G) of Cf proteins. The conserved KKRY motif in this domain appeared to be required for its retrieval from the Golgi apparatus to endoplasmic reticulum of Cf-9 and hence may be involved in the quality control of Cf-9 biogenesis (Jones *et al.*, 1994; Benghezal *et al.*, 2000), although it may not determine the final location of the protein ((Piedras *et al.*, 2000; van der Hoorn *et al.*, 2001b). Yeast two-hybrid assays using the cytosolic domain of Cf-9 as bait identified several interacting proteins including a Cf-9-interacting thioredoxin (CITRX) and a 'VAP27' protein (Laurent *et al.*, 2000; Rivas *et al.*, 2004). VIGS of CITRX resulted in enhanced Cf-9/Avr9-mediated HR and defence responses, indicating that it plays a negative regulatory role in Cf-9 signalling. However, the role of CITRX appeared to be specific to Cf-9 and not Cf-2 as silencing of CITRX did not alter Cf-2/Avr2-mediated defence responses (Rivas *et al.*, 2004). By contrast, the function of VAP27, a vesicle-associated membrane protein (VAMP)-like protein with a predicted role in protein trafficking in Cf-9-mediated resistance is yet to be demonstrated (Laurent *et al.*, 2000). Additionally, a Cf-2/Cf-9 domain swap containing the first 34 N-terminal LRRs of Cf-2 fused to the three C-terminal LRRs and remaining portion of Cf-9 including its cytosolic tail has been shown to mediate an Avr2- and Rcr3-dependent HR and resistance to *C. fulvum* infection (Krüger *et al.*, 2002). While CITRX is not involved in the regulation of Cf-2 signalling, silencing of CITRX enhanced an Avr2-dependent HR mediated by the Cf-2/Cf-9 domain swap (Rivas *et al.*, 2004), indicating that this chimeric protein induces plant defence through the Cf-9 signalling pathway.

Altogether, these data support a role of the variable N-terminus in ligand recognition and the conserved C-terminus in signal transduction of Cf proteins.

1.4.6 Cf-/Avr-mediated downstream signalling

Transgenic tobacco suspension-culture cells expressing *Cf-9* or *Cf-4* genes have been used successfully to identify an array of signalling events following activation of Cf-/Avr-mediated defence responses by the corresponding Avr9 and Avr4 elicitors. Early responses include changes in ion fluxes, reactive oxygen species (ROS) bursts, alkalization of the culture medium and activation of a calcium-dependent protein kinase (CDPK) and several mitogen-activated protein kinases (MAPKs), including a salicylic acid-induced protein kinase (SIPK) and a wound-induced protein kinase (WIPK) (Piedras *et al.*, 1998; Blatt *et al.*, 1999; de Jong *et al.*, 2000; Romeis *et al.*, 2000a; Romeis *et al.*, 2000b). Interestingly, activation of a phospholipase C (PLC)-mediated signalling pathway was shown to be involved in Cf-4/Avr4-mediated defence response (de Jong *et al.*, 2004). PLC signalling may to contribute to ROS production and downstream phosphorylation events involving protein kinases such as CDPK (de Jong *et al.*, 2004). VIGS of the tomato PLC isoforms 4 and 6 (SlPLC4 and SlPLC6) showed that both were essential for Cf-4–mediated resistance to *C. fulvum* whereas Cf-4/Avr4-induced HR appeared to be specifically mediated by SlPLC4 but not SlPLC6 (Vossen *et al.*, 2010).

Furthermore, gene expression profiling has identified a collection of *Avr9/Cf-9 rapidly elicited* (*ACRE*) genes induced in *Cf-9* tobacco cells within 15 to 30 min of Avr9 elicitor treatment (Durrant *et al.*, 2000). These include a gene encoding a serine/threonine protein kinase designated Avr9/Cf-9 induced kinase 1 (ACIK1). VIGS of ACIK1 showed that this protein is required for Cf-9/Avr9- and Cf-4/Avr4-mediated HR and Cf-9-mediated resistance to *C. fulvum* (Rowland *et al.*, 2005). Interestingly, ACIK1 was found to interact with CITRX and the cytosolic tail of Cf-9 in the presence of CITRX in yeast two- and three-hybrid assays, respectively, suggesting that CITRX may function as an adaptor protein that recruits ACIK1 in Cf-9/Avr9-mediated defence responses (Nekrasov *et al.*, 2006). Another *ACRE* gene required for Cf-9/Avr9- and Cf-4/Avr4-mediated HR and Cf-4-mediated resistance to *C. fulvum* was found to encode a CC-NB-LRR protein designated NRC1 (NB-LRR protein required for HR-associated cell death

1). Interestingly, NRC1 was found to be required for HR mediated by several resistance proteins from both the cell surface eLRR and cytoplasmic CC-NB-LRR classes as silencing of NRC1 abolished their HR induction (Gabriëls *et al.*, 2007), indicating an integration point in the downstream signalling of the two major different classes of R proteins.

Late responses observed following Cf-/Avr-mediated defence activation include accumulation of salicylic acid and ethylene (Hammond-Kosack *et al.*, 1996; Etalo *et al.*, 2013). For instance, infiltration of Cf-2 and Cf-9 tomato cotyledons with intercellular washing fluids (IF) containing the Avr2 and Avr9 peptides, respectively, resulted in accumulation of salicylic acid within 8 to 12 hours (Hammond-Kosack *et al.*, 1996). However, while salicylic acid was shown to be involved in the initiation of cell death response, it is not required for Cf-9- and Cf-2-mediated resistance to *C. fulvum* (Brading *et al.*, 2000), suggesting other defence signalling pathways are involved.

1.5 Autoactive R proteins

R protein-mediated defence, also designated ETI, involves a robust response which often leads to rapid induction of local cell death (Tsuda and Katagiri, 2010). Aberrant activation of plant defence is often associated with impaired plant growth. This can be observed in autoactive mutants associated with constitutive activation of plant defence in the absence of pathogens. These mutants show phenotypes comprising constitutive expression of plant defence marker genes and enhanced pathogen resistance but also altered plant development such as dwarfism (Krüger *et al.*, 2002; Shirano *et al.*, 2002; Zhang *et al.*, 2003; Howles *et al.*, 2005; Barker *et al.*, 2006b; Bomblies *et al.*, 2007; Bi *et al.*, 2010; Gou and Hua, 2012). The autoimmune response is an analogous phenomenon that occurs in the mammalian innate immune system (Anwar *et al.*, 2013). An interesting discussion about plant growth-defence tradeoffs has emerged wherein aberrant activation of plant defence imposes fitness costs on plants (Heil and Baldwin, 2002; Huot *et al.*, 2014). Indeed, plant defence activation is a high-energy-demand process requiring plant cells to undergo immense reprogramming of cellular processes in order to direct cellular resources towards plant defence (Etalo *et al.*, 2013). It is therefore important that plant defence is tightly regulated in the absence of pathogens. In the past decade, analysis of autoactive mutants has provided useful insights about the

activation of plant defence. This section will review a number of factors that can contribute to autoactivity in plants as a prelude to the subject of this thesis, which involves research about an autoactive mutant of the tomato *Cf-9* gene (Section 1.6). There are several types of mutations that can contribute to autoactivation of plant defence. These include mutations affecting the R protein itself or *trans*-acting components regulating R protein activity. Alternatively, mutations involving components that are not directly related to R protein activity such as the cyclic nucleotide-gated ion channel proteins involved in the *defence no death* (*dnd*) mutants, can also contribute to autoactivity (Lorrain *et al.*, 2003). These mutants are called 'lesion mimic' mutants but will not be further discussed here as they are not the subject of this study.

1.5.1 Mutations in the R protein

1.5.1.1 Autoactive NB-LRR proteins

Autoactivity caused by mutations in NB-LRR proteins include exchange of LRRs through domain swapping, loss of LRRs via truncation/deletion and point mutations. Autoactivity has been noted as a result of domain swapping (Hwang *et al.*, 2000; Howles *et al.*, 2005; Rairdan and Moffett, 2006; Slootweg *et al.*, 2013) and deletion (Bendahmane *et al.*, 2002; Michael Weaver *et al.*, 2006; Ade *et al.*, 2007; Qi *et al.*, 2012) involving the LRR domain in a number of NB-LRR proteins. For instance, domain swapping involving the first four N-terminal LRRs of the Arabidopsis CC-NB-LRR receptor RESISTANCE TO PSEUDOMONAS SYRINGAE 5 (RPS5) with its close homologue RPS2 or deletion of these LRRs has been demonstrated to cause autoactivity (Ade *et al.*, 2007; Qi *et al.*, 2012). Likewise, domain swapping analysis between the highly homologous potato Rx and Gpa2 CC-NB-LRR receptors showed that a minimum mismatch between the NB domain of Gpa2 and the first LRR of Rx is sufficient to cause autoactivity (Rairdan and Moffett, 2006; Slootweg *et al.*, 2013). These data suggest a role for the LRR domain in the negative regulation of resistance protein activity, in addition to its proposed role in pathogen recognition. Consistently, the expression of the Prf LRR domain by itself was found to repress activity of autoactive Prf mutants *in trans* (Du *et al.*, 2012).

Point mutations that lead to autoactivity in NB-LRR proteins include those located both inside the LRR domain (Bendahmane *et al.*, 2002; Farnham and Baulcombe, 2006) and outside (Shirano *et al.*, 2002; Hwang and Williamson, 2003; Zhang *et al.*, 2003). In particular, mutations in the conserved motifs involved in nucleotide binding and hydrolysis can cause autoactivity or loss of resistance function in these proteins (Howles *et al.*, 2005; Tameling *et al.*, 2006; van Ooijen *et al.*, 2008; Williams *et al.*, 2011). As autoactive NB-LRR proteins are often associated with ATP binding, it has been hypothesised that the 'on' and 'off' states of NB-LRR receptors are determined by binding of ATP and hydrolysis to ADP, respectively (Takken *et al.*, 2006). Collectively, it has been proposed that activation of NB-LRR receptors is regulated via interaction between the NB domain and adjacent N-terminal LRRs and involves ATP binding and hydrolysis (Collier and Moffett, 2009; Takken and Goverse, 2012). Although the NB-LRR proteins differ from the eLRR class in both their structure and function, reports on autoactive NB-LRR proteins nevertheless indicate negative inhibitory regulation of R protein activity in the absence of their cognate pathogen avirulence proteins.

1.5.1.2 Autoactive eLRR proteins

By shuffling selected *Cf* genes, Wulff *et al.*, (2004a) generated novel autoactive Cf proteins. These 'Cf autoactivators' induced HR differentially when transiently expressed in various tobacco species and were therefore classified into groups according to the distinct pattern of necrosis-inducing ability among the tobacco species tested (Wulff *et al.*, 2004a). Autoactivity among the Cf autoactivators may be caused by disruption of intra- and/or intermolecular interactions that existed in the progenitor sequences as a result of gene shuffling. Alternatively, but not exclusively, these autoactive proteins may differentially recognize endogenous necrosis-inducing factors present in tobacco. Accordingly, the presence or absence, relative concentration and amino acid polymorphism of these necrosis-inducing factors in each tobacco species may determine the differential HR-inducing activities of these autoactive proteins. In addition, VIGS analysis showed that these Cf autoactivators required the same downstream signalling components that are involved in Cf-9 signalling including CITRX, salicylic acid and the ubiquitin ligase-associated protein SGT1, indicating that these autoactive proteins signal through defence signalling pathways rather than causing a general cell toxicity associated with protein overexpression (Wulff *et al.*, 2004a).

A suppressor screen in Arabidopsis searching for signalling components functioning in NONEXPRESSOR OF PATHOGENESIS-RELATED GENES 1 (NPR1)-independent signalling identified two autoactive RLPs (Zhang *et al.*, 2010). RLP51 (also known as SNC2 for SUPPRESSOR OF NPR1-1 CONSTITUTIVE 2*)* and a close homologue RLP55 (SNC3), both contain point mutations in the conserved GXXXG motif in the transmembrane domain (Zhang *et al.*, 2010), which is also conserved among the Cf proteins, suggesting that this motif is important for the negative regulation of these RLPs. Both the *snc2* and *snc3* mutants showed dwarf morphology, accumulation of high levels of endogenous salicylic acid and enhanced resistance to the virulent oomycete *Hyaloperonospora arabidopsidis* Noco2 (Zhang *et al.*, 2010). The GxxxG motif has been implicated in homo-/heterodimerization of cell surface eLRR receptors (Zhang and Thomma, 2013). By contrast, a similar mutation in Cf-9 did not result in autoactivity but loss of function of the protein (Wulff *et al.*, 2004b), indicating different mechanisms may be involved in preventing autoactivity among these RLPs.

1.5.2 Heterologous expression of R proteins in foreign plant species

Some R proteins (including both the intracellular NB-LRR receptors and the cell surface eLRR receptors) have been reported to cause autoactivity when expressed heterologously. For instance, heterologous expression of the NB-LRR receptor RPS2 can cause an effector-independent HR in *N. benthamiana* (Day *et al.*, 2005). However, this was suppressed by co-expression of RIN4, indicating the negative regulatory role of RIN4 in RPS2-mediated defence (Day *et al.*, 2005). In another case, transient expression of the RPS4 TIR domain alone from the RPS4/RRS1 receptor pair (Section 1.2) in *N. benthamiana* has been observed to cause an AvrRps4-independent HR and this can be suppressed by co-expression of RRS1 TIR domain via heterodimerization (Williams *et al.*, 2014), suggesting that RRS1 is negatively regulating the activity of RPS4. It was proposed that RRS1 may act as the guardee of RPS4 in pathogen effector recognition, similar to the role of RIN4 in mediating pathogen recognition by RPS2 (Nishimura and Dangl, 2014). Interestingly, a similar phenomenon can also be found in the tomato eLRR Eix1/Eix2 receptor pair wherein overexpression of the Eix1 receptor attenuated Eix2-mediated signalling in response to the fungal Eix elicitor via

heterodimerization (Bar *et al.*, 2010), suggesting that Eix1 acts as a negative regulator in Eix2-mediated signalling. As the Eix elicitor has been shown to bind to both receptors (Ron and Avni, 2004), it is possible that the Eix1 receptor acts as the guardee of Eix2. However, whether the heterologous expression of Eix2 alone can cause autoactivity in tobacco remains to be demonstrated.

Transient expression of Cf-9B caused autonecrosis in *N. benthamiana* and the corresponding necrosis-inducing protein (NbNIP) recognized by Cf-9B was identified (Chakrabarti *et al.*, 2009). Similarly, heterologous expression of the Hcr9 proteins Peru1 and Peru2 from the wild tomato relative *S. peruvianum* also resulted in autonecrosis in various tobacco species including *N. tabacum* and *N. benthamiana* (Wulff *et al.*, 2004a). The recognition of NbNIP by Cf-9B is thought to be analogous to the recognition of $Rcr3^{lyc}$ by Cf-2 (Section 1.4) wherein NbNIP may be a structural mimic of its tomato homologue that mediates Cf-9B/Avr9B interaction. These examples can be related to a commonly observed phenomenon known as hybrid necrosis which occurs as a result of crosses between plants containing an *R* gene (guard) and plants containing a corresponding incompatible pathogenicity target gene (guardee) leading to aberrant activation of plant defence (Bomblies *et al.*, 2007; Spoel and Dong, 2012). Taken together, there are two hypotheses for autoactivity caused by heterologous expression of an R protein. One is the lack of an R protein guardee that act as a negative regulator in the foreign plant species and the other is the 'accidental' recognition of a structural variant (homologue) of an R protein guardee.

1.6 A tomato mutant that contains a recombinant *Hcr9* gene encoding an autoactive protein

In the transposon tagging experiment used to isolate the *Cf-9* gene, an *Avr9* transgene was used as a selection tool in crosses to tomato plants carrying *Cf-9* and a *Dissociation* (*Ds*) transposable element. Progeny containing a *Ds* insertion in *Cf-9* (thereby inactivating *Cf-9*) survived the selection whereas progeny carrying a *Ds* insertion elsewhere (and therefore containing a functional *Cf-9* gene) died (Jones *et al.*, 1994). One of the surviving progeny, designated M205, showed a distinct autoactive phenotype of stunted growth, wilting, progressive acropetal chlorosis and necrosis, and constitutive

expression of defence marker genes including *PR-1* and *PR-5* (Barker *et al.*, 2006b). Progeny testing indicated that the mutant phenotype was semidominant and Avr9-independent. These observations indicate that M205 mutant contained a gain-of-function mutation exhibiting low-level, constitutive activation of plant defence. Molecular genetic analysis revealed that M205 mutant contains an altered *Cf-9* locus arising from a transposon-induced recombination event that resulted in sequence exchange between *Cf-9* and its upstream paralogoue *Hcr9-9A* (Figure 1.5). This recombination event generated a chimeric gene designated *Hcr9-M205* which comprised an in-frame fusion between the 5' coding region of *Hcr9-9A* and the 3' coding region of *Cf-9*. Subsequently, Barker *et al.* (2006b) showed that transient expression of Hcr9-M205 protein, but not the proteins encoded by two remaining *Hcr9* genes at the *Cf-9* locus (i.e. the *Hcr9-9D* gene carrying a Ds insertion and *Hcr9-9E* as shown in Figure 1.5), caused chlorosis and accumulation of *PR-1* and *PR-5* transcripts in tobacco agroinfiltration assays, indicating that the chimeric protein is autoactive. Using a domain-swap analysis of Hcr9-M205, Anderson *et al.* (in preparation) identified three specific regions that may be responsible for the signalling activity of Cf-9. These included a signalling repression domain in LRRs 10-17 (whereby an Hcr9-9A substitution in this region allows autoactivity), a signalling activation domain (LRR 18) and a signalling enhancer domain (the loop-out region and LRRs 24-26) (see Section 5.1).

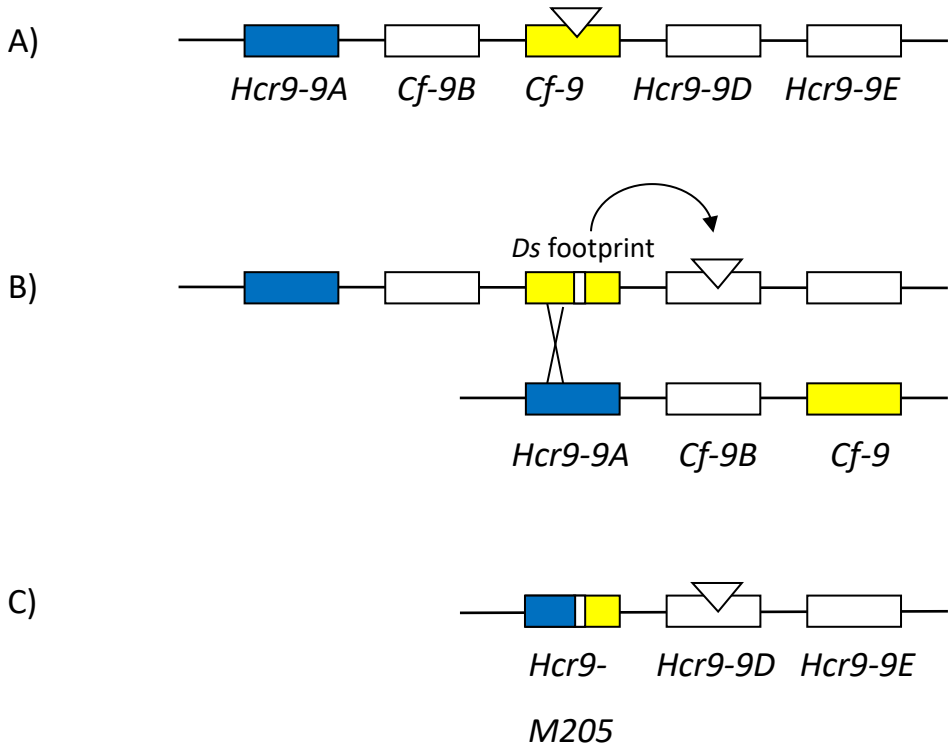

Figure 1.5 *Hcr9-M205* gene was generated by a complex transposon-induced recombination event. Data from molecular genetic analysis carried out by Barker *et al.*, (2006b) suggests the following sequence of events led to the generation of the altered *Cf-9* locus found in M205 mutant. A) The transposable element *Dissociation* (*Ds*) (indicated by an inverted triangle) first inserted into the *Cf-9* gene. B) A second transposition event involving *Ds* insertion into the adjacent *Hcr9-9D* gene occurred, leaving a footprint mutation in the *Cf-9* gene. Coincident with transposition, a homologous recombination occurred that fused *Cf-9* and its upstream paralogue *Hcr9-9A* resulting in the elimination of *Cf-9B*. C) The resulting mutated *Cf-9* locus in M205 contains three *Hcr9* genes i.e. *Hcr9-M205* encoding a chimeric 5' *Hcr9-9A–Cf-9* 3'gene, *Hcr9-9D* carrying a *Ds* insertion and *Hcr9-9E*. Figure adapted from Barker *et al.* (2006b).

1.7 Thesis aims

Analysis of the Hcr9-M205 mutant of tomato (Barker *et al.*, 2006b; Anderson *et al.*, in preparation), and of other autoactive resistance proteins, contributed to the realization that these proteins are likely being held in autoinhibitory states in the absence of pathogens (Section 1.5). More importantly, Hcr9-M205 provided a useful insight into

the nature of the autoinhibition in Cf-9 and provided a unique resource with which to investigate the phenomenon further. This knowledge would be difficult to obtain by analysis of wild type Cf-9 alone. Therefore, this thesis aimed to perform a structure-function analysis of Hcr9-M205 to unravel the underlying mechanisms of Cf-9 autoinhibition/activation. To assist in this analysis, a transgenic *PR-5* promoter: *gusA* reporter tobacco system was generated and the defence-inducible nature of this reporter examined to provide a means of making quantitative measurements of Hcr9-M205-mediated defence activation in agroinfiltration assays.

CHAPTER 2:

General Materials and Methods

2.1 DNA isolation

2.1.1 Isolation of plasmid DNA

Isolation of plasmid DNA was carried out based on the alkaline lysis method (Bimboim and Doly, 1979). A single colony of *Escherichia coli* (*E. coli*) Mach1 cells containing the plasmid of interest was inoculated from a freshly-streaked LB agar plate into 3–5 mL fresh liquid LB media (Appendix 1, Sambrook and Russell, 2001) containing appropriate antibiotics i.e. ampicillin (100 µg/mL) or kanamycin (100 µg/mL) and grown overnight at 37°C with constant shaking at 250 rpm. The cells were harvested by centrifugation at 8,000 x g for 4 min and resuspended in 250 µL Solution I (50 mM glucose, 25 mM Tris-HCl pH 8.0, 10 mM Na_2EDTA pH 8.0, 100 µg/mL RNase) by vortexing. The cells were lysed by adding 250 µL of Solution II (0.2 M NaOH, 1% (w/v) SDS), mixed several times by gentle inversion and left at room temperature for 4 min. Subsequently, 350 µL of Solution III (100 mL Solution III: 60 mL 5 M K acetate, 11.5 mL glacial acetic acid, 28.5 mL deionized water) was added and the samples were mixed by gentle inversion. The cells were centrifuged at 12,000 x g for 10 min and the supernatant was transferred to a new 1.5 mL micro-centrifuge tube. The plasmid DNA was precipitated by adding 0.6 volume isopropanol and centrifuged at 12,000 x g for 10 min. The supernatant was discarded and the pellet was washed with 70% (v/v) ethanol and air-dried at room temperature before dissolving in 50 µL deionized water. Rapid plasmid DNA isolation was performed using the AxiPrep Plasmid Miniprep kit (Axygen Biosciences) as per the manufacturer's instructions. The amount of plasmid DNA was quantified by a NanoDrop 1000 spectrophotometer (Thermo Scientific). The samples were stored at -20°C or used for molecular analyses as described in Section 2.2.

2.1.2 Genomic DNA extraction

Genomic DNA extraction was performed based on the CTAB method (Doyle, 1990) with modifications. For each sample, approximately 100 mg of leaf tissue were ground in 1 mL nuclear extraction buffer (7.5 mL nuclear lysis buffer (200 mM Tris-HCl pH 7.5, 50 mM Na_2EDTA, 2 M NaCl, 2% (w/v) CTAB), 5 mL deionized water, 0.2 g sodium bisulphite) and vortexed briefly. Subsequently, 200 µL of 5% (w/v) sarkosyl were added to the sample which was then mixed by inversion and incubated at 65°C for 20 min, then chilled on ice for 5 min. Following addition of 800 µL of phenol:

chloroform: isoamyl alcohol (25:24:1 v/v/v), the sample was vortexed and centrifuged at 16,000 x g for 15 min at room temperature. Phenol (buffer equilibrated) was obtained from Invitrogen, LifeTechnologies Australia. The supernatant was transferred to a new 1.5 mL micro-centrifuge tube and 0.6 volume of isopropanol was added. The sample was mixed by inversion and then centrifuged at 16,000 x g for 20 min at room temperature. The supernatant was discarded and the DNA pellet was washed with 70% (v/v) ethanol. The DNA pellet was allowed to air dry at room temperature and resuspended in 50 µL deionized water. The amount of DNA was quantified using a NanoDrop 1000 spectrophotometer (Thermo Scientific). The samples were then stored at -20°C or used for molecular analyses as described in Section 2.2.

2.2 Molecular cloning procedures

Molecular cloning methods were essentially performed as previously described by Sambrook and Russell (2001) unless stated otherwise.

2.2.1 PCR amplification

All PCR reactions were carried out in 200 µL polypropylene tubes using a PTC-200 Peltier Thermal Cycler (MJ Research). In general, PCR amplifications were conducted in a 20 µL reaction containing 20-50 ng of DNA template, 1 unit of Red*Taq* DNA polymerase enzyme (Sigma-Aldrich), 1x Red*Taq* buffer (Sigma-Aldrich), 200 µM of each dNTP (Bioline) and 0.5 µM of each primer. All primers were synthesized by Sigma-Aldrich or GeneWorks (Australia). Colony PCR was carried out by picking bacterial colonies grown on LB agar plates and adding a small amount directly to the PCR reaction as a template source. For PCR products that were amplified for cloning, iProof High-Fidelity (HF) DNA polymerase (Bio-Rad Laboratories) was used. The cycling parameters include an initial denaturation at 94°C for 1 min followed by 25-35 cycles of denaturation at 94°C for 30 s, primer annealing at 50-60°C (depending on the primer G and C content) for 30 s and product extension at 72°C for 1 min per kb of product. The reaction was terminated with a final extension step at 72°C for 10 min. Specific PCR conditions and cycling parameters such as a higher denaturation temperature at 98°C and a shorter product extension time of 15-30 s per kb of product

required for iProof HF DNA polymerase were carried out according to the manufacturer's recommendations. The PCR products were visualized by gel electrophoresis (Section 2.2.4) or subsequently used for TA cloning (Section 2.2.5).

2.2.2 Site-directed mutagenesis

Site-directed mutagenesis was carried out in a 50 µL reaction containing 100 ng plasmid DNA template, 2 units of iProof High-Fidelity (HF) DNA polymerase, 1x iProof HF buffer, 200 µM of each dNTP, 125 ng of each primer and 10% (v/v) DMSO. The mutagenic primers were designed using the PrimerX program available from the website http://www.bioinformatics.org/primerx/. If necessary, additional silent mutations were introduced to create or remove restriction sites to facilitate screening for successful mutations. PCR amplification was carried out using 18 cycles of denaturation at 98°C for 1 min, primer annealing at 50-60°C (depending on the primer G and C content) for 1 min and product extension at 72°C for 30 s per kb of product. The reaction was terminated by a final extension step at 72°C for 10 min. The amplification product was digested with 10 units of *Dpn*I at 37°C for 2-4 h to remove the parental DNA template. The reaction mixture was then purified by a Wizard® SV Gel and PCR Clean-Up System (Promega) and eluted in 20 µL of nuclease-free water. Four microliters of purified product were transformed into 45 µL of electrocompetent *E. coli* Mach1 cells and plated on LB agar (Appendix 1, Sambrook & Russell 2001) containing appropriate antibiotics. Plasmids were isolated from six independent colonies (Section 2.1.1) and screened for presence of the mutation by restriction digestion (Section 2.2.3). Two plasmids containing the mutation were sequenced for confirmation (Section 2.2.8).

2.2.3 Restriction digestion

Five to ten units of restriction enzyme (New England Biolab (NEB) or Promega) were added to 1 µg plasmid DNA in a 20 µL reaction containing 1x buffer (NEB or Promega) and 100 µg/ mL BSA (Promega, if required as specified by the manufacturer). The reaction was incubated at 37°C or a specific temperature required by the specific restriction enzyme for 2-4 h.

2.2.4 Gel electrophoresis and DNA gel purification

PCR products or digested DNA products were electrophoresed through a 0.8 to 1.5% (w/v) agarose (Invitrogen) gel containing 1x TAE (Appendix 1) and 1x SYBR® Safe DNA Gel Stain (Invitrogen) at 80 V for approximately 1 h. A ladder marker (Promega) was loaded into a separate lane on the gel to enable the size of the DNA fragments to be estimated. The gels were visualized using a Gel Doc^{TM} XR^{+} gel documentation system (Bio-Rad Laboratories). PCR products or digested DNA products were gel-purified using a Wizard® SV Gel and PCR Clean-Up System (Promega) according to the manufacturer's instructions.

2.2.5 TA cloning and ligation

For cloning of PCR products, gel-purified DNA (20-50 ng) (Section 2.2.4) was added into a 10 µL A-tailing reaction mixture containing 1 unit Red*Taq* DNA polymerase, 1x Red*Taq* buffer and 200 µM dATP, then incubated at 72^{o}C for 10 min prior to ligation into the pCR2.1 TA-cloning vector (Invitrogen). Ligation reactions were carried out in a total volume of 20 µL containing 50-100 ng vector DNA and insert DNA in a 1:1 to 1:3 (vector: insert molar ratio), 1 unit of T4 DNA Ligase (Fermentas) and 1x T4 DNA Ligase buffer (Fermentas). For cloning involving small vectors such as pBluescript and pCR2.1 (size of 3-3.9 kb), 50 ng of vector DNA was used, whereas 100 ng of vector DNA was used for cloning involving large vectors such as the pGREENII series of vectors (size of 6.1 kb). The reactions were incubated at 22°C overnight followed by enzyme deactivation at 65°C for 20 min. Five microliters of the reactions were used per 45 µL of electrocompetent *E. coli* cells for transformation (Section 2.2.7).

2.2.6 Preparation of electrocompetent *E. coli* Mach1 cells

Cells from a single colony of *E. coli* Mach1 grown on a freshly-streaked LB plate were inoculated into 50 mL LB liquid medium (Appendix 1, Sambrook and Russell 2001) and incubated overnight at 37°C with constant shaking at 250 rpm. Two aliquots of 500 mL pre-warmed LB liquid medium were each inoculated with 25 mL of the starter culture in two separate 2-liter flasks and incubated overnight at 37°C with constant shaking at 250 rpm until the OD_{600} reached a value of 0.6 to 0.8. The cells were chilled

on ice for 15 min and pelleted by centrifugation at 1000 x g for 15 min at 4°C. The cells were resuspended in 100 mL of sterile ice-cold deionized water and pelleted again by centrifugation. This washing step was repeated three times. After the final wash with water, the cells were resuspended in 10 mL ice-cold sterile 10% (v/v) glycerol and pelleted again by centrifugation. The cells were then resuspended in 1 mL ice-cold sterile GYT medium (10% (v/v) glycerol, 0.125% (w/v) yeast extract, 0.25% (w/v) Bacto tryptone). Aliquots of 100 µL of the suspended cells were transferred to pre-chilled 1.5 mL micro-centrifuge tubes and snap frozen in liquid nitrogen before storing at -80°C.

2.2.7 Transformation of electrocompetent *E. coli* Mach1 cells

An aliquot of 50 µL *E. coli* Mach1 cells was thawed on ice, 100 ng of plasmid (unless stated otherwise) was added and the cells were mixed gently. The cell/DNA mixture was transferred to a pre-chilled 2 mm gap electroporation cuvette (Bio-Rad Laboratories) and electroporated using a GenePulser electroporator (Bio-Rad Laboratories). The parameters used were 2.50 kV, 25 µF and 200 Ω. The cells were immediately revived by addition of 1 mL ice-cold SOC medium (Appendix 1, Sambrook and Russell 2001) and grown at 37°C with constant shaking at 250 rpm for 1.5 h. Cell aliquots of 100 µL and 200 µL were spread on LB agar plates containing the appropriate antibiotics i.e. ampicillin (100 µg/mL) or kanamycin (100 µg/mL) and incubated overnight at 37°C. Presence of the desired DNA construct in putative transformants was verified by colony PCR (Section 2.2.1).

2.2.8 DNA sequencing

Recombinant plasmids were sequenced by the Australian Genome Research Facility (AGRF), Brisbane, Australia. Samples were prepared in 10 µL reactions containing 6.4-10 pmol of each primer and 500-1000 ng plasmid DNA. The primers used were the universal M13-forward (5'-GTAAAACGACGGCCAGT-3') and M13-reverse (5'-AACAGCTATGACCATG-3') primers or gene-specific primers.

2.3 *Agrobacterium tumefaciens*-mediated transient gene expression in tobacco

All constructs were generated in a pGreenII binary vector that requires a helper plasmid pSOUP to provide replication functions *in trans* in *A. tumefaciens* (Appendix 2, Hellens *et al.*, 2000).

2.3.1 Preparation of *Agrobacterium tumefaciens* GV3101 cells

Cells from a single colony of *A. tumefaciens* GV3101 grown on a freshly-streaked LB plate were inoculated into 3 mL YEP media (Appendix 1, Sambrook & Russell 2001) containing rifampicin (50 µg/mL) and gentamycin (25 µg/mL) followed by incubation at 27°C for 36 h with constant shaking at 200 rpm. One milliliter of this starter culture was inoculated into 100 mL of YEP media containing the required antibiotics and grown overnight at 27°C with constant shaking at 200 rpm until the OD_{600} reached a value of 0.6-0.8. The cells were chilled on ice for 10 min and pelleted by centrifugation at 5,500 x g for 10 min at 4°C. The cells were resuspended in 100 mL of sterile ice-cold deionized water and pelleted again by centrifugation. This washing step was repeated three times. After the final wash with water, the cells were resuspended in 50 mL ice-cold sterile 10% (v/v) glycerol and pelleted again by centrifugation. The cells were then resuspended in 1 mL ice-cold sterile 10% (v/v) glycerol. Aliquots of 100 µL of the suspended cells were transferred to pre-chilled 1.5 mL micro-centrifuge tubes and snap frozen in liquid nitrogen before storing at -80°C.

2.3.2 Transformation of *A. tumefaciens* GV3101 by electroporation

An aliquot of 50 µL *A. tumefaciens* GV3101 cells was thawed on ice, 100 ng of a binary vector and 100 ng of pSOUP (Hellens *et al.*, 2000) were added with, and the cells were mixed gently. The cell/DNA mixture was transferred to a pre-chilled 2 mm gap electroporation cuvette (Bio-Rad Laboratories) and electroporated using the GenePulser electroporator (Bio-Rad Laboratories). The parameters used were 2.50 kV, 25 µF and 400 Ω. The cells were immediately revived by addition of 1 mL ice-cold SOC medium and grown at 27°C with constant shaking at 200 rpm for 4 h. Cell aliquots of 100 µL and 200 µL were spread on LB agar plates containing rifampicin (50 µg/mL),

gentamycin (25 µg/mL), kanamycin (100 µg/mL) and tetracycline (10 µg/mL) and were incubated at 27°C for 2-3 d. The presence of the binary vector in the transformants was verified by colony PCR (Section 2.2.1).

2.3.3 Transient gene expression in tobacco via agroinfiltration

Agroinfiltration experiments were performed based on the method described by Kapila *et al.* (1997). A single *A. tumefaciens* colony transformed with the binary vector as well as pSOUP and growing on a freshly streaked LB agar plate containing the required antibiotics was transferred to 1 mL YEP media supplemented with the same antibiotics and grown at 27°C for 16-24 h with constant shaking at 200 rpm. Two hundred microliters of this starter culture were then inoculated into 20 mL of YEP media supplemented with the appropriate antibiotics, MES pH 5.6 to a final concentration of 20 mM and acetosyringone (Sigma-Aldrich) to a final concentration of 20 µM and grown at 27°C for 16-24 h with constant shaking at 200 rpm. The cells were pelleted by centrifugation at 5,500 x g for 10 min at room temperature. The pellet was resuspended with 10-15 mL of infiltration buffer (1x MS salts (Sigma-Aldrich) pH 5.6, 10 mM MES pH 5.6, 3% (w/v) sucrose, 200 µM acetosyringone) and the OD_{600} was adjusted to 1.0 using the same buffer. Cultures were incubated at 27°C for 1.5 hr before infiltration. *Nicotiana tabacum* cv. Petit Havana or transgenic tobacco plants were grown under standard glasshouse conditions (20-24°C with ambient light and relative humidity) until two months old. Plants were watered 15-30 min prior to infiltration. The youngest fully expanded leaf, which generally corresponded to leaf five or six from the base of the plant was used for agroinfiltration. Leaf panels were infiltrated with the *A. tumefaciens* cultures through the abaxial leaf surface using a 1 mL disposable syringe without a needle. Plants were maintained under standard glasshouse conditions for the period of the experiment.

2.4 DNA gel blots

Twenty micrograms of genomic DNA were digested overnight with *Eco*RI or *Sca*I at 37°C using 1 unit of restriction enzyme per microgram of DNA. The digested DNA samples were visualized by gel electrophoresis (Section 2.2.4) in a 0.8% (w/v) agarose

gel run at a constant voltage of 30 V for 18-22 h. The gel was treated with a depurination solution (0.25 M HCl) for 15 min with slow orbital rotation, rinsed twice with deionized water and then treated with a denaturation solution (0.4 M NaOH) for 20 min with slow orbital rotation. DNA was transferred to a Hybond^{TM} N^{+} membrane (Amersham Pharmacia Biotech) by alkaline capillary transfer as described by Sambrook and Russell (2001). A DNA probe against the *nptII* sequence was generated by PCR amplification from a pCBJ306 plasmid (Appendix 2) using the nptIIF (5'-TCTGGATTCATCGACTGTGG-3') and nptIIR (5'-TGTCAAGGATCAGCTTGCAT-3') primers. The PCR product was radiolabelled with [α-^{32}P]dCTP using the oligolabelling kit (Amersham Pharmacia Biotech) according to the manufacturer's instructions. The ^{32}P-labelled DNA probe was purified using a QIAquick PCR purification kit (Qiagen) and denatured by boiling for 2 min. The membrane was pre-hybridized with 15 mL hybridization buffer (0.5 M Na_2HPO_4 pH 7.2, 7% (w/v) SDS, 1% (w/v) BSA, 1 mM Na_2EDTA pH 8.0) for 2.5-3 h at 65°C before addition of the freshly denatured probe. Hybridization was carried out overnight at 65°C. The probed membrane was washed with 30 mL wash buffer with increasing stringency (2x, 1x and 0.5x SSC (Appendix 2) with 0.1% (w/v) SDS), each for 20 min at 65°C. The membrane was air-dried then sealed in between thin plastic sheets and placed in an exposure cassette (Bio-Rad Laboratories) against a phosphorimaging screen (Kodak) for 5-7 d to allow the development of hybridization signal for detection using a Molecular Imager PharosFX™ System (Bio-Rad Laboratories).

2.5 Gene expression analysis

2.5.1 Total RNA extraction

Plant samples were snap frozen in liquid nitrogen and RNA was isolated using Trizol reagent (Invitrogen) according to the manufacturer's instructions. For each sample, approximately 100 mg of leaf tissue were ground in 1 mL Trizol reagent, mixed by vortexing and left at room temperature for 5 min. The homogenate was centrifuged at 8,000 x g for 10 min at 4°C. The supernatant was then transferred to a new 1.5 mL micro-centrifuge tube and 200 µL of chloroform were added. The sample was mixed by vortexing, left at room temperature for 5 min and centrifuged at 8,000 x g for 15 min at 4°C. The upper aqueous phase was then transferred to a new micro-centrifuge tube, 0.5

volume each of both isopropanol and a precipitating salt solution (0.8 M Na_3Citrate, 1.2 M NaCl) were added. The sample was mixed by gentle inversion, left at room temperature for 10 min and centrifuged at 8,000 x g for 30 min at 4°C. The supernatant was discarded and the RNA pellet was washed with 1 mL 70% (v/v) ethanol. The RNA pellet was allowed to semi-dry in air for 5–10 min and was then resuspended in 50 µL of RNAse-free deionized water. The amount of RNA was quantified by a NanoDrop 1000 spectrophotometer (Thermo Scientific). The samples were stored at -20°C or subsequently used for reverse transcription as described in Section 2.5.2.

2.5.2 Reverse transcription and cDNA synthesis

Total RNA was treated with DNase in a 20 µL reaction containing 2 µg RNA, 1x RQ1 RNase-Free DNase Reaction Buffer (Promega), 2 units RQ1 RNase-Free DNase (Promega) and 20 units RNaseOUT™ Recombinant RNase Inhibitor (Promega), then incubated at 30°C for 30 min followed by enzyme deactivation at 65°C for 10 min. First strand cDNA was generated in a 20 µL reaction containing 0.5 µg DNase-treated RNA, 300 ng oligo$(dT)_{12\text{-}18}$, 10 mM of each dNTP, 1x First-Strand Buffer (Invitrogen), 5 mM DTT, 20 units RNaseOUT™ Recombinant RNase Inhibitor (Promega) and 200 units SuperScript™ III reverse transcriptase (Invitrogen). Samples were incubated at 65°C for 5 min to denature the RNA before adding the reverse transcriptase. The reaction was incubated at 50°C for 1 h and terminated at 70°C for 15 min. PCR was carried out using 1 µL of the cDNA synthesis reaction per 20 µL reaction volume as described in Section 2.2.1. 'Minus-RT' (reverse transcriptase) negative control reactions were also included to check for contaminating genomic DNA in the cDNA samples. Primers NtGAPDH-F (5'- CGACTGGTGTCTTCACTGAC-3') and NtGAPDH- R (5'- CATCAACAGTTGGGACTCGG-3') were used to amplify a 426 bp product from the tobacco *glyceraldehyde-3-phosphate dehydrogenase (GAPDH)* gene (GenBank Accession number AJ133422). These primers flank an intron spliced out of the target cDNA sequence and therefore amplify a longer product (1.5 kb) from genomic DNA.

2.5.3 Quantitative real-time PCR (qRT-PCR)

qRT-PCR was carried out in triplicate for each sample in 15 µL reactions each containing 1x KAPA SYBR® FAST qPCR Master Mix (Kapa Biosystems), 200 nM of each primer and 5 µL of 1: 20 diluted cDNA. Primers E22q-F (5'-ACCCAATCAGGACTTTGTCG-3') and E22q-R (5'-AACTGTGCTGGGCATTGTTC-3') were used to amplify a 132 bp product from the *E22* gene (GenBank ID: X15224.1). Primers GUSq-F (5'-GTAATGTTCTGCGACGCTCAC-3') and GUSq-R (5'-AACGTATCCACGCCGTATTC-3') were used to amplify a 194 bp product from the *gusA* gene (GenBank ID: S69414.1). Thermal cycling was conducted in a Rotor-Gene 3000 Thermal Cycler (Corbett Research) using the cycling parameters of 95°C for 2 min followed by 40 cycles of denaturation at 95°C for 10 s, primer annealing at 60°C for 15 s and product extension at 72°C for 20 s. A subsequent melting cycle from 60°C to 95°C in 1°C increments was performed. Melt curve analysis was carried out by determining the change in peak fluorescence over time (dF/dT) to verify the specificity of amplified products. Negative control samples from the minus-RT reactions described in Section 2.5.2 were also included in the qPCR reactions. The *E22* and *gusA* gene transcript levels relative to *GAPDH* were calculated by the Comparative Quantification method using Rotor-Gene qPCR Analysis Software version 6.0 (Corbett Research), which provides quantification of the experimental gene transcript relative to the normalizing transcript by taking amplification efficiency into account.

2.6 Protein gel blots

2.6.1 SDS-Polyacrylamide Gel Electrophoresis (PAGE)

For each sample, approximately 100 mg of leaf tissue were ground in 200 µL of 3x Laemmli buffer (5 M Urea, 2% (w/v) SDS, 0.24 M Tris-HCl pH 6.8, 30% (v/v) glycerol, 16% (v/v) β-mercaptoethanol), boiled for 5 min and centrifuged at 16,000 x g for 10 min at 4°C to remove cellular debris. Protein concentration was determined by the dye-binding method of Bradford (1976) using the Bio-Rad protein assay reagent. Fifteen micrograms of total protein extract (the supernatant) for each sample were size fractionated by 5-10% SDS-PAGE (Laemmli, 1970): A stacking gel containing 5% (w/v) acrylamide/bis-acrylamide (37.5:1) (Bio-Rad Laboratories), 125 mM Tris-HCl pH

6.8, 0.1% (w/v) SDS, 0.05% (w/v) ammonium persulfate and 0.1% (v/v) tetramethylethylenediamine (TEMED) was layered on top of a resolving gel. The resolving gel contained 10% (w/v) acrylamide/bis-acrylamide (37.5:1), 375 mM Tris-HCl pH 8.8, 0.1% (w/v) SDS, 0.075% (w/v) ammonium persulfate and 0.05% (v/v) TEMED. The protein extracts were diluted 1:1 with 2 X SDS-PAGE sample buffer (125 mM Tris-HCl pH 6.8, 20% (v/v) glycerol, 4% (w/v) SDS, 10% (v/v) β-mercaptoethanol, 0.05% (w/v) bromophenol blue) and boiled for 5 min again before loading onto the gel. Electrophoresis was carried out in a 1x SDS-PAGE running buffer (25 mM Tris pH 8.3, 192 mM glycine, 1% (w/v) SDS) using a mini Protean II gel apparatus (Bio-Rad Laboratories), run at 60 V for approximately 30 min until the samples entered the resolving gel then run at 80 V for another 1.5 h at room temperature to ensure proper separation. Five microliters of Kaleidoscope^{TM} Precision Plus pre-stained molecular weight standards (Bio-Rad Laboratories) were included into the first lane of the gel for protein size estimation.

2.6.2 Western blot

Proteins were transferred from the gel onto a nitrocellulose membrane (Bio-Rad Laboratories) in 1x protein transfer buffer (25 mM Tris pH 8.3, 192 mM glycine, 20% (v/v) methanol) using the mini Protean II gel apparatus (Bio-Rad Laboratories), run at 60 V for 3 h or 20 V overnight at 4°C. Protein transfer from the gel to the membrane was confirmed by staining the membrane with 0.1% (w/v) Ponceau S (Sigma-Aldrich) in 5% (v/v) acetic acid for 5 min at room temperature with gentle agitation. Excess stain was removed by successive washes in deionized water until the lanes and bands were clearly visible. The membrane was allowed to dry and scanned using an Epson Perfection 4990 Photo scanner by inserting in between thin plastic sheets. The membrane was blocked with 5% (w/v) skim milk (Diploma Instant Skim Milk powder, Bonlac Foods Ltd, Australia) in TBST (0.5 M NaCl, 0.05% (v/v) Tween-20, 20 mM Tris-HCl pH 7.5) for 2 h by gentle agitation at room temperature and washed three times in TBST for 10 min each time. This was followed by an incubation in 10 mL of 200 ng/mL rat monoclonal anti-HA antibody clone 3F10 (Roche) in TBST with gentle agitation for 1 h at room temperature and subsequently three 10 min washes in TBST. The membrane was then incubated in 10 mL of a 1:10,000 dilution in TBST of mouse anti-rat antibody conjugated with horseradish peroxidase (Pierce) and washed three

times in TBST for 10 min each time. For protein detection, 3 mL of SuperSignal West Pico Chemiluminescent substrate (Pierce) was applied to the membrane, incubated for 5 min and excess solution was removed as per the manufacturer's instructions. The membrane was then allowed to air-dry before covering in between thin plastic sheets and exposure to X-ray film (Kodak) for 1-5 min. The film was developed using an AGFA CP1000 film processor.

2.7 β-Glucuronidase (GUS) reporter assays

2.7.1 Quantitative MUG assay

Protein was extracted from approximately 100 mg of leaf tissue ground in 200-250 μL protein extraction buffer (50 mM NaH_2PO_4 pH 7.0, 10 mM Na_2EDTA, 0.1% (v/v) Triton X-100, 0.1% (w/v) sarkosyl, 10 mM β-mercaptoethanol) followed by centrifugation at 16, 000 x g for 5 min at 4°C. GUS activity was measured at 37°C by a kinetic fluorimetric 4-methylumbelliferyl-β-glucuronide (MUG) assay based on the method described by Jefferson *et al.* (1987). Ten microliters of protein extract were mixed with 200 μL MUG substrate (2 mM MUG (Sigma-Aldrich) in the protein extraction buffer) in a 96-well microtiter plate (Thermo Scientific) and each sample was analyzed in triplicate. Fluorescence emission of 4-methylumbelliferone (MU) was measured at 455 nm following excitation at 365 nm. Measurements were taken every 2 min for up to 40 min using the Wallac 1420 Victor^{TM} fluorescence plate reader Version 2 (Perkin Elmer). GUS activity was calculated based on the resulting slope of MU fluorescence relative to the total amount of protein using Microsoft Excel. Protein concentration was determined by the dye-binding method of Bradford (1976) using the Bio-Rad protein assay reagent.

2.7.2 GUS histochemical assay

GUS histochemical assays were carried out according to the method described by Jefferson *et al.* (1987). Plant samples were fixed by vacuum infiltrating a fixative solution (0.1% (v/v) formaldehyde, 50 mM Na_2HPO_4 pH 7.0, 1 mM Na_2EDTA, 0.05% Triton X-100) for 10 min using a SpeedVac vacuum evaporator (Savant). The infiltrated samples were incubated on ice for 20 min followed by five washes in 50 mM ice cold

Na_2HPO_4 pH 7.0. Samples were then vacuum infiltrated with 5-bromo-4-chloro-3-indolyl-β-D-glucuronide (X-gluc) staining solution (1 mM X-gluc, 1 mM Na_2EDTA, 50 mM Na_2HPO_4 pH 7.0, 1 mM K ferricyanide, 1 mM K ferrocyanide, 0.05% (v/v) Triton X-100) for 10 min and incubated overnight at 37°C. X-gluc was obtained from X-Gluc Direct (ordered through www.X-gluc.com, United Kingdom). The stained materials were washed in 70% (v/v) ethanol to remove chlorophyll by gentle agitation and replacement of new solution several times until samples were decolorized. All samples subjected to the GUS histochemical staining were carried out with the fixation step unless stated otherwise.

2.8 Statistical analysis

Statistical analyses were conducted using the Genstat version 18 (licence under The Australian National University) and the data analysis function in Microsoft Excel.

CHAPTER 3:

Generation and Examination of a Quantitative Reporter for *Hcr9-M205*-mediated Defence Activation in Agroinfiltration Assays

3.1 Introduction

M205 is an autoactive mutant of tomato that exhibits a 'lesion mimic' phenotype showing a constitutive, low-level activation of plant defence including expression of *PR-1* and *PR-5* genes. Transient expression of the *Hcr9-M205* gene isolated from M205 induces chlorosis and expression of *PR-1* and *PR-5* in tobacco, indicating the gene encodes an autoactive disease resistance (R) protein (Barker *et al.*, 2006b; Section 1.6). Molecular dissection of Hcr9-M205 autoactivity provides a unique opportunity to understand the underlying mechanism of defence activation mediated by the tomato Hcr9 proteins (Chapter 5).

Agrobacterium-mediated transient gene expression, or agroinfiltration in brief, is a simple and effective method for studying the function of various plant R proteins (van der Hoorn *et al.*, 2000; Ma *et al.*, 2012; Zhang *et al.*, 2013). The conservation of the Cf-9 downstream signal transduction pathway among solanaceous plants has allowed the use of tobacco as a model plant species for a rapid study of the tomato Hcr9 proteins via transient gene expression (Hammond-Kosack *et al.*, 1998; van der Hoorn *et al.*, 2000). For example, agroinfiltration of matching *Cf/Avr* gene pairs or a number of autoactive *Hcr9* genes produced different intensities of necrotic response in tobacco, allowing comparison of the activity of the encoded R proteins (van der Hoorn *et al.*, 2000; Wulff *et al.*, 2004).

To date, assessment of R protein activity has relied mostly on visual inspection of necrosis upon agroinfiltration. However, a limitation of visual scoring of necrotic symptoms is that such a subjective qualitative assessment does not allow an objective quantitative distinction of subtle differences that involve continuous variation in the level of defence activation. Furthermore, development of necrosis is influenced by plant physiological state including leaf age and other external factors such as the environmental conditions. For example, relative humidity and temperature can influence development of necrosis (Hammond-Kosack and Jones, 1996; Hammond-Kosack *et al.*, 1996; Wang *et al.*, 2005a; Cheng *et al.*, 2013). These factors can contribute to suboptimal necrotic responses, making the assessment of defence activation based on necrotic symptoms alone less reliable. In light of the more quantitative nature of a defence gene promoter: reporter system compared to visual inspection of necrosis, a

transgenic *PR-5* promoter: *gusA* reporter tobacco system was generated in the present study to enable a more comprehensive assessment of defence activation by *Hcr9-M205* and its variants in agroinfiltration assays. Hcr9-M205 and CLB79, a domain-swap variant with low autoactivity generated by Anderson *et al.* (in preparation; see Section 5.1) were used for agroinfiltration experiments in transgenic tobacco to examine the ability of the reporter system to reflect the different levels of defence activation induced by these autoactive constructs.

3.1.1 *Pathogenesis-related (PR)* genes

First identified in tobacco mosaic virus (TMV)-infected tobacco and subsequently in many other plant species, the *pathogenesis-related* (*PR*) genes are defence-related genes induced in response to infection by various pathogens such as oomycetes, fungi, bacteria or viruses, and pest attacks (van Loon *et al.*, 2006). The products encoded by many of these genes possess antimicrobial activities that act via different mechanisms specific to the group they belong to. From five families (PR-1 to PR-5) defined initially to 17 families identified to date, the PR proteins are classified according to their amino acid sequence homology, serological relationship, cellular localization, biological activities and their induction in similar pathological or related conditions (van Loon, 1985; van Loon *et al.*, 2006).

Apart from the known inducers of biotic origin such as pathogens, insects, nematodes and herbivores, other important regulators of *PR* gene expression include the plant signalling hormones, physical stimuli such as wounding, ultraviolet (UV) light, and abiotic stresses such as drought, salinity and cold (Brederode *et al.*, 1991; van Loon, 1999; van Loon *et al.*, 2006; Pieterse *et al.*, 2012). The expression of *PR* genes also appears to occur naturally in healthy plants with constitutive expression in specific organs such as roots (Memelink *et al.*, 1990; Ohashi and Ohshima, 1992) or expression regulated by developmental cues during seed development and germination (Skadsen *et al.*, 2000), flowering (Memelink *et al.*, 1990; Neale *et al.*, 1990; van de Rhee *et al.*, 1993) or senescence (Quirino *et al.*, 1999). Van Loon *et al.* (2006) provide an excellent review about the 17 families of *PR* genes, which includes the *PR* gene of interest in this study, *PR-5*.

3.1.2 *PR-5* genes

The members of the PR-5 protein family, also known as the thaumatin-like proteins (TLPs) (due to their high amino acid sequence homology to the sweet-tasting protein thaumatin), include osmotin, osmotin-like protein, PR-R, PR-S, permatin and zeamatin (Anžlovar and Dermastia, 2003; van Loon *et al.*, 2006; Liu *et al.*, 2010). Similar to other PR proteins, PR-5 was identified in tobacco following induction by TMV infection (Cornelissen *et al.*, 1986; van Loon *et al.*, 1987; Stintzi *et al.*, 1991; Albrecht *et al.*, 1992; Koiwa *et al.*, 1994). The PR-R protein from tobacco cv. Xanthi-nc (Pierpoint *et al.*, 1987) and PR-S protein from Samsun NN tobacco (Cornelissen *et al.*, 1986; van Loon *et al.*, 1987), which were later identified as the E22 and E2 TLPs, respectively, share 95% amino acid sequence identity (van Kan *et al.*, 1989). The tobacco AP24 protein (an osmotin) was shown to inhibit the growth and development of *Phytophthora infestans in vitro* (Woloshuk *et al.*, 1991). The antifungal activity of osmotin is associated with its ability to permeabilise fungal plasma membranes (Abad *et al.*, 1996; Lee *et al.*, 2010). Some other PR-5 proteins also possess glucanase activity (Trudel *et al.*, 1998; Grenier *et al.*, 1999; Osmond *et al.*, 2001). Overexpression of *PR-5* by a transgenic approach also enhanced plant resistance to fungal infections (Datta *et al.*, 1999; Velazhahan and Muthukrishnan, 2003; Das *et al.*, 2011; Acharya *et al.*, 2012; Mahdavi *et al.*, 2012), indicating a role in disease resistance.

Promoters of osmotin and osmotin-like protein (which are basic and neutral PR-5 isoforms, respectively; see Section 4.1 on the various isoforms of PR proteins) have been well-characterized by generating transgenic plants containing promoter: reporter gene fusion (Kononowicz *et al.*, 1992; Nelson *et al.*, 1992; Zhu *et al.*, 1995a; Raghothama *et al.*, 1997). Osmotin was found to accumulate under osmotic adjustment in salt-adapted tobacco cells (Singh *et al.*, 1987; Singh *et al.*, 1989). The osmotin promoter is induced by salt stress, abscisic acid, ethylene and wounding (Neale *et al.*, 1990; Kononowicz *et al.*, 1992; LaRosa *et al.*, 1992; Nelson *et al.*, 1992; Liu *et al.*, 1995; Raghothama *et al.*, 1997). The osmotin-like protein gene is transcriptionally activated by salt stress, abscisic acid, ethylene and fungal infection (Zhu *et al.*, 1995a; Sato *et al.*, 1996). In addition, the expression of osmotin and osmotin-like protein genes was found to be spatially and developmentally regulated in healthy plants. These *PR-5* genes are constitutively expressed in roots (LaRosa *et al.*, 1992; Nelson *et al.*, 1992;

Koiwa *et al.*, 1994) and flowering organs (Neale *et al.*, 1990; Kononowicz *et al.*, 1992; Zhu *et al.*, 1995b). The E22 and E2 TLPs are both acidic isoforms. The promoter of the E2 TLP was characterized by generation of transgenic tobacco transformed with a series of promoter deletion: *gusA* reporter fusion constructs, leading to the identification of the promoter sequence involved in TMV induction (Albrecht *et al.*, 1992). Little information is currently available regarding regulation of the *E22* gene promoter except that it is induced by TMV (Cornelissen *et al.*, 1986; Pierpoint *et al.*, 1987). The *E22* promoter was chosen for the generation of transgenic *PR-5* promoter: *gusA* reporter tobacco plants as a quantitative reporter for Hcr9-M205-mediated defence activation in agroinfiltration assays (this chapter) and the defence-inducible nature of the *E22* promoter: *gusA* reporter system is examined further in Chapter 4.

3.2 Materials and methods

3.2.1 Generation of an *E22* promoter: *gusA* reporter: *E22* terminator (pCYT-1) cassette

The 5' *E22* regulatory sequence from -1051 to -4 relative to the translation start site +1 (Appendix 5) was PCR-amplified from the genomic DNA of *Nicotiana tabacum* cv. Petit Havana using an E22P-F forward primer containing a 5' terminal *Eco*RI site and an E22P-R primer containing a 3' terminal *Nde*I site (all primer sequences are listed in Table 3.1). The 1060 bp amplified product was cloned into pCR2.1 cloning vector (Life Technologies) by TA-cloning as per manufacturer's instructions to generate plasmid pE22P (Figure 3.1 A). The *gusA* reporter sequence was PCR-amplified from pSLJ10621 (Panter *et al.*, 2002) using a GusA-F forward primer containing a 5' terminal *Nde*I site and a GusA-R reverse primer. The *E22* stop codon and terminator sequence were PCR-amplified from the genomic DNA of *N. tabacum cv.* Petit Havana using an E22T-F forward primer and an E22T-R reverse primer containing a 3' terminal *Xba*I site. The 1812 bp *gusA* reporter and 540 bp *E22* terminator fragments were fused by PCR overlap extension based on the method described by Heckman and Pease, (2007). The *gusA* reporter: *E22* terminator fusion gene was then cloned into pCR2.1 vector to generate plasmid pGUS:E22T (Figure 3.1 B). The inserts in pE22P and pGUS:E22T were verified by DNA sequencing. Plasmid pCBJ306, a derivative binary vector of pGREENII (Appendix 2) generated by Chakrabarti et al. (2005) (Figure 3.1 C) was used as the recipient binary vector to generate binary vector pCYT-1. A three-way ligation was used to assemble the *Eco*RI/*Nde*I digested *E22* promoter fragment from pE22P, the *Nde*I/*Xba*I digested *gusA*: *E22* terminator fragment from pGUS:E22T and *Eco*RI/*Xba*I digested pCBJ306 to generate the binary vector pCYT-1 containing the *E22* promoter: *gusA* reporter: *E22* terminator cassette (Figure 3.1 D), which also eliminated the 35S promoter sequence from the T-DNA region of pCBJ306.

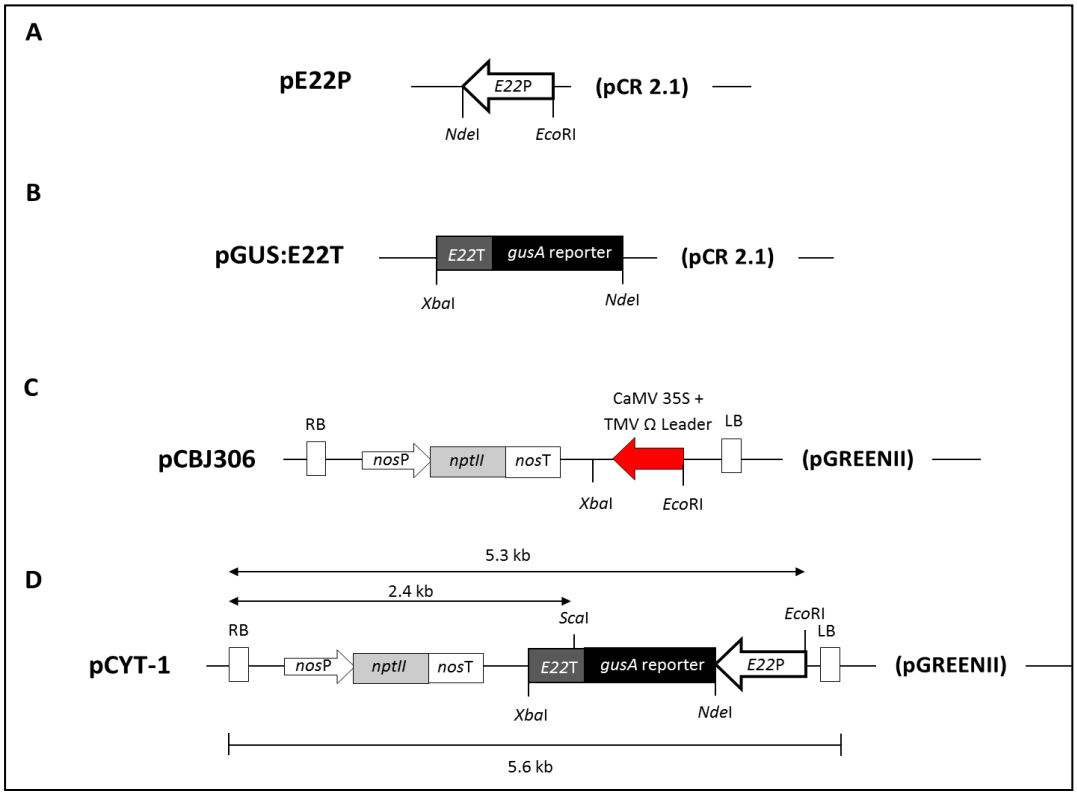

Figure 3.1 Diagrammatic representation of the intermediate plasmids involved in the generation of the pCYT-1 binary vector containing an *E22* promoter (*E22*P): *gusA* reporter: *E22* terminator (*E22*T) cassette. pE22P (A) and pGUS:E22T (B) are plasmids containing the *E22* promoter and *gusA* reporter-*E22* terminator fusion gene cloned into the pCR2.1 vector, respectively. pCBJ306 (C) is a derivative of the pGREEN II binary vector generated by Chakrabarti (2005). (D) Features of the pCYT-1 binary vector. LB and RB represent left and right borders of the T-DNA region. The T-DNA region contains the neomycin phosphotransferase (*nptII*) selectable marker gene for tobacco transformation. The positions of the nopaline synthase (*nos*) promoter (*nos*P) and terminator (*nos*T) are indicated. Positions of the restriction sites involved in cloning and DNA gel-blot analysis are shown. The distances of the restriction sites used in DNA gel-blot analysis from the RB are indicated. Size of the T-DNA region is 5.6 kb. Arrows indicate the direction of transcription. Drawings are not to scale.

Table 3.1 Primers used for generation of an *E22* promoter: *gusA* reporter: *E22*

Primers	Sequence 5'→3'	Restriction sites
E22P-F	GAATTCGGACTCCCAAATCACTATG	*Eco*RI
E22P-R	CATATGTTTTTTCTTTTTGTAAACTTGAG	*Nde*I
GusA-F	CATATGTTACGTCCTGTAGAAACC	*Nde*I
GusA-R	GTCATAATTTTGCAGGCTTCAATTTCATTGT TTGCCTCCCTGCTGCGG	-
E22T-F	CCGCAGCAGGGAGGCAAACAATGAAATTG AAGCCTGCAAAATTATGAC	-
E22T-R	TCTAGAGGTATTCTTCCAAGTCAGTTTAATG TG	*Xba*I

terminator (pCYT-1) cassette. Nucleotides encoding restriction sites are underlined.

3.2.2 Growth of tobacco seedlings in tissue culture

Tobacco seeds were soaked in 70% (v/v) ethanol for 2 min and disinfected in 10% (v/v) Domestos^{TM} (Lever Rexona) for 10 min before being washed three times in sterile water. The disinfected seeds were germinated on tobacco seedling media (TSM) containing 1 X MS salts (Sigma-Aldrich) pH 5.8, 1% (w/v) glucose and 2 g/L Gelrite^{TM} Gellan Gum (Sigma-Aldrich) and seedlings grown under a 16-hr light/8-hr dark photoperiod at 25°C. Four-week-old seedlings were used for tobacco transformation.

3.2.3 A*grobacterium*-mediated transformation of tobacco

Tobacco seedling leaf disks were transformed using the method of Horsch *et al.* (1985) with some modifications. A single colony of *A. tumefaciens* GV3101 transformed with pCYT-1 and pSOUP was inoculated into 15 mL YEP medium containing rifampicin (50 µg/mL), gentamycin (25 µg/mL), kanamycin (100 µg/mL), tetracycline (10 µg/mL), 20 mM MES, pH 5.7 and 20 µM acetosyringone, and incubated at 27°C for 16-24 h with constant shaking at 200 rpm. The cells were pelleted then resuspended in a solution of 1x MS salts (pH 5.7) containing 200 µM acetosyringone and the bacterial concentration adjusted to OD_{600} = 1.0. Leaves from 4-week-old Petit Havana tobacco seedlings grown in tissue culture were cut into approximately 1 cm^2 sections using a sterile scalpel and

submerged into the *Agrobacterium* suspension in Petri dishes for 5 min. The leaf sections were dried on filter paper, placed on tobacco regeneration media (TRM) containing 1x MS pH 5.7, 1x B5 Vitamins (Sigma-Aldrich), 3 mM MES, 3% (w/v) Sucrose and 0.2% (w/v) Gelrite, with the leaves adaxial face down and incubated at 25°C in darkness for 2-3 days. The explants were then transferred to TRM supplemented with 0.1 mg/L NAA, 1.0 mg/L BAP, 200 mg/L timentin and 200 mg/L kanamycin with the leaves adaxial face up to induce callus and shoot formation. Explants were transferred to fresh regeneration media every two weeks. In 3-4 weeks, developing shoots were excised from kanamycin resistant calli and placed on TRM supplemented with 0.1 mg/L NAA, 200 mg/L Timentin and 200 mg/L kanamycin to induce rooting. Multiple shoots cut from the same explant were considered to be clones of the same transgenic event until further verification by DNA gel-blot analysis and were labelled with the same event designation. For example, two shoots excised from explant number 3 were designated 3A and 3B. When the roots were approximately 2 cm long, plantlets were transferred to sterilized rehydrated Jiffy compressed-peat pots (4Seasons Seeds, Australia) in sealed plastic tubs containing water and grown under a 16-hr light/8-hr dark photoperiod at 25°C. When roots emerged from the Jiffy pots, plants were transferred to potting mix, given slow release fertilizer (Osmocote^{TM}, Scotts) and grown in a glasshouse. The primary transformants (T_1) were grown to flowering stage and allowed to self-pollinate to produce T_2 seeds.

3.2.4 Screening for homozygous transgenic *E22*: *gusA* reporter tobacco lines

T_2 transgenic tobacco seeds collected from the self-pollinated primary transformants of *E22*: *gusA* reporter (pCYT-1) tobacco lines were disinfected as described in Section 3.2.2. Approximately 100 seeds per line were germinated on TSM supplemented with 200 mg/L kanamycin and grown under a 16-hr light/8-hr dark photoperiod at 25°C. At four weeks post selection on kanamycin, the number of kanamycin resistant and sensitive seedlings for each transgenic line was recorded. Chi-square (χ^2) goodness-of-fit tests to known Mendelian ratios were used to analyse the observed segregation ratios to determine whether the transgenic lines carried single or multiple transgene loci. The χ^2 values were calculated on expected 3:1, 15:1 or 63:1 ratios using the formula (a-

$3b)^2/3n$, $(a-15b)^2/15n$ or $(a-63b)^2/63n$, respectively (a = number of antibiotic resistant seedlings, b = number of antibiotic sensitive seedlings and n = total number of seedlings tested). One degree of freedom and a 95% level of significance were used for all tests. To identify at least one homozygous line that produces 100% kanamycin resistant T_3 seedlings, nine or 45 kanamycin resistant T_2 plants were grown to maturity and self-pollinated for lines containing one or two transgene loci, respectively. T_3 seedlings were selected for kanamycin resistance as described above.

3.2.5 Constructs used for induction of the *E22*: *gusA* reporter

p802 is a plasmid expressing the coding region of the CLB79 domain swap and the *Cf-9* 3' UTR under the constitutive 35S promoter in the pBluescript SK+ vector (Figure 3.2). See Section 5.2.1 for the details of plasmid HA-Hcr9-M205. Plasmid HA-CLB79 was generated by substituting the coding region of CLB79 and *Cf-9* 3' UTR from plasmid p802 into HA-Hcr9-M205 through *Bst*AP1 and *Not*I sites (Figure 3.2). Plasmid pCBJ310 expressing the coding region and 3' UTR of *Cf-9* under the 35S promoter was generated by Chakrabarti (2005) (see Section 5.2.1). CLB18 is a plasmid expressing the coding region and 3' UTR of *Hcr9-M205* under the 35S promoter in the pCBJ10 binary vector (Figure 3.2). See Appendix 2 for details of pCBJ306 (empty vector).

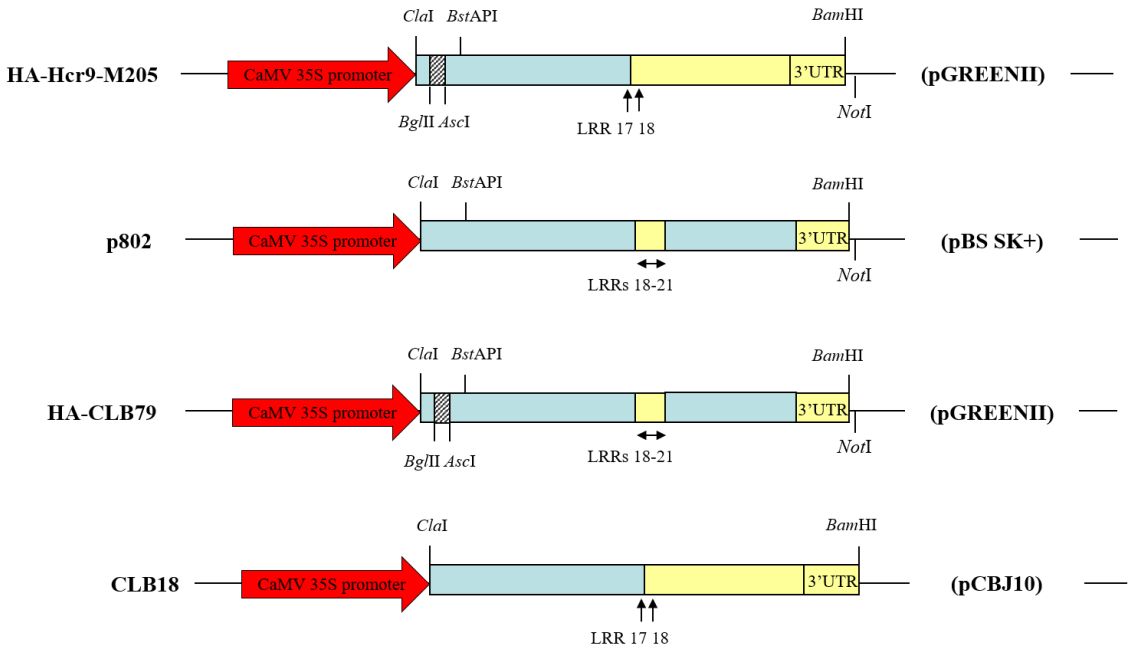

Figure 3.2 Constructs used for induction of the *E22*: *gusA* reporter. Plasmid HA-Hcr9-M205 was generated as described in Section 5.2.1. Plasmids p802 and CLB18 (Anderson *et al*., in preparation) were obtained from Dr Claire Anderson (Research School of Biology, The Australian National University). Plasmid HA-CLB79 was generated by substituting the *Bst*API-*Not*I fragment from plasmid p802 into HA-Hcr9-M205. All constructs were expressed under the constitutive CaMV 35S promoter. Blue, yellow and grey bars represent Hcr9-9A, Cf-9 and 3x HA tag sequences, respectively. 3' UTR = 3' untranslated region. Only restriction sites of interest are shown. The location of the junctions between Cf-9 and Hcr9-9A are indicated relative to specific LRRs. pBS SK+ = pBluescript SK+. See Appendix 2 for details of the pGREENII binary vector. The pCBJ10 binary vector is a derivative of pSLJ7292 (http://www.jic.bbsrc.ac.uk/sainsbury-lab/jj/plasmid.html) generated by insertion of a 1.4 kb *Eco*RI-*Bam*HI fragment containing the CaMV 35S promoter and omega leader sequence fragment from pSLJ10122 (Benghezal *et al.*, 2000) between the *Eco*RI and *Bam*HI sites of the pSLJ7292 polylinker. Drawings are not to scale.

3.3 Results

3.3.1 Generation of *E22*: *gusA* reporter (pCYT-1) primary transformants

To generate *E22*: *gusA* reporter (pCYT-1) transgenic tobacco plants containing the *E22* promoter: *gusA* reporter: *E22* terminator T-DNA construct, a total of 85 tobacco leaf disks were transformed with *A. tumefaciens* containing the pCYT-1 and pSOUP plasmids as described in Section 3.2.3 in two independent transformation experiments (Table 3.2). After four to six weeks on kanamycin selection, 16 antibiotic resistant explants (nine explants from the first transformation experiment and seven from the second) appeared healthy and formed calli and shoots. For the kanamycin resistant explants that generated more than one shoot, each shoot was grown to a whole plant by transferring onto rooting media and was not treated as an independent transformant until verification by DNA gel-blot analysis (Section 3.3.3). Among the 16 kanamycin resistant explants, two transformants were derived from explant numbers 3, 20 and 30 (and were thus labelled as 3A, 3B, 20A, 20B, 30A and 30B) and four transformants were derived from explant number 16 (and thus were designated as 16A to D), generating a total of 22 kanamycin resistant plants (Table 3.2). PCR amplification using the *GusA*-F and *E22*T primers (Table 3.1) confirmed the presence of the *E22* promoter: *gusA* reporter: *E22* terminator transgene in 12 transformants (3B, 9 and 14 from the first transformation experiment and 16A, 16B, 16C, 16D, 20A, 20B, 24, 30A and 30B from the second transformation experiment) (Table 3.2). To verify integration of the T-DNA construct into the host genome and to determine the pattern and number of independent transgene insertions, these PCR positive transformants were subjected to DNA gel-blot analysis (Section 3.3.3).

Table 3.2 Generation of tobacco primary transformants containing the *E22* promoter: *gusA* reporter: *E22* 3'UTR (pCYT-1) T-DNA transgene.

Transformation experiment	Number of explants	Number of kanamycin resistant plants generated (number of kanamycin resistant explants)	Number of PCR positive transformants (number of kanamycin resistant explants)	Number of independent transgenic lines verified by DNA gel-blot analysis
1	28	10(9)	3(3)	3
2	57	12(7)	9(4)	6
Total	85	22(16)	12(7)	9

3.3.2 Segregation analysis of T_2 progeny

All PCR positive transformants were grown to flowering stage and allowed to self-pollinate to produce T_2 progeny. The segregation for kanamycin resistance (R) or sensitivity (S) of T_2 seedlings in each independent transgenic line is summarized in Table 3.3. From the chi-square (χ^2) tests, the T_2 seedlings of lines 3B, 16B, 20A, 20B, 24, 30A and 30B appeared to segregate in a 3:1 (R:S) ratio among approximately 100 seedlings germinated for each line, indicating that these lines may carry a single T-DNA locus. In contrast, lines 9 and 14 segregated in a 15:1 (R:S) ratio among a total of at least 170 seedlings germinated for each line, indicating that these lines may contain two T-DNA loci. Line 24 was discarded as only 16 resistant T_2 seedlings were recovered in 100 seedlings germinated. This line may carry a weakly-expressing transgene locus wherein most seedlings were not able to survive under selection by 200 mg/L kanamycin.

Line	Number of seedlings tested	Number of resistant (R) seedlings	Number of sensitive (S) seedlings	χ^2 (3:1)	χ^2 (15:1)
3B	100	77	23	*0.21	47.88
9	170	163	7	39.54	*1.32
14	239	223	16	42.71	*0.08
16B	99	75	24	*0.03	54.70
20A	97	75	22	*0.28	44.69
20B	110	86	24	*0.59	45.50
24	100	16	84	n.d.	n.d.
30A	120	97	23	*2.18	34.17
30B	108	75	33	*1.78	108.89

Table 3.3 Segregation analysis of the self-progenies (T_2) of independent transgenic *E22* promoter: *gusA* reporter: *E22* 3'UTR (pCYT-1) tobacco lines under selection for kanamycin resistance. Chi-square (χ^2) tests with one degree of freedom have a rejection value greater than 3.84 at p = 0.05 (Peck and Devore, 2011). χ^2 values marked with asterisks (for those with the values of less than 3.84) indicate that the observed kanamycin resistance (R) to sensitivity (S) ratio fits the expected ratio of 3:1 or 15:1 for one or two T-DNA loci, respectively. Line 24 was discarded as only 16 resistant T_2 seedlings were generated out of 100. n.d. = not determined

In addition, lines 3B, 9 and 14 from the first transformation experiment were crossed to wild type tobacco (*N. tabacum*) to generate test cross progenies (TC_1) for segregation analysis (Table 3.4). From the chi-square (χ^2) tests, TC_1 plants for line 3B appeared to segregate in a 1:1 (R:S) ratio, consistent with the T_2 segregation suggesting a single T-DNA locus. However, TC_1 segregation for line 9 fit a 7:1 (R:S) ratio, suggesting that this line may contain three T-DNA loci, which is inconsistent with the results from the T_2 segregation suggesting two transgene loci. The T_2 segregation for line 9 (163:7 (R:S), Table 3.3) was also tested for a three locus segregation i.e. a 63:1 (R:S) ratio. While the χ^2 value did not fit this ratio, it is worth noting that a 165:5 (R:S) ratio would have fit a 3 locus model and that 163:7 (R:S) is not far off and the small number of sensitives expected has a disproportionate effect on the χ^2 value. Perhaps more T_2 seeds for line 9 could have been germinated for a more reliable interpretation for the T_2 segregation. However, line 9 was not used for subsequent study as it clearly contained more than one transgene locus. The segregation ratio for TC_1 plants of line 14 was inconclusive as it did not fit into any of the expected segregation ratios for one, two or three transgene loci. However, the 3:1 segregation ratio gave the lowest χ^2 value suggesting a two locus model gave the best fit, consistent with the conclusion reached from the T_2 data.

Line	Number of seedlings tested	Number of resistant (R) seedlings	Number of sensitive (S) seedlings	χ^2 (1:1)	χ^2 (3:1)	χ^2 (7:1)
3B	112	58	54	*0.14	32.19	130.61
9	245	218	27	148.90	25.54	*0.49
14	123	80	43	11.13	6.51	56.73

Table 3.4 Segregation analysis of the test cross progenies (TC_1) of independent transgenic *E22* promoter: *gusA* reporter: *E22* 3'UTR (pCYT-1) tobacco lines under selection for kanamycin resistance. Chi-square (χ^2) tests with one degree of freedom have a rejection value greater than 3.84 at p = 0.05 (Peck and Devore, 2011). χ^2 values marked with asterisks (for those with the values of less than 3.84) indicate that the observed kanamycin resistance (R) to sensitivity (S) ratio fits the expected ratio of 1:1, 3:1 or 7:1 ratio for one, two or three T-DNA loci, respectively.

To identify a homozygous line for each of the independent transgenic lines generated, the T_2 plants for each line except for lines 9 and 24 were self-pollinated to generate T_3

seeds. For this purpose, nine kanamycin resistant T_2 plants for each of the lines predicted to carry a single locus (i.e. lines 3B, 16b, 20a, 20b, 30a and 30b) and 45 kanamycin resistant T_2 plants for line 14 predicted to carry two transgene loci were self-pollinated. A homozygous T_2 plant that produced 100 % kanamycin resistant T_3 seedlings was identified for each line with a single T-DNA insertion locus and the T_3 seeds were used for subsequent experiments. Homozygous lines for each of the two T-DNA insertion loci present in line 14 were identified as described in Section 3.3.3.

3.3.3 Characterization of pCYT-1 tobacco transformants by DNA gel-blot analysis

For lines 3B and 14 generated in the first transformation experiment, leaf tissues from T_2 plants were used for DNA gel-blot analysis as leaf tissues from the primary transformants were not collected for these lines. As shown in Figure 3.3, all nine kanamycin resistant T_2 progeny from line 3B showed identical hybridization patterns in the DNA blots, consistent with a single T-DNA insertion locus. In addition, the multiple bands found in the blot of *Sca*I-digested DNA (Figure 3.3, right panel) suggest that this line contained multiple T-DNA insertions. By contrast, the kanamycin resistant T_2 plants of line 14 segregated into three different progeny classes as shown in Figure 3.4. The first progeny class consisted of ten plants that appeared to carry a single transgene copy which produced a band of approximately 2.5 kb following *Sca*I digestion. The second progeny class consisted of three plants that appeared to carry a tandem repeat of the transgene which produced two bands, one with an approximate size of the T-DNA fragment (5.6 kb; Figure 3.1) and the other with an approximate size of 10 kb following *Sca*I digestion. The third progeny class consisted of 33 plants that appeared to carry both T-DNA insertion loci. The segregation of hybridization banding patterns found on the DNA gel blots for these T_2 plants corroborates the segregation data obtained for kanamycin resistance suggesting two T-DNA insertion loci (described in Section 3.3.2 above). Among the T_2 segregants, plants 8 and 2 from the first and second progeny classes, respectively, produced 100% kanamycin resistant T_3 seedlings and were therefore identified as homozygous lines for each of the two T-DNA insertion loci present in line 14. These plants were designated lines 14(8) and 14(2) and were used in subsequent studies.

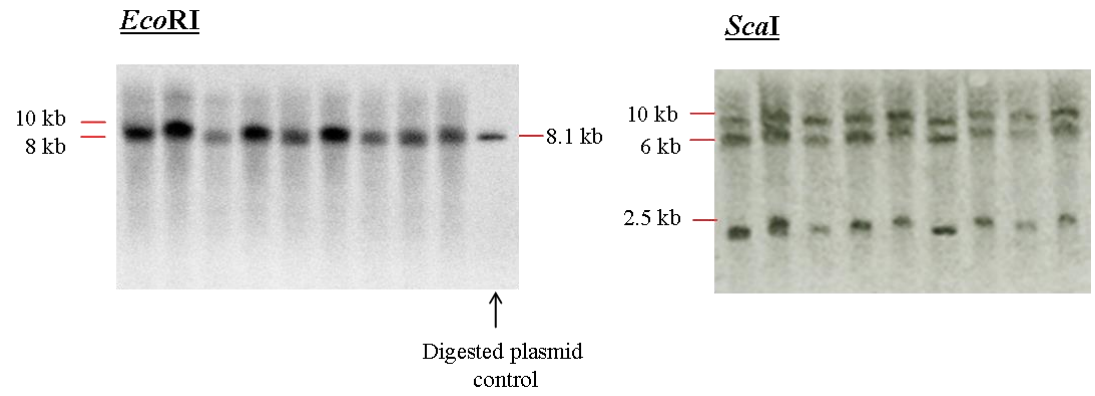

Figure 3.3 DNA gel blots of nine T_2 kanamycin resistant transgenic pCYT-1 tobacco plants for line 3B. 20 µg genomic DNA were digested with *Eco*RI or *Sca*I and hybridized with an *nptII* gene-specific probe. Locations of the restriction sites and the *nptII* gene in the T-DNA cassette are indicated in Figure 3.1. Positions of size markers are indicated to the left of each blot. *EcoR*I digested pCYT-1, with a known product size of 8.1 kb, was included in the *Eco*RI blot.

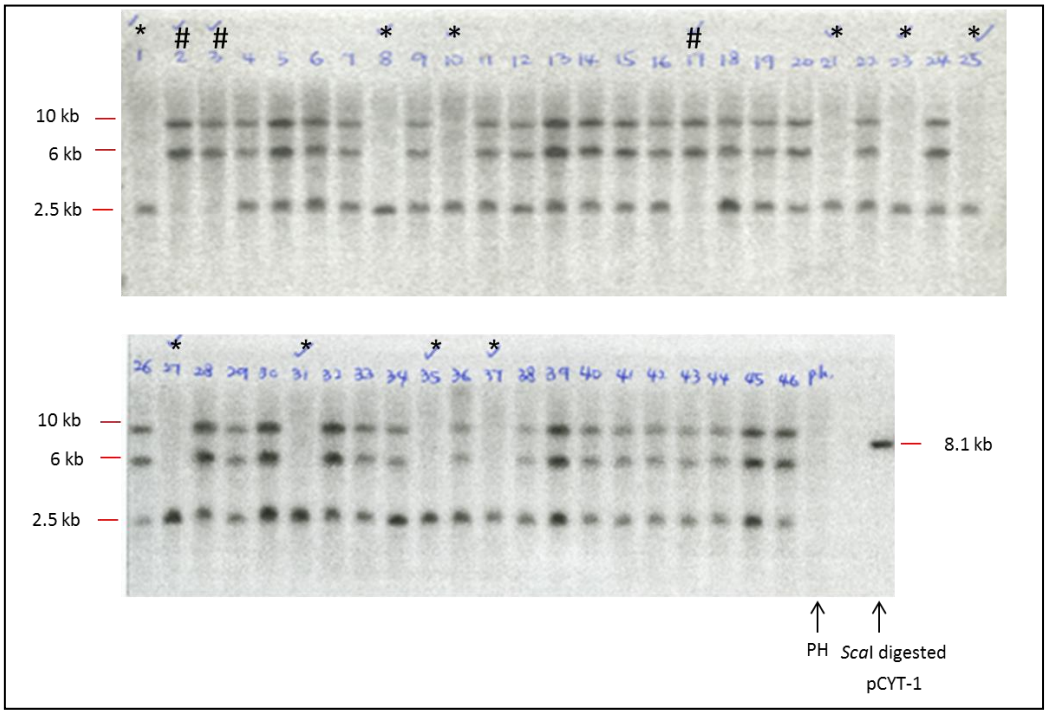

Figure 3.4 DNA gel blots showing segregation of 46 T_2 kanamycin resistant transgenic pCYT-1 tobacco plants for line 14. 20 µg of genomic DNA were digested with *Sca*I and hybridized with an *nptII* gene-specific probe. Locations of the restriction sites and the *nptII* gene in the T-DNA cassette are indicated in Figure 3.1.The number assigned to each plant is indicated at the top of each lane. PH: Genomic DNA from wild type *N. tabacum* cv. Petit Havana. Positions of sizes markers are indicated to the left of each blot. *Sca*I digested pCYT-1 with a known product size of 8.1 kb was included. The T_2 plants segregated into three different progeny classes. The first progeny class consisted of ten plants (indicated by asterisks) showing only a band of approximately 2.5 kb following *Sca*I digestion. The second progeny class consisted of three plants (indicated by hash tags) showing two bands with approximate sizes of 5.6 kb and 10 kb following *Sca*I digestion. The third progeny class consisted of 33 plants showing all three bands.

The DNA blots for each of the T_1 plants for lines 16A, 16B, 16C, 16D, 20A, 20B, 24, 30A and 30B generated from the second transformation experiment are shown in Figure 3.5. All four primary transformants (16A-D) for line 16 produced identical hybridization patterns in both *Eco*RI and *Sca*I digested DNA gel blots, indicating that these transformants were derived from the same T-DNA integration event. Therefore, only line 16B was used for subsequent study. By contrast, the two primary transformants generated from each of explants 20 (20A and 20B) and 30 (30A and 30B) produced different hybridization patterns in the DNA blots, indicating that these transformants were generated by independent insertion events despite being generated from the same explant. Altogether, there were a total of nine transgenic lines with independent insertion events, namely, lines 3B, 9, 14, 16B, 20A, 20B, 24, 30A and 30B generated from 85 tobacco explants used for transformation (Table 3.3). By including the two T_2 segregants obtained from line 14 i.e. lines 14(2) and 14(8), which carry different T-DNA insertions, this gave a total of ten independent transgenic lines generated in this study.

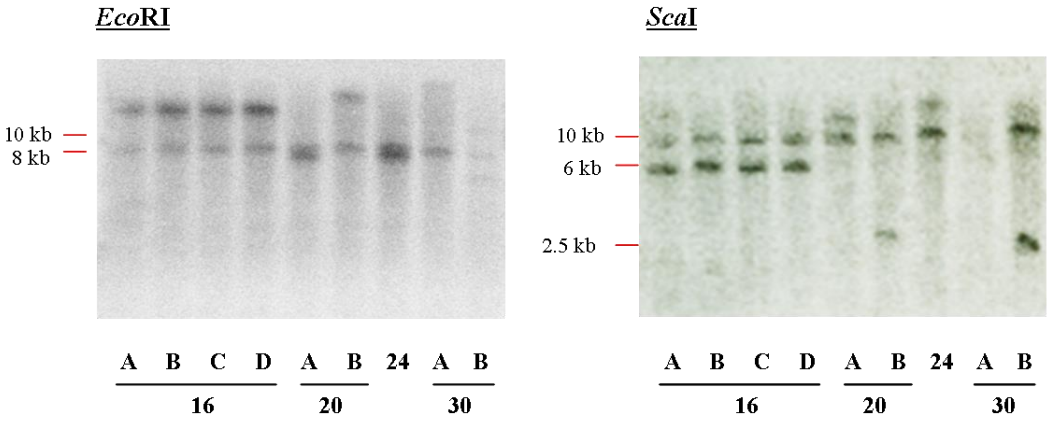

Figure 3.5 DNA gel blots of pCYT-1 primary transformants for lines 16B, 20A, 20B, 24, 30A and 30B. Genomic DNA (20 µg) was digested with *Eco*RI and *Sca*I and hybridized with *nptII* gene-specific probe. Positions of size markers are indicated to the left of each blot.

3.3.4 Selection of candidate transgenic lines for quantitative measurement of *Hcr9-M205*-mediated defence activation

To identify a suitable *E22*: *gusA* reporter line that could be used for quantifying *Hcr9-M205*-mediated defence activation in agroinfiltration assays, agroinfiltration of *Hcr9-M205* and *CLB79* (a domain swap derivative of *Hcr9-M205* shown to induce a low level of autoactivity by Anderson *et al.* (in preparation); Section 5.1), as well as *Cf-9* and empty vector (EV) controls was carried out to screen for the induction of GUS activity among the transgenic *E22*: *gusA* reporter lines 3B, 14(2), 14(8), 16B, 20A, 20B, 30A and 30B. *Hcr9-M205*, *CLB79* and *Cf-9* were expressed under the constitutive CaMV 35S promoter in the pGREENII binary vector and contain 3x HA epitope tag sequences at the 5' end of the regions encoding their mature N-termini (Section 3.2.5, Figure 3.2). *CLB79* was included in these experiments to examine the response of the *E22*: *gusA* reporter across a full range of autoactivity/necrosis induction. *CLB18* is a non-HA-tagged version of *Hcr9-M205* expressed by the 35S promoter in the pCBJ10 binary vector (Anderson *et al.*, in preparation; Section 3.2.5). In this section, the prefix 'HA' was added to Hcr9-M205 to differentiate it from CLB18, which does not contain a 3x HA tag. The same annotation also applied to the equivalent HA-tagged version of CLB79.

In preliminary experiments, lines 14(2) and 14(8) showed the highest fold induction of GUS activity by CLB18 or HA-Hcr9-M205 relative to the empty vector (Figure 3.6, Appendices 3 and 4). Interestingly, while the amplitude of GUS activity in line 14(8) was much lower compared to line 14(2) (Figure 3.6A), both lines 14(2) and 14(8) showed more than a three-fold induction by CLB18 or HA-Hcr9-M205 relative to empty vector (Figure 3.6B). By contrast, HA-Hcr9-M205 induced only a 1.5 to 2.5 fold greater GUS activity relative to the empty vector in lines 16B, 20A, 20B, 30A and 30B (Appendices 3 and 4). Importantly, GUS activity was barely detectable or at a very low level in uninfiltrated (healthy) or buffer infiltrated leaves in all transgenic lines tested (Figure 3.6, Appendices 3 and 4, data not shown for line 3B), indicating that the *E22* promoter was not induced by infiltration of the resuspension buffer alone. However, GUS activity was induced by agroinfiltration of the empty vector in all transgenic lines, indicating that the *E22* promoter is induced by *Agrobacterium* (Figure 3.6, Appendix 3). GUS activity induced by HA-Hcr9-M205 was lower compared to CLB18 (Figure 3.6). This could be due to reduced activity in HA-Hcr9-M205 caused by the presence of

epitope tag on the protein (van der Hoorn *et al.*, 2005) and/or by differences in the binary vector backbones of these two constructs, which might result in different levels of transgene expression and therefore protein production.

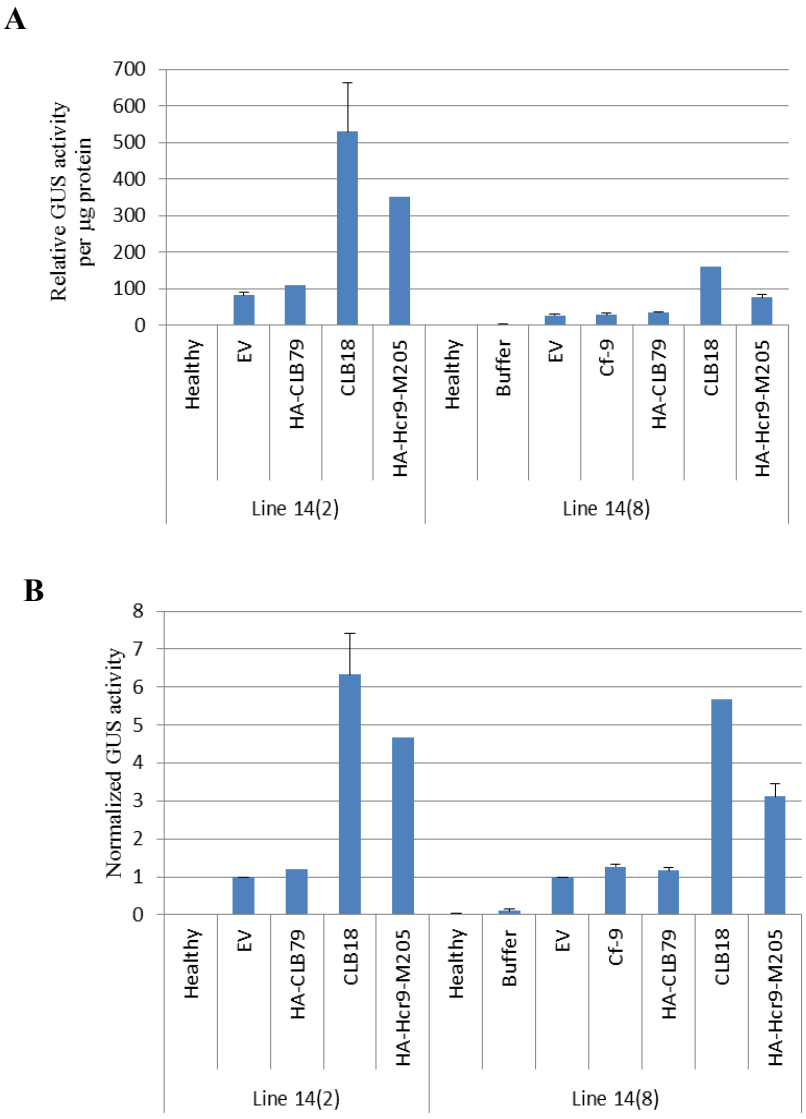

Figure 3.6 GUS activity induced by agroinfiltration of defence-activating constructs in transgenic pCYT-1 tobacco lines 14(8) and 14(2) at 5 dpi (days post infiltration). A) GUS activity measured by MUG assay in homogenates from five infiltrated leaf panels (combined together), one from each of five different plants for each construct. HA-CLB79, CLB18 and HA-Hcr9-M205 are defence-activating constructs obtained from Anderson *et al.* (in preparation) (Section 3.2.5). Cf-9 and resuspension buffer controls were included for line 14(8). Empty vector = EV, healthy = uninfiltrated leaf panels. Experiments were repeated at least twice but not with all constructs. HA-CLB79 and HA-Hcr9-M205 were only tested in one experiment for line

14(2) whereas CLB18 was tested in only one experiment for line 14(8). Error bars represent standard error (n ≥ 2 experiments). **B)** Normalized GUS activity relative to empty vector control from independent experiments (n ≥ 2) carried out in **(A)**.

Given the greater induction shown by lines 14(2) and 14(8), the choice of candidate transgenic line for further use in this study was between lines 14(2) and 14(8). However, induction of GUS activity in line 14(2) by the Hcr9-M205 domain swaps was inconsistent in subsequent studies (data not shown) and therefore, line 14(8) was selected for further analysis.

3.3.5 Induction of the *E22*: GUS reporter by Hcr9-M205 and its domain swap derivative CLB79 in a time course analysis

The induction of GUS activity by Hcr9-M205 and its domain swap derivative CLB79 in *E22*: *gusA* reporter tobacco was examined over three-day intervals following agroinfiltration. To examine whether the induction of GUS activity was consistent with expression of the endogenous *E22* gene and the *gusA* reporter gene, the induction of the *E22* and *gusA* genes was also investigated by quantitative RT-PCR. Infiltration of buffer alone did not induce any significant increase in GUS activity or *E22*/*gusA* transcript accumulation (Figure 3.7) and no significant induction was detected in non-infiltrated leaf panels from the same leaves (data not shown). Over the time course, Cf-9 induced lower levels of GUS activity or *E22*/*gusA* transcript accumulation similar to the empty vector (EV) control. In contrast, Hcr9-M205 and CLB79 induced much higher levels of GUS activity or *E22*/*gusA* transcript accumulation compared to the Cf-9 and EV controls (Figure 3.7).

Induction of GUS activity, or *E22*/*gusA* transcription by Hcr9-M205 and CLB79 were compared to examine the effectiveness of these measurements in detecting differences in induction by these defence-activating constructs. GUS activity induced by Hcr9-M205 was significantly higher than that induced by CLB79 at 3 dpi ($P < 0.05$) but not at later time points (Figure 3.7A). GUS activity increased substantially over time, probably due to accumulation of GUS protein (Jefferson *et al.*, 1987; Weinmann *et al.*, 1994). However, despite the lower GUS activity at 3 dpi, GUS activity induced by

Hcr9-M205 and CLB79 was 2.5 and 1.8 fold higher relative to Cf-9, respectively. In contrast, induction of the *E22* gene was highest at the early time points and decreased gradually thereafter (Figure 3.7B). *E22* gene transcript levels induced by Hcr9-M205 were significantly higher compared to those induced by CLB79 at 3 and 6 dpi ($P < 0.05$). At 3 dpi, the *E22* transcript levels induced by Hcr9-M205 and CLB79 were 2.1 and 1.6 fold higher relative to Cf-9, respectively, and 1.9 and 1.5 fold higher, respectively, at 6 dpi. The induction of *gusA* gene expression was similar to that of the *E22* gene (Figure 3.7C). *gusA* transcript levels induced by Hcr9-M205 were significantly higher than those for CLB79 at both 3 and 6 dpi ($P < 0.05$). At 3 dpi, *gusA* transcript levels induced by Hcr9-M205 and CLB79 were 3 and 2.1 fold higher relative to Cf-9, and reduced to 2.2 and 1.6 fold higher at 6 dpi, respectively. However, whereas the induction of the *E22* transcripts showed a marked decrease between 6 and 9 dpi (Figure 3.7B), the induction of *gusA* transcripts declined steadily from 3 to 12 dpi (Figure 3.7C). The detection of significant differences in the induction of *E22* and *gusA* transcript levels up to 6 dpi compared to only 3 dpi for GUS activity may reflect the greater sensitivity in detection of gene transcripts by RT-PCR compared to quantification of GUS activity by MUG enzymatic assays. Nevertheless, the greater differential induction of GUS activity by Hcr9-M205 and CLB79 at 3 dpi was in agreement with the transcript data for the *E22* and *gusA* genes indicating greater differential induction by the defence-activating constructs at the earliest sampling point of the time course i.e. at 3 dpi.

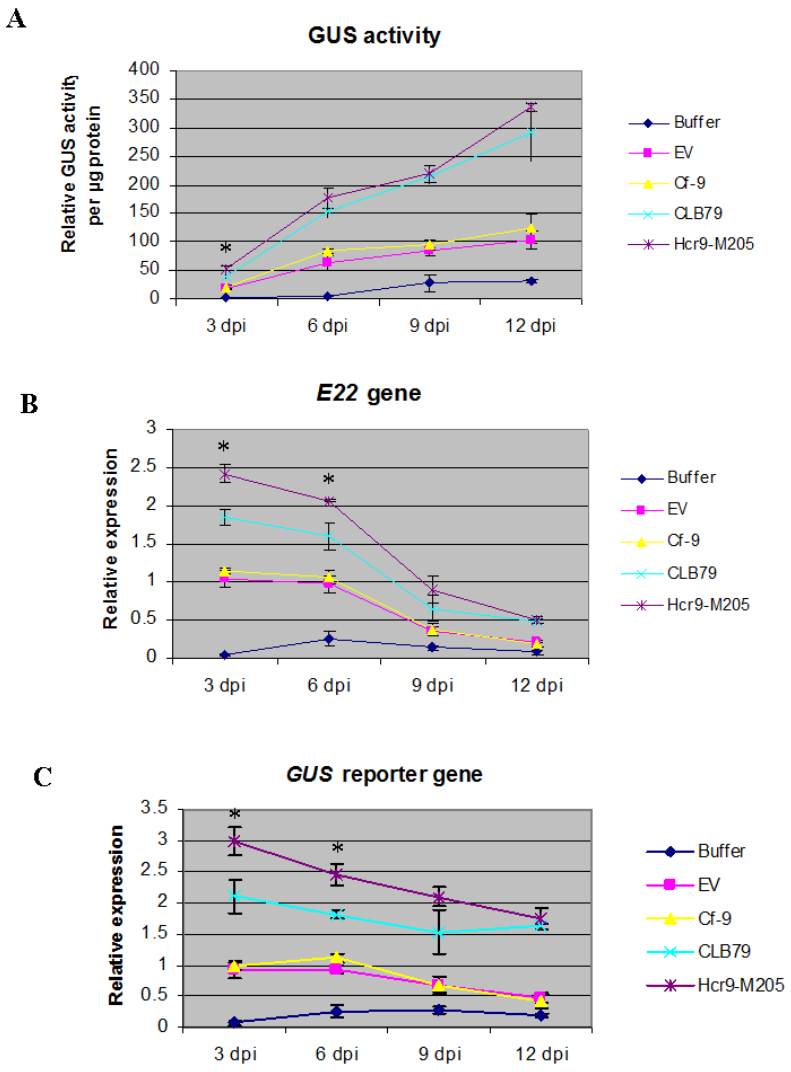

Figure 3.7 Time-course analysis comparing A) GUS activity B) expression of the endogenous *E22* gene and C) expression of the *gusA* reporter gene induced by agroinfiltration of selected defence-activating constructs at 3, 6, 9 and 12 dpi (days post infiltration). MUG assays and real-time quantitative reverse-transcriptase PCR analysis were carried out in homogenates of five infiltrated leaf panels (combined together), one from each of five different plants for each construct at each time point. Hcr9-M205 and CLB79 were obtained from Anderson *et al.* (in preparation). Agrobacterium resuspension buffer, empty vector (EV) and Cf-9 controls were included in these experiments. Relative gene expression was normalized to that of glyceraldehyde phosphate-3-dehydrogenase (GAPDH). Error bars represent the standard error in replicates from three independent experiments (n= 3, a total of 3 x 5 plants were used). Asterisks indicate significant differences ($P < 0.05$) in GUS activity or transcript levels induced by Hcr9-M205 compared to CLB79 as determined by Student's *t*-test.

3.3.6 Protein expression of Hcr9-M205 and domain swap CLB79

To confirm the expression of the selected constructs following agroinfiltration of transgenic pCYT-1 tobacco, protein expression was examined by protein immunoblot analysis using a 3x HA (hemagglutinin) epitope tag sequence engineered into the N-terminal region of the encoded protein (Section 3.2.5). Cf-9, Hcr9-M205 and CLB79 proteins were detected at 2 dpi (Figure 3.8). These data confirmed the expression of the epitope-tagged proteins prior to the induction of GUS activity measured at 3 dpi (Section 3.3.5).

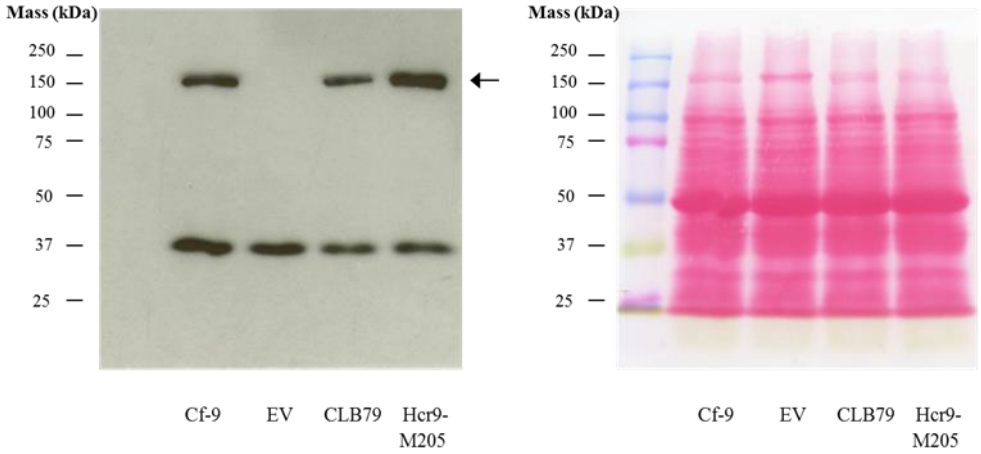

Figure 3.8 Protein immunoblot showing expression of 3x HA tagged Cf-9, domain swap CLB79 and Hcr9-M205 proteins at 2 dpi (days post infiltration) following *Agrobacterium*-mediated transient gene expression in *N. tabacum*. 20 μg of each total protein extract were size-separated by 10% SDS-PAGE. Left panel shows chemiluminescence detection of the HA-tagged Hcr9 proteins with an approximate size of 160 kDa (indicated by arrow) using rat anti-HA primary antibody (Roche) and mouse horseradish peroxidase-conjugated anti-rat secondary antibody (Pierce). No 160 kDa protein was detected in the empty vector (EV) control lane confirming the specificity of the anti-HA antibody for the expressed proteins. The presence of an additional band of approximately 37 kDa is probably due to non-specific binding of the primary or secondary antibody, which was also found in uninfiltrated tobacco leaves (data not shown). Right panel represents the loading control by Ponceau S staining of total proteins electroblotted onto a nitrocellulose membrane (Bio-Rad). A Kaleidoscope™ Precision Plus pre-stained molecular weight standard (Bio-Rad) was included in the first lane for protein size estimation.

3.4 Discussion

This study aimed to generate a quantitative reporter system for measuring plant defence activation by transient expression of the Hcr9-M205 protein and its domain swap variants in agroinfiltration assays. Independent transgenic tobacco lines carrying an *E22* promoter:*gusA* reporter construct were generated and tested with a range of defence activating and control constructs. Although these lines were not tested using *A. tumefaciens* GV3101 lacking a binary empty vector, the similar level of reporter induction by Cf-9 and EV controls suggests that there was a background level of activation by Agrobacterium per se in all lines. GUS activity induced by defence-activating constructs was therefore normalized to the empty vector control to allow comparisons between transgenic lines and between GUS activities triggered by various defence-activating constructs. The defence-activating constructs tested in this study each induced different amplitudes of GUS activity in the various transgenic lines tested (Section 3.3.4). These differences could be attributed to factors such as positional effects, transgene copy number, changes in the transgene organization following transgene integration or somaclonal variation occurring during transformant regeneration (Bhat and Srinivasan, 2002; Gelvin, 2003; Filipecki and Malepszy, 2006). Positional effects refer to the location of the T-DNA insertion in the host genome whereby insertions into or near a heterochromatic region may reduce transgene expression, whereas insertions into the vicinity of enhancer elements may elevate transgene expression. On the other hand, the effect of transgene copy number on the differences in GUS activity induced between transgenic lines could be exemplified by the much higher amplitude of GUS activity induced by line 14(2) carrying tandem T-DNA insertions compared to line 14(8) carrying a single T-DNA insertion (Section 3.3.3). Multiple copies of the *E22* promoter: *gusA* reporter fusion in the tandem repeat could potentially contribute to higher levels production of GUS protein following defence activation. The molecular characterization and screening of the *E22*: *gusA* reporter tobacco lines by agroinfiltration of Hcr9-M205 led to the choice of line 14(8) which carries a single transgene insertion and showed the greatest fold induction of GUS activity.

The time-course analysis measuring the induction of GUS activity and *E22* and *gusA* transcript levels indicated greater differential induction by Hcr9-M205 and CLB79 in all three measurements at the earliest sampling point of the time course (Figure 3.7). The

decreased differential induction at later stages could be due to decreased promoter responsiveness over time e.g. as a result of feedback inhibition. Early induction of defence-related genes has also been found to occur in an elicitor-dependent manner in other studies. For example, induction of the acidic chitinase and glucanase genes in incompatible tomato-*Cladosporium fulvum* interactions is highest at 4 days post inoculation, consistent with the production of the race-specific elicitor by the fungus (van den Ackerveken *et al.*, 1992; van Kan *et al.*, 1992). However, induction of *PR* gene expression by direct injection of Avr9 peptide into *Cf-9*-expressing tomato occurs much quicker i.e. within 6-24 hours of injection (Wubben *et al.*, 1996; van den Burg *et al.*, 2008). Therefore, the early induction of GUS activity and *E22/gusA* expression by agroinfiltration of the autoactive Hcr9-M205 protein is likely dependent on protein expression mediated by Agrobacterium-mediated transient transformation. The higher level of *E22* and *gusA* gene transcription during the early stage of the time course may be attributed to the higher level of protein expression mediated by agroinfiltration prior to post-transcriptional gene silencing (PTGS) that takes place at 3-4 dpi (Johansen and Carrington, 2001; Voinnet *et al.*, 2003). PTGS is a gene silencing mechanism against expression of foreign genes such as transgene expression mediated by Agrobacterium transformation or virus infection in plants (Johansen and Carrington, 2001; Vaucheret *et al.*, 2001). The differential induction of GUS activity at 3 dpi (Figure 3.7A) was consistent with detection of the proteins produced by the defence-activating constructs at 2-3 dpi (Figure 3.8). Taken together, the data from the time-course analysis showing greater differential induction and high-level induction of *E22/gusA* gene expression during the early stage following agroinfiltration suggest that 3 dpi would be best for measurement of GUS activity.

Co-expression of the *Cf-9/Avr9* gene pair by agroinfiltration resulted in necrosis at approximately 2-3 dpi (data not shown; van der Hoorn *et al.*, 2000) whereas necrosis induced by agroinfiltration of Hcr9-M205 occurred at approximately 5 dpi (data not shown, Section 5.3). The delayed induction of necrosis following GUS activity at 3 dpi was probably due to the weak signalling activity of Hcr9-M205 (Barker *et al.*, 2006b). Early induction preceding cell death has also been noted for other defence-related genes (van Kan *et al.*, 1992; Pontier *et al.*, 1994; Gopalan *et al.*, 1996a; Wubben *et al.*, 1996). For example, the tobacco *HSR203J* (HYPERSENSITIVITY RELATED 203J) and *HIN1* (HARPIN INDUCED 1) are specifically induced within 3-6 hours following

pathogen inoculation i.e. several hours before the appearance of HR lesions (Pontier *et al.*, 1994; Gopalan *et al.*, 1996a). The early induction of genes encoding the tomato apoplastic chitinase and glucanase and the accumulation of these proteins correlate with the inhibition of *C. fulvum* growth (Wubben *et al.*, 1996). Taken together, the early induction of defence-related genes such as the induction of *E22* promoter by Hcr9-M205 demonstrated in this study provides an early indication of defence activation without requiring prior induction of cell death.

The defence-related molecules such as ROS, nitric oxide (NO) and salicylic acid (SA) are important regulators of defence gene expression and cell death (Shirasu and Schulze-Lefert, 2000). For example, ROS has been reported to induce several defence-related genes including *PR-1*, glucanase and the pathogen-induced oxygenase (Castresana *et al.*, 1990; Green and Fluhr, 1995; Sanz *et al.*, 1998). However, induction of cell death may require concerted action of several defence-related signals. Whereas ROS alone are sufficient to induce defence gene expression (Levine *et al.*, 1994; Jabs *et al.*, 1997), induction of cell death requires synergistic action between ROS and NO or SA (Shirasu *et al.*, 1997; Delledonne *et al.*, 2001). Furthermore, the induction of cell death may be a consequence of escalation of signalling and/or accumulation of defence-related compounds to high concentration that may be toxic to plant cells (Hammond-Kosack and Jones, 1996; Coll *et al.*, 2011). The remaining high level of *E22* gene transcription (Figure 3.7B) during the onset of cell death at 5 dpi induced by agroinfiltration of Hcr9-M205 suggests that a continuous defence activation state or signalling input may be involved in the activation of cell death. For example, prolonged activation of MAP kinases is required for the induction of cell death (Zhang and Klessig, 1998; Zhang *et al.*, 2000). Overall, induction of defence gene expression and cell death may involve different thresholds depending on the amplitude and duration of exposure to defence-activating signals (Shirasu and Schulze-Lefert, 2000). The higher amplitude and longer duration required in the induction of cell death may serve as a regulatory mechanism in the induction of these defence responses whereby cell death is activated only when necessary.

3.4.1 *PR-5* may be a defence-activation marker specifically suited for infiltration experiments

Barker (2002) investigated the induction of three candidate defence marker genes for Hcr9-M205-mediated defence activation in tobacco agroinfiltration assays namely *PR-1a* (Ward *et al.*, 1991; Uknes *et al.*, 1993), *HSR203J* (Pontier *et al.*, 1998; Pontier *et al.*, 1999) and *AP24* (that encodes a basic PR-5 protein) (Singh *et al.*, 1989; Kononowicz *et al.*, 1992; Nelson *et al.*, 1992). Among these marker genes, *AP24* showed a strong and specific induction to Cf-9/Avr9-induced defence response without an apparent background response induced by infiltration of buffer, which was found in *PR-1a* and *HSR203J*. The induction of these defence genes by infiltration may be attributed to general stress-related responses associated with infiltration such as wounding or flooding. For example, the basic chitinase and glucanase genes of tomato are induced by infiltration of water (Ashfield *et al.*, 1994). As the basic *PR* genes are induced by wounding (Memelink *et al.*, 1990; Brederode *et al.*, 1991), it is possible that the induction of these genes by infiltration was due to wounding. However, Barker (2002) showed not only that the basic *PR-5*, *AP24* is not induced by infiltration, but counterintuitively, that *PR-1a* is induced by infiltration of buffer, which is unexpected for an acidic *PR* gene if the induction was due to wounding. These contradictory findings suggest that the inference that the infiltration-related induction of these defence-related genes is caused by wounding might not be valid.

On the other hand, Durrant *et al.* (2000) demonstrated that the cell death-specific marker genes *HSR203J* and *HIN1* are induced in tobacco by infiltration of water or buffer containing $MgCl_2$ or $MgSO_4$ but not by cutting, indicating that the induction of these genes was a response to flooding but not wounding. Thus, the same could be true for the induction of other defence-related genes by infiltration, including the induction of *PR-1a* observed by Barker (2002). In contrast, *PR-5* (both *E22* and *AP24)* are not induced by infiltration (this study; Barker, 2002) and this seems to be specific to *PR-5* amongst other defence-related genes. One possible explanation is that different defence-related genes may be induced by flooding to different extents wherein some are more inducible than another. However, it is possible that this characteristic may be related to the water stress tolerance property of *PR-5* (Singh *et al.*, 1987; Rajam *et al.*, 2007; Liu *et al.*, 2010; Munis *et al.*, 2010; Singh *et al.*, 2013; Weber *et al.*, 2014).

Despite the potential application of *E22:gusA* as a specific marker in infiltration experiments, the induction of the *E22* promoter by Agrobacterium seems to be unavoidable. Similar to the induction of *E22* gene transcription by Agrobacterium found in the present study, agroinfiltration also induces other defence-related genes including *PR-1* and other defence responses such as callose deposition, ROS production and activation of MAP kinases (Djamei *et al.*, 2007; Pruss *et al.*, 2008; Santos-Rosa *et al.*, 2008; van Verk *et al.*, 2008; Rico *et al.*, 2010; Sheikh *et al.*, 2014). These studies indicate that disarmed strains of Agrobacterium can induce host defence responses. Evidence supporting the notion that disarmed strains of Agrobacterium induce host defences also stems from the findings that agroinfiltration in tobacco leaves protects against subsequent pathogen infections accompanied by expression of *PR-1* (Pruss *et al.*, 2008; Rico *et al.*, 2010; Sheikh *et al.*, 2014), similar to that found following infiltration with *E. coli* (Pruss *et al.*, 2008). The induction of host defence by agroinfiltration may be caused by specific components present in *Agrobacterium* such as the cold shock protein which can act as MAMPs that trigger defence activation in solanaceous plants (Felix and Boller, 2003). Interestingly, Sheikh *et al.*, (2014) demonstrated that induction of host defence responses by agroinfiltration is in part caused by activation of cytokinin signalling due to the trans-zeatin synthase (*tzs*) gene present in the Ti plasmid of nopaline-producing Agrobacterium strain GV3101. In contrast, use of the octopine-producing Agrobacterium strain LBA4404 which lacks a *tzs* gene induces a much lower level of background response. This finding suggests that LAB4404 or an alternative strain of Agrobacterium that induces lower background response may be a potential solution to the problem of induction of the *E22* promoter by Agrobacterium that could perhaps improve the agroinfiltration assays based on the *E22*: *gusA* tobacco generated in the present study.

3.4.2 Advantages and limitations of the *E22*: *gusA* reporter system

The present study demonstrated the development and application of a quantitative reporter system for Hcr9-M205-mediated defence activation in agroinfiltration assays via measurement of induced GUS activity. The fluorometric GUS assay or MUG assay is a simple yet reliable method which is widely used in plant molecular analysis (Jefferson *et al.*, 1987). In this assay, GUS activity is measured quantitatively with high sensitivity by supplying the substrate i.e. 4-MUG (4-Methylumbelliferyl-β-D-glucuronide) for β-glucuronidase enzymatic reactions. This can be carried out in microtiter plates using a fluorescence plate reader, which is useful for simultaneous measurement of GUS activity for a large number of samples and is therefore time efficient. Measurement of GUS activity in the *E22*: *gusA* reporter tobacco allows a consistent quantification of plant defence activation expressed in terms of GUS activity and enables the use of statistical analysis for comparisons between the activities of different R protein constructs.

The early induction of GUS activity by Hcr9-M205 in this study provides an example of early detection of defence activation without relying on the visible necrotic/chlorotic symptoms that appear later. This reporter system could therefore be useful for other R proteins that exhibit weak levels of defence activation resulting in a reduced or delayed cell death response. Further, as the induction of GUS activity does not require prior induction of cell death, this reporter system allows detection of defence activation that does not involve cell death or it has been inhibited in suboptimal environmental conditions (Hammond-Kosack *et al.*, 1996). Therefore, the *E22*: *gusA* reporter system offers an advantage over other quantitative methods that rely on the occurrence of cell death such as electrolyte leakage and accumulation of autofluorescent compounds (Bennett *et al.*, 1996; Zhang *et al.*, 2004). Similar to the early induction of the *E22* promoter, changes in some plant physiological responses such as reduced photosynthetic capacity and local temperature rise can also be detected prior to the development of disease symptoms. These changes could be visualized and quantified by fluorescence imaging methods such as chlorophyll fluorescence and thermography (Chaerle *et al.*, 1999; Chaerle and van der Straeten, 2000). These methods allow live imaging and can therefore provide ongoing measurement of defence activation in a non-destructive manner. The advantage of the live imaging method over *in vitro* GUS assays

is that it does not require the labour-intensive and time-consuming procedures involved in sample preparation such as grinding of tissue samples and protein extraction. Nevertheless, live imaging methods require specialized robotic set-up in controlled environmental conditions and are therefore costly.

Another possible limitation of the present system is that cell death may reduce GUS activity (Gopalan *et al.*, 1996b; Obregón *et al.*, 2001) and this may interfere with the measurement of GUS activity in leaves undergoing necrosis. Based on the measurement of GUS activity in the time-course analysis, the effects of cell death on GUS activity may be minimal as GUS activity increased substantially at later time points after the onset of cell death but this does not exclude a limited reduction of GUS activity which may have contributed in part to the smaller differential induction at later time points. Hence, it would be best to measure GUS activity before the onset of cell death to avoid any possible effects of cell death on GUS activity. While protein expression of Hcr9-M205 was detected at 2 dpi, differential induction of GUS activity by Hcr9-M205 to approximately 2.5-3 fold higher than that for Cf-9 was only detected at 2.5 dpi (Section 5.3), suggesting a possible half-day lag for induction of GUS activity following protein expression. In this respect, a compromise may require measurements to be taken as soon as GUS activity is induced following transgene expression and before the onset of cell death and 2.5 dpi would perhaps be an ideal time point.

The *E22*: *gusA* tobacco line could possibly be used to quantify defence activation induced by autoactive derivatives of other R proteins or wild type R proteins by co-expression with their cognate Avr proteins via agroinfiltrations. Furthermore, this may also include screening of potential pathogen elicitors of tobacco via infiltration (either expressed via Agrobacterium–mediated transformation or in the form of a solution containing the elicitor) and identification of the cognate candidate host receptor proteins in tobacco. The availability of the draft genome of tobacco and *N. benthamiana* (Bombarely *et al.*, 2012; Sierro *et al.*, 2014) as well as an *E22*: *gusA* reporter for quantification of defence activation would enhance the use of tobacco in plant-microbe interaction research. In addition, the present study demonstrating the application of transgenic plants containing a defence gene promoter: reporter construct as a tool for quantification of plant defence activation provides a further proof-of-concept for

application in other plant species as documented previously (Shapiro and Zhang, 2001). The *E22*: *gusA* tobacco may allow other applications related to quantification of plant defence activation including screening of potential plant defence elicitors. The next chapter (Chapter 4) describes the application of the *E22*: *gusA* tobacco for screening of inducers/repressors of plant defence by adapting the leaf disk assays to a multi-well plate set-up.

CHAPTER 4:

Transcriptional Regulation of a Tobacco *Pathogenesis-Related (PR) 5* Gene in Plant Defence Signalling

4.1 Introduction

Chapter 3 described the generation and assessment of the transgenic *E22* promoter: *GUS* tobacco system for use as a quantitative tool in measuring defence activation mediated by Hcr9-M205 domain swaps in agroinfiltration assays. In contrast to other members of the *Pathogenesis-Related (PR) 5* gene family such as the osmotin and osmotin-like protein genes, little has been learnt about the transcriptional regulation of the *E22* gene since its identification by van Kan *et al.* (1989) apart from the knowledge that its expression is induced by Tobacco Mosaic Virus and the gene encodes an acidic PR-5 protein.

The five extensively studied *PR-1* to *PR-5* gene families encode proteins consisting of both acidic and basic isoforms, which are grouped according to the isoelectric point (*p*I), subcellular localization and biological activities of these proteins (Memelink *et al.*, 1990; Brederode *et al.,* 1991; Ohashi and Ohshima, 1992; Niki *et al.,* 1998). The amino acid sequences of these proteins have been demonstrated to determine the subcellular localization of the different PR isoforms. Generally, the acidic PR proteins are secreted into the extracellular space between plant cells and this is determined by an N-terminal signal peptide sequence whereas their basic counterparts contain an extended C-terminal pro-peptide sequence that targets these proteins to the vacuole (Melchers *et al.*, 1993). Interestingly, the acidic and basic PR proteins have been shown to exhibit distinct patterns of expression in response to *PR* gene regulators. Typically, expression of the acidic *PR* genes is strongly up-regulated by the salicylic acid (SA) pathway but less so the jasmonic acid/ethylene (JA/ET) pathway and wounding, whereas the basic *PR* genes are significantly induced by the JA/ET pathway and wounding but not the SA pathway and these regulators are mutually antagonistic (Niki *et al.*, 1998; Després *et al.*, 2003). The interplay between the SA and the JA/ET signalling pathways has been demonstrated to regulate plant response to different types of pathogens. Overall, the SA pathway is involved in the induction of plant defence against pathogens adopting a biotrophic lifestyle whereas the JA/ET pathway is activated in response to herbivores, chewing insects and necrotrophic pathogens (Glazebrook, 2005). The current view of plant defence is that the SA and JA/ET pathways form the backbone of plant defence signalling while other signalling molecules such as cytokinin (CK), abscisic acid (ABA), auxin and brassinosteroid can augment or repress signalling regulated by these two major pathways (Bari and Jones, 2009; Pieterse *et al.*, 2009). Furthermore, the basic *PR*

genes but not the acidic ones are often expressed constitutively in specific organs and tissues or during specific stages of plant development (Memelink *et al.*, 1990; Neale *et al.*, 1990; Ohashi and Ohshima, 1992; Zhu *et al.*, 1995b).

To date, little information about the *E22* promoter is known except that it is induced by tobacco mosaic virus infection (Cornelissen *et al.*, 1986; Pierpoint *et al.*, 1987). In this chapter, various aspects of *E22* promoter function in response to plant defence signalling were investigated. Organ- and tissue-specific expression and developmental regulation of the promoter were first examined in healthy transgenic *E22* promoter: *gusA* reporter tobacco plants. Subsequently, tobacco leaf disk assays were adapted to study the induction of the *E22* promoter: *gusA* reporter by the known *PR* gene regulators such as wounding and various plant defence signalling molecules including SA, JA, ET and CK, thereby unravelling the plant defence signalling pathways involved in activation of this reporter system. The regulation of *E22* promoter by salt stress (a common inducer of *PR-5* genes including the osmotin and the osmotin-like protein genes) was also investigated. The studies carried out in this chapter corroborate the defence-inducible nature of the *E22*: *gusA* reporter.

4.2 Materials and Methods

4.2.1 Promoter sequence analysis and identification of *cis*-acting elements

Identification of *cis*-acting elements was carried out by searching the 1048 bp *E22* promoter sequence (Appendix 5) against the plant promoter databases PLACE (URL : http://www.dna.affrc.go.jp/PLACE/) (Higo *et al.*, 1998) and PlantCARE (URL: http://bioinformatics.psb.ugent.be/webtools/plantcare/html/) (Lescot *et al.*, 2002).

4.2.2 Tobacco leaf disk assays

Leaf disks were punched from the youngest fully expanded leaves of 2.5-month old transgenic *E22* promoter: *gusA* reporter (pCYT-1) tobacco plants of line 14(8) (described in Chapter 3) using a cork borer with a diameter of 1.3 cm. This generally corresponds to leaf five and six as numbered from the base. Three leaf disks, one from each of three different plants, were collected and incubated with 7.5 mL solutions of chemical inducers (phytohormones or NaCl, Table 4.1) at specific concentrations with the lower (abaxial) surface up in 9.6 cm^2 wells of Nunc^{TM} 6-well plates (Thermo Scientific). Leaf disks were incubated at 25°C under fluorescent white light with light intensity of approximately 180 µmol m^{-2} s^{-1} in a 16 h light: 8 h dark photoperiod. Following incubation, chemical-treated leaf disks were briefly dried on a paper towel and collected into a 2 mL microfuge tube, snap frozen in liquid nitrogen and stored at -80°C. MUG assays were carried out on leaf samples homogenized using mini polypropylene pellet pestles (Sigma-Aldrich) as described in Section 2.7.1. Each experiment was repeated three times.

Chemical	Solvent	Stock concentration	Working concentration
Salicylic acid (SA, pH 7.0)	Water	2 mM	5, 50, 200 & 1000 μM
Methyl jasmonate (MeJA)	Water	100 μM	1, 5, 20 & 50 μM
Ethephon	Water	10 mM	1 mM
6-benzylaminopurine (BAP)	1 M NaOH	1 mM (10 mM NaOH)	100 μM (1 mM NaOH)
NaCl	Water	1 M	50 mM

Table 4.1 Preparation of phytohormone or salt solutions. All chemicals were obtained from Sigma-Aldrich except NaCl was obtained from Merck. The stock solution of salicylic acid (SA) was adjusted to pH 7.0 using 1 M KOH. Water was used as a negative control for SA, MeJA, ethephon and NaCl treatments. 1 mM NaOH was used as a negative control for BAP treatment. Stock solutions for phytohormones were stored at -20°C.

4.3 Results

4.3.1 Structure and sequence analysis of the *E22* promoter and E22 protein

Using bioinformatics tools currently available for promoter analysis, the *E22* promoter sequence was analysed *in silico* to identify known promoter elements and gain a picture about the possible transcriptional regulation of the *E22* promoter especially with respect to *PR* gene regulators. Analysis of the 1048 bp *E22* promoter sequence (Appendix 5) by PLACE and PlantCARE revealed the presence of putative *cis*-elements involved in biotic (pathogen), hormone (i.e. salicylic acid (SA), ethylene (ET), cytokinin (CK) and abscisic acid (ABA)) and abiotic (salinity, drought and cold) stress responses, light-regulated responses and tissue-/cell-specific expression (such as mesophyll-, guard-cell- and seed-specific expression) as listed in Table 4.2. Analysis of the E22 protein (UniProtID: P13046) sequence via http://web.expasy.org/compute_pi/ predicted a theoretical pI of 5.38, confirming that E22 is an acidic PR protein. This provided a clue as to the types of regulatory molecules that should be investigated in order to characterize the regulation of its promoter as described in each of the following sections.

Table 4.2 List of putative *cis*-acting elements identified in the *E22* promoter. Underlined = W-box core motif. R = A/G, W = A/T, Y = C/T, N = A/T/G/C. Note the salicylic acid-responsive element (SARE), which contains the 'TTCGACC' sequence, was originally identified as the Elicitor Responsive Element (ElRE) by PlantCARE but was re-annotated s a SARE in accordance with Shah and Klessig (1996) and Liu *et al.* (2013) in this study. SARE is different from the Elicitor Responsive Element (ElRE), which contains the 'TTGACC' sequence identified in the parsley *PR-1* promoter (Rushton *et al.*, 1996).

Response/ Function	*cis*-element	Consensus Sequence	Organism	PLACE ID	Copy number	Reference
Pathogen and salicylic acid (SA) responsive	W-box	TTGAC	*Arabidopsis thaliana*	S000390	4	Rushton *et al.* (2010)
	Elicitor-Responsive Element (ElRE)	TTGACC	*Petroselinum crispum, Arabidopsis thaliana*	S000142	1	Rushton *et al.* (1996); Eulgem *et al.* (1999)
	as-1 element	TGACG	*Nicotiana tabacum*	S000024	2	Jupin & Chua (1996) ; Strompen *et al.* (1998)
Pathogen responsive	WBOXNTCHN48	CTGACY	*Nicotiana tabacum*	S000508	1	Yamamoto *et al.* (2004)
NaCl and pathogen responsive	GT-1 box	GAAAAA	*Glycine max, Arabidopsis thaliana*	S000453	3	Park *et al.* (2004)
SA responsive	Salicylic Acid-Responsive Element (SARE)	TTCGACC	*Nicotiana tabacum*	PlantCARE	1	Shah & Klessig (1996), Liu *et al.* (2013)
	GT-element	GRWAAW	*Nicotiana tabacum*	S000198	11	Buchel *et al.* (1999); Zhou (1999)

Response/ Function	*cis*-element	Consensus Sequence	Organism	PLACE ID	Copy Number	Reference
Ethylene (ET) responsive	Ethylene-Responsive Element (ERE)	AWTTCAAA	*Solanum lycopersicum, Dianthus caryophyllus*	S000037	1	Tapia *et al.* (2005)
Cytokinin (CK) responsive	ARR1-binding element	GATT	*Arabidopsis thaliana*	S000454	10	Sakai *et al.* (2001), Taniguchi *et al.* (2007)
	Cytokinin-dependent protein binding motif	TATTAG	*Cucumis sativus*	S000491	2	Fusada *et al.* (2005)
Drought, salinity and abscisic acid (ABA) responsive	ABA-Responsive Element (ABRE)	ACGTG	*Arabidopsis thaliana*	S000414	1	Nakashima *et al.* (2006)
Drought and ABA responsive	MYB1AT	WAACCA	*Arabidopsis thaliana*	S000408	1	Abe *et al.* (2003)
	MYCCONSENSUSAT	CANNTG	*Arabidopsis thaliana*	S000407	8	Abe *et al.* (2003)
	MYCATERD1	CATGTG	*Arabidopsis thaliana*	S000413	2	Tran *et al.* (2004)
	MYCATRD22	CACATG	*Arabidopsis thaliana*	S000174	2	Abe *et al.* (1997)
Cold, drought and ABA responsive	LTRECOREATCOR15	CCGAC	*Arabidopsis thaliana*	S000153	1	Baker *et al.* (1994)
Mesophyll-specific	CACTFTPPCA1	YACT	*Flaveria trinervia*	S000449	16	Gowik *et al.* (2004)

Response/ Function	*cis*-element	Consensus Sequence	Organism	PLACE ID	Copy Number	Reference
Guard cell-specific	TAAAG element	(T/A)AAAG	*Solanum tuberosum, Gossypium barbadense*	S000387	8	Plesch *et al.* (2001), Han *et al.* (2013)
Seed-/embryo-specific, ABA responsive	2S SEEDPROTBAMNAPA	CAAACAC	*Brassica napus*	S000143	1	Stålberg *et al.* (1996)
	E-box	CANNTG	*Brassica napus*	S000144	8	Stålberg *et al.* (1996)
	DPBFCOREDCDC3	ACACNNG	*Daucus carota*	S000292	3	Kim *et al.* (1997)
Embryo- and endosperm-specific	$(CA)_n$ element	CNAACAC	*Brassica napus*	S000148	1	Ellerström *et al.* (1996)
Light regulated	I-box	GATAA	Monocots and dicots	S000199	1	Terzaghi & Cashmore (1995)
	Inr (Initiator) element	YTCANTYY	*Nicotiana tabacum*	S000395	4	Nakamura *et al.* (2002)
	SORLIP5AT	GAGTGAG	*Arabidopsis thaliana*	S000486	1	Jiao *et al.* (2005)
	T-box	ACTTTG	*Arabidopsis thaliana*	S000383	1	Chan *et al.* (2001)
Dof transcription factor binding site	DOFCOREZM	AAAG	Monocots and dicots	S000265	12	Yanagisawa (2004)

4.3.2 Developmental regulation of the *E22* promoter in healthy transgenic *E22* promoter: *gusA* reporter tobacco plants

To investigate the constitutive activity and developmental regulation of the *E22* promoter, different parts of healthy line 14(8) transgenic *E22* promoter: *gusA* reporter (pCYT-1) tobacco at different developmental stages i.e. seedlings, mature plants, flowering plants and senescing plants (1-, 2-, 3- and 4-month old, respectively) were tested for GUS activity by MUG assay and GUS histochemical staining. GUS activity was barely detectable in the cotyledons and roots of transgenic pCYT-1 tobacco seedlings or in leaves, stems and roots of mature transgenic plants. In flowering transgenic tobacco plants, GUS activity was detected in the sepals but not in other flower parts such as the corolla, pistil and stamen (Figure 4.1). GUS activity was not detected in pollen or fruits at various stages of development (from immature to desiccated) following GUS histochemical staining (data not shown). As a positive control for GUS staining, GUS histochemical assays were also performed on leaves, flower parts and fruits at various stages of development from a transgenic 35S: *gusA* reporter tobacco obtained from Wang *et al.* (2008b). GUS expression was detected in all of these parts following GUS histochemical staining (data not shown). Interestingly, GUS histochemical staining was observed in senescing leaves of four-month old transgenic pCYT-1 tobacco plants (Figure 4.2), with the most intense expression in leaves undergoing senescence (Figure 4.2, middle panels) but less expression in leaves prior to or at the end of senescence (second and fourth panels).

Figure 4.1 Tissue-specific GUS activity in the flower parts of healthy transgenic *E22* promoter: *gusA* reporter (pCYT-1) tobacco detected by GUS histochemical staining. GUS activity was detected in the sepals at the tips (indicated by arrows). GUS activity was absent in other flower parts such as in the corolla, pistil and stamen. Size of samples (in cm) is indicated by inclusion of a ruler in the photograph.

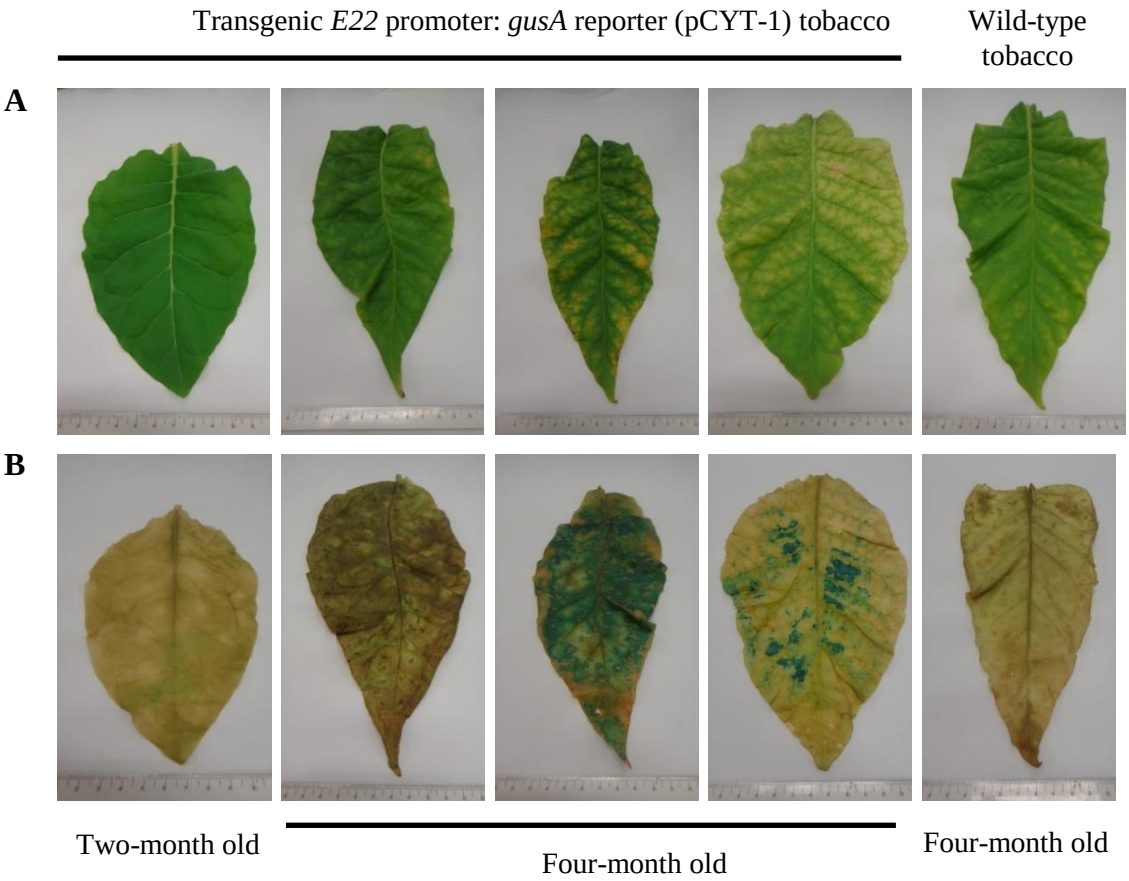

Figure 4.2 GUS activity in leaves of mature and senescing transgenic *E22* promoter: *gusA* reporter (pCYT-1) tobacco plants. Leaf samples **A)** prior to and **B)** after GUS histochemical staining carried out by incubation with 1 mM X-Gluc overnight followed by chlorophyll removal using 70% (v/v) ethanol. Leaves of mature (two-month old) and senescing (four-month old) plants from transgenic and negative-control non-transgenic tobacco were stained. Sizes of samples (in cm) are indicated by inclusion of a ruler in each photograph.

4.3.3 Regulation of the *E22* promoter by *PR* gene regulators

The acidic *PR* genes are known to be induced by SA but less so by JA and wounding (Niki *et al.*, 1998). The acidic nature of E22 and the presence of SA-responsive elements in the promoter (Table 4.2) prompted an investigation of *E22* promoter activation by SA, JA and wounding. Freshly prepared leaf disks from *E22* promoter: *gusA* reporter (pCYT-1) tobacco plants were incubated with SA and/or methyl-jasmonate (MeJA) solution at different concentrations and GUS activity was determined after 48 hours of incubation. As shown in Figure 4.3, GUS activity was very low in leaf disks incubated with water, indicating that the *E22* promoter is not induced by wounding. By contrast, GUS activity increased in response to an increase in SA concentration from 5 to 1000 µM, indicating that the *E22* promoter is up-regulated by SA in a dose-dependent manner. MeJA did not induce the *E22* promoter but it appeared to inhibit promoter activity as shown by a reduction of SA-induced GUS activity in leaf disks incubated with 1 to 20 µM MeJA compared to the water control (Figure 4.3). The effect of inhibition was more pronounced with increasing MeJA concentration and SA-induced GUS activity was completely inhibited at 50 µM MeJA (data not shown). Overall, the results indicate that the *E22* promoter is activated by SA but repressed by MeJA, indicating an antagonistic interplay between SA and JA signalling pathways in regulating the *E22* promoter.

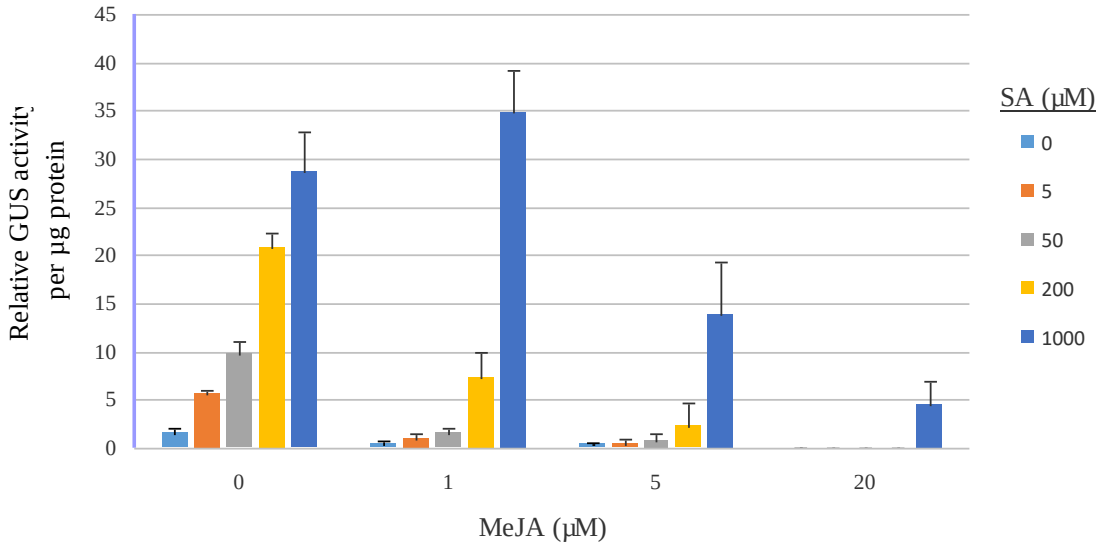

Figure 4.3 Effects of SA and MeJA on GUS activity in *E22* promoter: *gusA* leaf disks after 48 hours of incubation. Freshly prepared leaf disks were incubated with salicylic acid (SA) and/or methyl-jasmonate (MeJA) at the indicated concentrations. The water negative control is indicated by '0' concentration in both treatments. The histogram shows mean relative GUS activity for each treatment as determined by MUG assays from three independent experiments with error bars representing the standard error (n = 3). In each independent experiment, GUS activity was measured in pooled homogenates of three pCYT-1 tobacco leaf disks, one from each of three different plants.

In preliminary experiments, the GUS activity was also found to be induced by ET and CK. Furthermore, a time-dependent induction of *PR* genes by CK has been reported previously (Sano *et al.*, 1996). This prompted an analysis of the induction of *E22* promoter: *gusA* reporter activity by SA, ET and CK over time. Leaf disks were incubated with solutions containing 1 mM SA, 100 µM 6-benzylaminopurine (BAP, a synthetic cytokinin) or 1 mM ethephon (an ethylene-releasing compound) for three days and samples were collected at 12 hour intervals during incubation for measurement of GUS activity by MUG assay. As shown in Figure 4.4, GUS activity was induced by 1 mM SA as early as 12 hours of incubation followed by a steady increase from 12 to 72 hours of incubation. Interestingly, under incubation with 100 µM BAP, GUS activity

remained very low for 12 to 48 hours and this was followed by a marked (6.6 fold) increase in activity at 60 hours, indicating a delayed induction of the *E22* promoter by CK. Similar to SA, 1 mM ethephon also resulted in a consistent increase in GUS activity but showed a greater induction than SA at later time points (Figure 4.4). These results indicate that the *E22* promoter is differentially induced by SA, CK and ET in a time-dependent manner. Consistent with these findings, GUS histochemical staining also showed a time-dependent increase in GUS activity in *E22* promoter: *gusA* reporter (pCYT-1) tobacco leaf disks incubated with 2 mM SA for 24 to 72 hours (Figure 4.5).

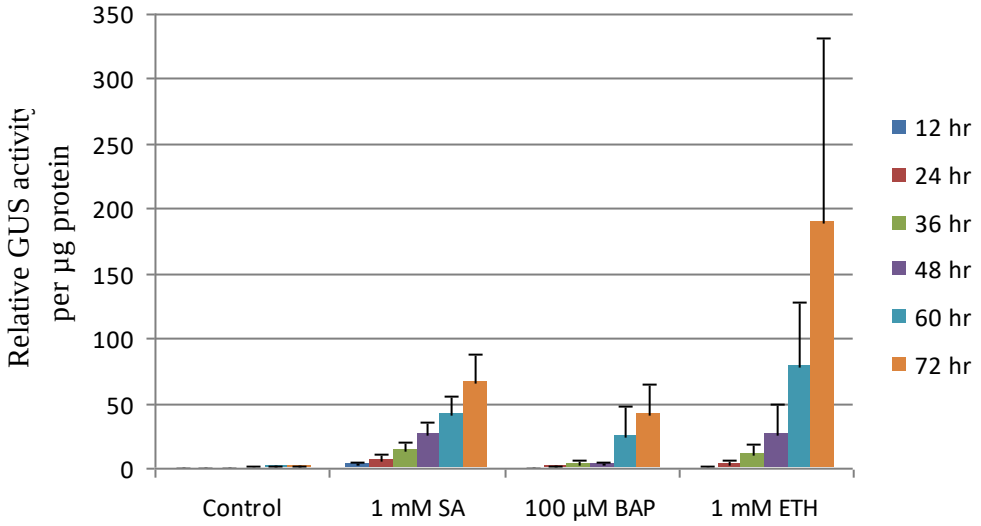

Figure 4.4 Time-course analysis of the induction of GUS activity in *E22* promoter: *gusA* leaf disks by salicylic acid (SA), cytokinin (CK) and ethylene (ET) after 12, 24, 36, 48, 60 and 72 hours of incubation. Freshly prepared leaf disks were incubated with water (negative control), 1 mM SA, 100 µM 6-benzylaminopurine (BAP) and 1 mM ethephon. The histogram shows mean relative GUS activity for each treatment as determined by MUG assays from three independent experiments with error bars representing the standard error (n = 3). In each independent experiment, GUS activity was measured in pooled homogenates of three pCYT-1 tobacco leaf disks, one from each of three different plants.

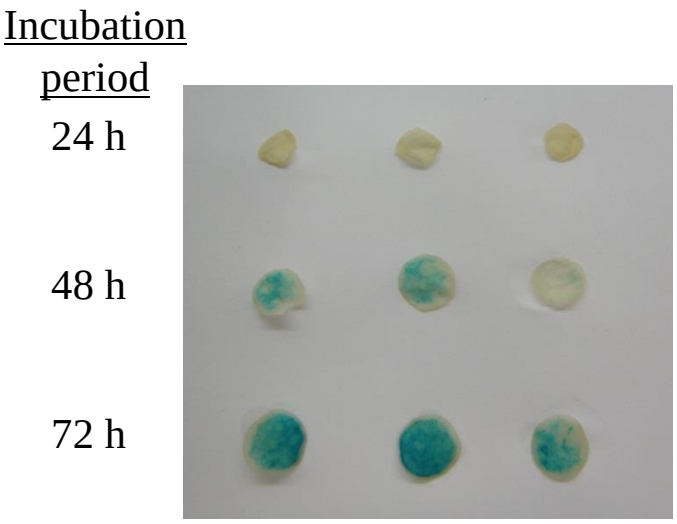

Figure 4.5 GUS activity in transgenic *E22* promoter: *gusA* reporter (pCYT-1) tobacco leaf disks incubated with 2 mM salicylic acid (SA) after 24, 48 and 72 hours of incubation revealed by GUS histochemical staining. Three freshly prepared leaf disks, one from each of three different transgenic tobacco plants were used for each time point.

As SA and CK have been reported to act synergistically to induce the expression of some defence genes (Choi *et al.*, 2010; Jiang *et al.*, 2013a), the induction of *E22* promoter activity following simultaneous application of SA and CK was investigated using leaf disk MUG assays. GUS activity was determined after incubation for 60 hours which is the time point that the *E22* promoter: *gusA* reporter first shows an increase in GUS activity in response to CK. As shown in Figure 4.6, GUS activity was significantly enhanced in leaf disks incubated with the solution containing a combination of both 100 µM BAP and 1 mM SA with 4.2 fold and 2.6 fold increase in GUS activity compared to 100 µM BAP and 1 mM SA, respectively ($P < 0.05$), indicating a possible synergistic effect on induction of the *E22* promoter resulting from simultaneous application of CK and SA.

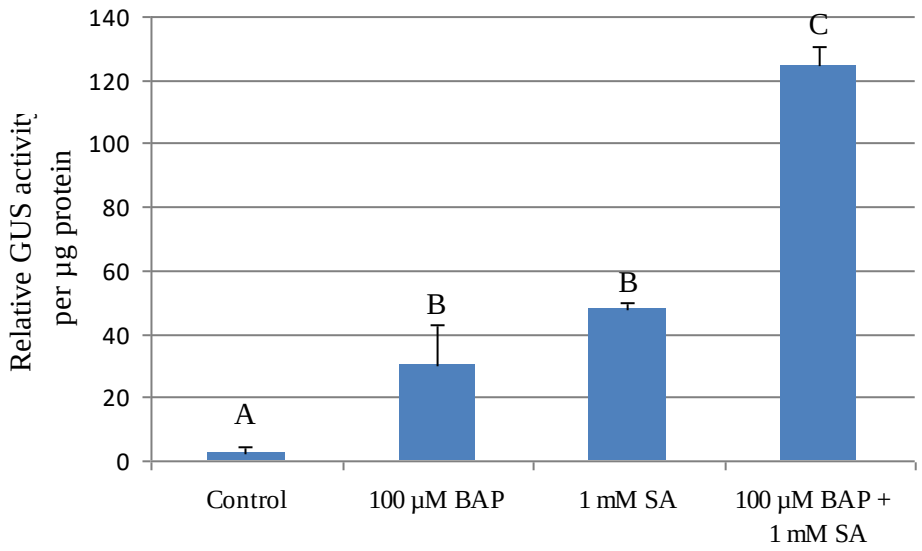

Figure 4.6 Effects of combined cytokinin (CK) and salicylic acid (SA) application on GUS activity in *E22* promoter: *gusA* leaf disks after incubation for 60 hours. Freshly prepared leaf disks were floated on water, 6-benzylaminopurine (BAP) and/or SA at the indicated concentrations. Control treatment was 1 mM NaOH (as described in section 4.2.2). The histogram shows mean relative GUS activity for each treatment as determined by MUG assays from three independent experiments with error bars representing the standard error (n = 3). In each independent experiment, GUS activity was measured in pooled homogenates of three pCYT-1 tobacco leaf disks, one from each of three different plants. Significant differences indicated by letters above the histograms were determined using ANOVA, followed by Fisher's least significant difference analysis at the 95% confidence level (P = 0.05).

The reported induction of *PR-5* genes by salt stress (Singh *et al.*, 1987; LaRosa *et al.*, 1992; Nelson *et al.*, 1992) and the detection of salt-responsive *cis*-acting elements also prompted an investigation of the salt inducibility of *E22* promoter by leaf disk assays. Incubation of the *E22* promoter: *gusA* reporter (pCYT-1) tobacco leaf disks in 50 mM NaCl resulted in a significant increase in GUS activity compared to the water control after 48 hours (P< 0.001, Figure 4.7).

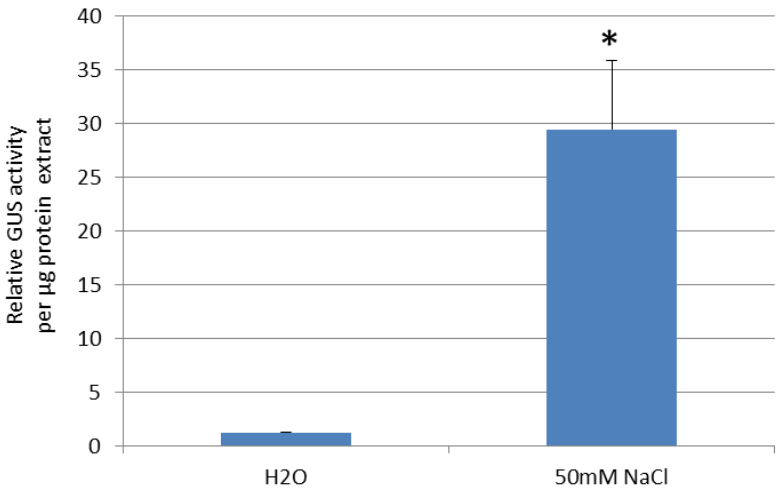

Figure 4.7 Induction of GUS activity in *E22* promoter: *gusA* leaf disks by 50 mM NaCl after 48 hours of incubation. Freshly prepared leaf disks were incubated with water (negative control) or 50 mM NaCl. The histogram shows mean relative GUS activity for each treatment as determined by MUG assays from three independent experiments with error bars representing the standard error (n = 3). In each independent experiment, GUS activity was measured in pooled homogenates of three pCYT-1 tobacco leaf disks, one from each of three different plants. Significant difference was determined by Student *t*-Test, * = P< 0.001.

4.4 Discussion

4.4.1 Developmental regulation of the *E22* promoter in healthy transgenic *E22* promoter: *gusA* reporter tobacco plants

Constitutive expression of tobacco *PR-5* genes encoding osmotin and the osmotin-like protein in roots and flowering organs is well-documented (Neale *et al.*, 1990; Kononowicz *et al.*, 1992; LaRosa *et al.*, 1992; Nelson *et al.*, 1992; Koiwa *et al.*, 1994; Zhu *et al.*, 1995b; Sato *et al.*, 1996; Kitajima *et al.*, 1998). In contrast, the *E22* promoter is not active in roots as evidenced by the absence of GUS activity in the roots of healthy transgenic *E22* promoter: *gusA* reporter tobacco seedlings and mature plants, supporting the notion that constitutive expression in roots is a general characteristic of the basic *PR* genes but not the acidic ones like *E22* (Memelink *et al.*, 1990; Ohashi and Ohshima, 1992). In contrast to a high level of osmotin and osmotin-like protein gene expression in mature flowers and desiccating fruits (Neale *et al.*, 1990; Kononowicz *et al.*, 1992; Zhu *et al.*, 1995b), *E22* promoter activity was not detected in these organs. Interestingly, *E22* promoter activity was detected in sepals (Figure 4.1), consistent with previous reports showing the expression of acidic PR-1, PR-2 (glucanases) and PR-4 (endochitinases) proteins in sepals (Lotan *et al.*, 1989; Côté *et al.*, 1991; Uknes *et al.*, 1993). However, the aforementioned studies also reported the expression of PR-2 and PR-4 proteins in the pedicle, anthers and ovaries in addition to sepals whereas in this study *E22* promoter activity was only found in sepals but not in other flower parts and fruits. The expression of *PR* genes in the flowering organs and fruits may serve a protective function in these organs during flower development. The detection of various *PR* gene activities in different parts of the flowering organs may indicate that each of these genes serve different protective roles in these tissues.

Interestingly, *E22* promoter activity was also detected during leaf senescence (Figure 4.2). Senescence is an age-dependent slow form of cell death involving breakdown and remobilization of plant cell materials and nutrients into developing organs of the plants such as younger leaves, flowers and fruits (Lim *et al.*, 2007). Expression of defence-related genes during plant senescence has been reported previously. For instance, PR-1a and chitinase genes are expressed during early senescence in *Brassica napus* (Hanfrey *et al.*, 1996). The expression of several HR-associated genes were also found during senescence (Olszak *et al.*, 2006). While this process is developmentally regulated,

premature senescence can be induced by external stimuli such as UV, starvation, drought, shading and pathogen attack (Love *et al.*, 2008). Furthermore, phytohormones particularly ethylene, are well-known to play a role in promoting senescence (Love *et al.*, 2008). The induction of *E22* promoter activity during senescence is consistent with the strong induction of GUS activity by ET as shown by this study.

4.4.2 Regulation of the *E22* promoter by *PR* gene regulators

Plants respond to pathogens by the induction of signalling hormones including SA, JA, ET and CK (Bari and Jones, 2009; Pieterse *et al.*, 2009). Exogenous application of plant signalling hormones also leads to activation of defence responses including the induction of *PR* gene expression. As shown in Section 4.3.3, the *E22* promoter is not induced by wounding. This allowed the use of leaf disk assays to study regulation of the *E22* promoter with a low background of activity. This result is also consistent with previous findings reporting that the basic *PR* genes but not their acidic counterparts are wound-inducible (Brederode *et al.*, 1991; Sano *et al.*, 1996; Niki *et al.*, 1998). The *E22* promoter showed a marked responsiveness to SA but SA-induced *E22* promoter activity was repressed by JA (Figure 4.3), demonstrating the classic antagonistic interplay between SA and JA signalling pathways in the regulation of *PR* gene expression. SA also plays an important role in plant defence by mediating systemic acquired resistance (SAR) (Hammond-Kosack and Jones, 1996; Durrant and Dong, 2004; Vlot *et al.*, 2009). The SA responsiveness of the *E22* promoter is in line with previous findings that *PR-1*, *PR-2* and *PR-5*, particularly those encoding acidic isoforms such as *PR-1a*, acidic glucanases (*PR-2*) and acidic *PR-5*, are strongly up-regulated by SA (Ohashi and Ohshima, 1992; Hennig *et al.*, 1993; Uknes *et al.*, 1993; van de Rhee *et al.*, 1993; Niki *et al.*, 1998; van Verk *et al.*, 2008; Ono *et al.*, 2011; Molinari *et al.*, 2014). The presence of multiple *cis*-elements involved in SA responsiveness such as the W-box, *as-1* element, SARE and GT-element in the *E22* promoter (Table 4.2) is consistent with the SA inducibility of the promoter as shown in this study. For example, the *as-1* element, which is a binding site for the TGA1 transcription factor, has been identified in the promoter region of many SA-inducible genes including the tobacco acidic *PR-1a* gene (Jupin and Chua, 1996; Yang *et al.*, 2000; Garretón *et al.*, 2002; Redman *et al.*, 2002; Després *et al.*, 2003). The presence of W-box motifs, which are highly enriched in the promoters of many defence-related genes in plants including the *FLARE* (*Flagellin*

Rapidly Elicited) genes, genes induced by SAR (systemic acquired resistance) and during HR (Maleck *et al.*, 2000; Navarro *et al.*, 2004; Etalo *et al.*, 2013), is consistent with a role for the *E22* gene in plant defence.

In the time-course analysis, the *E22* promoter was also shown to be induced by ET, which induces high level expression of osmotin (a basic PR-5 protein) and osmotin-like protein (a neutral PR-5 protein) (Brederode *et al.*, 1991; Koiwa *et al.*, 1994; Sato *et al.*, 1996; Kitajima *et al.*, 1998). Previous studies indicate that the basic *PR* genes are highly induced by ET whereas the acidic ones are only moderately induced (Memelink *et al.*, 1990; Brederode *et al.*, 1991; Eyal *et al.*, 1993; Tornero *et al.*, 1997). However, in this study, the *E22* promoter activity showed a greater increase in activity at 60 and 72 hours after incubation in response to ET compared to SA despite induction by ET being lower at 12, 24 and 36 hours and similar to that of SA at 48 hours. A comparison between induction by SA and ET taken at any one of the earlier time points would lead to the conclusion that the induction of the *E22* promoter by ET is lower or at a similar level compared to SA. If the same were true for other *PR* genes, this may have contributed to the notion that the acidic *PR* genes are only moderately induced by ET and highly induced by SA as reported by the previous studies cited above. This result shows the importance of conducting an analysis that involves monitoring over a time course to gain a 'true picture' of the induction of *PR* genes. Alternatively, the Ethylene-Responsive Element (ERE) (5'-AWTTCAAA-3') present in the *E22* promoter (Table 4.2), which differs from the GCC element (5'-AGCCGCC-3') known to mediate the ethylene responsiveness of the basic *PR* genes including the osmotin and osmotin-like protein genes (Sato *et al.*, 1996; Tornero *et al.*, 1997) and to be responsible for constitutive expression of the osmotin-like protein gene in roots (Kitajima *et al.*, 1998), may account for both the differences in ethylene responsiveness and the absence of constitutive activity in roots shown by the *E22* promoter compared to other *PR-5* promoters.

An emerging role of CK in plant defence (Choi *et al.*, 2011) along with the presence of a CK-responsive sequence motif in the *E22* promoter (Table 4.2) prompted an investigation of *E22* promoter induction by this defence-related signalling molecule. Tobacco mutants with elevated endogenous CK or exogenous application of CK in wild type tobacco leaves leads to accumulation of acidic *PR* genes (Sano *et al.*, 1996;

Synkova *et al.*, 2004). Consistent with these observations, this study demonstrated that application of CK induced the *E22* promoter, in a time-dependent manner (Figure 4.4). Sano *et al.* (1996) showed that CK indirectly up-regulates the expression of acidic *PR* genes through induction of the SA pathway by altering endogenous JA levels, leading to a time-dependent induction of *PR* gene expression (in which a surge of *PR* gene transcript accumulation was observed after 24 hours incubation with CK). Recently, several studies reported that CK promotes the SA signalling pathway by acting synergistically with SA to induce the expression of several defence genes (Choi *et al.*, 2010; Jiang *et al.*, 2013a). Similarly, simultaneous application of SA and CK additively enhanced *E22* promoter activity compared to the application of SA or CK alone (Figure 4.6). The induction of *PR* genes by a pathogen-induced increase in the cellular SA level or via exogenous application of SA is regulated by the activity of the transcription co-activator NPR1 (NONEXPRESSOR OF *PATHOGENESIS-RELATED* GENES 1) (Zhou *et al.*, 2000; Spoel *et al.*, 2009). Following an increase in cellular SA, NPR1 translocates into the nucleus to interact with TGA transcription factors (Kinkema *et al.*, 2000; Subramaniam *et al.*, 2001; Fan and Dong, 2002). NPR1 stimulates the DNA binding activity of TGA transcription factors to SA-responsive *cis*-elements such as the *as-1* element present in the *PR-1* promoter (Strompen *et al.*, 1998; Després *et al.*, 2003; Johnson *et al.*, 2003). Interestingly, binding of the cytokinin signalling regulated transcription factor ARABIDOPSIS RESPONSE REGULATOR 2 (ARR2) during activation of the *PR-1* promoter is promoted by NPR1 and the TGA3 transcription factor, indicating a role of NPR1 in CK/SA-mediated signalling (Choi *et al.*, 2010). Whilst NPR1 regulates the antagonism between the SA and JA signalling pathways (Spoel *et al.*, 2003), the evidence reported in the studies mentioned above correlate with the findings by Sano *et al.* (1996) suggesting that the regulation of *PR* gene expression by CK is achieved via modulation of endogenous SA and JA levels. Taken together, these data suggest that the delayed induction of the *E22* promoter by CK observed in this study may be attributed to modulation of the SA and JA signalling pathways by CK. In addition, there are eleven copies of the ARR1-binding motif present in the *E22* promoter (Table 4.2). ARR1 is a cytokinin-regulated transcription factor and the ARR1 binding site is identified in the promoter region of several cytokinin primary response genes such as ARR6 and some putative disease resistance genes (Sakai *et al.*, 2001; Taniguchi *et al.*, 2007). The presence of ARR1-binding motifs in the *E22* promoter suggests an alternative regulation of the promoter by CK via ARR1 or in addition to

regulation by NPR1 via endogenous SA: JA ratio as discussed above. Furthermore, ET also plays a role in modulating SA-JA antagonism through NPR1 (Leon-Reyes *et al.*, 2009), adding to the complexity of the interplay between the signalling pathways in the regulation of plant defence. Therefore, the tobacco leaf disks assays adopted in this study could be extended to investigate the induction of the *E22* promoter by other combinations of the signalling hormones tested above. This could include SA and ET, which have been reported to act synergistically to induce defence gene expression (Lieberherr *et al.*, 2003), and JA and ET, which have been shown to synergistically activate expression of basic *PR* genes (Xu *et al.*, 1994). In fact, preliminary experiments indicated that the *E22* promoter: *gusA* reporter is additively induced by the combination of SA and ET but not induced by the combination of JA and ET. These studies were not completed due to the inability to carry out replicate experiments owing to time constraints but they may be worth following up.

Similar to other members of the *PR-5* family (Singh *et al.*, 1987; LaRosa *et al.*, 1992; Nelson *et al.*, 1992; Koiwa *et al.*, 1994), the *E22* promoter is also induced by salt stress. While it might seem that only the basic *PR-5* genes are induced by salt stress, a soybean acidic osmotin-like protein GmOLP is found to be induced in roots 24 hr after application of high salt solution and in leaf and stem tissues at 48 hr and 72 hr under similar conditions (Onishi *et al.*, 2006). Together with the observation that the acidic *E22* gene promoter is induced by salt stress, these results suggest that salt inducibility may be a general characteristic of the *PR-5* genes. In this study, salt inducibility of the *E22* promoter was only investigated in leaf tissues. This investigation could therefore be extended to other organs such as in roots.

4.4.3 Conclusion

As discussed in Chapter 3, *PR-5* could be used as an alternative to *PR-1* as a marker of plant defence in experiments involving transient expression assays by agroinfiltration. The data presented in this chapter showed that the *E22* promoter is regulated by various defence-activating signalling molecules such as SA, JA, ET and CK, indicating that the *E22* promoter is a defence-inducible promoter. In addition to the primary application of the *E22* promoter: *gusA* reporter system for the analysis of Hcr9-M205 constructs in agroinfiltration assays, the investigation reported in this chapter about the regulation of *E22* promoter activity using tobacco leaf disk assays has demonstrated the effectiveness of the reporter system in the quantification of plant defence activation. The *E22* promoter: *gusA* reporter system showed the capability to respond to activation and repression of defence signalling as exemplified by the antagonistic regulation of *E22* promoter activity by SA and JA. The reporter system also responded to enhanced defence signalling through the concerted action of SA and CK and time-dependent induction by SA, ET and CK, with an output ranging from barely detectable GUS activity in healthy leaves to a high level of GUS activity induced by ET at later time points. An investigation to compare GUS activity and endogenous *E22* expression, as carried out in Chapter 3, in response to *PR* regulators in leaf disk assays would determine whether GUS activity responded in the same manner as the endogenous *E22* gene. The results from the agroinfiltration assays in Chapter 3 indicate that line 14(8) used in this study is an excellent transgenic line in this respect. Importantly, the *E22* promoter: *gusA* reporter system was capable of responding to micromolar changes in the amount of signalling input applied, indicating the sensitivity of the reporter system.

The investigations reported in this chapter have provided new insights into the regulation of a *PR-5* promoter in plant defence. Nevertheless, the regulatory functions of the *cis*-elements identified in the promoter region require further verification by a functional study such as a promoter deletion analysis. This will address the functional relevance of the *cis*-elements identified *in silico* to the transcriptional regulation of the *E22* promoter. Such an investigation was not carried out as part of this study because this aspect was not of direct interest to the research being undertaken. However, several motifs present in the *E22* promoter such as the W-box and SARE motifs have been shown to function in isolation in transgenic tobacco containing synthetic promoter: reporter constructs (Rushton *et al.*, 2002; Liu *et al.*, 2013). By functional investigation

of synthetic minimal promoters containing several defence related *cis*-elements, Rushton *et al.* (2002) demonstrated that defence signalling is largely conserved across plant species at the promoter element level. In addition, the spacing, copy number and orientation of specific *cis*-elements, as well as their combinatorial regulation in conjunction with other *cis*-elements are other important determinants of gene expression (Buchel *et al.*, 1999; Rushton *et al.*, 2002; Gurr and Rushton, 2005; Venter, 2007). For example, increasing the copy number of W-boxes from 1, 2, 4 to 8 copies increases the promoter strength in response to elicitor treatment progressively but this was also associated with an increase in background activity (Rushton *et al.*, 2002).

Potential applications of the *E22* promoter: *gusA* reporter system include the use as a tool to screen for activators of plant defence and as a biosensor to detect pathogen attack and adverse environmental conditions such as high salinity. A suggestion for future study includes investigation of the responsiveness of the *E22* reporter to attack by different pathogens. For example, it would be interesting to investigate if there is any differential induction of the *E22* promoter by biotrophic and necrotrophic pathogens that activate the SA and JA/ET pathways, respectively. As *PR-5* genes have been demonstrated with antifungal activity against several pathogens including *Fusarium oxysporum* and *Phytophthora infestans* (Woloshuk *et al.*, 1991; Liu *et al.*, 2010), the induction of *E22* promoter activity by these pathogens is worth further investigation.

CHAPTER 5:

Structure-function Analysis of an Autoactive Chimeric Cf-9 Disease Resistance Protein, Hcr9-M205

5.1 Introduction

An autoactive Cf-9 mutant designated M205 was identified as part of the Cf-9 transposon tagging experiment conducted by Jones *et al.* (1994) and the mutant was characterized by Barker *et al.* 2006a (Section 1.6). Subsequently, a domain swapping analysis by Anderson *et al.* (in preparation) has identified three key regions responsible for control of the signalling activity of the Hcr9-M205 protein comprising a mismatch between Hcr9-9A sequence in LRRs 10-17 (designated the signalling repression domain) and Cf-9 LRR 18 (designated the signal activation domain) required for a basal level of autoactivity and an additional C-terminal region consisting of the loop-out region and LRRs 24-26 (designated the signalling enhancer domain) required for complete autoactivity. This introduction gives a brief summary of the evidence relating to these domains, which provides the basis for further investigation in the present study.

Transient expression of Hcr9-M205 protein but not its progenitors Cf-9 and Hcr9-9A in *N. tabacum* resulted in necrosis (Figure 5.1). Transient expression of domain swap CLB101 containing a reciprocal fusion comprising the N-terminus of Cf-9 and the C-terminus of Hcr9-9A also did not result in necrosis, indicating that Hcr9-M205 autoactivity requires a specific mismatch consisting of the N-terminus of Hcr9-9A and the C-terminus of Cf-9 (Figure 5.1). Furthermore, domain swaps between Hcr9-9A and Cf-9 with junctions located at other positions were not autoactive (Figure 5.2). In particular, domain swaps CLB93, which contains a junction just one LRR upstream compared to Hcr9-M205, and CLB94, which contains a junction just one LRR downstream, were not autoactive (Figure 5.2). These results are consistent with the postulated role of the N- and C-terminal regions of Cf proteins in recognition specificity and signalling output, respectively, with the N-terminus repressing signalling by the C-terminus in the absence of recognition (Wulff *et al.*, 2009a).

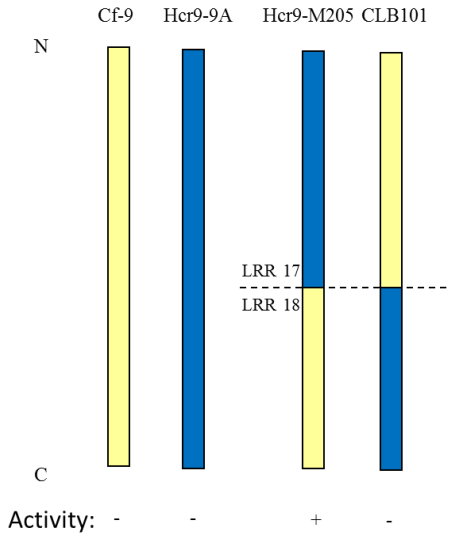

Figure 5.1 Autoactivity of Hcr9-M205 protein, its progenitors Cf-9 and Hcr9-9A, and the reciprocal domain swap CLB101. Yellow and blue bars represent Cf-9 and Hcr9-9A sequences, respectively. N and C represent the N- and C-termini of the proteins, respectively. The location of the junctions between Cf-9 and Hcr9-9A are indicated relative to specific LRRs. Activity is represented as autoactive (+) or non-autoactive (-).

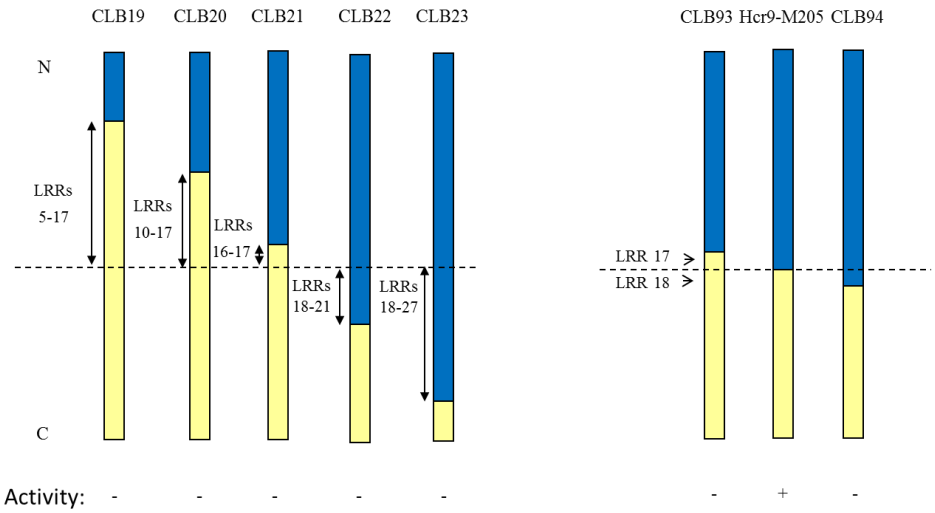

Figure 5.2 Domain swaps that define the position of the junction between Hcr9-9A and Cf-9 required for autoactivity. Yellow and blue bars represent Cf-9 and Hcr9-9A sequences, respectively. N and C represent the N- and C-termini of the proteins, respectively. The location of the junctions between Cf-9 and Hcr9-9A are indicated relative to specific LRRs. Activity is represented as autoactive (+) or non-autoactive (-).

Further domain swaps enabled the identification of two regions located in the C-terminal Cf-9 portion of Hcr9-M205 that may play an important role in signal transduction (Figure 5.3). Substitution of Cf-9 LRR 18 into Hcr9-9A appears to be necessary for a gain of autoactivity albeit at a low level (indicated by the activity of domain swaps CLB79, CLB83 and CLB91). LRR 18 is therefore referred to as the signal activation domain. The second region located at the C-terminal end comprising the loop-out region and LRRs 24-26 (hereafter referred to as the signal enhancer domain), did not trigger autoactivity by itself (indicated by domain swap CLB89), but was required to induce full autoactivity in the presence of Cf-9 LRR 18 (domain swap CLB91).

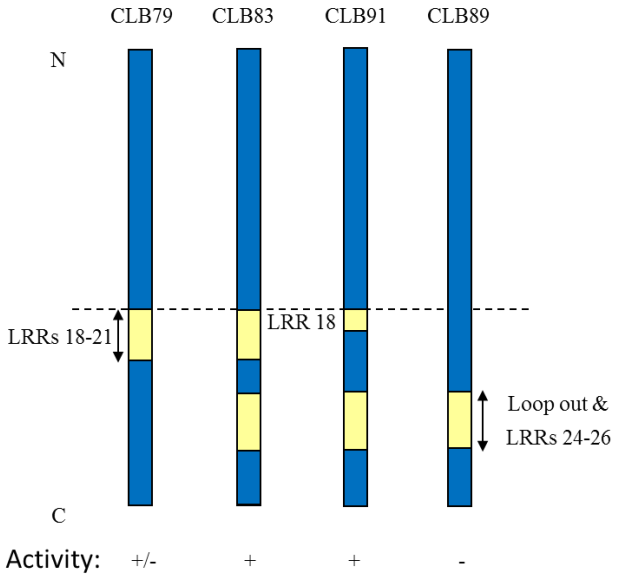

Figure 5.3 Domain swaps dissecting the C-terminal region required for signal transduction of Hcr9-M205. Yellow and blue bars represent Cf-9 and Hcr9-9A sequences, respectively. N and C represent the N- and C-termini of the proteins, respectively. The location of the junctions between Cf-9 and Hcr9-9A are indicated relative to specific LRRs. Activity is represented as autoactive (+), basal level of autoactivity (+/-) or non-autoactive (-).

Domain swaps were also used to dissect the Hcr9-9A region required for Hcr9-M205 autoactivity. Reduction of Hcr9-9A to LRRs 10-17 in CLB103 did not alter autoactivity whereas a further reduction to LRRs 16-17 in CLB104 abolished autoactivity (Figure 5.4). These findings indicate that autoactivity, and by inference disruption of signalling

repression, is regulated by a region extending from LRR17 to somewhere between LRR10 and LRR16. Consistent with a role of LRRs 10-17 in signalling repression, Anderson *et al.* (in preparation) showed that the introduction into Hcr9-M205 of LRR 16 and/or LRR 17 from Cf-9 as represented by CLB21, CLB92 and CLB93 abolished autoactivity (Figure 5.4), indicating that LRR 16 and 17 may both be important for repression of signal activation mediated by LRR 18. Interestingly, there is only one amino acid difference between Cf-9 and Hcr9-9A in LRR 17 (L481 in Cf-9 corresponding to S483 in Hcr9-9A). In essence, domain swap CLB93 represents Hcr9-M205 containing an S483L mutation leading to the hypothesis that L481 in LRR 17 may be an important residue involved in repression of signalling.

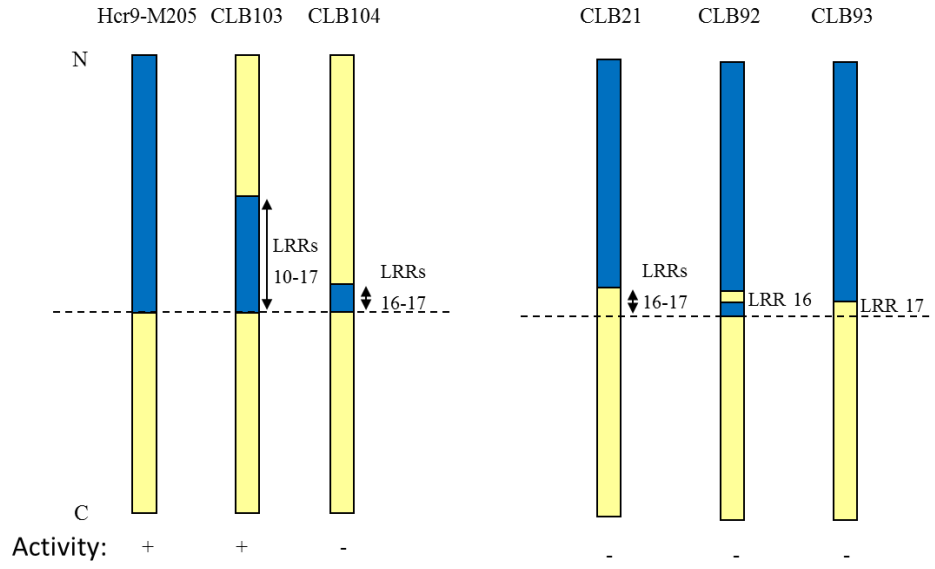

Figure 5.4 Domain swaps dissecting the N-terminal Hcr9-9A sequence required for Hcr9-M205 autoactivity. Yellow and blue bars represent Cf-9 and Hcr9-9A sequences, respectively. N and C represent the N- and C-termini of the proteins, respectively. The location of the junctions between Cf-9 and Hcr9-9A are indicated relative to specific LRRs. Activity is represented as autoactive (+) or non-autoactive (-).

The role of the C-terminal region in signal transduction, including six amino acid residues in the loop-out region and LRRs 24-26 that differentially contributed to enhanced signalling, has been well-defined by Anderson *et al.* (in preparation). By contrast, the extent of N-terminal Hcr9-9A sequence required prior to LRRs 16-17 for autoactivity was not investigated. Therefore, this region was investigated by domain

swapping analysis in this study. Interestingly, the major Cf-9 specificity-determining region located in LRRs 13-16 (Wulff *et al.*, 2001; Wulff *et al.*, 2009b) overlap the proposed signalling repression domain, indicating that ligand interaction and the negative regulation of signalling may occur in the same region in Cf-9. This study has explored the relationship between Cf-9 specificity and signalling repression by the use of site-directed mutagenesis, including the possibility that L481 may not only be involved in signal repression but also involved in Avr9 recognition.

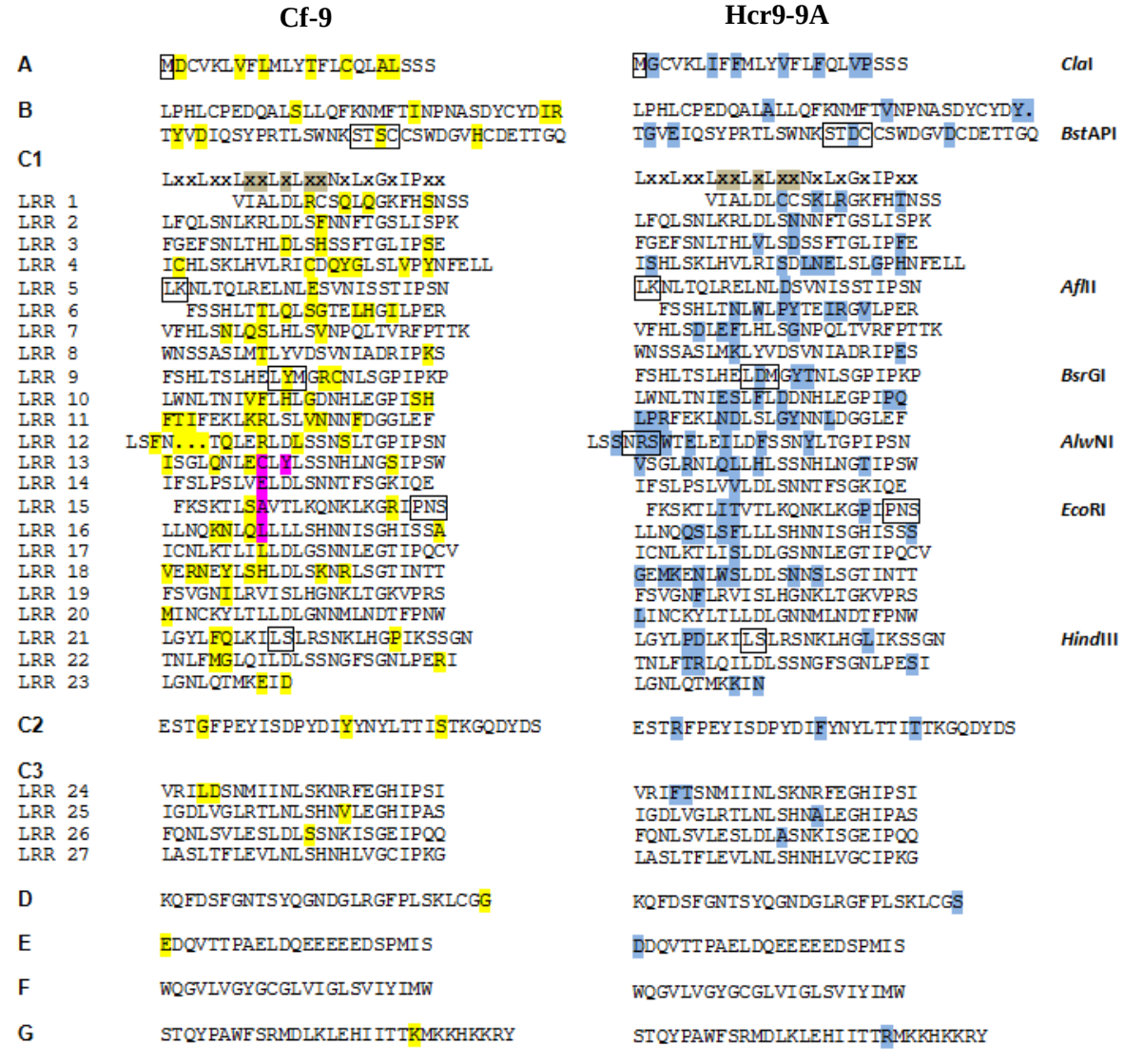

Figure 5.5 Comparison between Cf-9 and Hcr9-9A proteins. Leucine-rich repeats (LRR) are numbered 1 to 27. The amino acid polymorphisms between Cf-9 and Hcr9-9A are highlighted in yellow (Cf-9) and blue (Hcr9-9A). All five previously identified Cf-9 specificity-determining residues (Wulff *et al.*, 2001; Wulff *et al.*, 2009b) overlapping the polymorphic positions are highlighted in pink. Structural domains of Hcr9 proteins (Jones and Jones, 1997) are indicated on the left: A, signal peptide; B, predicted mature amino terminus; C, LRR domain; D, connecting domain; E, acidic domain; F, transmembrane domain; G, basic domain. The conserved structural motifs of plant extracellular LRR proteins are indicated above the LRR sequences. The predicted solvent-exposed positions (x) in the β-sheet (xxLxLxx) typical of LRR proteins (Kobe and Kajava, 2001; Bella *et al.*, 2008) are highlighted in brown. Deletions in Cf-9 relative to Hcr9-9A, and vice versa, are indicated by dots. The amino acids whose coding DNAs contain restriction sites (indicated on the right) used in the generation of chimeric constructs are boxed.

5.2 Materials and methods

5.2.1 Plant materials

Nicotiana tabacum cv. Petit Havana tobacco plants were used in agroinfiltration experiments for necrosis assessment of the autoactive constructs and protein gel-blot analysis. Transgenic tobacco plants expressing *Avr9* (SLJ6201A) (Hammond-Kosack et al., 1994) were used in agroinfiltration experiments for assessment of Avr9-dependent necrosis. Transgenic *E22* promoter: *gusA* reporter (pCYT-1) tobacco plants (Chapter 3) were used in agroinfiltration experiments for *E22* promoter: *gusA* reporter activity quantification.

5.2.2 Starting plasmids

Progenitor plasmids p494, p925, p997 and p999 containing the coding regions of the Hcr9-M205, CLB93, CLB103 and CLB104 domain swaps in pBluescript SK+, respectively, and the *Cf-9* 3'UTR, were generated by Anderson *et al.* (in preparation) (Figure 5.6). Plasmid pCBJ109, which contains the *Cf-9* promoter, *Cf-9* coding region tagged with a 3x hemagglutinin (HA) epitope at the N-terminus and *Cf-9* 3' UTR in pBluescript SK+, was developed by Benghezal *et al.* (2000) (Figure 5.6). Plasmid pCBJ310, containing the CaMV 35S promoter, *Cf-9* coding region tagged with a 3x HA epitope at the N-terminus and *Cf-9* 3' UTR in a pGREENII binary vector, was generated by Chakrabarti (2005) (Figure 5.6). An HA-tagged version of the Hcr9-M205 domain swap in a pGREENII binary vector, here designated HA-Hcr9-M205, was generated as described in Figure 5.7. To generate HA-tagged versions of domain swaps CLB103 and CLB104 in a pGREENII binary vector, the coding regions and 3' UTRs in p997 and p999 were substituted into pCBJ310 by utilizing the *Bst*API and *Not*I sites located just downstream of the 3x HA sequence and Cf-9 3' UTR, respectively (Figure 5.8). Similarly, an HA-tagged version of CLB93 in a pGREENII binary vector was generated by substituting the coding region and 3' UTR of p925 into HA-Hcr9-M205 plasmid through *Bst*AP1 and *Not*I sites (Figure 5.9). All domain swaps and site-directed mutants in this study were first made in pBluescript SK+ using the existing plasmids shown in Figure 5.6 and then transferred into pCBJ310 or HA-Hcr9-M205 by utilizing *Bst*API and *Not*I restriction sites to generate the HA-tagged version of these constructs in a pGREENII binary vector. Depending on the N-terminal sequences of the domain swaps and mutants, those that contain Cf-9 5' coding region (Section 5.2.2) were

transferred into pCBJ310 whereas those containing Cf-9A 5' coding region (Section 5.2.3) were transferred into HA-Hcr9-M205.

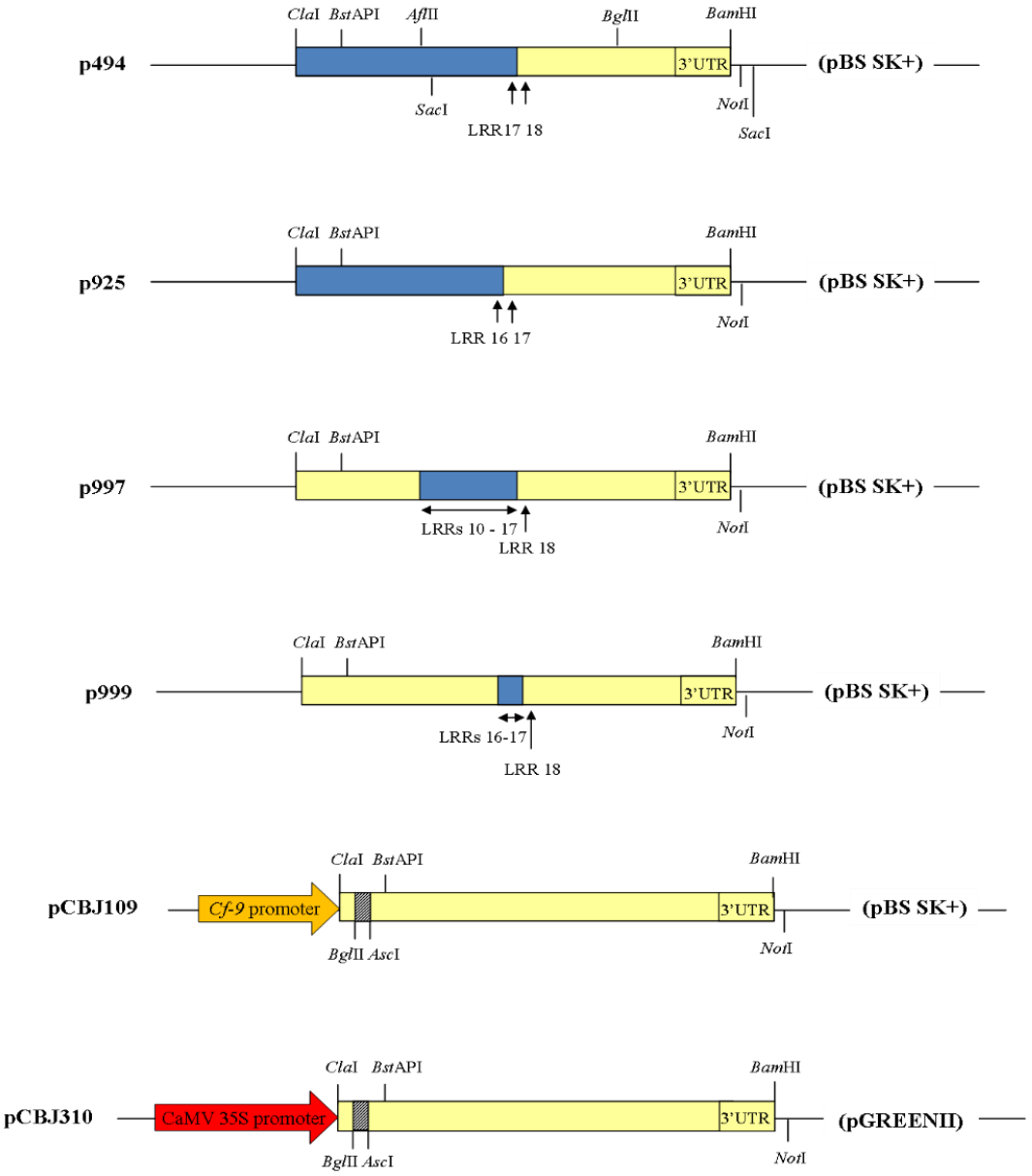

Figure 5.6 Existing plasmids used in this study for construction of domain swaps and generation of site-directed mutants. Blue, yellow and grey bars represent Hcr9-9A, Cf-9 and 3x HA tag sequences, respectively. 3' UTR = 3' untranslated region. Only restriction sites of interest are shown. The location of the junctions between Cf-9 and Hcr9-9A are indicated relative to specific LRRs. pBS SK+ = pBluescript SK+. See Appendix 2 for features of the pGREENII binary vector. Drawings are not to scale.

Figure 5.7 Construction of the HA-Hcr9-M205 plasmid. Plasmids pCBJ109 and p494 were used as the source of the 3x HA sequence and Hcr9-M205 coding sequence, respectively. The pGREENII-derived empty vector, pCBJ306 was developed by Chakrabarti (2005). **Step 1**: Generation of an intermediate plasmid of p494 containing a 3x HA sequence at the N-terminus of Hcr9-M205 coding region: Plasmid p494 was digested with *Sac*I to remove the C-terminal region of the Hcr9-M205 coding sequence containing a *Bgl*II site and flanked by two *Sac*I sites, one located in the coding region and the other located downstream of the 3'UTR. Re-ligation of the *Sac*I digested p494 generated an intermediate plasmid (a) into which *Bgl*II and *Asc*I sites (indicated by asterisks) were introduced sequentially at equivalent positions to those flanking the 3x HA sequence in the *Cf-9* coding region of pCBJ109 by site-directed mutagenesis (b) using the Hcr9-M205(*Bgl*II) forward and reverse primers and Hcr9-M205(*Asc*I) forward and reverse primers listed in Table 5.1. The 3x HA sequence from pCBJ109 was excised and ligated into the modified p494 plasmid via *Bgl*II and *Asc*I sites (c). **Step 2**: Plasmid HA-Hcr9-M205 was generated by a three-way ligation between a 668 bp *Cla*I-*Afl*II fragment from the modified p494 plasmid with the 3x HA sequence incorporated, a 2457 bp *Afl*II-*Bam*HI fragment from p494 containing the rest of the Hcr9-M205 coding region and *Cf-9* 3'UTR, and the 6.1 kb *Cla*I-*Bam*HI digested pCBJ306. Blue, yellow and grey bars represent Hcr9-9A, Cf-9 and 3x HA tag sequences, respectively. 3' UTR = 3' untranslated region. Only restriction sites of interest are shown. Drawings are not to scale.

Step 1

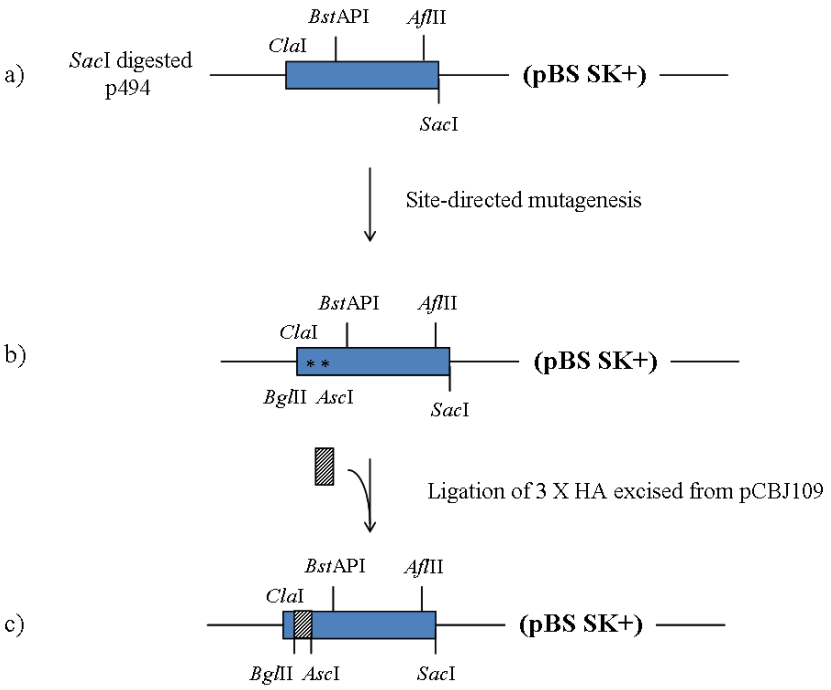
a)
SacI digested p494
BstAPI
AflII
ClaI
SacI
(pBS SK+)
Site-directed mutagenesis
b)
BstAPI
AflII
ClaI
BglII AscI
SacI
(pBS SK+)
Ligation of 3 X HA excised from pCBJ109
c)
BstAPI
AflII
ClaI
BglII AscI
SacI
(pBS SK+)

Step 2

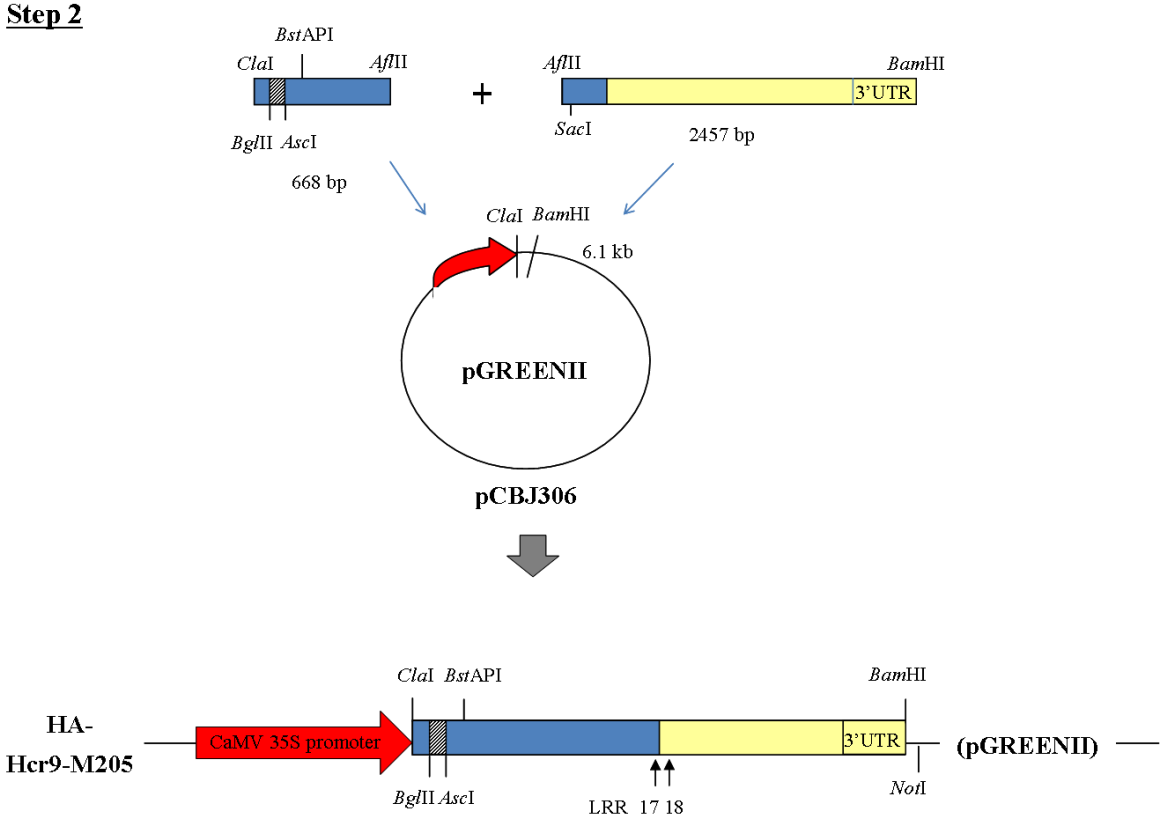
BstAPI
ClaI
AflII
BglII AscI
668 bp
+
AflII
BamHI
3'UTR
SacI
2457 bp
ClaI BamHI
6.1 kb
pGREENII
pCBJ306
HA-Hcr9-M205
CaMV 35S promoter
ClaI BstAPI
BglII AscI
LRR 17 18
BamHI
3'UTR
NotI
(pGREENII)

Primers	Sequence 5' ⟶ 3'	Mutation	Restriction Site
Hcr9-M205(*Bgl*II)F	CGTCATCCTTAgaTCtTTTGTGCCCCG	-	*Bgl*II
Hcr9-M205(*Bgl*II)R	CGGGGCACAAAaGAtcTAAGGATGACG		
Hcr9-M205(*Asc*I)F	CTTTCAACTTGTTCCCggGcgcgCCTTACCTCATTTGTG	-	*Asc*I
Hcr9-M205(*Asc*I)R	CACAAATGAGGTAGGcgcgcccGGGAACAAGTTGAAAG		
Hcr9-M205(L389C)F	GGACTACGAAATCTgCAg**Tgt**CTCCACTTGTCATC	L389C	*Pst*I
Hcr9-M205(L389C)R	GATGACAAGTGGAG**acA**cTGcAGATTTCGTAGTCC		
Hcr9-M205(H391Y)F	CGAAATCTACAATTACTg**tAC**TTGTCATCAAACCAC	H391Y	*Rsa*I
Hcr9-M205(H391Y)R	GTGGTTTGATGACAA**GTa**cAGTAATTGTAGATTTCG		
Hcr9-M205(V413E)F	CCCTTCCTTCACTGGTA**GaG**cTcGACTTGAGCAATAACAC	V413E	*Sac*I
Hcr9-M205(V413E)R	GTGTTATTGCTCAAGTCgAg**CtC**TACCAGTGAAGGAAGGG		
Hcr9-M205(T435A)F	CAAGTCCAAAACATTAATT**gCa**GTgACCCTAAAACAAAATAAGC	T435A	*Bts*I
Hcr9-M205(T435A)R	GCTTATTTTGTTTTAGGGTcAC**tGc**AATTAATGTTTTGGACTTG		
Hcr9-M205(F459L)F	CCAGCAGAGCCTAagc**TTa**CTTCTCCTTTCAC	F459L	*Hin*dIII
Hcr9-M205(F459L)R	GTGAAAGGAGAAGtAAgctTAGGCTCTGCTGG		
Cf-9(L481S)F	CTGAAAACATTGATATcGTTAGACTTGGGAAG	L481S	*Eco*RV
Cf-9(L481S)R	CTTCCCAAGTCTAACgATATCAATGTTTTCAG		

Table 5.1 List of mutagenic primers. Mutagenic nucleotides are shown in lower case. Nucleotides encoding restriction sites are underlined. Mutations involved changes of amino acid residue are in bold.

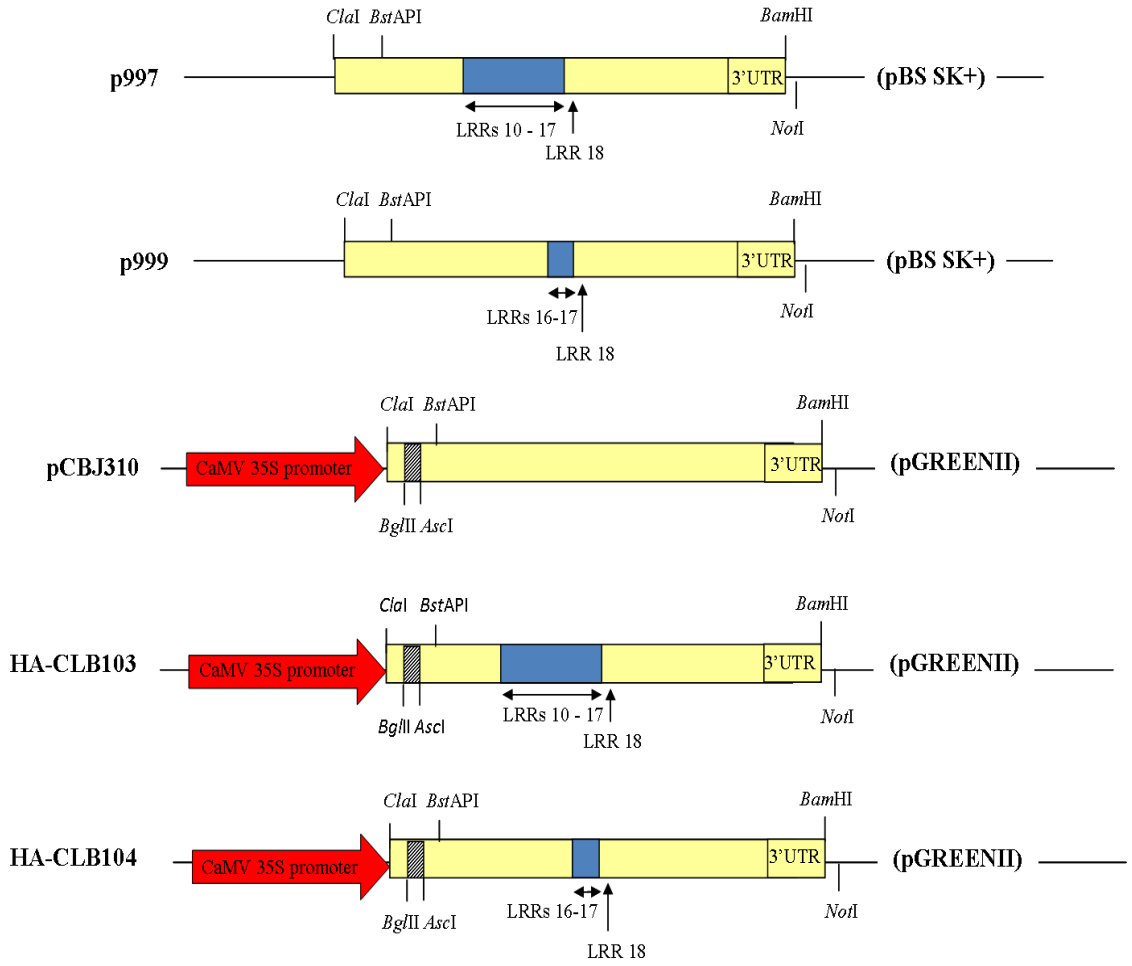

Figure 5.8 Generation of HA-tagged CLB103 and CLB104 in a pGREENII binary vector. The coding regions flanked by *Bst*API and *Not*I sites for domain swap CLB103 and CLB104 in plasmids p997 and p999 were substituted into the corresponding region in pCBJ310 using *Bst*API and *Not*I sites to generate HA-CLB103 and HA-CLB104, respectively. Blue, yellow and grey bars represent Hcr9-9A, Cf-9 and 3x HA tag sequences, respectively. 3' UTR = 3' untranslated region. Only restriction sites of interest are shown. The location of the junctions between Cf-9 and Hcr9-9A are indicated relative to specific LRRs. Drawings are not to scale.

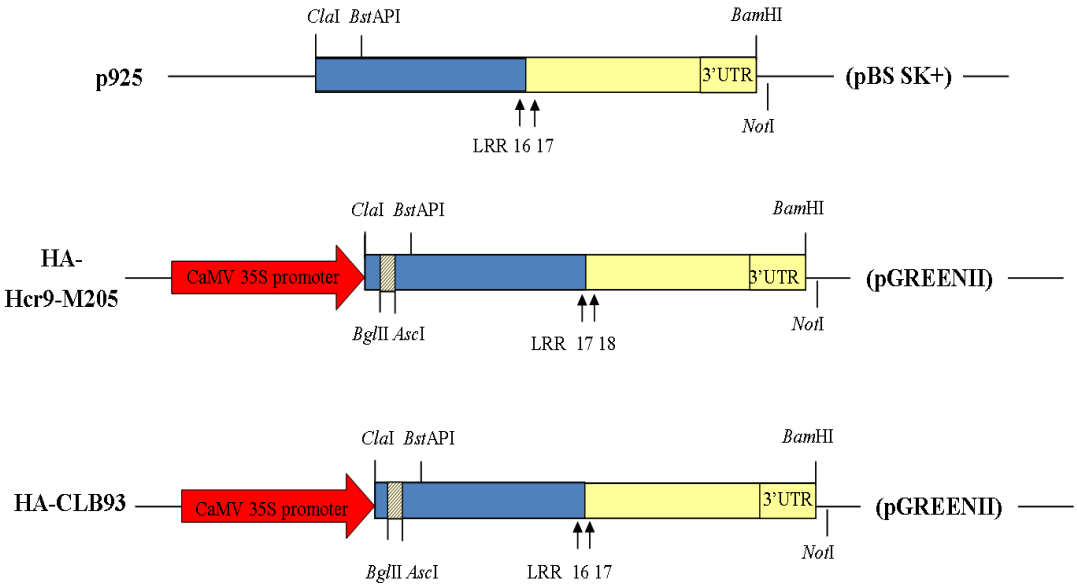

Figure 5.9 Generation of HA-tagged CLB93 in a pGREENII binary vector. The coding region flanked by *Bst*API and *Not*I sites for domain swap CLB93 in plasmid p925 was substituted into the corresponding region in pCBJ310 using *Bst*API and *Not*I sites to generate HA-CLB93. Blue, yellow and grey bars represent Hcr9-9A, Cf-9 and 3x HA tag sequences, respectively. 3' UTR = 3' untranslated region. Only restriction sites of interest are shown. The location of the junctions between Cf-9 and Hcr9-9A are indicated relative to specific LRRs. Drawings are not to scale.

5.2.3 Construction of CLB103 domain swap derivatives, Cf-9(L481S) mutant and Cf-9(SR) mutant

To generate the CLB103 domain swap derivatives CLB103V(11), CLB103V(12), CLB103V(13) and CLB103V(14), subregions containing these domain swaps were synthesized by Genscript USA Inc. or Integrated DNA Technologies Inc. and transferred into p997 as described in Figure 5.9. CLB103V(15) was generated by introducing a V413E mutation into the coding region of CLB103V(14) via site-directed mutagenesis using the M205(V413E)F and M205(V413E)R mutagenic primers listed in Table 5.1. The Cf-9(L481S) mutant was generated by introduction of L481S mutation into the Cf-9 coding region in pCBJ109 via site-directed mutagenesis using the Cf-9(L481S)F and Cf-9(L481S)R mutagenic primers listed in Table 5.1. To generate the Cf-9 (Specificity Replacement) or briefly Cf-9(SR) mutant that contains a replacement of all six specificity-determining residues (C387, Y389, E411, A433, L457 and L481) in the coding region of Cf-9 by the corresponding Cf-9A residues, the *Bsr*GI-*Hind*III fragment of the Cf-9 coding region (Figure 5.5) containing the six mutations i.e. C387L,

Y389H, E411V, A433T, L457F and L481S, was synthesized by Genscript USA Inc. and transferred into pCBJ109 via *Bsr*GI and *Hind*III sites. The coding regions and 3' UTRs of the CLB103 domain swap derivatives, Cf-9(L481S) mutant and Cf-9(SR) mutant were transferred from pBS SK+ into pCBJ310 by utilizing *Bst*API and *Not*I sites to generate HA-tagged versions of these constructs in a pGREENII binary vector, similar to the generation of HA-CLB103 and HA-CLB104 described in Section 5.2.1.

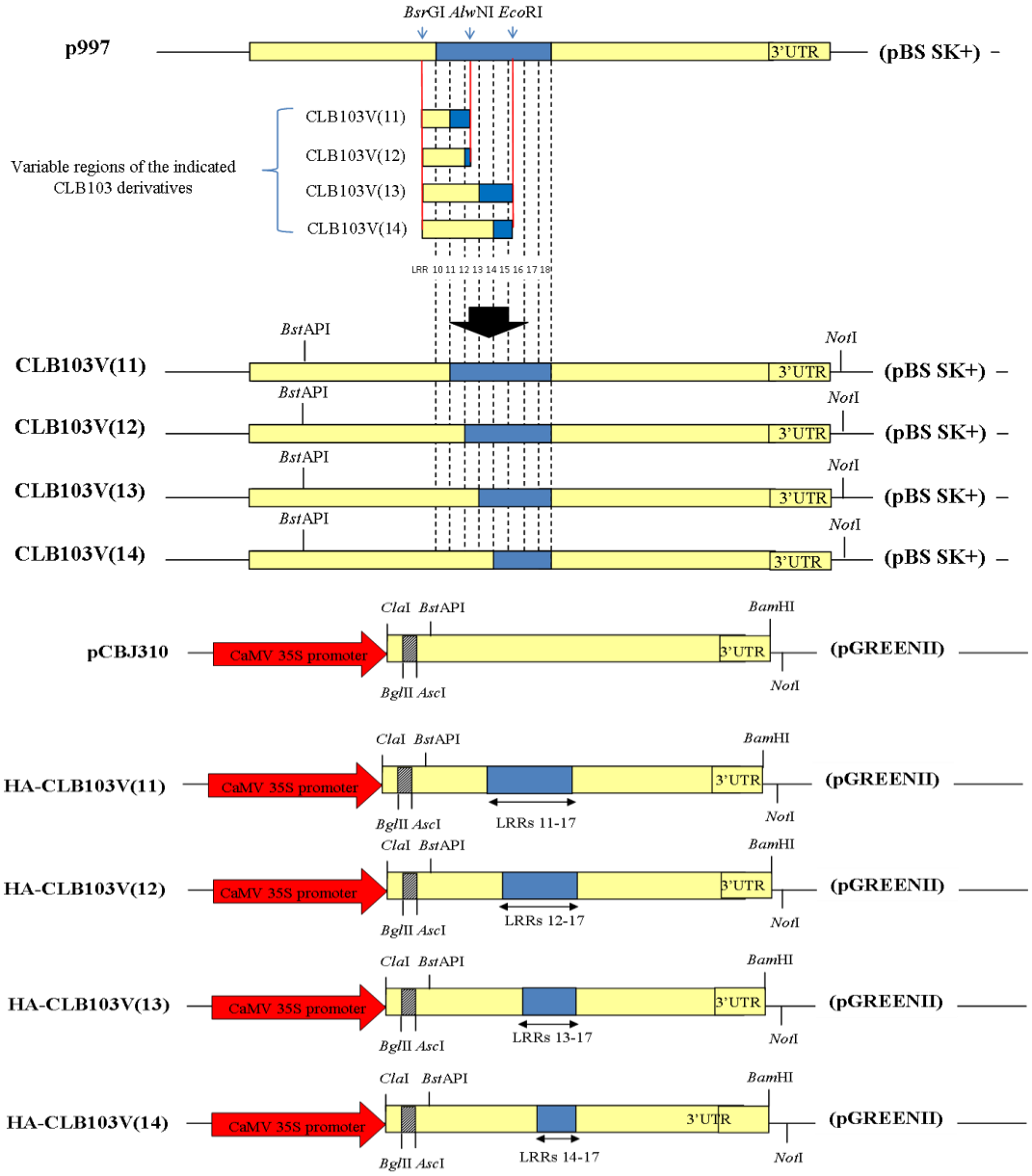

Figure 5.10 Generation of CLB103 domain swap derivatives. Subregions containing domain swaps flanked by the nearest internal restriction sites were synthesized and transferred into p997 to generate the respective CLB103 domain swap derivatives in pBS SK+. For example, the subregion synthesized for CLB103V(11) encompasses a domain swap between LRRs 11 and 12 flanked by *Bsr*GI and *Alw*NI sites. The coding

regions flanked by *Bst*API and *Not*I sites for CLB103 domain swap derivatives were substituted into the corresponding region in pCBJ310 using *Bst*API and *Not*I sites to generate HA-tagged version of these domain swaps. Blue, yellow and grey bars represent Hcr9-9A, Cf-9 and 3x HA tag sequences, respectively. 3' UTR = 3' untranslated region. Only restriction sites of interest are shown. The location of the junctions between Cf-9 and Hcr9-9A are indicated relative to specific LRRs. Drawings are not to scale.

5.2.4 Construction of Hcr9-M205 site-directed mutants

The Hcr9-M205 site-directed mutants containing the desired mutations i.e. L389C, H391Y, V413E, T435A or F459L were generated by introducing these mutations into the coding region of Hcr9-M205 via site-directed mutagenesis in p494 using the specified mutagenic primers listed in Table 5.1. The coding regions and 3' UTRs of the Hcr9-M205 site-directed mutants in pBS SK+ were subcloned into HA-Hcr9-M205 plasmid by utilizing *Bst*API and *Not*I sites to generate the HA-tagged version of these mutants in a pGREENII binary vector, similar to the generation of HA-CLB93 described in Section 5.2.1.

5.2.5 Transfer of binary vectors into *Agrobacterium tumefaciens* and *A. tumefaciens*-mediated transient gene expression in tobacco

The binary vectors were co-transformed with pSOUP (Hellens *et al.*, 2000) into *A. tumefaciens* GV3101 as described in Section 2.3.2. The presence of the binary vector in the transformants was verified by colony PCR (Section 2.2.1) using Cf-9-F (5'-GACATAAGAACATACGTA-3') and Cf-9-R (5'-GCCGTTCAAGTTGGGTGT-3') primers for constructs containing Cf-9 5' coding region (Section 5.2.3) or Hcr9-M205-F (5'-CACTCCTAAACCAGCAGAGCCTATCTT-3') and Hcr9-M205-R (5'-CATATGGATCAGAAATATACTCTGGGAA-3') primers for constructs containing the Hcr9-M205 5' coding region (Section 5.2.4). Transient gene expression of the constructs into tobacco was carried out via agroinfiltration as described in Section 2.3.3.

5.3 Results

5.3.1 A minimum Hcr9-9A substitution in LRRs 15-17 of Cf-9 is sufficient for autoactivity

An Hcr9-9A substitution in LRRs 10-17 but not in LRRs 16-17 of Cf-9 was sufficient to cause autoactivity (shown by the activity of the CLB103 and CLB104 domain swaps, respectively), indicating that signalling repression domain may involve a larger region than LRRs 16-17 but smaller than LRRs 10-17 (Section 5.1). To investigate the extent of the region involved in signalling repression, domain swapping analysis was carried out to determine the minimum Hcr9-9A substitution required for autoactivity. A series of domain swap derivatives of CLB103 were generated containing progressive reductions of the Hcr9-9A sequence from LRRs 10-17 down to LRRs 16-17 one LRR at a time (Figure 5.11 A). Agrobacterium-mediated transient expression of domain swaps Hcr9-M205, CLB103, CLB103V(11), CLB103V(12), CLB103V(13), CLB103V(14) and CLB103V(15) caused necrosis in tobacco (*N. tabacum* cv. Petit Havana) (Figures 5.11 B, and C). In contrast, CLB104 did not induce necrosis except for the occasional appearance of one or two necrotic spots (Figures 5.11 B and C). The CLB103V(14) domain swap caused a stronger and accelerated necrosis compared to Hcr9-M205 and other domain swaps, indicating enhanced autoactivity (Figure 5.11 D). Taken together, these data indicated that a minimum Hcr9-9A substitution in LRRs 15-17 of Cf-9 was sufficient to cause autoactivity.

A

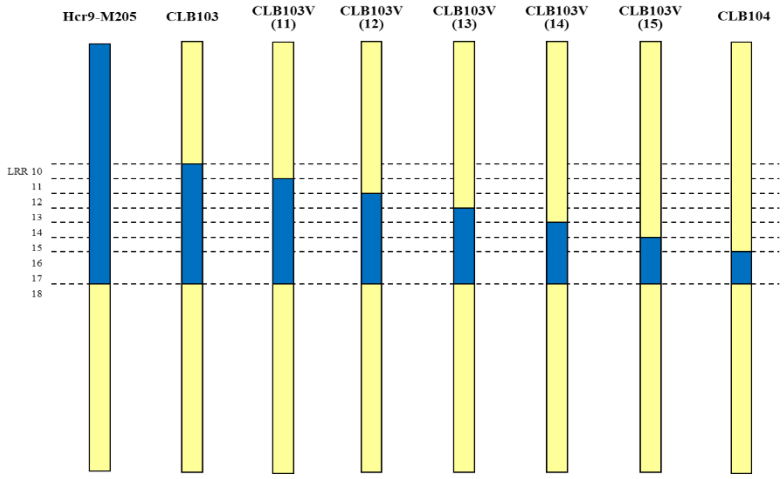

B

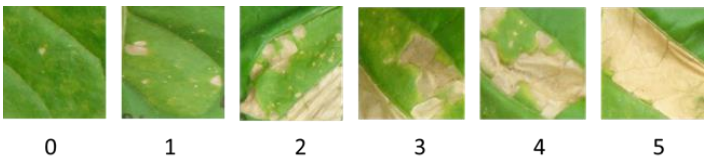

C

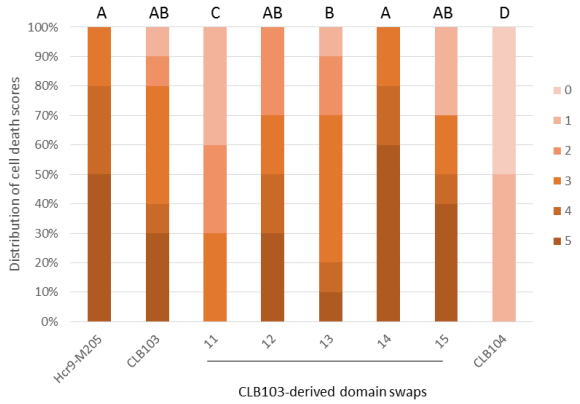

D

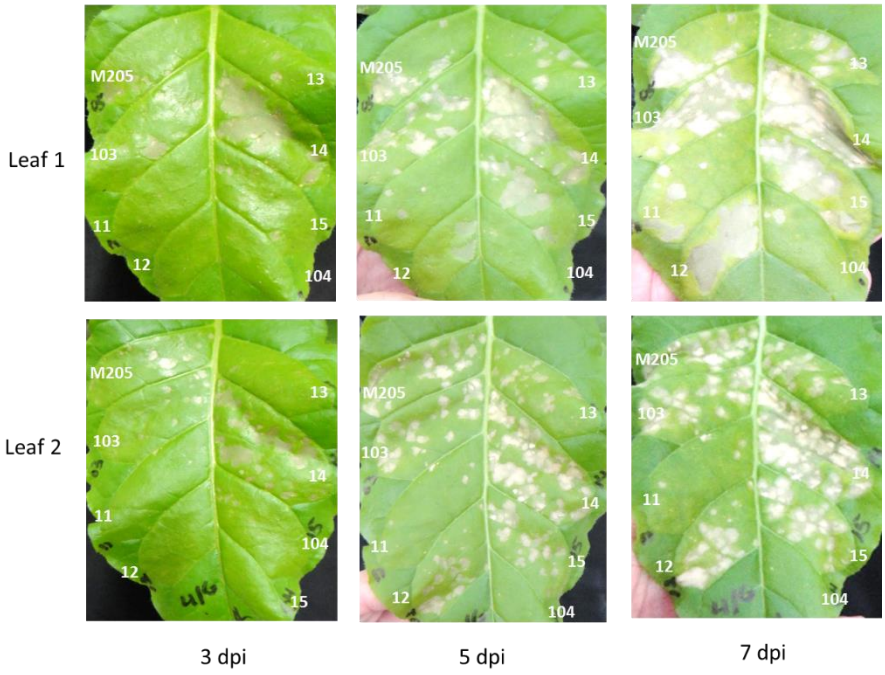

Figure 5.11 Dissection of the N-terminal Hcr9-9A sequence required for Hcr9-M205 autoactivity by domain swapping analysis. A) Domain swaps containing Hcr9-9A replacement at the N-terminus of Cf-9. Hcr9-9A-specific and Cf-9-specific sequences are indicated in blue and yellow, respectively. The extent of Hcr9-9A sequence was reduced by replacing with the corresponding Cf-9 sequence. These domain swaps were named using the prefix CLB103V to represent variants of domain swap CLB103 and the numbers in parentheses indicate the LRR where the Hcr9-9A sequences commence. For example, CLB103V(11) represents a CLB103 derivative containing Hcr9-9A sequence commencing at LRR 11. **B)** Examples of cell death responses representative for each score (ranging from 0 to 5) in the scoring system used

in this study to evaluate the necrotic response induced by agroinfiltration of Hcr9-M205-derived domain swaps in tobacco (*N. tabacum* cv. Petit Havana). 0: no visual symptoms, 1: chlorosis and/or one to three necrotic spots, 2: necrosis in approximately 25% of infiltrated area, 3: necrosis in approximately 50% of infiltrated area, 4: necrosis in approximately 75% of infiltrated area, 5: confluent necrosis. **C)** Cell death scores of Hcr9-M205, CLB103, CLB104 and CLB103-derived domain swaps at 12 dpi (days post infiltration) in *N. tabacum* based on the scoring scale indicated in **(B)**. A total of ten infiltrated leaves from at least two independent agroinfiltration experiments was scored. Letters A to D represent significant differences in cell death scores between constructs determined by pairwise one-tailed Mann–Whitney tests ($P < 0.05$). **D)** Progression of necrosis induced by Hcr9-M205 and Hcr9-M205-derived domain swaps. The CLB103V(14) domain swap consistently caused an accelerated and stronger necrotic response. Photographs were taken at 3, 5 and 7 dpi. Representative leaves from at least two independent agroinfiltration experiments (with at least five plants in each experiment) are shown.

To exclude the possibility that a reduction or loss of autoactivity in the domain swaps was due to a reduced level or lack of protein, protein gel-blot analysis was carried out on total protein extracted from *N. tabacum* leaves transiently expressing the domain swaps using anti-HA antibody. From this analysis, bands with an approximate size of 160 kDa, similar to the size of epitope-tagged Cf-9 protein observed in previous studies (Rivas *et al.*, 2002; Chakrabarti *et al.*, 2016), were detected for Hcr9-M205 and the domain swap proteins (Figure 5.12). The levels of domain swap proteins were found to be similar to that of Cf-9 or Hcr9-M205 (Figure 5.12), indicating that a reduction or loss of autoactivity in some domain swaps was not due to lack of protein or reduced protein stability. No protein band with a similar apparent molecular mass to that of Cf-9 was detected for the lane loaded with empty vector, confirming the specificity of anti-HA antibody for HA-tagged proteins in this position on the protein gel blot.

A

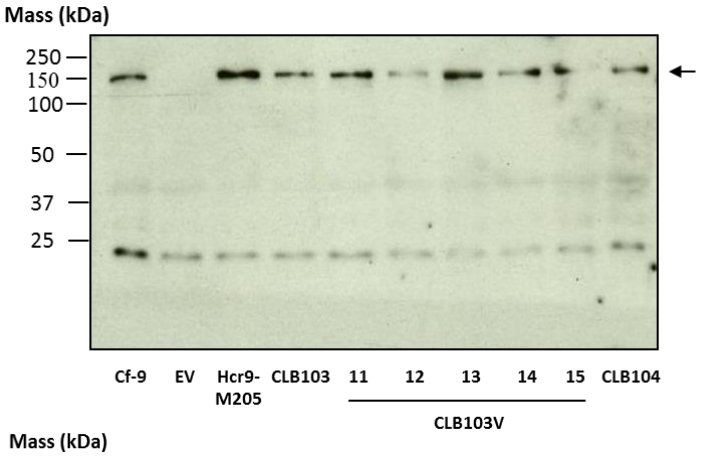

B

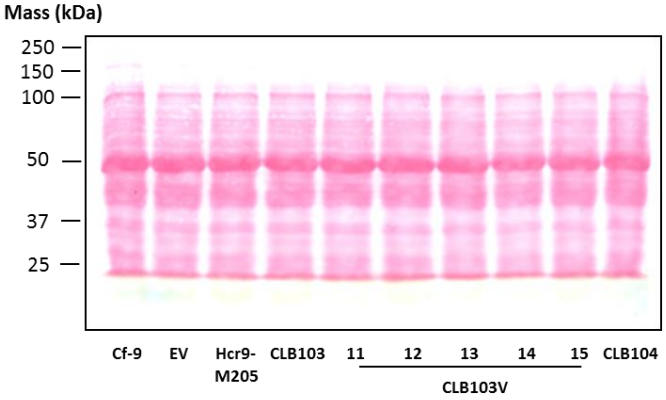

Figure 5.12 Protein expression of domain swaps defining the signalling repression domain in LRRs 10-17. A) A protein blot showing chemiluminescent detection of HA-tagged constructs using anti-HA antibody probed against total protein extracted at 2 dpi from *N. tabacum* agroinfiltrated with the denoted constructs and empty vector (EV). The positions of the HA-tagged Cf-9, Hcr9-M205 and Hcr9-M205-derived domain swaps are indicated by an arrow on the right. A representative blot from two independent experiments is shown. In each independent experiment, each construct was infiltrated into three leaf panels one from each of three different plants, which were then pooled prior to extracting proteins. **B)** Ponceau S staining of protein blot showing equal loading and transfer of protein. 15 µg of total protein extract were separated by 10% SDS-PAGE. Protein masses for Kaleidoscope™ Precision Plus pre-stained molecular weight standards (Bio-Rad) are indicated on the left.

5.3.2 Role of the Cf-9 specificity-determining residues in signalling repression

L481 in LRR 17 has been proposed to play a role in signalling repression as introduction of this residue into the corresponding position in Hcr9-M205 abolished autoactivity (shown by the inactivity of domain swap CLB93, Section 5.1). The major specificity-determining residues C387, Y389, E411, A433 and L457 located in LRRs 13-16 (Wulff *et al.*, 2001; Wulff *et al.*, 2009b) reside at similar positions to L481 in the solvent-exposed positions of the β-strand of the concave eLRR region and overlap the polymorphic positions involved in autoactivity (Figure 5.5), suggesting that they may play a role in signalling repression. To examine the role of these residues in signalling repression, a Cf-9 mutant containing a collective substitution of all five specificity-determining residues in LRRs 13-16 together with L481 in LRR 17 by the corresponding Hcr9-9A residues, designated Cf-9(SR) (SR for Specificity Replacement) (Figure 5.13 A) was generated to look for autoactivity. Transient expression of the Cf-9(SR) mutant in *N. tabacum* resulted in chlorosis with occasional necrotic flecks (Figures 5.13 B), indicating gain-of-autoactivity. These data indicate that among the 16 polymorphic positions in LRRs 13-17, substitution of six overlapping residues located at the specificity-determining positions in LRRs 13-16 and L481 in LRR 17 (Figure 5.5) was sufficient to induce a low level of autoactivity.

Further, these residues were each introduced into the corresponding positions in Hcr9-M205 by site-directed mutagenesis generating L389C (in LRR 13), H391Y (LRR 13), V413E (LRR 14), T435A (LRR 15) and F459L (LRR 16) mutations in Hcr9-M205 (Figure 5.13 A) to look for loss of autoactivity. The site-directed mutants of Hcr9-M205 generated were each transiently expressed in *N. tabacum* for assessment of necrosis induction. Domain swap CLB93 containing an S483L mutation in LRR 17 of Hcr9-M205 (Anderson *et al.* in preparation, Section 5.1; designated as Hcr9-M205(S483L) mutant in this study) was also included in this analysis (Figure 5.13 A). Note that the numbering of the amino acid residues in Hcr9-M205 differs by two from Cf-9 due to a net difference of two amino acid residues between Hcr9-M205 and Cf-9 (owing to a deletion of R57 and an insertion of three amino acids (RSW) in LRR12 of Hcr9-9A relative to Cf-9) (Figure 5.5). The response induced by the site-directed mutants compared to that of Hcr9-M205 upon agroinfiltration in tobacco indicated that the

F459L mutation in LRR 16 completely abolished necrosis, similar to the S483L mutation in LRR 17 whereas the T435A mutation in LRR 15 marginally impaired necrosis (Figure 5.13 B). In contrast, the H391Y and V413E mutations in LRRs 13 and 14, respectively did not significantly reduce necrosis (Figure 5.13 B). Unexpectedly, the L389C mutation in LRR 13 caused a stronger and accelerated necrosis compared to Hcr9-M205 (Figure 5.13 C), indicating enhanced autoactivity. Taken together, these data suggest that A433 in LRR 15 and L457 in LRR16 play a role signalling repression, similar to L481 in LRR 17 and that those located the closest to LRR 18 required for signal activation (Section 5.1) showed the greatest effect on signalling repression.

A

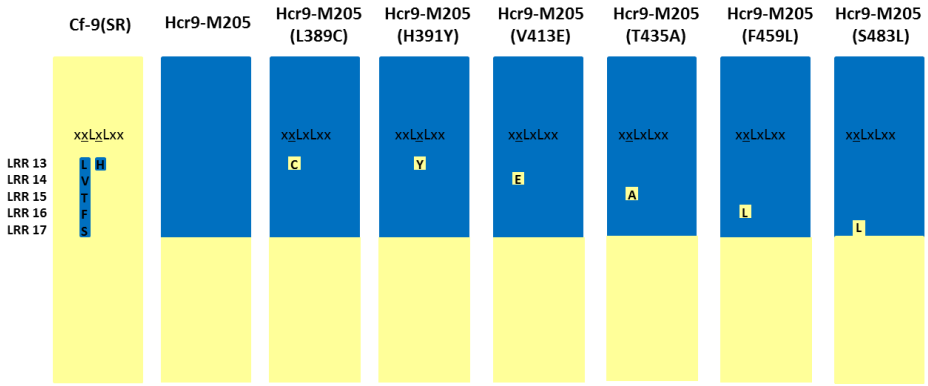

B

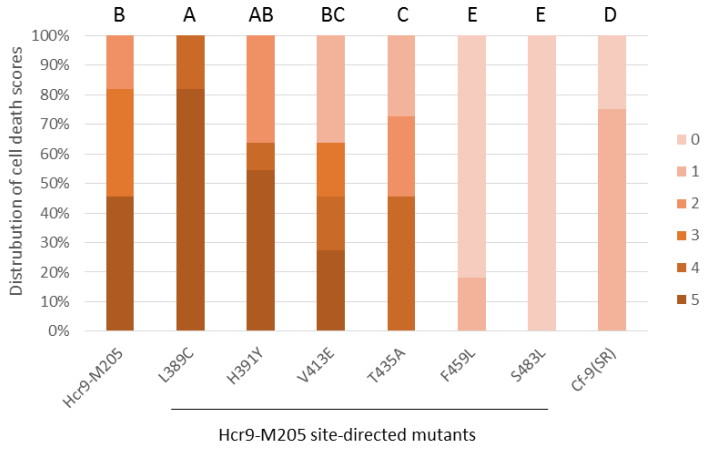

C

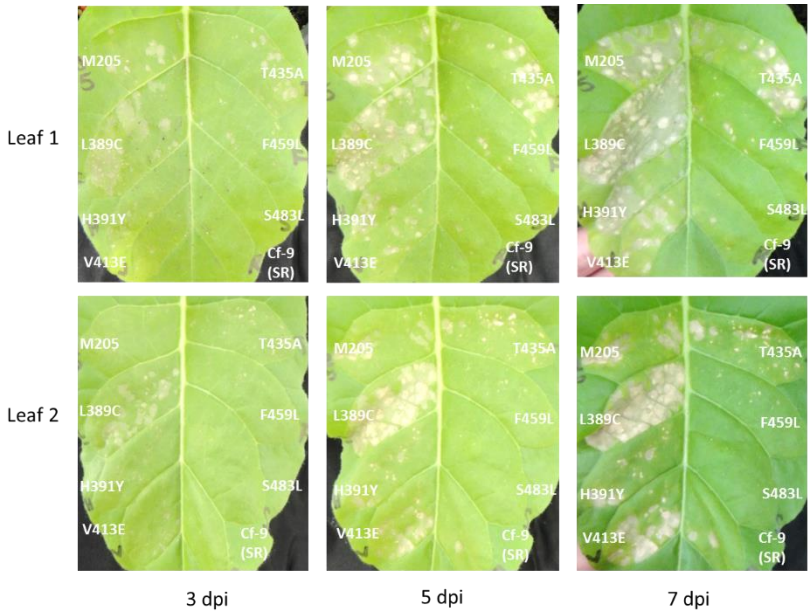

Figure 5.13 Role of the Cf-9 specificity-determining residues in autoactivity. A) Graphic representation showing the Cf-9 Specificity Replacement mutant Cf-9(SR), Hcr9-M205 and Hcr9-M205 site-directed mutants. Hcr9-9A- and Cf-9-specific residues are shown in blue and yellow, respectively. The Cf-9(SR) mutant contains a collective replacement of the Cf-9 specificity-determining residues and L481 by the corresponding Hcr9-9A residues generating six mutations comprising C387L, Y389H, E411V, A433T, L457F and L481S. The Hcr9-M205 site-directed mutants contain mutations at Cf-9 specificity-determining positions in the LRR β-sheet region (xxLxLxx) that replace the Hcr9-9A residues by the corresponding Cf-9 residues. Mutant Hcr9-M205(S483L) (also known as domain swap CLB93) from Anderson *et al.* (in preparation) was included for comparison of autoactivity. **B)** Cell death scores for Hcr9-M205, Hcr9-M205 site-directed mutants and Cf-9(SR) at 12 dpi in *N. tabacum* based on the scoring system described in Figure 5.11 (B). A total number of 11 infiltrated leaves from at least three independent agroinfiltration experiments were scored. Each constructs was included in all infiltrated leaves except for Cf-9(SR) tested in eight out of 11 leaves. Letters A to E represent significant differences in cell death scores between constructs determined by pairwise one-tailed Mann–Whitney tests ($P < 0.05$). **C)** Progression of necrosis induced by Hcr9-M205, Hcr9-M205 site-directed mutants and Cf-9(SR). The Hcr9-M205(L389C) mutant consistently caused a stronger and accelerated necrotic response. Photographs were taken at 3, 5 and 7 dpi. Representative leaves from at least three

independent agroinfiltration experiments (with at least three plants in each experiment) are shown.

Additionally, the activity of Cf-9(SR) and the Hcr9-M205 site-directed mutants were assessed by their ability to induce *E22* promoter upon agroinfiltration into the *E22*: *gusA* reporter tobacco plants generated in Chapter 3. Agroinfiltration of Cf-9(SR) in *E22*: *gusA* reporter tobacco caused an increase in GUS activity intermediate between Cf-9 and Hcr9-M205 or CLB103V(13) (Figure 5.14 A), consistent with the gain-of-autoactivity phenotype shown by the chlorotic response induced by agroinfiltration of Cf-9(SR) in *N. tabacum* (Figure 5.13 B). GUS activities induced in *E22: gusA* reporter plants by the Hcr9-M205(F459L) and Hcr9-M205(S483L) mutants were significantly reduced compared to those induced by Hcr9-M205 whereas GUS activities induced by the Hcr9-M205(H391Y), Hcr9-M205(V413E) and Hcr9-M205(T435A) mutants were at similar levels to that of Hcr9-M205 (Figure 5.14 B). In contrast, GUS activity induced by Hcr9-M205(L389C) was significantly elevated (Figure 5.14 B). Overall, the ranking of GUS activity between the Hcr9-M205 site-directed mutants was in agreement with their necrotic response (Figure 5.13 B). Unfortunately, this experiment could not be consolidated with additional biological replicates due to time constraints. These data nevertheless provide preliminary evidence on the activity of these constructs in addition to their necrosis-inducing abilities.

A

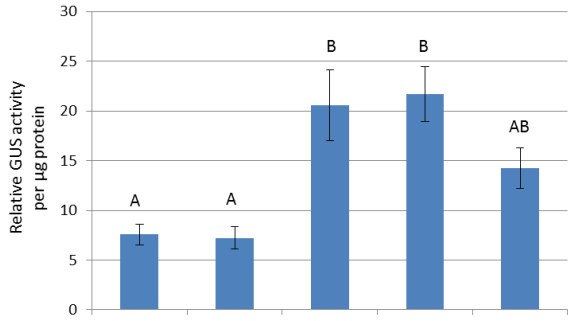

B

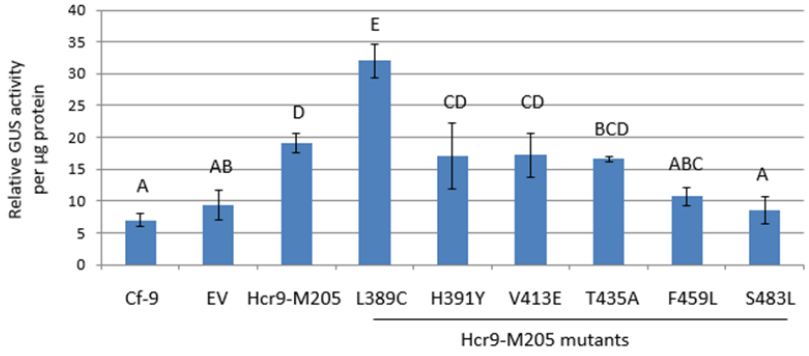

Figure 5.14 GUS activity induced in *E22* promoter: *gusA* leaf disks by site-directed mutants of Hcr9-M205 and Cf-9(SR). A) GUS activity induced by Cf-9, empty vector (EV), Hcr9-M205, the CLB103V(13) domain swap and the Cf-9(SR) mutant at 2.5 dpi following agroinfiltration into pCYT-1 (*E22: gusA*) tobacco leaves. The histogram shows the mean GUS activity from five plants (n = 5) with error bars representing standard error. **B)** GUS activity induced by agroinfiltration of Cf-9, empty vector (EV), Hcr9-M205 and its mutants at 2.5 dpi into the pCYT-1 (*E22: gusA*) tobacco leaves. The histogram shows the mean of GUS activity from three plants (n = 3) with error bars representing standard error. Statistically significant differences indicated by letters A to E were determined using ANOVA, followed by Fisher's protected Least Significant Difference (LSD) analysis ($P < 0.05$).

Protein gel-blot analysis showed accumulation of the Hcr9-M205 mutant and Cf-9(SR) proteins (Figure 5.15), indicating the reduction or loss of autoactivity observed for some of the mutants was not due to reduced level or lack of protein.

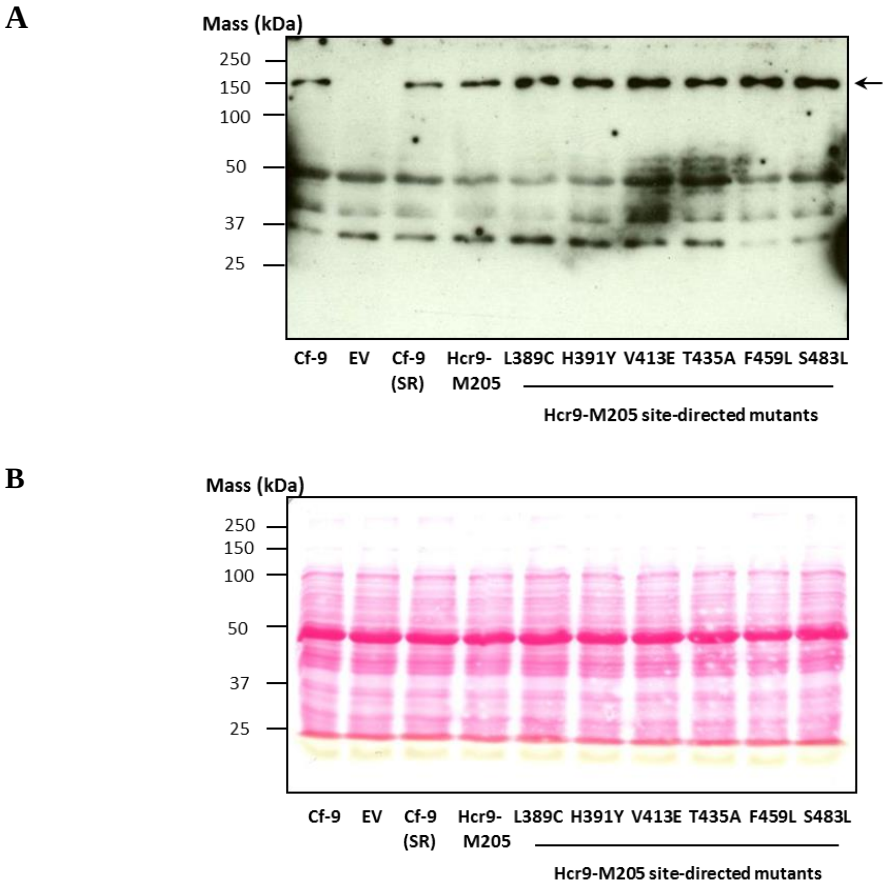

Figure 5.15 Protein expression of Hcr9-M205 site-directed mutants defining the role of the Cf-9 specificity-determining residues in LRRs 13-16 in Hcr9-M205 autoactivity. A) A protein blot showing chemiluminescent detection of protein expression using anti-HA antibody probed against total protein extracted at 2 dpi from *N. tabacum* agroinfiltrated with the denoted constructs and empty vector (EV). Positions of the HA-tagged Cf-9, Cf-9(SR), Hcr9-M205 and mutants of Hcr9-M205 are indicated by an arrow on the right. A representative blot from two independent experiments is shown. In each independent experiment, each construct was infiltrated into three leaf panels one from each of three different plants, which were then pooled prior to extracting proteins. **B)** Ponceau S staining of protein blot showing equal loading and transfer of protein. 15 µg of total protein extract were separated by 10% SDS-PAGE. Protein masses for Kaleidoscope™ Precision Plus pre-stained molecular weight standards (Bio-Rad) are indicated on the left.

5.3.3 L481 in LRR 17 is required for Avr9-dependent necrosis

L481 is located in a similar position to solvent-exposed residues in the β-strand region of LRRs 13-16 required for Avr9 recognition (Figure 5.5). Whereas L481 in LRR 17 has been implicated in signalling repression like other specificity-determining residues in LRRs 15-16 (Anderson *et al.*, in preparation; Section 5.3.2), the role of this residue in Avr9-dependent necrosis was not investigated previously. Therefore, a Cf-9 construct containing a mutation of L481 to the corresponding serine of Hcr9-9A, designated Cf-9(L481S), was generated by site-directed mutagenesis and agroinfiltrated into tobacco expressing *Avr9*. The L481S mutation in Cf-9 resulted in severely attenuated necrosis compared to wild type Cf-9 response (Figure 5.16), indicating that L481 of LRR 17 is essential for Avr9-dependent necrosis. Additionally, the Cf-9(L481S) mutant did not induce necrosis in the absence of Avr9 (data not shown), indicating that this mutant is not autoactive. As L481 is the only polymorphic residue in LRR 17 (Figure 5.5), the Cf-9(L481S) mutant is conceptually equivalent to a domain swap of Cf-9 containing an Hcr9-9A substitution in LRR 17 (Figure 5.18). The result showing this construct was not autoactive was consistent with the data from the domain swapping analysis showing a minimum Hcr9-9A substitution in LRRs 15-17 of Cf-9 is required to induce autoactivity (Section 5.3.1).

Figure 5.16 L481 in LRR17 is required for Avr9-dependent necrosis. Cf-9, the Cf-9(L481S) mutant (L481S) and empty vector control (EV) were agroinfiltrated into tobacco expressing *Avr9* to look for Avr9-dependent necrosis. Photographs were taken at 12 dpi. Representative leaves from at least three independent agroinfiltration experiments are shown.

To exclude the possibility that the loss of Avr9-dependent necrosis in the Cf-9(L481S) mutant was due to a reduced level or lack of protein, protein gel-blot analysis was carried out on total protein extracted from *N. tabacum* leaves transiently expressing Cf-9, the Cf-9(L481S) mutant and the empty vector using anti-HA antibody. From this analysis, the Cf-9(L481S) mutant protein was found to accumulate to a similar level to that of the wild-type Cf-9 protein (Figure 5.17), indicating that the L481S mutation did not affect the abundance of Cf-9 protein and therefore that the loss of Avr9-dependent necrosis was due to a loss of protein function.

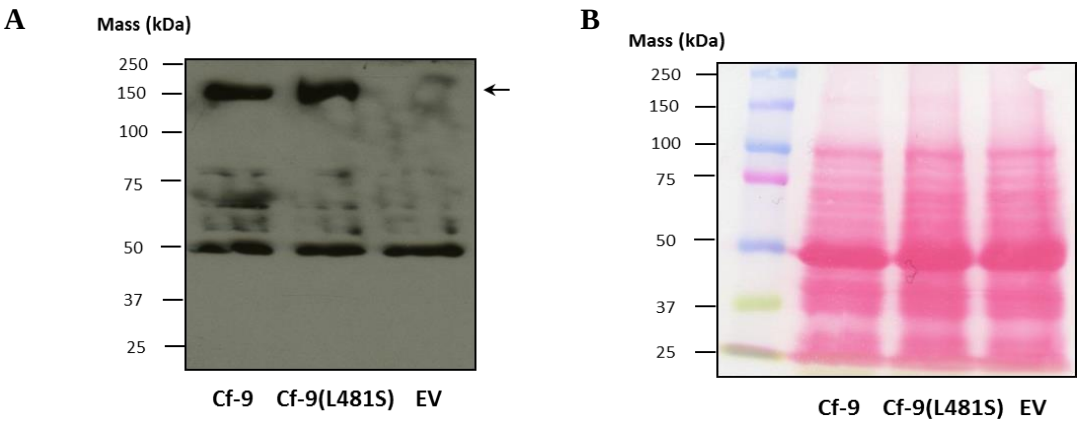

Figure 5.17 Protein expression of Cf-9 and Cf-9(L481S) mutant. A) A protein immunoblot showing chemiluminescence detection of HA-tagged Cf-9 and the Cf-9(L481S) mutant using anti-HA antibody probed against total protein extracted at 2 dpi from *N. tabacum* agroinfiltrated with Cf-9, the Cf-9(L481S) mutant and empty vector (EV). Position of the HA-tagged Cf-9 and the Cf-9(L481S) mutant are indicated by an arrow on the right. A representative blot from three independent experiments is shown. In each independent experiment, each construct was infiltrated into three leaf panels one from each of three different plants, which were then pooled prior to extracting proteins. **B)** Ponceau S staining of the protein blot showing equal loading and transfer of total proteins electroblotted onto a nitrocellulose membrane. 15 µg of total protein extract for each sample were separated by 10% SDS-PAGE. The first lane contains Kaleidoscope^{TM} Precision Plus pre-stained molecular weight standards (Bio-Rad) with the protein masses indicated on the left.

5.4 Discussion

Barker *et al.* (2006b) described a novel recombinant *Hcr9* gene designated *Hcr9-M205* that encodes an autoactive disease resistance protein. By domain swapping analysis, Anderson *et al.* (in preparation) revealed three regions involved in regulation of autoactivity: LRRs 10-17 proposed to be involved in signalling repression, LRR 18 proposed to be involved in signal activation and a C-terminal region containing the loop-out region and LRRs 24-26 proposed to be involved in enhancement of signalling (Section 5.1). The present study focused on LRRs 10-17, which may play a role in signalling repression. The identification of the molecular determinants in signalling repression was based on the hypothesis that substitution of Cf-9-specific sequences may disrupt the interactions involved in autoinhibition and cause autoactivity whereas re-introduction of these sequences may restore these autoinhibitory interactions and therefore represses autoactivity. Domain swapping analysis in LRRs 10-17 indicated that a minimum Hcr9-9A substitution in LRRs 15-17 was sufficient to cause autoactivity (Section 5.3.1). Site-directed mutagenesis revealed that similar to L481 in LRR 17 (Anderson *et al.*, in preparation; Section 5.1), the Cf-9 specificity-determining residues A433 in LRR 15 and L457 in LRR16 but not C387 and Y389 in LRR 13 and E411 in LRR 14 are involved in signalling repression (Section 5.3.2). Interestingly, the specificity-determining residues located proximate to LRR 18 showed greater effects on signalling repression, consistent with previous findings by Anderson *et al.* (in preparation) suggesting that signal activation controlled by LRR 18 is repressed by LRRs 10-17 located upstream. Taken together, these data suggest that LRRs 15-17 and LRR 18 may be involved in interactions that autoinhibit Cf-9 activity and that an Hcr9-9A substitution in LRRs 15-17 may have abrogated the autoinhibitory interactions resulting in autoactivity.

In contrast to the involvement of residues in LRRs 15-17 in signalling repression, C387 in LRR 13 enhanced autoactivity upon introduction into the Hcr9-M205 mutant Hcr9-M205(L389C) (Figure 5.13 C) Interestingly, the CLB103V(14) domain swap also exhibited accelerated and stronger necrosis (Figure 5.11 D). Both constructs contain the Cf-9-specific residue C387 in LRR 13 (Figure 5.18), indicating that C387 may enhance autoactivity. However, CLB103V(15), CLB104 and Cf-9(L481S) also contain C387 in LRR 13 but did not exhibit enhanced autoactivity, indicating that there are additional requirements for enhanced autoactivity. CLB103V(14) and Hcr9-M205(L389C) share

an Hcr9-9A substitution spanning the entire signalling repression region in LRRs 15-17 in addition to the presence of C387 in LRR 13 (Figure 5.18), suggesting that disruption of signalling repression in LRRs 15-17 can allow enhanced autoactivity by C387. CLB103, CLB103V(11), CLB103V(12) and CLB103V(13) contain Hcr9-9A substitutions in LRRs 15-17 but lack C387 in LRR 13, and therefore did not exhibit enhanced autoactivity. Conversely, CLB104 and Cf-9(L481S) contain C387 but did not exhibit enhanced autoactivity, probably because these constructs contain Cf-9 residues involved in signalling repression in LRR 15 and LRRs 15-16, respectively, that countered the effect of C387. However, CLB103V(15) contains both C387 in LRR 13 and an Hcr9-9A substitution in LRRs 15-17 but did not exhibit enhanced autoactivity. CLB103V(15) contains the Cf-9-specific residue E411 in LRR 14 which is not present in both Hcr9-M205(L389C) and CLB103V(14) (Figure 5.18), suggesting that the presence of E411 may counter the activity promoting effect by C387. Conceivably, E411 in LRR 14 may have a small contribution in signalling repression as the V413E mutation in Hcr9-M205 marginally reduced autoactivity but the effect was not sufficient to cause a significant reduction in either the cell death scores or GUS activity (Figures 5.13 B and 5.14 B).

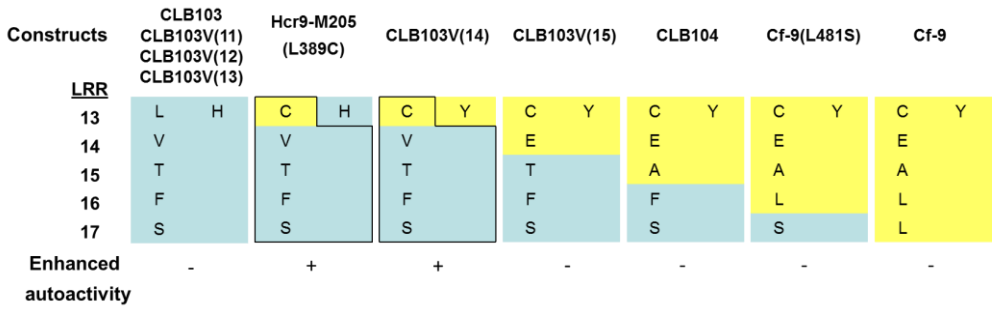

Figure 5.18 Molecular determinants of enhanced autoactivity. Diagram shows LRRs 13-17 in the Hcr9-M205 or Cf-9 domain swaps and mutants indicating the specificity-determining positions in this region. Cf-9 and Hcr9-9A residues are indicated in yellow and blue, respectively. The phenotypes of the denoted constructs that exhibited enhanced autoactivity (+), or no enhanced autoactivity (-) are indicated. The residues/regions that contribute to enhanced autoactivity are indicated by the boxed regions.

Hcr9-M205 is a recombinant Cf-9 protein that confers a weaker level of defence activation compared to Cf-9 when activated by Avr9. Seedlings from the crosses

between *Cf-9*- and *Avr9*-expressing tomato plants die soon after germination whereas the mutant M205 tomato plants survive up to maturity despite showing symptoms of defence activation (Jones *et al.*, 1994; Barker *et al.*, 2006b; Section 1.6). The reason why Hcr9-M205 confers a weaker level of activation is unclear. Inferences about Hcr9-M205 autoactivity are based on the premise that Hcr9-9A substitutions in the polymorphic positions of Cf-9 may have disrupted the autoinhibitory interactions leading to Avr9-independent immune activation. However, substitutions of these polymorphic residues may also have replaced Cf-9 residues required for activity in addition to those involved in autoinhibition. In this respect, C387 may be one such example and introduction of this residue into Hcr9-M205 may have restored interactions required for wild type activity of Cf-9. Therefore, it is postulated that an Hcr9-9A substitution in LRRs 15-17 in Cf-9 may allow a state that mimics Avr9-induced derepression; whereas introduction of C387 into the 'derepressed' protein may enhance that state, suggesting that C387 may enhance signal activation upon Avr9-induced derepression of Cf-9.

5.4.1 Role of the specificity-determining residues in Cf-9 activation

Previous domain swapping analysis, gene shuffling and site-directed mutagenesis identified the solvent-exposed β-sheet residues C387 and Y389 of LRR 13, E411 of LRR 14, A433 of LRR 15 and L457 of LRR 16 as the major specificity-determining residues of Cf-9 required for Avr9 recognition (Wulff *et al.*, 2001; Wulff *et al.*, 2009b). In plant eLRR receptors, the solvent-exposed residues in the concave surface of the eLRR domain are involved in ligand binding specificity (Leckie *et al.*, 1999; van der Hoorn *et al.*, 2001a; Di Matteo *et al.*, 2003; Dunning *et al.*, 2007; Sun *et al.*, 2013; Zhang *et al.*, 2014b). For example, site-directed mutagenesis indicates that solvent-exposed positions in the concave β-sheet of eLRRs 9-16 as being essential for flagellin recognition, which was further supported by crystal structures showing binding of flg22 to the concave β-sheet of FLS2 (Dunning *et al.*, 2007; Sun *et al.*, 2013). The involvement of the Cf-9 specificity-determining residues in the concave β-sheet surface of Cf-9 eLRRs in both Avr9 recognition and autoinhibition may provide a means of ligand-regulated receptor activation, whereby ligand recognition directly competes with autoinhibitory interactions for receptor activation. The differential involvement of the specificity-determining residues in autoinhibition, as shown by a gradient of increasing

contribution of the specificity-determining residues located proximate to LRR 18 in signaling repression may explain how Avr9 recognition induces Cf-9 activation. Given that the specificity-determining residues C387 and Y389 in LRR 13 are not involved in autoinhibition, these residues may play a role in priming ligand recognition. Full ligand recognition then outcompetes the autoinhibitory interactions located downstream in LRRs 15-18, allowing LRR 18 to facilitate signal activation upon Avr9-induced conformational change e.g. via dimerization (Section 6.1).

The present study also showed that L481 in LRR 17 is required for Avr9-dependent response (Section 5.3.3). In contrast to the specificity-determining residues located in LRRs 13-16, the conserved L481 (Parniske *et al.*, 1997; Wulff *et al.*, 2009b) may play a role in signaling per se, such as relaying signals from Avr9 recognition to allow signal activation mediated by LRR 18. It would therefore be interesting to examine the role in Avr9-dependent necrosis of H506 in LRR 18, which is located in the second solvent-exposed position of the concave β-sheet of LRR18 similar to the specificity-determining residues in LRRs 13-16 and L481 in LRR 17 (Figure 5.5). Currently, it is not known how Cf-9 recognizes Avr9. As Cf-9 does not recognize Avr9 directly and the interaction may be mediated by a high-affinity Avr9 binding site (HABS; (Kooman-Gersmann *et al.*, 1996; Kooman-Gersmann *et al.*, 1998; Luderer *et al.*, 2001), the specificity-determining residues in LRRs 13-16 or L481 in LRR 17 or H506 in LRR18 may be involved in interactions with the HABS or a HABS-Avr9 complex. Crystallography studies are needed to elucidate the structures of Cf-9 in both the autoinhibited conformation and the activated state upon Avr9 recognition and determine the interactions at the ligand recognition surface that are modified by Avr9 recognition.

5.4.2 The contribution of other polymorphic residues in LRRs 13-17 to autoinhibition

The low level of autoactivity of Cf-9(SR) compared to the CLB103V(15) domain swap indicates that polymorphic residues located in other positions in LRRs 15-17 may also contribute to autoinhibition. Therefore the six polymorphic residues i.e. S432 and R444 in LRR 15 and K453, N454, Q456 and A472 in LRR 16, additional to the three solvent-exposed residues A433 in LRR 15, L457 in LRR 16 and L457 in LRR 17 that have already been investigated, may contribute to autoinhibition (Figure 5.19). The contribution of some of these polymorphic residues in autoinhibition may have already

been addressed in part by the identification of over-represented residues among the autoactive Hcr9 proteins generated by gene shuffling compared to those that are non-autoactive (Wulff *et al.*, 2004a; Wulff *et al.*, 2009a and accompanying Supplementary Material; Figure 5.19). Nine over-represented residues were identified in these studies and these residues are located in LRRs 2 and LRRs 15 to 21 (Figure 5.19). Four out of nine of these residues namely R444, N454, L457 and A472 are located at polymorphic positions in LRRs 15 and 16 (Figure 5.19), supporting the data from the present study showing LRRs 15-17 are involved in autoinhibition. Among these residues, L457 located at the second solvent-exposed position in the β-sheet 1 region of LRR16 (Figure 5.19) was shown to be involved in autoinhibition in the present study. The other three residues include N454 and A472 located in or near the 3_{10}-helix region and R444 located in the β-sheet 2 region specific to the eLRR domain of plant eLRR proteins, suggesting that polymorphic residues located in the 3_{10} helix and β-sheet 2 may also contribute to signalling repression. These residues are potential targets for site-directed mutagenesis to examine their role in autoinhibition in future investigations.

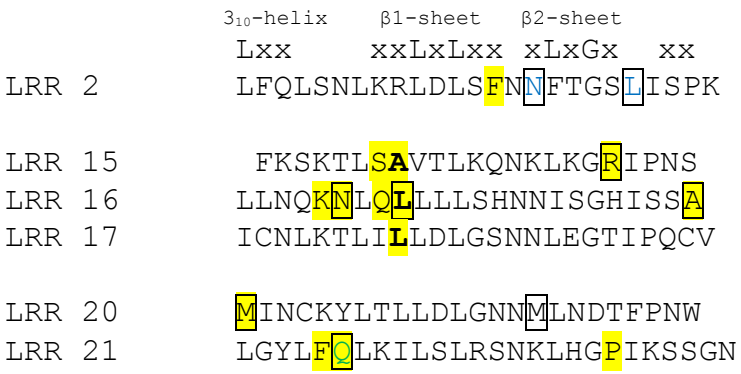

Figure 5.19 Amino acid residues that may contribute to autoinhibition. This figure shows Cf-9-specific residues in LRRs containing amino acid residues potentially involved in autoinhibition identified from the study of Hcr9-M205 autoactivity and over-represented among the autoactive Hcr9 gene shufflants (Wulff *et al.*, 2004a; Wulff *et al.* 2009a and accompanying supplementary materials). Residues polymorphic with Hcr9-M205 are highlighted in yellow. L481 demonstrated to play a role in signalling repression by Anderson *et al.* (in preparation) and A433 and L457 by the present study are shown in bold text. Positions of over-represented residues among the autoactive Hcr9 gene shufflants (Wulff *et al.*, 2004a; Wulff *et al.*, 2009a) are boxed. N127 and L132 in LRR 2 in blue text correspond to the over-represented Cf-4/Cf-4E-specific residues D127 and P132. Q575 in green text corresponds to the over-represented Cf-9B

residue H579. LRR numbers are indicated on the left. Positions of residues in the 3_{10} helix, β-sheet 1 and β-sheet 2 are indicated above the sequence.

Nevertheless, among the three solvent-exposed residues in LRRs 15-17 demonstrated to play a role in autoinhibition, only L457 was identified among the over-represented residues (Figure 5.19). This may be in part due to the fact that Hcr9-9A was not included in the gene shuffling experiment carried out by Wulff *et al.* (2004). On the other hand, only the specificity-determining residues were targeted in the present study to investigate the relationship between autoinhibition and Avr9 recognition in Cf-9 activation. These residues are located at some of the most variable positions among the Hcr9 proteins (Parniske *et al.*, 1997; Wulff *et al.*, 2009b). Therefore, these residues may not be identifiable as over-represented residues among the autoactive Hcr9 gene shufflants because of their high variability. In fact, only three out of nine over-represented residues i.e. N454 and L457 in LRR 16 and the Cf-9B-specific residue H579 in LRR 21 are highly variable residues (Figure 5.19; Figure 5 of Wulff *et al.*, 2009b). As the specificity-determining residues are located at some of the most variable positions in the Hcr9 proteins (Parniske *et al.*, 1997; Wulff *et al.*, 2009b), the higher substitution rates of specificity-determining residues also responsible for autoinhibition compared to those in other positions may lead to a greater possibility of causing autoactivation. Therefore, the involvement of residues in other positions/regions in autoinhibition may serve as additional controls to prevent or limit autoactivation by providing multiple contacts for signalling repression to ensure tight regulation of receptor activation. On the other hand, the involvement of the specificity-determining residues in the regulation of autoinhibition provides a means of ligand-specific regulation of Cf-9 activation by direct competition between ligand binding and autoinhibitory interactions.

CHAPTER 6:

General Discussion

6.1 Possible mechanisms of Cf-9 autoinhibition and activation

Evidence for autoinhibition mediated by the eLRR domain has been found in the *Drosophilla* Toll and mammalian Toll-like cell-surface receptors. For example, domain swapping and deletions of the N-terminal LRRs of Toll-like receptor 4 (TLR4) causes a ligand-independent immune activation, indicating that the eLRR domain is involved in preventing aberrant immune activation (Panter and Jerala, 2011). Similarly, deletion studies of the Toll eLRR domain indicate the presence of autoinhibitory interactions that prevent ventralization of the *Drosophilla* embryo (Winans and Hashimoto, 1995; Weber *et al.*, 2005). Other types of cell surface (non eLRR) receptors such as the human epidermal growth factor (EGF) receptor are also held in autoinhibited states via the ectodomain and ligand recognition releases these autoinhibitory interactions to enable receptor activation (Garrett *et al.*, 2002; Alvarado *et al.*, 2009).

The current model of plant eLRR receptor activation involves ligand-induced dimerization with co-receptors (Han *et al.*, 2014; Postma *et al.*, 2016). For example, FLS2 heterodimerizes with the eLRR RLK co-receptor BAK1 upon flg22 recognition to allow defence signalling (Chinchilla *et al.*, 2007; Schulze *et al.*, 2010; Sun *et al.*, 2013). Recent crystallographic studies demonstrate that BRI1 and FLS2 interact with their co-receptors SERK1 and BAK1 following the binding of brassinosteroid and flg22, respectively (Santiago *et al.*, 2013; Sun *et al.*, 2013). A recent study by Postma *et al.* (2016) has demonstrated that Cf-4 and Cf-9 interact with BAK1 in the presence of Avr4 and Avr9, respectively and that BAK1 is essential for Cf-4-mediated defence responses, suggesting that BAK1 may act as a co-receptor for these Cf receptors, similar to the role it plays with BRI1 and FLS2. On the other hand, the eLRR RLK SOBIR1 was found to associate constitutively with several plant eLRR RLPs including Cf-4 and Cf-9 irrespective of the presence of their cognate ligands (Liebrand *et al.*, 2013; Postma *et al.*, 2016). These findings suggest that SOBIR1 acts as a signalling adaptor for the eLRR RLPs, which together form an RLP-SOBIR1 heterodimer equivalent to an eLRR RLK (Liebrand *et al.*, 2013; Gust and Felix, 2014; Postma *et al.*, 2016).

Based on the data obtained from the structure/function analysis of the Cf-9 autoactive derivative, Hcr9-M205, carried out in the present study, it is postulated that autoinhibition mediated by interactions between LRRs 14-17 and LRR 18 may prevent the C-terminus of Cf-9 from interacting with BAK1 for defence signalling in the absence of Avr9 and that an Hcr9-9A substitution in LRRs 14-17 involved in signalling

repression may have abrogated these autoinhibitory interactions to allow defence signalling which normally only occurs upon a conformational change induced by Avr9 recognition. Previously, a study by Barker *et al.* (2006a) demonstrated dominant negative interference of Cf-9 activity and Hcr9-M205 autoactivity by C-terminal truncated mutants of Cf-9 terminating in LRRs 20-23. Analysis of the dominant negative interference phenomenon suggested that the regions located directly upstream and downstream of LRRs 20-23 may be involved in homodimerization and interaction with signalling partners (Barker *et al.*, 2006a). The truncation points that causes interference lies precisely between the signal activation domain (LRR 18) and signal enhancer domain (the loop-out region and LRRs 24-26) delineated by Anderson *et al.* (in preparation) (Section 5.1), suggesting that these regions may be involved in these functions. Therefore, autoinhibition may prevent one of these domains from interacting with BAK1 for signal transduction.

Several models of autoinhibition are proposed. Models of regulation of Cf-9 autoinhibition by intra- and/or intermolecular interactions between LRRs 14-17 and LRR 18 are currently conceivable. The first model proposes intramolecular interactions between LRRs 14-17 and LRR 18 in the regulation of autoinhibition (Figure 6.1 A). Crystal structures of the eLRR receptors BRI1 and FLS2 showed that the eLRR domain adopts a superhelical structure and is flexible (Hothorn *et al.*, 2011; She *et al.*, 2011; Sun *et al.*, 2013). Therefore, the specificity-determining residues in LRRs 14-17 may interact directly with LRR 18 via the side chains of these residues or indirectly via the side chains of intervening LRRs to prevent signal activation. A variation of this model might involve similar autoinhibitory interactions between LRRs 14-17 and LRR 18 within a Cf-9 dimer as illustrated in the second model (Figure 6.1 B). The second model is supported by the fact that a number of plant eLRR receptors exist in dimers prior to interaction with their cognate ligands (Wang *et al.*, 2005b; Naithani *et al.*, 2007; Sun *et al.*, 2012; Afzal *et al.*, 2013) and by genetic evidence that Cf-9 may dimerize (Barker *et al.*, 2006a). Activation of some Toll-like receptors (such as TLRs 7, 8 and 9) involves ligand-induced conformational changes of pre-formed homodimers into activated states that allow the C-termini to come into close proximity to recruit their signalling partner proteins (Gay *et al.*, 2006; Latz *et al.*, 2007; Kang and Lee, 2011; Tanji *et al.*, 2013). Similar to the Toll-like receptors, an activated homodimeric conformation of Cf-9 may be required for interactions with BAK1. It is postulated that autoinhibition in a pre-formed dimer may prevent the formation of an activated dimeric conformation which

allows interaction with BAK1 for signal transduction. In this respect, the signal activation and signal enhancer domains (Anderson *et al.*, in preparation) may be involved in mediating dimerization for signal activation and interaction with BAK1 to allow signal transduction, respectively. The biological significance of these pre-formed dimers remains unknown but it is tempting to speculate that dimerization in the absence of a ligand may play a role in autoinhibition. This leads to a third model which postulates autoinhibition mediated by intermolecular interactions between LRRs 14-17 and LRR 18 via reciprocal interactions between Cf-9 monomers in a Cf-9 dimer (Figure 6.1 C). This model is supported by the observation that the M205 phenotype is partially suppressed in the presence of the Cf-9 haplotype (Barker *et al.*, 2006b), suggesting that Cf-9 or other Hcr9 proteins present in the Cf-9 haplotype (Section 1.4.3; Barker *et al*., 2006b) may repress Hcr9-M205 autoactivity via *in trans* association. For example, signal activation in LRR 18 may be repressed by LRRs 14-17 from Cf-9 or another Hcr9 protein *in trans*.

Model four envisions autoinhibition mediated by indirect interactions between LRRs 14-17 and LRR 18 via a host protein acting as a negative regulator constitutively associated with these regions to prevent defence signalling *in trans* (Figure 6.1 D-i). As recognition of Avr9 by Cf-9 may be mediated by a host protein, it is postulated that the host protein may act as the negative regulator of Cf-9 activation in the absence of Avr9, similar to the notion that the tomato cysteine protease Rcr3 acts as a negative regulator of Cf-2 (Wulff *et al.*, 2009a). It has been proposed that Cf-2 activation may be repressed by constitutive association with Rcr3 and that Avr2 recognition may induce a conformational change in Rcr3, thereby releasing its autoinhibitory interaction to activate Cf-2 (Rooney *et al.*, 2005; Wulff *et al.*, 2009a). Similarly, Avr9 recognition may induce a conformational change of a target host protein, which may promote dissociation of this protein from Cf-9 to allow defence signalling. However, it is also possible the host protein might remain associated with Cf-9 upon ligand-induced derepression and act as an upstream signalling partner. Model four does not exclude the possibility of autoinhibition by the host protein in a Cf-9 dimer (Figure 5.21 D-ii).

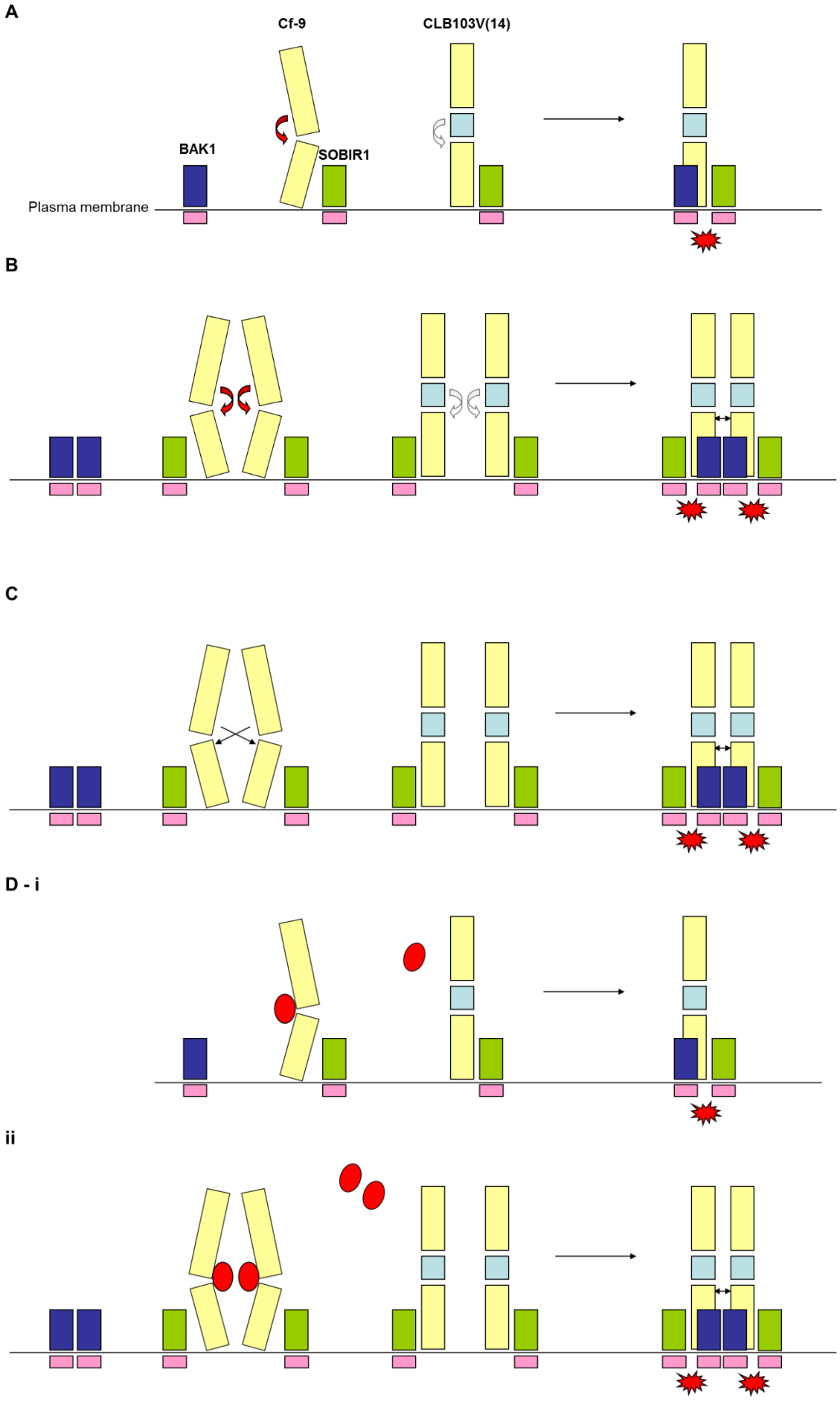
A
Cf-9
CLB103V(14)
BAK1
SOBIR1
Plasma membrane
B
C
D - i
ii

Figure 6.1 Schematic diagram representing models of autoinhibition.

A) The first model postulates that autoinhibition is regulated by intramolecular interactions between LRRs 14-17 and LRR 18 (indicated by a red arrow). Cf-9 (represented by two yellow bending rectangles depicting the twisted eLRR domain) is maintained in an autoinhibited monomeric conformation which may prevent an interaction with the co-receptor BAK1, a short eLRR RLK (dark blue). Cf-9 possibly functions as a heterodimer complex (hereafter referred to as a protomer) containing SOBIR1 (green). In the case of Hcr9-M205, an Hcr9-9A substitution (light blue) in LRRs 14-17, as exemplified by domain swap CLB103V(14) may have disrupted the autoinhibited conformation (indicated by a colourless arrow), allowing interaction with BAK1 for signal transduction possibly by transphosphorylation between the kinase domains (pink) of BAK1 and SOBIR1 (depicted by red stars).

B) Model two depicts autoinhibition in a 'Cf-9 dimer' complex consisting of two Cf-9-SOBIR1 protomers. Similar to model one, BAK1 may exist in a separate pool and only interacts with an activated Cf-9 dimer. Disruption of the autoinhibitory interactions by an Hcr9-9A substitution in LRRs 14-17 may allow formation of an activated dimer probably mediated by LRR 18 (depicted by a double head arrow). An activated dimeric conformation may be required for interaction with BAK1 for signal transduction.

C) Model three depicts autoinhibition in a Cf-9 dimer, which involves repression of signal activation in LRR 18 by LRRs 14-17 regulated by reciprocal interactions between the protomers (indicated by arrows).

D) Model four depicts autoinhibition mediated by a host protein (red oval) acting as a negative regulator by constitutive association with the autoinhibitory region to prevent signalling. This model proposes that autoinhibition may occur in the form of Cf-9 monomer (i) or in a Cf-9 dimer (ii). For the latter, Cf-9 and the host protein may form a 2:2 complex. An Hcr9-9A substitution in LRRs 14-17 may disrupt interactions with the negative regulator, allowing signalling of defence activation following interaction with BAK1 (i) or formation of an activated Cf-9 dimer required for this interaction (ii).

6.2 Future directions

The mechanisms of Cf-9 autoinhibition and activation proposed in this study are based on the model of ligand-induced interaction with BAK1 (Section 6.1). Whereas defence activation by the Cf-9 receptor is achieved by Avr9-induced interaction with BAK1, it is postulated that Hcr9-M205 may constitutively interact with BAK1 for signal transduction. Hence, future investigations may include possible interactions between Hcr9-M205 and BAK1. In addition, it would be worth investigating the downstream signal transduction pathways induced by Hcr9-M205-mediated defence activation including the involvement of BAK1 and SOBIR1 by gene silencing analysis (including Cf-9 as a control).

To test the model of ligand-induced conformational change of pre-formed dimers in Cf-9 activation, the next aspect that may be of interest for future investigations is the dimerization status of Cf-9. In contrast to the current findings indicating some of the plant eLRR receptors may be involved in dimerization (Wang *et al.*, 2005b; Naithani *et al.*, 2007; Sun *et al.*, 2012; Afzal *et al.*, 2013), crystal structures suggest that FLS2 and BRI1 do not dimerize (Hothorn *et al.*, 2011; She *et al.*, 2011; Sun *et al.*, 2013). However, the latter may not reflect the situations *in vivo*. An alternative model that could explain these discrepancies is that these cell surface receptors may exist as both monomers and higher oligomeric forms. While the role of oligomerization of cell surface receptors remains unclear, it may be involved in signal amplification (Weiss and Schlessinger, 1998). Conversely, as proposed in the models of autoinhibition (model 3) in Section 6.1, oligomeric associations may play a role in autoinhibition of defence signalling. In this respect, it may be worth investigating possible interactions between Cf-9 or other Hcr9 from the Cf-9 haplotype and Hcr9-M205 as proposed in that model suggesting signalling repression *in trans* and functionally testing possible repression of necrosis induced by Hcr9-M205 by co-expression with Cf-9 or other Hcr9 from the Cf-9 haplotype via agroinfiltration in tobacco. By taking the advantage of the availability of the transgenic *E22* promoter: *gusA* reporter tobacco generated in Chapter 3, repression of autoactivity could also be investigated by examining the induction of *E22*: GUS activity following co-expression of Hcr9-M205 and Cf-9 or other Hcr9 from the Cf-9 haplotype via agroinfiltration.

The role of the Cf-9 specificity-determining residues in LRRs 13-16 in Avr9 recognition has been investigated previously. A limitation of domain swapping analyses involving resistance proteins with different known specificities such as those carried out previously between Cf-9 and Cf-4 and between Cf-9 and Cf-9B is that such analyses may only allow the identification of the residues involved in ligand specificity or do not allow residues involved in Cf-9 activation or signal transduction to be distinguished from those involved in recognition or both. In the case of Hcr9-M205, residues that play a role in signal repression or signal activation were revealed by incompatible Cf-9/Hcr9-9A polymorphisms involved in the Avr9-independent activation of Hcr9-M205. Therefore, domain-swap analysis of Hcr9-M205 allows identification of molecular determinants involved in Cf-9 activation and signal transduction (a study of the latter having already been carried out by Anderson *et al.*, in preparation) and the present study focused on those involved in signal activation.

Additionally, a very interesting finding obtained from the analysis of Hcr9-M205 in the present study is the enhanced autoactivity caused by introduction of the Cf-9-specificity-determining residue C387 in LRR 13. In this respect, it may be significant to first answer the question of why Hcr9-M205 has a lower activity than the wild type Cf-9 protein, which is probably due to the loss of Cf-9-specific residues at polymorphic positions in the N-terminal half of the protein (Section 5.4). An example of enhanced receptor activity in an eLRR receptor protein due to a point mutation is provided by the $BRI1_{sud}$ mutant, which contains a Gly643→Glu mutation in the loop-out region and exhibits an elevated response to brassinolide. Indeed, crystallographic analysis showed that this mutation results in stabilization of the loop-out region, leading to enhanced interaction with BAK1 (Santiago *et al.*, 2013). In contrast, the L389C mutation of Hcr9-M205 is located N-terminal to the loop-out region of Cf-9, suggesting that enhanced interaction with BAK1 is unlikely. Conceivably, C387 may interact with an upstream partner such as the HABS or a hypothetical guardee of Cf-9 or Hcr9-9A. Alternatively, C387 may be involved in dimerization upon Avr9-induced conformational change in a pre-formed Cf-9 dimer (Models 2 and 3, Section 6.1), and it may be informative to investigate the dimerization status of Cf-9, Hcr9-M205 and the Hcr9-M205(L389C) mutant. An important next step would then be to elucidate the structural basis of Avr9 recognition by Cf-9.

The Hcr9-M205 domain swaps and site-directed mutants that exhibit different levels of defence activation may represent different states of Cf-9 activation ranging from autoinhibited to activated states of the receptor. These domain swaps or mutants are valuable tools that could be included in the generation of crystal structures in future investigations to elucidate receptor conformation in comparison to that of Cf-9. In this respect, it would be of great interest to investigate the protein conformation of the Hcr9-M205(L389C) mutant that exhibits enhanced level of signalling activity. Finally, as activation of defence signalling by plant cell surface eLRR receptors is often associated with receptor internalization or endocytosis (Beck *et al.*, 2012), including Cf-4, which undergoes endocytosis in the presence of Avr4 (Postma *et al.*, 2016), it would be interesting to examine the subcellular localization of Hcr9-M205, which exhibits constitutive defence activation. Determining the subcellular localization of Hcr9-M205 may further our understanding of the role of endocytosis in cell surface receptor-mediated defence signalling. In this respect, it would also be interesting to examine the subcellular localization of the Hcr9-M205(L389C) mutant, which confers an elevated level of defence signalling.

REFERENCES

Abad, Laura R; D'Urzo, Matilde Paino; Liu, Dong; Narasimhan, Meena L; Reuveni, Moshe; Zhu, Jian Kang; Niu, Xiaomu; Singh, Narendra K; Hasegawa, Paul M & Bressan, Ray A 1996. Antifungal activity of tobacco osmotin has specificity and involves plasma membrane permeabilization. *Plant Science,* **118,** 11-23.

Abe, Hiroshi; Urao, Takeshi; Ito, Takuya; Seki, Motoaki; Shinozaki, Kazuo & Yamaguchi-Shinozaki, Kazuko 2003. Arabidopsis AtMYC2 (bHLH) and AtMYB2 (MYB) function as transcriptional activators in abscisic acid signaling. *Plant Cell* **15,** 63-78.

Abe, Hiroshi; Yamaguchi-Shinozaki, Kazuko; Urao, Takeshi; Iwasaki, Toshisuke; Hosokawa, Daijiro & Shinozaki, Kazuo 1997. Role of *Arabidopsis* MYC and MYB homologs in drought-and abscisic acid-regulated gene expression. *Plant Cell* **9,** 1859-1868.

Acharya, Karan; Pal, Awadhesh K; Gulati, Arvind; Kumar, Sanjay; Singh, Anil K & Ahuja, Paramvir S 2012. Overexpression of *Camellia sinensis* thaumatin-like protein, CsTLP in potato confers enhanced resistance to *Macrophomina phaseolina* and *Phytophthora infestans* infection. *Molecular Biotechnology,* 1-14.

Ade, Jules; DeYoung, Brody J; Golstein, Catherine & Innes, Roger W 2007. Indirect activation of a plant nucleotide binding site–leucine-rich repeat protein by a bacterial protease. *Proceedings of the National Academy of Sciences,* **104,** 2531-2536.

Afzal, Ahmed; Srour, Ali; Goil, Abhishek; Vasudaven, Sheeja; Liu, Tianyun; Samudrala, Ram; Dogra, Navneet; Kohli, Punit; Malakar, Ayan & Lightfoot, David 2013. Homo-dimerization and ligand binding by the leucine-rich repeat domain at RHG1/RFS2 underlying resistance to two soybean pathogens. *BMC Plant Biology,* **13,** 43.

Albrecht, Huguette; van de Rhee, Miranda D & Bol, John F 1992. Analysis of *cis*-regulatory elements involved in induction of a tobacco *PR-5* gene by virus infection. *Plant Molecular Biology,* **18,** 155-158.

Alfano, James R & Collmer, Alan 2004. Type III secretion system effector proteins: double agents in bacterial disease and plant defense. *Annual Review of Phytopathology,* **42,** 385-414.

Alvarado, Diego; Klein, Daryl E & Lemmon, Mark A 2009. ErbB2 resembles an autoinhibited invertebrate epidermal growth factor receptor. *Nature,* **461,** 287-291.

Anwar, Muhammad Ayaz; Basith, Shaherin & Choi, Sangdun 2013. Negative regulatory approaches to the attenuation of Toll-like receptor signaling. *Experimental & Molecular Medicine,* **45,** e11.

Anžlovar, Sabina & Dermastia, Marina 2003. The comparative analysis of osmotins and osmotin-like PR-5 proteins. *Plant Biology,* **5,** 116-124.

Asai, Tsuneaki; Tena, Guillaume; Plotnikova, Joulia; Willmann, Matthew R; Chiu, Wan-Ling; Gomez-Gomez, Lourdes; Boller, Thomas; Ausubel, Frederick M & Sheen, Jen 2002. MAP kinase signalling cascade in *Arabidopsis* innate immunity. *Nature,* **415,** 977-983.

Ashfield, Tom; Hammond-Kosack, Kim E; Harrison, Kate & Jones, Jonathan DG 1994. *Cf* gene-dependent induction of a β-1, 3-glucanase promoter in tomato plants infected with *Cladosporium fulvum*. *Molecular Plant-Microbe Interactions,* **7,** 645-656.

Ausubel, Frederick M 2005. Are innate immune signaling pathways in plants and animals conserved? *Nature Immunology,* **6,** 973-979.

Axtell, Michael J & Staskawicz, Brian J 2003. Initiation of *RPS2*-Specified Disease Resistance in *Arabidopsis* Is Coupled to the AvrRpt2-Directed Elimination of RIN4. *Cell,* **112,** 369-377.

Baker, Stokes S; Wilhelm, Kathy S & Thomashow, Michael F 1994. The 5′ -region of *Arabidopsis thaliana cor15a* has *cis*-acting elements that confer cold-, drought-and ABA-regulated gene expression. *Plant Molecular Biology,* **24,** 701-713.

Bar, Maya; Sharfman, Miya; Ron, Mily & Avni, Adi 2010. BAK1 is required for the attenuation of ethylene-inducing xylanase (Eix) induced defense responses by the decoy receptor LeEix1. *The Plant Journal,* **63,** 791-800.

Bari, Rajendra & Jones, Jonathan DG 2009. Role of plant hormones in plant defence responses. *Plant Molecular Biology,* **69,** 473-488.

Barker, Claire L. **2002**. An examination of the signalling capacity of the tomato Cf-9 disease resistance protein. Ph.D. thesis submitted to the Australian National University (ANU), Canberra, Australia.

Barker, Claire L; Baillie, Brett K; Hammond-Kosack, Kim E; Jones, Jonathan DG & Jones, David A 2006a. Dominant-negative interference with defence signalling by truncation mutations of the tomato *Cf-9* disease resistance gene. *The Plant Journal,* **46,** 385-399.

Barker, Claire L; Talbot, Stephen J; Jones, Jonathan DG & Jones, David A 2006b. A tomato mutant that shows stunting, wilting, progressive necrosis and constitutive expression of defence genes contains a recombinant *Hcr9* gene encoding an autoactive protein. *The Plant Journal,* **46,** 369-384.

Beck, Martina; Heard, William; Mbengue, Malick & Robatzek, Silke 2012. The INs and OUTs of pattern recognition receptors at the cell surface. *Current Opinion in Plant Biology,* **15,** 367-374.

Belfanti, Enrico; Silfverberg-Dilworth, Eve; Tartarini, Stefano; Patocchi, Andrea; Barbieri, Massimo; Zhu, Jun; Vinatzer, Boris A; Gianfranceschi, Luca; Gessler, Cesare & Sansavini, Silviero 2004. The *HcrVf2* gene from a wild apple confers scab resistance to a transgenic cultivated variety. *Proceedings of the National Academy of Sciences* **101,** 886-890.

Belkhadir, Youssef; Nimchuk, Zachary; Hubert, David A; Mackey, David & Dangl, Jeffery L 2004. Arabidopsis RIN4 negatively regulates disease resistance mediated by RPS2 and RPM1 downstream or independent of the NDR1 signal modulator and is not required for the virulence functions of bacterial type III effectors AvrRpt2 or AvrRpm1. *Plant Cell,* **16,** 2822-2835.

Bell, Jessica K; Mullen, Gregory ED; Leifer, Cynthia A; Mazzoni, Alessandra; Davies, David R & Segal, David M 2003. Leucine-rich repeats and pathogen recognition in Toll-like receptors. *Trends in Immunology,* **24,** 528-533.

Bella, J; Hindle, KL; McEwan, PA & Lovell, SC 2008. The leucine-rich repeat structure. *Cellular and Molecular Life Sciences,* **65,** 2307-2333.

Bendahmane, Abdelhafid; Farnham, Garry; Moffett, Peter & Baulcombe, David C 2002. Constitutive gain-of-function mutants in a nucleotide binding site–leucine rich repeat protein encoded at the *Rx* locus of potato. *The Plant Journal,* **32,** 195-204.

Benghezal, Mohammed; Wasteneys, Geoffrey O & Jones, David A 2000. The C-terminal dilysine motif confers endoplasmic reticulum localization to type I membrane proteins in plants. *Plant Cell,* **12,** 1179-1201.

Bennett, Mark; Gallagher, Matthew; Fagg, Jean; Bestwick, Charles; Paul, Teresa; Beale, Michael & Mansfield, John 1996. The hypersensitive reaction,

membrane damage and accumulation of autofluorescent phenolics in lettuce cells challenged by *Bremia lactucae*. *The Plant Journal,* **9,** 851-865.

Bernoux, Maud; Ve, Thomas; Williams, Simon; Warren, Christopher; Hatters, Danny; Valkov, Eugene; Zhang, Xiaoxiao; Ellis, Jeffrey G; Kobe, Bostjan & Dodds, Peter N 2011. Structural and functional analysis of a plant resistance protein TIR domain reveals interfaces for self-association, signaling, and autoregulation. *Cell Host & Microbe,* **9,** 200-211.

Bhat, SR & Srinivasan, S 2002. Molecular and genetic analyses of transgenic plants: Considerations and approaches. *Plant Science,* **163,** 673-681.

Bi, Dongling; Cheng, Yu Ti; Li, Xin & Zhang, Yuelin 2010. Activation of plant immune responses by a gain-of-function mutation in an atypical receptor-like kinase. *Plant Physiology,* **153,** 1771-1779.

Bimboim, HC & Doly, J 1979. A rapid alkaline extraction procedure for screening recombinant plasmid DNA. *Nucleic Acids Research,* **7,** 1513-1523.

Blatt, Michael R; Grabov, Alexander; Brearley, Jane; Hammond-Kosack, Kim & Jones, Jonathan DG 1999. K+ channels of *Cf-9* transgenic tobacco guard cells as targets for *Cladosporium fulvum Avr9* elicitor-dependent signal transduction. *The Plant Journal,* **19,** 453-462.

Boller, Thomas & Felix, Georg 2009. A renaissance of elicitors: perception of microbe-associated molecular patterns and danger signals by pattern-recognition receptors. *Annual Review of Plant Biology,* **60,** 379-406.

Boller, Thomas & He, Sheng Yang 2009. Innate immunity in plants: an arms race between pattern recognition receptors in plants and effectors in microbial pathogens. *Science* **324,** 742.

Bolton, Melvin D; van Esse, H Peter; Vossen, Jack H; de Jonge, Ronnie; Stergiopoulos, Ioannis; Stulemeijer, Iris JE; van den Berg, Grardy; Borrás-Hidalgo, Orlando; Dekker, Henk L & de Koster, Chris G 2008. The novel *Cladosporium fulvum* lysin motif effector Ecp6 is a virulence factor with orthologues in other fungal species. *Molecular Microbiology,* **69,** 119-136.

Bombarely, Aureliano; Rosli, Hernan G; Vrebalov, Julia; Moffett, Peter; Mueller, Lukas A & Martin, Gregory B 2012. A draft genome sequence of *Nicotiana benthamiana* to enhance molecular plant-microbe biology research. *Molecular Plant-Microbe Interactions,* **25,** 1523-1530.

Bomblies, Kirsten; Lempe, Janne; Epple, Petra; Warthmann, Norman; Lanz, Christa; Dangl, Jeffery L & Weigel, Detlef 2007. Autoimmune response as a mechanism for a Dobzhansky-Muller-type incompatibility syndrome in plants. *PLoS Biology,* **5,** e236.

Bond, TET 1938. Infection experiments with *Cladosporium fulvum* Cooke and related species. *Annals of Applied Biology,* **25,** 277-307.

Bowen, Joanna K; Mesarich, Carl H; Bus, Vincent GM; Beresford, Robert M; Plummer, Kim M & Templeton, Matthew D 2011. *Venturia inaequalis*: the causal agent of apple scab. *Molecular Plant Pathology,* **12,** 105-122.

Bradford, Marion M 1976. A rapid and sensitive method for the quantitation of microgram quantities of protein utilizing the principle of protein-dye binding. *Analytical Biochemistry,* **72,** 248-254.

Brading, Penny A; Hammond-Kosack, Kim E; Parr, Adrian & Jones, Jonathan DG 2000. Salicylic acid is not required for Cf-2- and Cf-9-dependent resistance of tomato to *Cladosporium fulvum*. *The Plant Journal,* **23,** 305-318.

Brederode, Frans T; Linthorst, Huub JM & Bol, John F 1991. Differential induction of acquired resistance and *PR* gene expression in tobacco by virus infection, ethephon treatment, UV light and wounding. *Plant Molecular Biology,* **17,** 1117-1125.

Buchel, Annemarie S; Brederode, Frans T; Bol, John F & Linthorst, Huub JM 1999. Mutation of GT-1 binding sites in the *PR-1A* promoter influences the level of inducible gene expression *in vivo*. *Plant Molecular Biology,* **40,** 387-396.

Castresana, Carmen; de Carvalho, Fernanda; Gheysen, Godelieve; Habets, Marianne; Inzé, Dirk & van Montagu, Marc 1990. Tissue-specific and pathogen-induced regulation of a *Nicotiana plumbaginifolia* β-1,3-glucanase gene. *Plant Cell,* **2,** 1131-1143.

Catanzariti, Ann-Maree; Dodds, Peter N; Ve, Thomas; Kobe, Bostjan; Ellis, Jeffrey G & Staskawicz, Brian J 2010. The AvrM effector from flax rust has a structured C-terminal domain and interacts directly with the M resistance protein. *Molecular Plant-Microbe Interactions,* **23,** 49-57.

Chaerle, Laury; Caeneghem, Wim Van; Messens, Eric; Lambers, Hans; van Montagu, Marc & van der Straeten, Dominique 1999. Presymptomatic visualization of plant-virus interactions by thermography. *Nature Biotechnology,* **17,** 813-816.

Chaerle, Laury & van der Straeten, Dominique 2000. Imaging techniques and the early detection of plant stress. *Trends in Plant Science,* **5,** 495-501.

Chakrabarti, Apratim. **2005**. Structure-function analysis of Cf-9 and Cf-9B resistance proteins from tomato (*Lycopersicon esculentum* Mill.). Ph.D. thesis submitted to the Australian National University (ANU), Canberra, Australia.

Chakrabarti, Apratim; Panter, Stephen N; Harrison, Kate; Jones, Jonathan DG & Jones, David A 2009. Regions of the Cf-9B disease resistance protein able to cause spontaneous necrosis in *Nicotiana benthamiana* lie within the region controlling pathogen recognition in tomato. *Molecular Plant-Microbe Interactions,* **22,** 1214-1226.

Chakrabarti, Apratim; Velusamy, Thilaga; Tee, Choon Yang & Jones, David A 2016. A mutational analysis of the cytosolic domain of the tomato Cf-9 disease-resistance protein shows that membrane-proximal residues are important for Avr9-dependent necrosis. *Molecular Plant Pathology,* **17,** 565-576.

Chan, Chui-Sien; Guo, Lankai & Shih, Ming-Che 2001. Promoter analysis of the nuclear gene encoding the chloroplast glyceraldehyde-3-phosphate dehydrogenase B subunit of *Arabidopsis thaliana*. *Plant Molecular Biology,* **46,** 131-141.

Cheng, Cheng; Gao, Xiquan; Feng, Baomin; Sheen, Jen; Shan, Libo & He, Ping 2013. Plant immune response to pathogens differs with changing temperatures. *Nature Communications,* **4,** 2530.

Chinchilla, Delphine; Zipfel, Cyril; Robatzek, Silke; Kemmerling, Birgit; Nürnberger, Thorsten; Jones, Jonathan DG; Felix, Georg & Boller, Thomas 2007. A flagellin-induced complex of the receptor FLS2 and BAK1 initiates plant defence. *Nature,* **448,** 497-500.

Choi, Jaemyung; Choi, Daeseok; Lee, Seungchul; Ryu, Choong-Min & Hwang, Ildoo 2011. Cytokinins and plant immunity: old foes or new friends? *Trends in Plant Science,* **16,** 388-394.

Choi, Jaemyung; Huh, Sung Un; Kojima, Mikiko; Sakakibara, Hitoshi; Paek, Kyung-Hee & Hwang, Ildoo 2010. The Cytokinin-Activated Transcription Factor ARR2 Promotes Plant Immunity via TGA3/NPR1-Dependent Salicylic Acid Signaling in Arabidopsis. *Developmental Cell,* **19,** 284-295.

Clark, SE; Williams, RW & Meyerowitz, EM 1997. The *CLAVATA1* gene encodes a putative receptor kinase that controls shoot and floral meristem size in Arabidopsis. *Cell,* **89,** 575 - 585.

Coll, NS; Epple, P & Dangl, JL 2011. Programmed cell death in the plant immune system. *Cell Death & Differentiation,* **18,** 1247-1256.

Collier, Sarah M & Moffett, Peter 2009. NB-LRRs work a "bait and switch" on pathogens. *Trends in Plant Science,* **14,** 521-529.

Cooke, MC 1883. New american fungi. *Grevillea,* **12,** 22-33.

Cornelissen, Ben J. C.; Hooft van Huijsduijnen, Rob A. M. & Bol, John F. 1986. A tobacco mosaic virus-induced tobacco protein is homologous to the sweet-tasting protein thaumatin. *Nature,* **321,** 531-532.

Côté, François; Cutt, John R.; Asselin, Alain & Klessig, Daniel F. 1991. Pathogenesis-related acidic *β*-1,3-glucanase genes of tobacco are regulated by both stress and developmental signals. *Molecular Plant-Microbe Interactions,* **4,** 173-181.

Dangl, Jeffery L & Jones, Jonathan DG 2001. Plant pathogens and integrated defence responses to infection. *Nature,* **411,** 826-833.

Das, Manaswini; Chauhan, Harsh; Chhibbar, Anju; Haq, Qazi Mohd Rizwanul & Khurana, Paramjit 2011. High-efficiency transformation and selective tolerance against biotic and abiotic stress in mulberry, *Morus indica* cv. K2, by constitutive and inducible expression of tobacco osmotin. *Transgenic Research,* **20,** 231-246.

Datta, K; Velazhahan, R; Oliva, N; Ona, I; Mew, T; Khush, GS; Muthukrishnan, S & Datta, SK 1999. Over-expression of the cloned rice thaumatin-like protein (PR-5) gene in transgenic rice plants enhances environmental friendly resistance to *Rhizoctonia solani* causing sheath blight disease. *Theoretical and Applied Genetics,* **98,** 1138-1145.

Day, Brad; Dahlbeck, Douglas; Huang, Jeffrey; Chisholm, Stephen T; Li, Donghui & Staskawicz, Brian J 2005. Molecular basis for the RIN4 negative regulation of RPS2 disease resistance. *Plant Cell,* **17,** 1292-1305.

de Jong, Camiel F; Honee, Guy; Joosten, Matthieu HAJ & de Wit, Pierre JGM 2000. Early defence responses induced by AVR9 and mutant analogues in tobacco cell suspensions expressing the *Cf-9* resistance gene. *Physiological and Molecular Plant Pathology,* **56,** 169-177.

de Jong, Camiel F; Laxalt, Ana M; Bargmann, Bastiaan OR; de Wit, Pierre JGM; Joosten, Matthieu HAJ & Munnik, Teun 2004. Phosphatidic acid accumulation is an early response in the *Cf-4/Avr4* interaction. *The Plant Journal,* **39,** 1-12.

de Jong, Camiel F; Takken, Frank LW; Cai, Xinzhong; de Wit, Pierre JGM & Joosten, Matthieu HAJ 2002. Attenuation of Cf-mediated defense responses at elevated temperatures correlates with a decrease in elicitor-binding sites. *Molecular Plant-Microbe Interactions,* **15,** 1040-1049.

de Jonge, Ronnie; van Esse, H Peter; Kombrink, Anja; Shinya, Tomonori; Desaki, Yoshitake; Bours, Ralph; van der Krol, Sander; Shibuya, Naoto; Joosten, Matthieu HAJ & Thomma, Bart PHJ 2010. Conserved fungal LysM effector Ecp6 prevents chitin-triggered immunity in plants. *Science,* **329,** 953-955.

de Jonge, Ronnie; van Esse, Peter H; Maruthachalam, Karunakaran; Bolton, Melvin D; Santhanam, Parthasarathy; Saber, Mojtaba Keykha; Zhang, Zhao; Usami, Toshiyuki; Lievens, Bart; Subbarao, Krishna V & Thomma, Bart PHJ 2012. Tomato immune receptor Ve1 recognizes effector of multiple fungal pathogens uncovered by genome and RNA sequencing. *Proceedings of the National Academy of Sciences,* **109,** 5110-5115.

de Kock, Maarten JD; Brandwagt, Bas F; Bonnema, Guusje; de Wit, Pierre JGM & Lindhout, Pim 2005. The tomato Orion locus comprises a unique class of *Hcr9* genes. *Molecular Breeding,* **15,** 409-422.

de Wit, Pierre JGM 1977. A light and scanning-electron microscopic study of infection of tomato plants by virulent and avirulent races of *Cladosporium fulvum*. *Netherlands Journal of Plant Pathology,* **83,** 109-122.

de Wit, Pierre JGM 1992. Molecular characterization of gene-for-gene systems in plant-fungus interactions and the application of avirulence genes in control of plant pathogens. *Annual Review of Phytopathology,* **30,** 391-418.

de Wit, Pierre JGM; Van Der Burgt, Ate; Ökmen, Bilal; Stergiopoulos, Ioannis; Abd-Elsalam, Kamel A; Aerts, Andrea L; Bahkali, Ali H; Beenen, Henriek G; Chettri, Pranav & Cox, Murray P 2012. The genomes of the fungal plant pathogens *Cladosporium fulvum* and *Dothistroma septosporum* reveal adaptation to different hosts and lifestyles but also signatures of common ancestry. *PLoS Genetics,* **8,** e1003088.

Delledonne, Massimo; Zeier, Jürgen; Marocco, Adriano & Lamb, Chris 2001. Signal interactions between nitric oxide and reactive oxygen intermediates in the plant hypersensitive disease resistance response. *Proceedings of the National Academy of Sciences,* **98,** 13454-13459.

Després, Charles; Chubak, Catherine; Rochon, Amanda; Clark, Rena; Bethune, Terry; Desveaux, Darrell & Fobert, Pierre R 2003. The Arabidopsis NPR1 disease resistance protein is a novel cofactor that confers redox regulation of DNA binding activity to the basic domain/leucine zipper transcription factor TGA1. *Plant Cell,* **15,** 2181-2191.

Di Matteo, A; Federici, L; Mattei, B; Salvi, G; Johnson, KA; Savino, C; De Lorenzo, G; Tsernoglou, D & Cervone, F 2003. The crystal structure of polygalacturonase-inhibiting protein (PGIP), a leucine-rich repeat protein involved in plant defense. *Proceedings of the National Academy of Sciences,* **100,** 10124-10128.

Dixon, Mark S; Golstein, Catherine; Thomas, Colwyn M; van der Biezen, Erik A & Jones, Jonathan DG 2000. Genetic complexity of pathogen perception by plants: the example of *Rcr3*, a tomato gene required specifically by *Cf-2*. *Proceedings of the National Academy of Sciences,* **97,** 8807-8814.

Dixon, Mark S; Hatzixanthis, Kostas; Jones, David A; Harrison, Kate & Jones, Jonathan DG 1998. The tomato *Cf-5* disease resistance gene and six homologs show pronounced allelic variation in leucine-rich repeat copy number. *Plant Cell,* **10,** 1915-1925.

Dixon, Mark S; Jones, David A; Keddie, James S; Thomas, Colwyn M; Harrison, Kate & Jones, Jonathan DG 1996. The tomato *Cf-2* disease resistance locus comprises two functional genes encoding leucine-rich repeat proteins. *Cell,* **84,** 451-459.

Djamei, Armin; Pitzschke, Andrea; Nakagami, Hirofumi; Rajh, Iva & Hirt, Heribert 2007. Trojan horse strategy in *Agrobacterium* transformation: abusing MAPK defense signaling. *Science,* **318,** 453-456.

Dodds, Peter N; Lawrence, Gregory J; Catanzariti, Ann-Maree; Teh, Trazel; Wang, Ching-IA; Ayliffe, Michael A; Kobe, Bostjan & Ellis, Jeffrey G 2006. Direct protein interaction underlies gene-for-gene specificity and coevolution of the flax resistance genes and flax rust avirulence genes. *Proceedings of the National Academy of Sciences,* **103,** 8888-8893.

Dodds, Peter N; Lawrence, Gregory J & Ellis, Jeffrey G 2001. Six amino acid changes confined to the leucine-rich repeat β-strand/β-turn motif determine the difference between the *P* and *P2* rust resistance specificities in flax. *Plant Cell* **13,** 163-178.

Dodds, Peter N & Rathjen, John P 2010. Plant immunity: towards an integrated view of plant–pathogen interactions. *Nature Reviews Genetics,* **11,** 539-548.

Doyle, Jeff J 1990. Isolation of plant DNA from fresh tissue. *Focus,* **12,** 13-15.

Du, Xinran; Miao, Min; Ma, Xinrong; Liu, Yongsheng; Kuhl, Joseph C; Martin, Gregory B & Xiao, Fangming 2012. Plant programmed cell death caused by an autoactive form of Prf is suppressed by co-expression of the Prf LRR domain. *Molecular Plant,* **5,** 1058-1067.

Dunning, F Mark; Sun, Wenxian; Jansen, Kristin L; Helft, Laura & Bent, Andrew F 2007. Identification and mutational analysis of Arabidopsis FLS2 leucine-rich repeat domain residues that contribute to flagellin perception. *Plant Cell,* **19,** 3297-3313.

Durrant, Wendy E & Dong, Xinnian 2004. Systemic acquired resistance. *Annual Review of Phytopathology,* **42,** 185-209.

Durrant, Wendy E; Rowland, Owen; Piedras, Pedro; Hammond-Kosack, Kim E & Jones, Jonathan DG 2000. cDNA-AFLP reveals a striking overlap in race-specific resistance and wound response gene expression profiles. *Plant Cell* **12,** 963-977.

Ellerström, Mats; Stålberg, Kjell; Ezcurra, Inés & Rask, Lars 1996. Functional dissection of a napin gene promoter: identification of promoter elements required for embryo and endosperm-specific transcription. *Plant Molecular Biology,* **32,** 1019-1027.

Ellis, Jeff 2006. Insights into nonhost disease resistance: can they assist disease control in agriculture? *Plant Cell* **18,** 523-528.

Ellis, Jeff; Dodds, Peter & Pryor, Tony 2000. The generation of plant disease resistance gene specificities. *Trends in Plant Science,* **5,** 373-379.

Ellis, Jeffrey G; Dodds, Peter N & Lawrence, Gregory J 2007. Flax rust resistance gene specificity is based on direct resistance-avirulence protein interactions. *Annual Review of Phytopathology,* **45,** 289-306.

Enya, Junichiro; Ikeda, Kentaro; Takeuchi, Taeko; Horikoshi, Norio; Higashi, Takahiko; Sakai, Takako; Iida, Yuichiro; Nishi, Kazufumi & Kubota, Masaharu 2009. The first occurrence of leaf mold of tomato caused by races 4.9 and 4.9.11 of *Passalora fulva* (syn. *Fulvia fulva*) in Japan. *Journal of General Plant Pathology,* **75,** 76-79.

Etalo, Desalegn W; Stulemeijer, Iris JE; van Esse, Peter H; de Vos, Ric CH; Bouwmeester, Harro J & Joosten, Matthieu HAJ 2013. System-wide hypersensitive response-associated transcriptome and metabolome reprogramming in tomato. *Plant Physiology,* **162,** 1599-1617.

Eulgem, Thomas; Rushton, Paul J; Schmelzer, Elmon; Hahlbrock, Klaus & Somssich, Imre E 1999. Early nuclear events in plant defence signalling: rapid gene activation by WRKY transcription factors. *The EMBO Journal,* **18,** 4689-4699.

Eyal, Yoram; Meller, Yael; Lev-Yadun, Simcha & Fluhr, Robert 1993. A basic-type PR-1 promoter directs ethylene responsiveness, vascular and abscission zone-specific expression. *The Plant Journal,* **4,** 225-234.

Fan, Jun & Doerner, Peter 2012. Genetic and molecular basis of nonhost disease resistance: complex, yes; silver bullet, no. *Current Opinion in Plant Biology,* **15,** 400-406.

Fan, Weihua & Dong, Xinnian 2002. *In vivo* interaction between NPR1 and transcription factor TGA2 leads to salicylic acid–mediated gene activation in Arabidopsis. *Plant Cell* **14,** 1377-1389.

Farnham, Garry & Baulcombe, David C 2006. Artificial evolution extends the spectrum of viruses that are targeted by a disease-resistance gene from potato. *Proceedings of the National Academy of Sciences,* **103,** 18828-18833.

Felix, Georg & Boller, Thomas 2003. Molecular sensing of bacteria in plants: The highly conserved RNA-binding motif RNP-1 of bacterial cold shock proteins is recognized as an elicitor signal in tobacco. *Journal of Biological Chemistry,* **278,** 6201-6208.

Filipecki, Marcin & Malepszy, Stefan 2006. Unintended consequences of plant transformation: a molecular insight. *Journal of Applied Genetics,* **47,** 277-286.

Flood, Julie 2010. The importance of plant health to food security. *Food Security,* **2,** 215-231.

Flor, Harold H 1971. Current status of the gene-for-gene concept. *Annual Review of Phytopathology,* **9,** 275-296.

Fradin, E. F.; Abd-El-Haliem, A.; Masini, L.; van den Berg, G. C. M.; Joosten, Matthieu H.A.J. & Thomma, Bart P.H.J. 2011. Interfamily transfer of tomato *Ve1* mediates *Verticillium* resistance in *Arabidopsis*. *Plant Physiology,* **156,** 2255-2265.

Fradin, Emilie F; Zhang, Zhao; Ayala, Juan C Juarez; Castroverde, Christian DM; Nazar, Ross N; Robb, Jane; Liu, Chun-Ming & Thomma, Bart PHJ 2009. Genetic dissection of *Verticillium* wilt resistance mediated by tomato Ve1. *Plant Physiology,* **150,** 320-332.

Fradin, Emilie F; Zhang, Zhao; Rovenich, Hanna; Song, Yin; Liebrand, Thomas WH; Masini, Laura; van den Berg, Grardy CM; Joosten, Matthieu HAJ & Thomma, Bart PHJ 2014. Functional analysis of the tomato immune receptor Ve1 through domain swaps with its non-functional homolog Ve2. *PloS One,* **9,** e88208.

Fritz-Laylin, Lillian K; Krishnamurthy, Nandini; Tör, Mahmut; Sjölander, Kimmen V & Jones, Jonathan DG 2005. Phylogenomic analysis of the receptor-like proteins of rice and Arabidopsis. *Plant Physiology,* **138,** 611-623.

Fusada, Naoki; Masuda, Tatsuru; Kuroda, Hirofumi; Shimada, Hiroshi; Ohta, Hiroyuki & Takamiya, Ken-ichiro 2005. Identification of a novel *cis*-element exhibiting cytokinin-dependent protein binding *in vitro* in the 5′ -region of NADPH-protochlorophyllide oxidoreductase gene in cucumber. *Plant Molecular Biology,* **59,** 631-645.

Gabriëls, Suzan HEJ; Vossen, Jack H; Ekengren, Sophia K; Ooijen, Gerben van; Abd-El-Haliem, Ahmed M; Berg, Grardy; Rainey, Daphne Y; Martin, Gregory B; Takken, Frank LW & de Wit, Pierre JGM 2007. An NB-LRR protein required for HR signalling mediated by both extra- and intracellular resistance proteins. *The Plant Journal,* **50,** 14-28.

Gao, Minghui; Wang, Xia; Wang, Dongmei; Xu, Fang; Ding, Xiaojun; Zhang, Zhibin; Bi, Dongling; Cheng, Yu Ti; Chen, She & Li, Xin 2009. Regulation of cell death and innate immunity by two receptor-like kinases in Arabidopsis. *Cell Host & Microbe,* **6,** 34.

Garretón, Virginia; Carpinelli, Jorge; Jordana, Xavier & Holuigue, Loreto 2002. The *as-1* promoter element is an oxidative stress-responsive element and salicylic acid activates it via oxidative species. *Plant Physiology,* **130,** 1516-1526.

Garrett, Thomas PJ; McKern, Neil M; Lou, Meizhen; Elleman, Thomas C; Adams, Timothy E; Lovrecz, George O; Zhu, Hong-Jian; Walker, Francesca; Frenkel, Morry J; Hoyne, Peter A; Jorissen, Robert N; Nice, Edouard C; Burgess, Antony W & Ward, Colin W 2002. Crystal structure of a truncated epidermal growth factor receptor extracellular domain bound to transforming growth factor α. *Cell,* **110,** 763-773.

Gay, Nicholas J; Gangloff, Monique & Weber, Alexander NR 2006. Toll-like receptors as molecular switches. *Nature Reviews Immunology,* **6,** 693-698.

Gelvin, Stanton B 2003. *Agrobacterium*-mediated plant transformation: the biology behind the "gene-jockeying" tool. *Microbiology and Molecular Biology Reviews,* **67,** 16-37.

Glazebrook, Jane 2005. Contrasting mechanisms of defense against biotrophic and necrotrophic pathogens. *Annual Review of Phytopathology,* **43,** 205-227.

Gomez-Gomez, L & Boller, T 2000. FLS2: an LRR receptor-like kinase involved in the perception of the bacterial elicitor flagellin in *Arabidopsis*. *Molecular Cell,* **5,** 1003 - 1011.

González-Lamothe, Rocío; Mitchell, Gabriel; Gattuso, Mariza; Diarra, Moussa S.; Malouin, François & Bouarab, Kamal 2009. Plant antimicrobial agents and their effects on plant and human pathogens. *International Journal of Molecular Sciences,* **10,** 3400-3419.

Gopalan, S; Wei, W & He, SY 1996a. *hrp* gene-dependent induction of *hin1*: a plant gene activated rapidly by both harpins and the *avrPto* gene-mediated signal. *The Plant Journal,* **10,** 591-600.

Gopalan, Suresh; Bauer, David W; Alfano, James R; Loniello, Amy O; He, Shen Yang & Collmer, Alan 1996b. Expression of the *Pseudomonas syringae* avirulence protein AvrB in plant cells alleviates its dependence on the hypersensitive response and pathogenicity (Hrp) secretion system in eliciting genotype-specific hypersensitive cell death. *Plant Cell,* **8,** 1095-105.

Gou, Mingyue & Hua, Jian 2012. Complex regulation of an *R* gene *SNC1* revealed by autoimmune mutants. *Plant Signaling & Behavior,* **7,** 213-216.

Gowik, Udo; Burscheidt, Janet; Akyildiz, Meryem; Schlue, Ute; Koczor, Maria; Streubel, Monika & Westhoff, Peter 2004. *cis*-Regulatory elements for mesophyll-specific gene expression in the C_4 plant *Flaveria trinervia*, the promoter of the C_4 phosphoenolpyruvate carboxylase gene. *Plant Cell,* **16,** 1077-1090.

Green, R & Fluhr, R 1995. UV-B-induced PR-1 accumulation is mediated by active oxygen species. *Plant Cell,* **7,** 203-212.

Grenier, Jean; Potvin, Claude; Trudel, Jean & Asselin, Alain 1999. Some thaumatin-like proteins hydrolyse polymeric β-1, 3-glucans. *The Plant Journal,* **19,** 473-480.

Gurr, Sarah J & Rushton, Paul J 2005. Engineering plants with increased disease resistance: what are we going to express? *Trends in Biotechnology,* **23,** 275-282.

Gust, Andrea A & Felix, Georg 2014. Receptor like proteins associate with SOBIR1-type of adaptors to form bimolecular receptor kinases. *Current Opinion in Plant Biology,* **21,** 104-111.

Haanstra, JPW; Laugé, Richard; Meijer-Dekens, F; Bonnema, G; de Wit, Pierre JGM & Lindhout, Pim 1999. The *Cf-ECP2* gene is linked to, but not part of, the *Cf-4/Cf-9* cluster on the short arm of chromosome 1 in tomato. *Molecular and General Genetics* **262,** 839-845.

Haanstra, JPW; Meijer-Dekens, F; Lauge, Richard; Seetanah, DC; Joosten, Matthieu HAJ; de Wit, Pierre JGM & Lindhout, Pim 2000. Mapping strategy for resistance genes against *Cladosporium fulvum* on the short arm of chromosome 1 of tomato: *Cf-ECP5* near the *Hcr9* Milky Way cluster. *Theoretical and Applied Genetics,* **101,** 661-668.

Hammond-Kosack, Kim E & Jones, Jonathan DG 1996. Resistance gene-dependent plant defense responses. *Plant Cell,* **8,** 1773.

Hammond-Kosack, Kim E & Parker, Jane E 2003. Deciphering plant–pathogen communication: fresh perspectives for molecular resistance breeding. *Current Opinion in Biotechnology,* **14,** 177-193.

Hammond-Kosack, Kim E; Silverman, Paul; Raskin, Ilya & Jones, Jonathan DG 1996. Race-specific elicitors of *Cladosporium fulvum* induce changes in cell morphology and the synthesis of ethylene and salicylic acid in tomato plants carrying the corresponding *Cf* disease resistance gene. *Plant Physiology,* **110,** 1381-1394.

Hammond-Kosack, Kim E; Tang, Saijun; Harrison, Kate & Jones, Jonathan DG 1998. The tomato *Cf-9* disease resistance gene functions in tobacco and potato to confer responsiveness to the fungal avirulence gene product Avr9. *Plant Cell* **10,** 1251-1266.

Han, Lei; Han, Ya-Nan & Xiao, Xing-Guo 2013. Truncated Cotton Subtilase Promoter Directs Guard Cell-Specific Expression of Foreign Genes in Tobacco and Arabidopsis. *PloS One,* **8,** e59802.

Han, Zhifu; Sun, Yadong & Chai, Jijie 2014. Structural insight into the activation of plant receptor kinases. *Current Opinion in Plant Biology,* **20,** 55-63.

Hanfrey, Colin; Fife, Mark & Buchanan-Wollaston, Vicky 1996. Leaf senescence in *Brassica napus*: expression of genes encoding pathogenesis-related proteins. *Plant Molecular Biology,* **30,** 597-609.

Hardham, Adrienne R; Jones, David A & Takemoto, Daigo 2007. Cytoskeleton and cell wall function in penetration resistance. *Current Opinion in Plant Biology,* **10,** 342-348.

Heckman, Karin L & Pease, Larry R 2007. Gene splicing and mutagenesis by PCR-driven overlap extension. *Nature protocols,* **2,** 924-932.

Heese, A; Hann, DR; Gimenez-Ibanez, S; Jones, AM; He, K; Li, J; Schroeder, JI; Peck, SC & Rathjen, JP 2007. The receptor-like kinase SERK3/BAK1 is a central regulator of innate immunity in plants. *Proceedings of the National Academy of Sciences,* **104,** 12217 - 12222.

Heil, Martin & Baldwin, Ian T 2002. Fitness costs of induced resistance: emerging experimental support for a slippery concept. *Trends in Plant Science,* **7,** 61-67.

Hellens, Roger P; Edwards, E Anne; Leyland, Nicola R; Bean, Samantha & Mullineaux, Philip M 2000. pGreen: a versatile and flexible binary Ti vector for *Agrobacterium*-mediated plant transformation. *Plant Molecular Biology,* **42,** 819-832.

Hennig, Jacek; Dewey, Ralph E; Cutt, John R & Klessig, Daniel F 1993. Pathogen, salicylic acid and developmental dependent expression of a β-1, 3-glucanase/GUS gene fusion in transgenic tobacco plants. *The Plant Journal,* **4,** 481-493.

Higo, Kenichi; Ugawa, Yoshihiro; Iwamoto, Masao & Higo, Hiromi 1998. PLACE: a database of plant *cis*-acting regulatory DNA elements. *Nucleic Acids Research,* **26,** 358-359.

Horsch, RB; Fry, JE; Hoffmann, NL; Eichholtz, D; Rogers, SG and & Fraley, RT 1985. A simple and general method for transferring genes into plants. *Science,* **227,** 1229-1231.

Hothorn, Michael; Belkhadir, Youssef; Dreux, Marlene; Dabi, Tsegaye; Noel, Joseph P; Wilson, Ian A & Chory, Joanne 2011. Structural basis of steroid hormone perception by the receptor kinase BRI1. *Nature,* **474,** 467-471.

Howles, Paul; Lawrence, Greg; Finnegan, Jean; McFadden, Helen; Ayliffe, Michael; Dodds, Peter & Ellis, Jeff 2005. Autoactive alleles of the flax *L6* rust resistance gene induce non-race-specific rust resistance associated with the hypersensitive response. *Molecular Plant-Microbe Interactions,* **18,** 570-582.

Huot, Bethany; Yao, Jian; Montgomery, Beronda L & He, Sheng Yang 2014. Growth-defense tradeoffs in plants: a balancing act to optimize fitness. *Molecular Plant,* **7,** 1267-1287.

Hwang, Chin-Feng; Bhakta, Amit V; Truesdell, Gina M; Pudlo, Waclawa M & Williamson, Valerie Moroz 2000. Evidence for a role of the N terminus and leucine-rich repeat region of the *Mi* gene product in regulation of localized cell death. *Plant Cell,* **12,** 1319-1329.

Hwang, Chin-Feng & Williamson, Valerie M 2003. Leucine-rich repeat-mediated intramolecular interactions in nematode recognition and cell death signaling by the tomato resistance protein Mi. *The Plant Journal,* **34,** 585-593.

Jabs, T; Colling, C; Tschöpe, M; Hahlbrock, K & Scheel, D 1997. Elicitor-stimulated ion fluxes and reactive oxygen species from the oxidative burst signal defense gene activation and phytoalexin synthesis in parsley. *Proceedings of the National Academy of Sciences,* **94,** 4800-4805.

Jaillais, Yvon; Belkhadir, Youssef; Balsemão-Pires, Emilia; Dangl, Jeffery L & Chory, Joanne 2011. Extracellular leucine-rich repeats as a platform for receptor/coreceptor complex formation. *Proceedings of the National Academy of Sciences,* **108,** 8503-8507.

Jefferson, Richard A; Kavanagh, Tony A & Bevan, Michael W 1987. GUS fusions: β-glucuronidase as a sensitive and versatile gene fusion marker in higher plants. *The EMBO Journal,* **6,** 3901.

Jehle, Anna Kristina; Lipschis, Martin; Albert, Markus; Fallahzadeh-Mamaghani, Vahid; Fürst, Ursula; Mueller, Katharina & Felix, Georg 2013. The Receptor-Like Protein ReMAX of Arabidopsis Detects the Microbe-Associated Molecular Pattern eMax from *Xanthomonas*. *Plant Cell,* **25,** 2330-2340.

Jiang, Chang-Jie; Shimono, Masaki; Sugano, Shoji; Kojima, Mikiko; Liu, Xinqiong; Inoue, Haruhiko; Sakakibara, Hitoshi & Takatsuji, Hiroshi 2013a. Cytokinins act synergistically with salicylic acid to activate defense gene expression in rice. *Molecular Plant-Microbe Interactions,* **26,** 287-296.

Jiang, Zhengning; Ge, Shuai; Xing, Liping; Han, Dejun; Kang, Zhensheng; Zhang, Guoqin; Wang, Xiaojie; Wang, Xiue; Chen, Peidu & Cao, Aizhong 2013b. *RLP1*. *1*, a novel wheat receptor-like protein gene, is involved in the defence response against *Puccinia striiformis* f. sp. *tritici*. *Journal of Experimental Botany,* **64,** 3735-3746.

Jiao, Yuling; Ma, Ligeng; Strickland, Elizabeth & Deng, Xing Wang 2005. Conservation and divergence of light-regulated genome expression patterns during seedling development in rice and Arabidopsis. *Plant Cell,* **17,** 3239-3256.

Johansen, Lisa K & Carrington, James C 2001. Silencing on the spot. Induction and suppression of RNA silencing in the *Agrobacterium*-mediated transient expression system. *Plant Physiology,* **126,** 930-938.

Johnson, Christopher; Boden, Erin & Arias, Jonathan 2003. Salicylic acid and NPR1 induce the recruitment of trans-activating TGA factors to a defense gene promoter in Arabidopsis. *Plant Cell* **15,** 1846-1858.

Jones, David A & Jones, Jonathan DG 1997. The role of leucine-rich repeat proteins in plant defences. *Advances in Botanical Research,* **24,** 89-167.

Jones, David A & Takemoto, Daigo 2004. Plant innate immunity–direct and indirect recognition of general and specific pathogen-associated molecules. *Current Opinion in Immunology,* **16,** 48-62.

Jones, David A; Thomas, Colwyn M; Hammond-Kosack, Kim E; Balint-Kurti, Peter J & Jones, Jonathan DG 1994. Isolation of the tomato *Cf-9* gene for resistance to *Cladosporium fulvum* by transposon tagging. *Science,* **266,** 789-793.

Jones, Jonathan DG & Dangl, Jeffery L 2006. The plant immune system. *Nature,* **444,** 323-329.

Joosten, Matthieu HAJ; Cozijnsen, Ton J & de Wit, Pierre JGM 1994. Host resistance to a fungal tomato pathogen lost by a single base-pair change in an avirulence gene. *Nature,* **367,** 384-386.

Joosten, Matthieu HAJ & de Wit, Pierre JGM 1999. The tomato-*Cladosporium fulvum* interaction: A versatile experimental system to study plant-pathogen interactions. *Annual Review of Phytopathology,* **37,** 335-367.

Joosten, Matthieu HAJ; Vogelsang, Ralph; Cozijnsen, Ton J; Verberne, Marianne C & de Wit, Pierre JGM 1997. The biotrophic fungus *Cladosporium fulvum* circumvents *Cf-4*-mediated resistance by producing unstable AVR4 elicitors. *Plant Cell* **9,** 367-379.

Jupin, I & Chua, NH 1996. Activation of the CaMV *as-1 cis*-element by salicylic acid: differential DNA-binding of a factor related to TGA1a. *The EMBO Journal,* **15,** 5679.

Kang, Jin Young & Lee, Jie-Oh 2011. Structural biology of the Toll-like receptor family. *Annual Review of Biochemistry,* **80,** 917-941.

Kapila, J.; de Rycke, R.; van Montagu, M. & Angenon, G. 1997. An *Agrobacterium*-mediated transient gene expression system for intact leaves. *Plant Science,* **122,** 101-108.

Kawai, Taro & Akira, Shizuo 2010. The role of pattern-recognition receptors in innate immunity: update on Toll-like receptors. *Nature Immunology,* **11,** 373-384.

Kawchuk, Lawrence M; Hachey, John; Lynch, Dermot R; Kulcsar, Frank; van Rooijen, Gijs; Waterer, Doug R; Robertson, Albert; Kokko, Eric; Byers, Robert & Howard, Ronald J 2001. Tomato *Ve* disease resistance genes encode cell surface-like receptors. *Proceedings of the National Academy of Sciences,* **98,** 6511-6515.

Kayes, Jeffrey M & Clark, Steven E 1998. CLAVATA2, a regulator of meristem and organ development in Arabidopsis. *Development,* **125,** 3843-3851.

Kim, Soo Young; Chung, Hwa ‐ Jee & Thomas, Terry L 1997. Isolation of a novel class of bZIP transcription factors that interact with ABA-responsive and embryo-specification elements in the *Dc3* promoter using a modified yeast one-hybrid system. *The Plant Journal,* **11,** 1237-1251.

Kinkema, Mark; Fan, Weihua & Dong, Xinnian 2000. Nuclear localization of NPR1 is required for activation of *PR* gene expression. *Plant Cell* **12,** 2339-2350.

Kitajima, S; Koyama, T; Yamada, Y & Sato, F 1998. Constitutive expression of the neutral PR-5 (OLP, PR-5d) gene in roots and cultured cells of tobacco is mediated by ethylene-responsive *cis*-element AGCCGCC sequences. *Plant Cell Reports,* **18,** 173-179.

Kobe, Bostjan & Deisenhofer, Johann 1993. Crystal structure of porcine ribonuclease inhibitor, a protein with leucine-rich repeats. *Nature,* **366,** 751-756.

Kobe, Bostjan & Deisenhofer, Johann 1996. Mechanism of ribonuclease inhibition by ribonuclease inhibitor protein based on the crystal structure of its complex with ribonuclease A. *Journal of Molecular Biology,* **264,** 1028-1043.

Kobe, Bostjan & Kajava, Andrey V 2001. The leucine-rich repeat as a protein recognition motif. *Current Opinion in Structural Biology,* **11,** 725-732.

Koiwa, Hisashi; Sato, Fumihiko & Yamada, Yasuyuki 1994. Characterization of accumulation of tobacco PR-5 proteins by IEF-immunoblot analysis. *Plant and Cell Physiology,* **35,** 821-827.

Kononowicz, Andrzej K; Nelson, Donald E; Singh, Narendra K; Hasegawa, Paul M & Bressan, Ray A 1992. Regulation of the osmotin gene promoter. *Plant Cell,* **4,** 513-524.

Kooman-Gersmann, Miriam; Honee, Guy; Bonnema, Guusje & de Wit, Pierre JGM 1996. A high-affinity binding site for the AVR9 peptide elicitor of

Cladosporium fulvum is present on plasma membranes of tomato and other Solanaceous plants. *Plant Cell* **8,** 929-938.

Kooman-Gersmann, Miriam; Vogelsang, Ralph; Vossen, Paul; van Den Hooven, Henno W; Mahé, Eve; Honée, Guy & de Wit, Pierre JGM 1998. Correlation between binding affinity and necrosis-inducing activity of mutant AVR9 peptide elicitors. *Plant Physiology,* **117,** 609-618.

Krasileva, Ksenia V; Dahlbeck, Douglas & Staskawicz, Brian J 2010. Activation of an Arabidopsis resistance protein is specified by the *in planta* association of its leucine-rich repeat domain with the cognate oomycete effector. *Plant Cell,* **22,** 2444-2458.

Krüger, Julia; Thomas, Colwyn M; Golstein, Catherine; Dixon, Mark S; Smoker, Matthew; Tang, Saijun; Mulder, Lonneke & Jones, Jonathan DG 2002. A tomato cysteine protease required for *Cf-2*-dependent disease resistance and suppression of autonecrosis. *Science,* **296,** 744-747.

Kruijt, Marco; de Kock, Maarten JD & de Wit, Pierre JGM 2005. Receptor-like proteins involved in plant disease resistance. *Molecular Plant Pathology,* **6,** 85-97.

Laemmli, U. K. 1970. Cleavage of Structural Proteins during the Assembly of the Head of Bacteriophage T4. *Nature,* **227,** 680-685.

Larkan, NJ; Lydiate, DJ; Parkin, IAP; Nelson, MN; Epp, DJ; Cowling, WA; Rimmer, SR & Borhan, MH 2013. The *Brassica napus* blackleg resistance gene *LepR3* encodes a receptor-like protein triggered by the *Leptosphaeria maculans* effector AVRLM1. *New Phytologist,* **197,** 595-605.

LaRosa, P Christopher; Chen, Zutang; Nelson, Donald E; Singh, Narendra K; Hasegawa, Paul M & Bressan, Ray A 1992. Osmotin gene expression is posttranscriptionally regulated. *Plant Physiology,* **100,** 409-415.

Latz, Eicke; Verma, Anjali; Visintin, Alberto; Gong, Mei; Sirois, Cherilyn M; Klein, Dionne CG; Monks, Brian G; McKnight, C James; Lamphier, Marc S & Duprex, W Paul 2007. Ligand-induced conformational changes allosterically activate Toll-like receptor 9. *Nature Immunology,* **8,** 772-779.

Laugé, Richard; Dmitriev, Alexander P; Joosten, Matthieu HAJ & de Wit, Pierre JGM 1998. Additional resistance gene(s) against *Cladosporium fulvum* present on the *Cf-9* introgression segment are associated with strong PR protein accumulation. *Molecular Plant-Microbe Interactions,* **11,** 301-308.

Laugé, Richard; Goodwin, Paul H; de Wit, Pierre JGM & Joosten, Matthieu HAJ 2000. Specific HR-associated recognition of secreted proteins from *Cladosporium fulvum* occurs in both host and non-host plants. *The Plant Journal,* **23,** 735-745.

Laurent, Franck; Labesse, Gilles & de Wit, Pierre 2000. Molecular cloning and partial characterization of a plant VAP33 homologue with a major sperm protein domain. *Biochemical and Biophysical Research Communications,* **270,** 286-292.

Lazarovits, George & Higgins, Verna J 1976. Ultrastructure of susceptible, resistant, and immune reactions of tomato to races of *Cladosporium fulvum*. *Canadian Journal of Botany,* **54,** 235-249.

Leckie, F; Mattei, B; Capodicasa, C; Hemmings, A; Nuss, L; Aracri, B; De Lorenzo, G & Cervone, F 1999. The specificity of polygalacturonase-inhibiting protein (PGIP): a single amino acid substitution in the solvent-exposed β-strand/β-turn region of the leucine-rich repeats (LRRs) confers a new recognition capability. *EMBO J,* **18,** 2352-2363.

Lee, Hyeseung; Damsz, Barbara; Woloshuk, Charles P; Bressan, Ray A & Narasimhan, Meena L 2010. Use of the plant defense protein osmotin to

identify *Fusarium oxysporum* genes that control cell wall properties. *Eukaryotic Cell,* **9,** 558-568.

Leon-Reyes, Antonio; Spoel, Steven H; De Lange, Elvira S; Abe, Hiroshi; Kobayashi, Masatomo; Tsuda, Shinya; Millenaar, Frank F; Welschen, Rob AM; Ritsema, Tita & Pieterse, Corné MJ 2009. Ethylene modulates the role of NONEXPRESSOR OF PATHOGENESIS-RELATED GENES1 in cross talk between salicylate and jasmonate signaling. *Plant Physiology,* **149,** 1797-1809.

Lescot, Magali; Déhais, Patrice; Thijs, Gert; Marchal, Kathleen; Moreau, Yves; Van de Peer, Yves; Rouzé, Pierre & Rombauts, Stephane 2002. PlantCARE, a database of plant *cis*-acting regulatory elements and a portal to tools for *in silico* analysis of promoter sequences. *Nucleic Acids Research,* **30,** 325-327.

Leslie, Michelle E; Lewis, Michael W; Youn, Ji-Young; Daniels, Mark J & Liljegren, Sarah J 2010. The EVERSHED receptor-like kinase modulates floral organ shedding in *Arabidopsis*. *Development,* **137,** 467-476.

Levine, Alex; Tenhaken, Raimund; Dixon, Richard & Lamb, Chris 1994. H_2O_2 from the oxidative burst orchestrates the plant hypersensitive disease resistance response. *Cell,* **79,** 583-593.

Li, Jianming 2011. Direct involvement of leucine-rich repeats in assembling ligand-triggered receptor–coreceptor complexes. *Proceedings of the National Academy of Sciences,* **108,** 8073-8074.

Lieberherr, Damien; Wagner, Ulrich; Dubuis, Pierre-Henri; Métraux, Jean-Pierre & Mauch, Felix 2003. The rapid induction of glutathione *S*-transferases *AtGSTF2* and *AtGSTF6* by avirulent *Pseudomonas syringae* is the result of combined salicylic acid and ethylene signaling. *Plant and Cell Physiology,* **44,** 750-757.

Liebrand, Thomas WH; Smit, Patrick; Abd-El-Haliem, Ahmed; de Jonge, Ronnie; Cordewener, Jan HG; America, Antoine HP; Sklenar, Jan; Jones, Alexandra ME; Robatzek, Silke & Thomma, Bart PHJ 2012. Endoplasmic reticulum-quality control chaperones facilitate the biogenesis of Cf receptor-like proteins involved in pathogen resistance of tomato. *Plant Physiology,* **159,** 1819-1833.

Liebrand, Thomas WH; van den Berg, Grardy CM; Zhang, Zhao; Smit, Patrick; Cordewener, Jan HG; America, Antoine HP; Sklenar, Jan; Jones, Alexandra ME; Tameling, Wladimir IL & Robatzek, Silke 2013. Receptor-like kinase SOBIR1/EVR interacts with receptor-like proteins in plant immunity against fungal infection. *Proceedings of the National Academy of Sciences,* **110,** 10010-10015.

Liebrand, Thomas WH; van den Burg, Harrold A. & Joosten, Matthieu HAJ 2014. Two for all: receptor-associated kinases SOBIR1 and BAK1. *Trends in Plant Science,* **19,** 123-132.

Lim, Pyung Ok; Kim, Hyo Jung & Gil Nam, Hong 2007. Leaf Senescence. *Annual Review of Plant Biology,* **58,** 115-136.

Liu, Dong; Narasimhan, Meena L; Xu, Yi; Raghothama, Kashchandra G; Hasegawa, Paul M & Bressan, Ray A 1995. Fine structure and function of the osmotin gene promoter. *Plant Molecular Biology,* **29,** 1015-1026.

Liu, JJ; Sturrock, R & Ekramoddoullah, AKM 2010. The superfamily of thaumatin-like proteins: its origin, evolution, and expression towards biological function. *Plant Cell Reports,* **29,** 419-436.

Liu, Wusheng; Mazarei, Mitra; Rudis, Mary R; Fethe, Michael H; Peng, Yanhui; Millwood, Reginald J; Schoene, Gisele; Burris, Jason N & Stewart, C Neal 2013. Bacterial pathogen phytosensing in transgenic tobacco and Arabidopsis plants. *Plant Biotechnology Journal,* **11,** 43-52.

Lorrain, Séverine; Vailleau, Fabienne; Balagué, Claudine & Roby, Dominique 2003. Lesion mimic mutants: keys for deciphering cell death and defense pathways in plants? *Trends in Plant Science,* **8,** 263-271.

Lotan, Tamar; Ori, Naomi & Fluhr, Robert 1989. Pathogenesis-related proteins are developmentally regulated in tobacco flowers. *Plant Cell* **1,** 881-887.

Love, Andrew J.; Milner, Joel J. & Sadanandom, Ari 2008. Timing is everything: regulatory overlap in plant cell death. *Trends in Plant Science,* **13,** 589-595.

Lozano-Torres, Jose L; Wilbers, Ruud HP; Gawronski, Piotr; Boshoven, Jordi C; Finkers-Tomczak, Anna; Cordewener, Jan HG; America, Antoine HP; Overmars, Hein A; Van 't Klooster, John W; Baranowski, Lukasz; Sobczak, Miroslaw; Ilyas, Muhammad; van der Hoorn, Renier AL; Schots, Arjen; de Wit, Pierre JGM; Bakker, Jaap; Goverse, Aska & Smant, Geert 2012. Dual disease resistance mediated by the immune receptor Cf-2 in tomato requires a common virulence target of a fungus and a nematode. *Proceedings of the National Academy of Sciences,* **109,** 10119-10124.

Luck, Joanne E; Lawrence, Gregory J; Dodds, Peter N; Shepherd, Kenneth W & Ellis, Jeffrey G 2000. Regions outside of the leucine-rich repeats of flax rust resistance proteins play a role in specificity determination. *Plant Cell* **12,** 1367-1377.

Luderer, Rianne; Rivas, Susana; Nürnberger, Thorsten; Mattei, Benedetta; van den Hooven, Henno W; van der Hoorn, Renier AL; Romeis, Tina; Wehrfritz, Josa- M; Blume, Beatrix & Nennstiel, Dirk 2001. No evidence for binding between resistance gene product Cf-9 of tomato and avirulence gene product AVR9 of *Cladosporium fulvum*. *Molecular Plant-Microbe Interactions,* **14,** 867-876.

Luderer, Rianne; Takken, Frank LW; de Wit, Pierre JGM & Joosten, Matthieu HAJ 2002. *Cladosporium fulvum* overcomes *Cf-2*-mediated resistance by producing truncated AVR2 elicitor proteins. *Molecular Microbiology,* **45,** 875-884.

Lusser, Maria; Parisi, Claudia; Plan, Damien & Rodriguez-Cerezo, Emilio 2012. Deployment of new biotechnologies in plant breeding. *Nature Biotechnology,* **30,** 231-239.

Maekawa, Takaki; Cheng, Wei; Spiridon, Laurentiu N; Töller, Armin; Lukasik, Ewa; Saijo, Yusuke; Liu, Peiyuan; Shen, Qian-Hua; Micluta, Marius A & Somssich, Imre E 2011a. Coiled-coil domain-dependent homodimerization of intracellular barley immune receptors defines a minimal functional module for triggering cell death. *Cell Host & Microbe,* **9,** 187-199.

Maekawa, Takaki; Kufer, Thomas A & Schulze-Lefert, Paul 2011b. NLR functions in plant and animal immune systems: so far and yet so close. *Nature Immunology,* **12,** 817-826.

Mahdavi, F; Sariah, M & Maziah, M 2012. Expression of rice thaumatin-like protein gene in transgenic banana plants enhances resistance to fusarium wilt. *Applied Biochemistry and Biotechnology,* **166,** 1008-1019.

Maleck, Klaus; Levine, Aaron; Eulgem, Thomas; Morgan, Allen; Schmid, Jürg; Lawton, Kay A; Dangl, Jeffery L & Dietrich, Robert A 2000. The transcriptome of *Arabidopsis thaliana* during systemic acquired resistance. *Nature Genetics,* **26,** 403-410.

Marmeisse, Roland; van den Ackerveken, Guido FJM; Goosen, Theo; de Wit, Pierre JGM & van den Broek, Henk WJ 1993. Disruption of the avirulence gene *Avr9* in two races of the tomato pathogen *Cladosporium fulvum* causes virulence on tomato genotypes with the complementary resistance gene *Cf-9*. *Molecular Plant Microbe Interactions,* **6,** 412-412.

Marone, Daniela; Russo, Maria A; Laidò, Giovanni; De Leonardis, Anna M & Mastrangelo, Anna M 2013. Plant Nucleotide Binding Site–Leucine-Rich Repeat (NBS-LRR) Genes: Active Guardians in Host Defense Responses. *International Journal of Molecular Sciences,* **14,** 7302-7326.

McDowell, John M & Simon, Stacey A 2008. Molecular diversity at the plant–pathogen interface. *Developmental & Comparative Immunology,* **32,** 736-744.

Melchers, Leo S; Sela-Buurlage, Marianne B; Vloemans, Sandra A; Woloshuk, Charles P; van Roekel, Jeroen SC; Pen, Jan; van den Elzen, Peter JM & Cornelissen, Ben JC 1993. Extracellular targeting of the vacuolar tobacco proteins AP24, chitinase and β-1,3-glucanase in transgenic plants. *Plant Molecular Biology,* **21,** 583-593.

Memelink, Johan; Linthorst, Huub JM; Schilperoort, Rob A & Hoge, J Harry C 1990. Tobacco genes encoding acidic and basic isoforms of pathogenesis-related proteins display different expression patterns. *Plant Molecular Biology,* **14,** 119-126.

Mesarich, Carl Hayden; Griffiths, Scott A; van der Burgt, Ate; Ökmen, Bilal; Beenen, Henriek G; Etalo, Desalegn W; Joosten, Matthieu HAJ & de Wit, Pierre JGM 2014. Transcriptome sequencing uncovers the *Avr5* avirulence gene of the tomato leaf mould pathogen *Cladosporium fulvum*. *Molecular Plant-Microbe Interactions,* **27,** 846-857.

Michael Weaver, L; Swiderski, Michal R; Li, Yan & Jones, Jonathan DG 2006. The *Arabidopsis thaliana* TIR-NB-LRR R protein, RPP1A; protein localization and constitutive activation of defence by truncated alleles in tobacco and Arabidopsis. *The Plant Journal,* **47,** 829-840.

Molinari, Sergio; Fanelli, Elena & Leonetti, Paola 2014. Expression of tomato salicylic acid (SA)-responsive pathogenesis-related genes in *Mi-1*-mediated and SA-induced resistance to root-knot nematodes. *Molecular Plant Pathology,* **15,** 255-264.

Monaghan, Jacqueline & Zipfel, Cyril 2012. Plant pattern recognition receptor complexes at the plasma membrane. *Current Opinion in Plant Biology,* **15,** 349-357.

Munis, M; Tu, Lili; Deng, Fenglin; Tan, Jiafu; Xu, Li; Xu, Shicheng; Long, Lu & Zhang, Xianlong 2010. A thaumatin-like protein gene involved in cotton fiber secondary cell wall development enhances resistance against *Verticillium dahliae* and other stresses in transgenic tobacco. *Biochemical and Biophysical Research Communications,* **393,** 38-44.

Naithani, Sushma; Chookajorn, Thanat; Ripoll, Daniel R & Nasrallah, June B 2007. Structural modules for receptor dimerization in the S-locus receptor kinase extracellular domain. *Proceedings of the National Academy of Sciences,* **104,** 12211-12216.

Nakamura, Masayuki; Tsunoda, Tatsuhiko & Obokata, Junichi 2002. Photosynthesis nuclear genes generally lack TATA-boxes: a tobacco photosystem I gene responds to light through an initiator. *The Plant Journal,* **29,** 1-10.

Nakashima, Kazuo; Fujita, Yasunari; Katsura, Koji; Maruyama, Kyonoshin; Narusaka, Yoshihiro; Seki, Motoaki; Shinozaki, Kazuo & Yamaguchi-Shinozaki, Kazuko 2006. Transcriptional regulation of ABI3-and ABA-responsive genes including RD29B and RD29A in seeds, germinating embryos, and seedlings of Arabidopsis. *Plant Molecular Biology,* **60,** 51-68.

Navarro, Lionel; Zipfel, Cyril; Rowland, Owen; Keller, Ingo; Robatzek, Silke; Boller, Thomas & Jones, Jonathan DG 2004. The transcriptional innate

immune response to flg22. Interplay and overlap with *Avr* gene-dependent defense responses and bacterial pathogenesis. *Plant Physiology,* **135,** 1113-1128.

Neale, Alan D; Wahleithner, Jill A; Lund, Marianne; Bonnett, Howard T; Kelly, Alan; Meeks-Wagner, D Ry; Peacock, W James & Dennis, Elizabeth S 1990. Chitinase, β-1, 3-glucanase, osmotin, and extensin are expressed in tobacco explants during flower formation. *Plant Cell* **2,** 673-684.

Nekrasov, Vladimir; Ludwig, Andrea A & Jones, Jonathan DG 2006. CITRX thioredoxin is a putative adaptor protein connecting Cf-9 and the ACIK1 protein kinase during the Cf-9/Avr9-induced defence response. *FEBS Letters,* **580,** 4236-4241.

Nelson, Donald E; Raghothama, Kashchandra G; Singh, Narendra K; Hasegawa, Paul M & Bressan, Ray A 1992. Analysis of structure and transcriptional activation of an osmotin gene. *Plant Molecular Biology,* **19,** 577-588.

Newman, Mari-Anne; Sundelin, Thomas; Nielsen, Jon T & Erbs, Gitte 2013. MAMP (microbe-associated molecular pattern) triggered immunity in plants. *Frontiers in Plant Science,* **4,** 139.

Niki, Tomoya; Mitsuhara, Ichiro; Seo, Shigemi; Ohtsubo, Norihiro & Ohashi, Yuko 1998. Antagonistic effect of salicylic acid and jasmonic acid on the expression of pathogenesis-related (PR) protein genes in wounded mature tobacco leaves. *Plant and Cell Physiology,* **39,** 500-507.

Nishimura, Marc T. & Dangl, Jeffery L. 2014. Paired Plant Immune Receptors. *Science,* **344,** 267-268.

Obregón, Patricia; Martín, Raquel; Sanz, Ana & Castresana, Carmen 2001. Activation of defence-related genes during senescence: a correlation between gene expression and cellular damage. *Plant Molecular Biology,* **46,** 67-77.

Ohashi, Yuko & Ohshima, Masahiro 1992. Stress-induced expression of genes for pathogenesis-related proteins in plants. *Plant and Cell Physiology,* **33,** 819-826.

Olszak, Brian; Malinovsky, Frederikke Gro; Brodersen, Peter; Grell, Morten; Giese, Henriette; Petersen, Morten & Mundy, John 2006. A putative flavin-containing mono-oxygenase as a marker for certain defense and cell death pathways. *Plant Science,* **170,** 614-623.

Onishi, M; Tachi, H; Kojima, T; Shiraiwa, M & Takahara, H 2006. Molecular cloning and characterization of a novel salt-inducible gene encoding an acidic isoform of PR-5 protein in soybean (*Glycine max* [L.] Merr.). *Plant Physiology and Biochemistry,* **44,** 574-580.

Ono, Sachiko; Kusama, Masahiro; Ogura, Rieko & Hiratsuka, Kazuyuki 2011. Evaluation of the use of the tobacco *PR-1a* promoter to monitor defense gene expression by the luciferase bioluminescence reporter system. *Bioscience, Biotechnology, and Biochemistry,* **75,** 1796-1800.

Osmond, Ronald IW; Hrmova, Maria; Fontaine, Fabien; Imberty, Anne & Fincher, Geoffrey B 2001. Binding interactions between barley thaumatin-like proteins and (1, 3)-β-D-glucans. *European Journal of Biochemistry,* **268,** 4190-4199.

Padmanabhan, Meenu; Cournoyer, Patrick & Dinesh-Kumar, SP 2009. The leucine-rich repeat domain in plant innate immunity: a wealth of possibilities. *Cellular Microbiology,* **11,** 191-198.

Panstruga, Ralph & Dodds, Peter N 2009. Terrific protein traffic: the mystery of effector protein delivery by filamentous plant pathogens. *Science (New York, NY),* **324,** 748.

Panter, Gabriela & Jerala, Roman 2011. The ectodomain of the Toll-like receptor 4 prevents constitutive receptor activation. *Journal of Biological Chemistry,* **286,** 23334-23344.

Panter, Stephen N; Hammond-Kosack, Kim E; Harrison, Kate; Jones, Jonathan DG & Jones, David A 2002. Developmental control of promoter activity is not responsible for mature onset of *Cf-9B*-mediated resistance to leaf mold in tomato. *Molecular Plant-Microbe Interactions,* **15,** 1099-1107.

Park, Hyeong Cheol; Kim, Man Lyang; Kang, Yun Hwan; Jeon, Joo Mi; Yoo, Jae Hyuk; Kim, Min Chul; Park, Chan Young; Jeong, Jae Cheol; Moon, Byeong Cheol & Lee, Ju Huck 2004. Pathogen-and NaCl-induced expression of the SCaM-4 promoter is mediated in part by a GT-1 box that interacts with a GT-1-like transcription factor. *Plant Physiology,* **135,** 2150-2161.

Parniske, Martin; Hammond-Kosack, Kim E; Golstein, Catherine; Thomas, Colwyn M; Jones, David A; Harrison, Kate; Wulff, Brande BH & Jones, Jonathan DG 1997. Novel disease resistance specificities result from sequence exchange between tandemly repeated genes at the *Cf-4/9* locus of tomato. *Cell,* **91,** 821-832.

Parniske, Martin & Jones, Jonathan DG 1999. Recombination between diverged clusters of the tomato *Cf-9* plant disease resistance gene family. *Proceedings of the National Academy of Sciences,* **96,** 5850-5855.

Peck, Roxy & Devore, Jay 2011. *Statistics: The Exploration & Analysis of Data,* Boston, USA, Cengage Learning.

Piedras, Pedro; Hammond-Kosack, Kim E; Harrison, Kate & Jones, Jonathan DG 1998. Rapid, *Cf-9*- and Avr9-dependent production of active oxygen species in tobacco suspension cultures. *Molecular Plant-Microbe Interactions,* **11,** 1155-1166.

Piedras, Pedro; Rivas, Susana; Dröge, Swenja; Hillmer, Stephan & Jones, Jonathan DG 2000. Functional, c-myc-tagged *Cf-9* resistance gene products are plasma-membrane localized and glycosylated. *The Plant Journal,* **21,** 529-536.

Pierpoint, WS; Tatham, AS & Pappin, DJC 1987. Identification of the virus-induced protein of tobacco leaves that resembles the sweet-protein thaumatin. *Physiological and Molecular Plant Pathology,* **31,** 291-298.

Pieterse, Corné MJ; Leon-Reyes, Antonio; van der Ent, Sjoerd & van Wees, Saskia CM 2009. Networking by small-molecule hormones in plant immunity. *Nature Chemical Biology,* **5,** 308-316.

Pieterse, Corné MJ; van der Does, Dieuwertje; Zamioudis, Christos; Leon-Reyes, Antonio & van Wees, Saskia CM 2012. Hormonal modulation of plant immunity. *Annual Review of Cell and Developmental Biology,* **28,** 489-521.

Plesch, Gunnar; Ehrhardt, Thomas & Mueller-Roeber, Bernd 2001. Involvement of TAAAG elements suggests a role for Dof transcription factors in guard cell-specific gene expression. *The Plant Journal,* **28,** 455-464.

Pontier, Dominique; Gan, Susheng; Amasino, Richard M; Roby, Dominique & Lam, Eric 1999. Markers for hypersensitive response and senescence show distinct patterns of expression. *Plant Molecular Biology,* **39,** 1243-1255.

Pontier, Dominique; Godiard, Laurence; Marco, Yves & Roby, Dominique 1994. *hsr*203J, a tobacco gene whose activation is rapid, highly localized and specific for incompatible plant/pathogen interactions. *The Plant Journal,* **5,** 507-521.

Pontier, Dominique; Tronchet, Maurice; Rogowsky, Peter; Lam, Eric & Roby, Dominique 1998. Activation of *hsr203,* a plant gene expressed during incompatible plant-pathogen interactions, is correlated with programmed cell death. *Molecular Plant-Microbe Interactions,* **11,** 544-554.

Postma, Jelle; Liebrand, Thomas W. H.; Bi, Guozhi; Evrard, Alexandre; Bye, Ruby R.; Mbengue, Malick; Kuhn, Hannah; Joosten, Matthieu H. A. J. & Robatzek, Silke 2016. Avr4 promotes Cf-4 receptor-like protein association

with the BAK1/SERK3 receptor-like kinase to initiate receptor endocytosis and plant immunity. *New Phytologist,* **210,** 627-642.

Pruss, Gail J; Nester, Eugene W & Vance, Vicki 2008. Infiltration with *Agrobacterium tumefaciens* induces host defense and development-dependent responses in the infiltrated zone. *Molecular Plant-Microbe Interactions,* **21,** 1528-1538.

Qi, Dong; DeYoung, Brody J & Innes, Roger W 2012. Structure-function analysis of the coiled-coil and leucine-rich repeat domains of the RPS5 disease resistance protein. *Plant Physiology,* **158,** 1819-1832.

Quirino, Betania F; Normanly, Jennifer & Amasino, Richard M 1999. Diverse range of gene activity during *Arabidopsis thaliana* leaf senescence includes pathogen-independent induction of defense-related genes. *Plant Molecular Biology,* **40,** 267-278.

Raghothama, KG; Maggio, Albino; Narasimhan, Meena L; Kononowicz, Andrzej K; Wang, Guangli; D'Urzo, Matilde Paino; Hasegawa, Paul M & Bressan, Ray A 1997. Tissue-specific activation of the osmotin gene by ABA, C_2H_4 and NaCl involves the same promoter region. *Plant Molecular Biology,* **34,** 393-402.

Rairdan, Gregory J & Moffett, Peter 2006. Distinct domains in the ARC region of the potato resistance protein Rx mediate LRR binding and inhibition of activation. *Plant Cell,* **18,** 2082-2093.

Rajam, MV; Chandola, N; Goud, P Saiprasad; Singh, D; Kashyap, V; Choudhary, ML & Sihachakr, D 2007. Thaumatin gene confers resistance to fungal pathogens as well as tolerance to abiotic stresses in transgenic tobacco plants. *Biologia Plantarum,* **51,** 135-141.

Ramonell, Katrina; Berrocal-Lobo, Marta; Koh, Serry; Wan, Jinrong; Edwards, Herb; Stacey, Gary & Somerville, Shauna 2005. Loss-of-function mutations in chitin responsive genes show increased susceptibility to the powdery mildew pathogen *Erysiphe cichoracearum*. *Plant Physiology,* **138,** 1027-1036.

Ravensdale, Michael; Bernoux, Maud; Ve, Thomas; Kobe, Bostjan; Thrall, Peter H; Ellis, Jeffrey G & Dodds, Peter N 2012. Intramolecular interaction influences binding of the flax L5 and L6 resistance proteins to their AvrL567 ligands. *PLoS Pathogens,* **8,** e1003004.

Redman, J; Whitcraft, J; Johnson, C & Arias, J 2002. Abiotic and biotic stress differentially stimulate *as-1* element activity in Arabidopsis. *Plant Cell Reports,* **21,** 180-185.

Reina-Pinto, José J. & Yephremov, Alexander 2009. Surface lipids and plant defenses. *Plant Physiology and Biochemistry,* **47,** 540-549.

Rico, Arantza; Bennett, Mark H; Forcat, Silvia; Huang, Wei E & Preston, Gail M 2010. Agroinfiltration reduces ABA levels and suppresses *Pseudomonas syringae*-elicited salicylic acid production in *Nicotiana tabacum*. *PloS One,* **5,** e8977.

Rivas, Susana; Romeis, Tina & Jones, Jonathan DG 2002. The Cf-9 disease resistance protein is present in an ~420-kilodalton heteromultimeric membrane-associated complex at one molecule per complex. *Plant Cell* **14,** 689-702.

Rivas, Susana; Rougon-Cardoso, Alejandra; Smoker, Matthew; Schauser, Leif; Yoshioka, Hirofumi & Jones, Jonathan DG 2004. CITRX thioredoxin interacts with the tomato Cf-9 resistance protein and negatively regulates defence. *The EMBO Journal,* **23,** 2156-2165.

Rivas, Susana & Thomas, Colwyn M 2005. Molecular interactions between tomato and the leaf mold pathogen *Cladosporium fulvum*. *Annual Review of Phytopathology,* **43,** 395-436.

Romeis, Tina; Piedras, Pedro & Jones, Jonathan DG 2000a. Resistance gene-dependent activation of a calcium-dependent protein kinase in the plant defense response. *Plant Cell,* **12,** 803-815.

Romeis, Tina; Tang, Saijun; Hammond-Kosack, Kim; Piedras, Pedro; Blatt, Mike & Jones, Jonathan DG 2000b. Early signalling events in the Avr9/Cf-9-dependent plant defence response. *Molecular Plant Pathology,* **1,** 3-8.

Ron, Mily & Avni, Adi 2004. The receptor for the fungal elicitor ethylene-inducing xylanase is a member of a resistance-like gene family in tomato. *Plant Cell,* **16,** 1604-1615.

Rooney, Henrietta CE; van't Klooster, John W; van der Hoorn, Renier AL; Joosten, Matthieu HAJ; Jones, Jonathan DG & de Wit, Pierre JGM 2005. Cladosporium Avr2 inhibits tomato Rcr3 protease required for *Cf-2*-dependent disease resistance. *Science,* **308,** 1783-1786.

Rowland, Owen; Ludwig, Andrea A; Merrick, Catherine J; Baillieul, Fabienne; Tracy, Frances E; Durrant, Wendy E; Fritz-Laylin, Lillian; Nekrasov, Vladimir; Sjölander, Kimmen & Yoshioka, Hirofumi 2005. Functional analysis of *Avr9/Cf-9 rapidly elicited* genes identifies a protein kinase, ACIK1, that is essential for full Cf-9–dependent disease resistance in tomato. *Plant Cell,* **17,** 295-310.

Rushton, Paul J; Reinstädler, Anja; Lipka, Volker; Lippok, Bernadette & Somssich, Imre E 2002. Synthetic plant promoters containing defined regulatory elements provide novel insights into pathogen-and wound-induced signaling. *Plant Cell,* **14,** 749-762.

Rushton, Paul J; Somssich, Imre E; Ringler, Patricia & Shen, Qingxi J 2010. WRKY transcription factors. *Trends in Plant Science,* **15,** 247-258.

Rushton, Paul J; Torres, Jorge Tovar; Parniske, Martin; Wernert, Petra; Hahlbrock, K & Somssich, IE 1996. Interaction of elicitor-induced DNA-binding proteins with elicitor response elements in the promoters of parsley *PR1* genes. *The EMBO Journal,* **15,** 5690.

Sakai, Hiroe; Honma, Takashi; Aoyama, Takashi; Sato, Shusei; Kato, Tomohiko; Tabata, Satoshi & Oka, Atsuhiro 2001. ARR1, a transcription factor for genes immediately responsive to cytokinins. *Science,* **294,** 1519-1521.

Sano, H.; Seo, S.; Koizumi, N.; Niki, T.; Iwamura, H. & Ohashi, Y. 1996. Regulation by cytokinins of endogenous levels of jasmonic and salicylic acids in mechanically wounded tobacco plants. *Plant and Cell Physiology,* **37,** 762-769.

Santiago, Julia; Henzler, Christine & Hothorn, Michael 2013. Molecular mechanism for plant steroid receptor activation by somatic embryogenesis co-receptor kinases. *Science,* **341,** 889-892.

Santos-Rosa, M; Poutaraud, A; Merdinoglu, D & Mestre, P 2008. Development of a transient expression system in grapevine via agro-infiltration. *Plant Cell Reports,* **27,** 1053-1063.

Sanz, Ana; Moreno, Juan Ignacio & Castresana, Carmen 1998. PIOX, a new pathogen-induced oxygenase with homology to animal cyclooxygenase. *Plant Cell,* **10,** 1523-1537.

Sato, F.; Kitajima, S. & Koyama, T. 1996. Ethylene-induced gene expression of osmotin-like protein, a neutral isoform of tobacco PR-5, is mediated by the AGCCGCC *cis*-sequence. *Plant and Cell Physiology,* **37,** 249-255.

Schulze, Birgit; Mentzel, Tobias; Jehle, Anna K.; Mueller, Katharina; Beeler, Seraina; Boller, Thomas; Felix, Georg & Chinchilla, Delphine 2010. Rapid heteromerization and phosphorylation of ligand-activated plant transmembrane receptors and their associated kinase BAK1. *Journal of Biological Chemistry,* **285,** 9444-9451.

Seear, Paul J & Dixon, Mark S 2003. Variable leucine-rich repeats of tomato disease resistance genes *Cf-2* and *Cf-5* determine specificity. *Molecular Plant Pathology,* **4,** 199-202.

Segonzac, Cécile & Zipfel, Cyril 2011. Activation of plant pattern-recognition receptors by bacteria. *Current Opinion in Microbiology,* **14,** 54-61.

Senthil-Kumar, Muthappa & Mysore, Kirankumar S 2013. Nonhost resistance against bacterial pathogens: retrospectives and prospects. *Annual Review of Phytopathology,* **51,** 407-427.

Shabab, Mohammed; Shindo, Takayuki; Gu, Christian; Kaschani, Farnusch; Pansuriya, Twinkal; Chintha, Raju; Harzen, Anne; Colby, Tom; Kamoun, Sophien & van der Hoorn, Renier AL 2008. Fungal effector protein AVR2 targets diversifying defense-related cys proteases of tomato. *Plant Cell* **20,** 1169-1183.

Shah, Jyoti & Klessig, Daniel F 1996. Identification of a salicylic acid-responsive element in the promoter of the tobacco pathogenesis-related β-1,3-glucanase gene, *PR-2d*. *The Plant Journal,* **10,** 1089-1101.

Shapiro, Allan D & Zhang, Chu 2001. The role of NDR1 in avirulence gene-directed signaling and control of programmed cell death in Arabidopsis. *Plant Physiology,* **127,** 1089-1101.

She, Ji; Han, Zhifu; Kim, Tae-Wuk; Wang, Jinjing; Cheng, Wei; Chang, Junbiao; Shi, Shuai; Wang, Jiawei; Yang, Maojun & Wang, Zhi-Yong 2011. Structural insight into brassinosteroid perception by BRI1. *Nature,* **474,** 472-476.

Sheikh, Arsheed Hussain; Raghuram, Badmi; Eschen-Lippold, Lennart; Scheel, Dierk; Lee, Justin & Sinha, Alok Krishna 2014. Agroinfiltration by cytokinin-producing *Agrobacterium* sp. strain GV3101 primes defense responses in *Nicotiana tabacum*. *Molecular Plant-Microbe Interactions,* **27,** 1175-1185.

Shen, Yunping & Diener, Andrew C 2013. *Arabidopsis thaliana RESISTANCE TO FUSARIUM OXYSPORUM 2* Implicates Tyrosine-Sulfated Peptide Signaling in Susceptibility and Resistance to Root Infection. *PLoS Genetics,* **9,** e1003525.

Shirano, Yumiko; Kachroo, Pradeep; Shah, Jyoti & Klessig, Daniel F 2002. A gain-of-function mutation in an Arabidopsis Toll Interleukin1 Receptor–Nucleotide Binding Site–Leucine-Rich Repeat type R gene triggers defense responses and results in enhanced disease resistance. *Plant Cell* **14,** 3149-3162.

Shirasu, K; Nakajima, H; Rajasekhar, VK; Dixon, RA & Lamb, C 1997. Salicylic acid potentiates an agonist-dependent gain control that amplifies pathogen signals in the activation of defense mechanisms. *Plant Cell,* **9,** 261-70.

Shirasu, Ken & Schulze-Lefert, Paul 2000. Regulators of cell death in disease resistance. *Plant Molecular Biology,* **44,** 371-385.

Shiu, Shin-Han; Karlowski, Wojciech M; Pan, Runsun; Tzeng, Yun-Huei; Mayer, Klaus FX & Li, Wen-Hsiung 2004. Comparative analysis of the receptor-like kinase family in Arabidopsis and rice. *Plant Cell,* **16,** 1220-1234.

Sierro, Nicolas; Battey, James ND; Ouadi, Sonia; Bakaher, Nicolas; Bovet, Lucien; Willig, Adrian; Goepfert, Simon; Peitsch, Manuel C & Ivanov, Nikolai V 2014. The tobacco genome sequence and its comparison with those of tomato and potato. *Nature Communications,* **5,** 3833.

Singh, Narendra K; Bracker, Charles A; Hasegawa, Paul M; Handa, Avtar K; Buckel, Scott; Hermodson, Mark A; Pfankoch, ED; Regnier, Fred E & Bressan, Ray A 1987. Characterization of osmotin: A thaumatin-like protein associated with osmotic adaptation in plant cells. *Plant Physiology,* **85,** 529-536.

Singh, Narendra K; Nelson, Donald E; Kuhn, David; Hasegawa, Paul M & Bressan, Ray A 1989. Molecular cloning of osmotin and regulation of its

expression by ABA and adaptation to low water potential. *Plant Physiology,* **90,** 1096-1101.

Singh, Naveen Kumar; Kumar, Koppolu Raja Rajesh; Kumar, Dilip; Shukla, Pawan & Kirti, PB 2013. Characterization of a pathogen induced thaumatin-like protein gene *AdTLP* from *Arachis diogoi*, a wild peanut. *PloS One,* **8,** e83963.

Skadsen, RW; Sathish, P & Kaeppler, HF 2000. Expression of thaumatin-like permatin *PR-5* genes switches from the ovary wall to the aleurone in developing barley and oat seeds. *Plant Science,* **156,** 11-22.

Slootweg, Erik J; Spiridon, Laurentiu N; Roosien, Jan; Butterbach, Patrick; Pomp, Rikus; Westerhof, Lotte; Wilbers, Ruud; Bakker, Erin; Bakker, Jaap & Petrescu, Andrei-José 2013. Structural Determinants at the Interface of the ARC2 and LRR Domains Control the Activation of the NB-LRR Plant Immune Receptors Rx1 and Gpa2. *Plant Physiology*.

Song, Jing; Win, Joe; Tian, Miaoying; Schornack, Sebastian; Kaschani, Farnusch; Ilyas, Muhammad; van der Hoorn, Renier AL & Kamoun, Sophien 2009. Apoplastic effectors secreted by two unrelated eukaryotic plant pathogens target the tomato defense protease Rcr3. *Proceedings of the National Academy of Sciences,* **106,** 1654-1659.

Song, Wen-Yuan; Wang, Guo-Liang; Chen, Li-Li; Kim, Han-Suk; Pi, Li-Ya; Holsten, Tom; Gardner, J; Wang, Bei; Zhai, Wen-Xue & Zhu, Li-Huang 1995. A receptor kinase-like protein encoded by the rice disease resistance gene, *Xa21*. *Science,* **270,** 1804-1806.

Soumpourou, Eleni; Iakovidis, Michael; Chartrain, Laetitia; Lyall, Verity & Thomas, Colwyn M 2007. The *Solanum pimpinellifolium Cf-ECP1* and *Cf-ECP4* genes for resistance to *Cladosporium fulvum* are located at the *Milky Way* locus on the short arm of chromosome 1. *Theoretical and Applied Genetics,* **115,** 1127-1136.

Spoel, Steven H & Dong, Xinnian 2012. How do plants achieve immunity? Defence without specialized immune cells. *Nature Reviews Immunology,* **12,** 89-100.

Spoel, Steven H; Mou, Zhonglin; Tada, Yasuomi; Spivey, Natalie W; Genschik, Pascal & Dong, Xinnian 2009. Proteasome-mediated turnover of the transcription coactivator NPR1 plays dual roles in regulating plant immunity. *Cell,* **137,** 860-872.

Spoel, Steven H.; Koornneef, Annemart; Claessens, Susanne M. C.; Korzelius, Jerôme P.; van Pelt, Johan A.; Mueller, Martin J.; Buchala, Antony J.; Métraux, Jean-Pierre; Brown, Rebecca; Kazan, Kemal; van Loon, Leendert C.; Dong, Xinnian & Pieterse, Corné M. J. 2003. NPR1 Modulates Cross-Talk between Salicylate- and Jasmonate-Dependent Defense Pathways through a Novel Function in the Cytosol. *Plant Cell,* **15,** 760-770.

Stålberg, Kjell; Ellerström, Mats; Ezcurra, Inès; Ablov, Sergei & Rask, Lars 1996. Disruption of an overlapping E-box/ABRE motif abolished high transcription of the napA storage-protein promoter in transgenic *Brassica napus* seeds. *Planta,* **199,** 515-519.

Stergiopoulos, Ioannis; de Kock, Maarten JD; Lindhout, Pim & de Wit, Pierre JGM 2007. Allelic variation in the effector genes of the tomato pathogen *Cladosporium fulvum* reveals different modes of adaptive evolution. *Molecular Plant-Microbe Interactions,* **20,** 1271-1283.

Stergiopoulos, Ioannis & de Wit, Pierre JGM 2009. Fungal effector proteins. *Annual Review of Phytopathology,* **47,** 233-263.

Stergiopoulos, Ioannis; van den Burg, Harrold A; Ökmen, Bilal; Beenen, Henriek G; van Liere, Sabine; Kema, Gert HJ & de Wit, Pierre JGM 2010. Tomato

Cf resistance proteins mediate recognition of cognate homologous effectors from fungi pathogenic on dicots and monocots. *Proceedings of the National Academy of Sciences,* **107,** 7610-7615.

Stintzi, A; Heitz, T; Kauffmann, S; Legrand, M & Fritig, B 1991. Identification of a basic pathogenesis-related, thaumatin-like protein of virus-infected tobacco as osmotin. *Physiological and Molecular Plant Pathology,* **38,** 137-146.

Stotz, Henrik U; Mitrousia, Georgia K; de Wit, Pierre JGM & Fitt, Bruce DL 2014. Effector-triggered defence against apoplastic fungal pathogens. *Trends in Plant Science,* **19,** 491-500.

Strompen, Georg; Grüner, Rose & Pfitzner, Ursula M 1998. An *as-1*-like motif controls the level of expression of the gene for the pathogenesis-related protein 1a from tobacco. *Plant Molecular Biology,* **37,** 871-883.

Subramaniam, Rajagopal; Desveaux, Darrell; Spickler, Catherine; Michnick, Stephen W & Brisson, Normand 2001. Direct visualization of protein interactions in plant cells. *Nature Biotechnology,* **19,** 769-772.

Sun, Wenxian; Cao, Yangrong; Labby, Kristin Jansen; Bittel, Pascal; Boller, Thomas & Bent, Andrew F 2012. Probing the *Arabidopsis* flagellin receptor: FLS2-FLS2 association and the contributions of specific domains to signaling function. *Plant Cell,* **24,** 1096-1113.

Sun, Yadong; Li, Lei; Macho, Alberto P; Han, Zhifu; Hu, Zehan; Zipfel, Cyril; Zhou, Jian-Min & Chai, Jijie 2013. Structural basis for flg22-induced activation of the *Arabidopsis* FLS2-BAK1 immune complex. *Science,* **342,** 624-628.

Synkova, Helena; Semorádová, Šárka & Burketova, Lenka 2004. High content of endogenous cytokinins stimulates activity of enzymes and proteins involved in stress response in *Nicotiana tabacum*. *Plant Cell, Tissue and Organ Culture,* **79,** 169-179.

Takemoto, Daigo; Hayashi, Makoto; Doke, Noriyuki; Nishimura, Mikio & Kawakita, Kazuhito 2000. Isolation of the gene for EILP, an elicitor-inducible LRR receptor-like protein, from tobacco by differential display. *Plant and Cell Physiology,* **41,** 458-464.

Takemoto, Daigo & Jones, David A 2005. Membrane release and destabilization of Arabidopsis RIN4 following cleavage by *Pseudomonas syringae* AvrRpt2. *Molecular Plant-Microbe Interactions,* **18,** 1258-1268.

Takken, Frank LW; Albrecht, Mario & Tameling, Wladimir IL 2006. Resistance proteins: molecular switches of plant defence. *Current Opinion in Plant Biology,* **9,** 383-390.

Takken, Frank LW & Goverse, Aska 2012. How to build a pathogen detector: structural basis of NB-LRR function. *Current Opinion in Plant Biology,* **15,** 375-384.

Takken, Frank LW; Thomas, Colwyn M; Joosten, Matthieu HAJ; Golstein, Catherine; Westerink, Nienke; Hille, Jacques; Nijkamp, H John J; de Wit, Pierre JGM & Jones, Jonathan DG 1999. A second gene at the tomato *Cf-4* locus confers resistance to *Cladosporium fulvum* through recognition of a novel avirulence determinant. *The Plant Journal,* **20,** 279-288.

Tameling, Wladimir IL; Vossen, Jack H; Albrecht, Mario; Lengauer, Thomas; Berden, Jan A; Haring, Michel A; Cornelissen, Ben JC & Takken, Frank LW 2006. Mutations in the NB-ARC domain of I-2 that impair ATP hydrolysis cause autoactivation. *Plant Physiology,* **140,** 1233-1245.

Taniguchi, Masatoshi; Sasaki, Naokazu; Tsuge, Tomohiko; Aoyama, Takashi & Oka, Atsuhiro 2007. ARR1 directly activates cytokinin response genes that

encode proteins with diverse regulatory functions. *Plant and Cell Physiology,* **48,** 263-277.

Tanji, Hiromi; Ohto, Umeharu; Shibata, Takuma; Miyake, Kensuke & Shimizu, Toshiyuki 2013. Structural reorganization of the Toll-like receptor 8 dimer induced by agonistic ligands. *Science,* **339,** 1426-1429.

Tapia, Gerardo; Verdugo, Isabel; Yañez, Mónica; Ahumada, Iván; Theoduloz, Cristina; Cordero, Cecilia; Poblete, Fernando; González, Enrique & Ruiz-Lara, Simón 2005. Involvement of ethylene in stress-induced expression of the *TLC1. 1* retrotransposon from *Lycopersicon chilense* Dun. *Plant Physiology,* **138,** 2075-2086.

Terzaghi, William B & Cashmore, Anthony R 1995. Light-regulated transcription. *Annual Review of Plant Biology,* **46,** 445-474.

Thomas, Colwyn M; Jones, David A; Parniske, Martin; Harrison, Kate; Balint-Kurti, Peter J; Hatzixanthis, Kostas & Jones, Jonathan DG 1997. Characterization of the tomato *Cf-4* gene for resistance to *Cladosporium fulvum* identifies sequences that determine recognitional specificity in *Cf-4* and *Cf-9*. *Plant Cell,* **9,** 2209-2224.

Thomas, Colwyn M; Tang, Saijun; Hammond-Kosack, Kim & Jones, Jonathan DG 2000. Comparison of the hypersensitive response induced by the tomato *Cf-4* and *Cf-9* genes in *Nicotiana* spp. *Molecular Plant-Microbe Interactions,* **13,** 465-469.

Thomma, Bart PHJ; Nürnberger, Thorsten & Joosten, Matthieu HAJ 2011. Of PAMPs and effectors: the blurred PTI-ETI dichotomy. *Plant Cell* **23,** 4-15.

Thomma, Bart PHJ; van Esse, H Peter; Crous, Pedro W & de Wit, Pierre JGM 2005. *Cladosporium fulvum* (syn. *Passalora fulva*), a highly specialized plant pathogen as a model for functional studies on plant pathogenic Mycosphaerellaceae. *Molecular Plant Pathology,* **6,** 379-393.

Tian, Miaoying; Win, Joe; Song, Jing; van der Hoorn, Renier AL; van der Knaap, Esther & Kamoun, Sophien 2007. A *Phytophthora infestans* cystatin-like protein targets a novel tomato papain-like apoplastic protease. *Plant Physiology,* **143,** 364-377.

Tornero, Pablo; Gadea, José; Conejero, Vicente & Vera, Pablo 1997. Two *PR-1* genes from tomato are differentially regulated and reveal a novel mode of expression for a pathogenesis-related gene during the hypersensitive response and development. *Molecular Plant-Microbe Interactions,* **10,** 624-634.

Tran, Lam-Son Phan; Nakashima, Kazuo; Sakuma, Yoh; Simpson, Sean D; Fujita, Yasunari; Maruyama, Kyonoshin; Fujita, Miki; Seki, Motoaki; Shinozaki, Kazuo & Yamaguchi-Shinozaki, Kazuko 2004. Isolation and functional analysis of Arabidopsis stress-inducible NAC transcription factors that bind to a drought-responsive *cis*-element in the *early responsive to dehydration stress 1* promoter. *Plant Cell* **16,** 2481-2498.

Trudel, Jean; Grenier, Jean; Potvin, Claude & Asselin, Alain 1998. Several thaumatin-like proteins bind to β-1,3-glucans. *Plant Physiology,* **118,** 1431-1438.

Tsuda, Kenichi & Katagiri, Fumiaki 2010. Comparing signaling mechanisms engaged in pattern-triggered and effector-triggered immunity. *Current Opinion in Plant Biology,* **13,** 459-465.

Uknes, Scott; Dincher, Sandra; Friedrich, Leslie; Negrotto, David; Williams, Shericca; Thompson-Taylor, Hope; Potter, Sharon; Ward, Eric & Ryals, John 1993. Regulation of pathogenesis-related protein-1a gene expression in tobacco. *Plant Cell* **5,** 159-169.

van't Klooster, John W; van der Kamp, Marc W; Vervoort, Jacques; Beekwilder, Jules; Boeren, Sjef; Joosten, Matthieu HAJ; Thomma, Bart PHJ & de Wit,

Pierre JGM 2011. Affinity of Avr2 for tomato cysteine protease Rcr3 correlates with the Avr2-triggered Cf-2-mediated hypersensitive response. *Molecular Plant Pathology,* **12,** 21-30.

van de Rhee, Miranda D; Lemmers, R & Bol, JF 1993. Analysis of regulatory elements involved in stress-induced and organ-specific expression of tobacco acidic and basic β-1,3-glucanase genes. *Plant Molecular Biology,* **21,** 451-461.

van den Ackerveken, Guido FJM; van Kan, Jan AL & de Wit, Pierre JGM 1992. Molecular analysis of the avirulence gene *avr9* of the fungal tomato pathogen *Cladosporium fulvum* fully supports the gene-for-gene hypothesis. *The Plant Journal,* **2,** 359-366.

van den Ackerveken, Guido FJM; van Kan, Jan AL; Joosten, Matthieu HAJ; Muisers, José M; Verbakel, Henk M & de Wit, Pierre JGM 1993. Characterization of two putative pathogenicity genes of the fungal tomato pathogen *Cladosporium fulvum*. *Molecular Plant-Microbe Interactions,* **6,** 210-215.

van den Burg, Harrold A; Harrison, Stuart J; Joosten, Matthieu HAJ; Vervoort, Jacques & de Wit, Pierre JGM 2006. *Cladosporium fulvum* Avr4 protects fungal cell walls against hydrolysis by plant chitinases accumulating during infection. *Molecular Plant-Microbe Interactions,* **19,** 1420-1430.

van den Burg, Harrold A; Tsitsigiannis, Dimitrios I; Rowland, Owen; Lo, Jane; Rallapalli, Ghanasyam; MacLean, Daniel; Takken, Frank LW & Jones, Jonathan DG 2008. The F-box protein ACRE189/ACIF1 regulates cell death and defense responses activated during pathogen recognition in tobacco and tomato. *Plant Cell* **20,** 697-719.

van den Burg, Harrold A; Westerink, Nienke; Francoijs, Kees-Jan; Roth, Ronelle; Woestenenk, Esmeralda; Boeren, Sjef; de Wit, Pierre JGM; Joosten, Matthieu HAJ & Vervoort, Jacques 2003. Natural disulfide bond-disrupted mutants of AVR4 of the tomato pathogen *Cladosporium fulvum* are sensitive to proteolysis, circumvent *Cf-4*-mediated resistance, but retain their chitin binding ability. *Journal of Biological Chemistry,* **278,** 27340-27346.

van der Biezen, Erik A & Jones, Jonathan DG 1998. Plant disease-resistance proteins and the gene-for-gene concept. *Trends in Biochemical Sciences,* **23,** 454-456.

van der Hoorn, Renier AL & Kamoun, Sophien 2008. From guard to decoy: a new model for perception of plant pathogen effectors. *Plant Cell* **20,** 2009-2017.

van der Hoorn, Renier AL; Laurent, Franck; Roth, Ronelle & de Wit, Pierre JGM 2000. Agroinfiltration is a versatile tool that facilitates comparative analyses of *Avr9*/*Cf-9*-induced and *Avr4*/*Cf-4*-induced necrosis. *Molecular Plant-Microbe Interactions,* **13,** 439-446.

van der Hoorn, Renier AL; Roth, Ronelle & de Wit, Pierre JGM 2001a. Identification of distinct specificity determinants in resistance protein Cf-4 allows construction of a Cf-9 mutant that confers recognition of avirulence protein AVR4. *Plant Cell* **13,** 273-285.

van der Hoorn, Renier AL; van der Ploeg, Anke; de Wit, Pierre JGM & Joosten, Matthieu HAJ 2001b. The C-terminal dilysine motif for targeting to the endoplasmic reticulum is not required for Cf-9 function. *Molecular Plant-Microbe Interactions,* **14,** 412-415.

van der Hoorn, Renier AL; Wulff, Brande BH; Rivas, Susana; Durrant, Marcus C; van der Ploeg, Anke; de Wit, Pierre JGM & Jones, Jonathan DG 2005. Structure-function analysis of Cf-9, a receptor-like protein with extracytoplasmic leucine-rich repeats. *Plant Cell,* **17,** 1000-1015.

van Esse, H Peter; Bolton, Melvin D; Stergiopoulos, Ioannis; de Wit, Pierre JGM & Thomma, Bart PHJ 2007. The chitin-binding *Cladosporium fulvum* effector

protein Avr4 is a virulence factor. *Molecular Plant-Microbe Interactions,* **20,** 1092-1101.

van Esse, H Peter; van't Klooster, John W; Bolton, Melvin D; Yadeta, Koste A; van Baarlen, Peter; Boeren, Sjef; Vervoort, Jacques; de Wit, Pierre JGM & Thomma, Bart PHJ 2008. The *Cladosporium fulvum* virulence protein Avr2 inhibits host proteases required for basal defense. *Plant Cell* **20,** 1948-1963.

van Etten, Hans D; Mansfield, John W; Bailey, John A & Farmer, Edward E 1994. Two classes of plant antibiotics: Phytoalexins versus" Phytoanticipins". *Plant Cell,* **6,** 1191.

van Kan, Jan AL; Joosten, Matthieu HAJ; Wagemakers, Cornelia AM; van den Berg-Velthuis, Grardy CM & de Wit, Pierre JGM 1992. Differential accumulation of mRNAs encoding extracellular and intracellular PR proteins in tomato induced by virulent and avirulent races of *Cladosporium fulvum*. *Plant Molecular Biology,* **20,** 513-527.

van Kan, Jan AL; van de Rhee, Miranda D; Zuidema, D; Cornelissen, Ben JC & Bol, John F 1989. Structure of tobacco genes encoding thaumatin-like proteins. *Plant Molecular Biology,* **12,** 153-155.

van Loon, LC; Gerritsen, YAM & Ritter, CE 1987. Identification, purification, and characterization of pathogenesis-related proteins from virus-infected Samsun NN tobacco leaves. *Plant Molecular Biology,* **9,** 593-609.

van Loon, Leendert C. 1985. Pathogenesis-related proteins. *Plant Molecular Biology,* **4,** 111-116.

van Loon, Leendert C. 1999. Occurrence and properties of plant pathogenesis-related proteins. *Pathogenesis-related proteins in plants***,** 1-19.

van Loon, Leendert C.; Rep, Martijn & Pieterse, Corné MJ 2006. Significance of inducible defense-related proteins in infected plants. *Annual Review of Phytopathology,* **44,** 135-162.

van Ooijen, Gerben; Mayr, Gabriele; Kasiem, Mobien MA; Albrecht, Mario; Cornelissen, Ben JC & Takken, Frank LW 2008. Structure–function analysis of the NB-ARC domain of plant disease resistance proteins. *Journal of Experimental Botany,* **59,** 1383-1397.

van Verk, Marcel C; Pappaioannou, Dimitri; Neeleman, Lyda; Bol, John F & Linthorst, Huub JM 2008. A novel WRKY transcription factor is required for induction of *PR-1a* gene expression by salicylic acid and bacterial elicitors. *Plant Physiology,* **146,** 1983-1995.

Vaucheret, Hervé; Béclin, Christophe & Fagard, Mathilde 2001. Post-transcriptional gene silencing in plants. *Journal of Cell Science,* **114,** 3083-3091.

Velazhahan, R & Muthukrishnan, S 2003. Transgenic tobacco plants constitutively overexpressing a rice thaumatin-like protein (PR-5) show enhanced resistance to *Alternaria alternata*. *Biologia Plantarum,* **47,** 347-354.

Venter, Mauritz 2007. Synthetic promoters: genetic control through *cis* engineering. *Trends in Plant Science,* **12,** 118-124.

Vervoort, Jacques; van den Hooven, Henno W; Berg, Axel; Vossen, Paul; Vogelsang, Ralph; Joosten, Matthieu HAJ & de Wit, Pierre JGM 1997. The race-specific elicitor AVR9 of the tomato pathogen *Cladosporium fulvum*: a cystine knot protein: Sequence-specific ^{1}H NMR assignments, secondary structure and global fold of the protein. *FEBS Letters,* **404,** 153-158.

Vlot, A Corina; Dempsey, D'Maris Amick & Klessig, Daniel F 2009. Salicylic acid, a multifaceted hormone to combat disease. *Annual Review of Phytopathology,* **47,** 177-206.

Voinnet, Olivier; Rivas, Susana; Mestre, Pere & Baulcombe, David 2003. An enhanced transient expression system in plants based on suppression of gene

silencing by the p19 protein of tomato bushy stunt virus. *The Plant Journal,* **33,** 949-956.

Vossen, Jack H.; Abd-El-Haliem, Ahmed; Fradin, Emilie F.; Van Den Berg, Grardy C. M.; Ekengren, Sophia K.; Meijer, Harold J. G.; Seifi, Alireza; Bai, Yuling; Ten Have, Arjen; Munnik, Teun; Thomma, Bart P. H. J. & Joosten, Matthieu H. A. J. 2010. Identification of tomato phosphatidylinositol-specific phospholipase-C (PI-PLC) family members and the role of PLC4 and PLC6 in HR and disease resistance. *The Plant Journal,* **62,** 224-239.

Wang, Changchun; Cai, Xinzhong & Zheng, Zhong 2005a. High humidity represses Cf-4/Avr4-and Cf-9/Avr9-dependent hypersensitive cell death and defense gene expression. *Planta,* **222,** 947-956.

Wang, Guodong; Ellendorff, Ursula; Kemp, Ben; Mansfield, John W; Forsyth, Alec; Mitchell, Kathy; Bastas, Kubilay; Liu, Chun-Ming; Woods-Tör, Alison & Zipfel, Cyril 2008a. A genome-wide functional investigation into the roles of receptor-like proteins in Arabidopsis. *Plant Physiology,* **147,** 503-517.

Wang, Ming-Bo; Helliwell, Christopher A; Wu, Li-Min; Waterhouse, Peter M; Peacock, W James & Dennis, Elizabeth S 2008b. Hairpin RNAs derived from RNA polymerase II and polymerase III promoter-directed transgenes are processed differently in plants. *RNA,* **14,** 903-913.

Wang, Xuelu; Li, Xiaoqing; Meisenhelder, Jill; Hunter, Tony; Yoshida, Shigeo; Asami, Tadao & Chory, Joanne 2005b. Autoregulation and homodimerization are involved in the activation of the plant steroid receptor BRI1. *Developmental Cell,* **8,** 855-865.

Ward, ER; Uknes, SJ; Williams, SC; Dincher, SS; Wiederhold, DL; Alexander, DC; Ahl-Goy, P; Metraux, JP & Ryals, JA 1991. Coordinate gene activity in response to agents that induce systemic acquired resistance. *Plant Cell,* **3,** 1085-1094.

Weber, Alexander NR; Moncrieffe, Martin C; Gangloff, Monique; Imler, Jean-Luc & Gay, Nicholas J 2005. Ligand-receptor and receptor-receptor interactions act in concert to activate signaling in the *Drosophila* toll pathway. *Journal of Biological Chemistry,* **280,** 22793-22799.

Weber, Ricardo LM; Wiebke-Strohm, Beatriz; Bredemeier, Christian; Margis-Pinheiro, Márcia; de Brito, Giovani G; Rechenmacher, Ciliana; Bertagnolli, Paulo F; de Sá, Maria EL; Campos, Magnólia de Araújo; de Amorim, Regina MS; Beneventi, Magda A; Margis, Rogério; Grossi-de-Sa, Maria F & Bodanese-Zanettini, Maria H 2014. Expression of an osmotin-like protein from *Solanum nigrum* confers drought tolerance in transgenic soybean. *BMC Plant Biology,* **14,** 343.

Weinmann, Pamela; Gossen, Manfred; Hillen, Wolfgang; Bujard, Hermann & Gatz, Christiane 1994. A chimeric transactivator allows tetracycline-responsive gene expression in whole plants. *The Plant Journal,* **5,** 559-569.

Weiss, Arthur & Schlessinger, Joseph 1998. Switching signals on or off by receptor dimerization. *Cell,* **94,** 277-280.

Westerink, Nienke; Brandwagt, Bas F; de Wit, Pierre JGM & Joosten, Matthieu HAJ 2004. *Cladosporium fulvum* circumvents the second functional resistance gene homologue at the *Cf-4* locus (*Hcr9-4E*) by secretion of a stable avr4E isoform. *Molecular Microbiology,* **54,** 533-545.

Westerink, Nienke; Roth, Ronelle; Van den Burg, Harrold A; de Wit, Pierre JGM & Joosten, Matthieu HAJ 2002. The AVR4 elicitor protein of *Cladosporium fulvum* binds to fungal components with high affinity. *Molecular Plant-Microbe Interactions,* **15,** 1219-1227.

Williams, Simon J; Sornaraj, Pradeep; deCourcy-Ireland, Emma; Menz, R Ian; Kobe, Bostjan; Ellis, Jeffrey G; Dodds, Peter N & Anderson, Peter A 2011. An autoactive mutant of the M flax rust resistance protein has a preference for binding ATP, whereas wild-type M protein binds ADP. *Molecular Plant-Microbe Interactions,* **24,** 897-906.

Williams, Simon J.; Sohn, Kee Hoon; Wan, Li; Bernoux, Maud; Sarris, Panagiotis F.; Segonzac, Cecile; Ve, Thomas; Ma, Yan; Saucet, Simon B.; Ericsson, Daniel J.; Casey, Lachlan W.; Lonhienne, Thierry; Winzor, Donald J.; Zhang, Xiaoxiao; Coerdt, Anne; Parker, Jane E.; Dodds, Peter N.; Kobe, Bostjan & Jones, Jonathan D. G. 2014. Structural basis for assembly and function of a heterodimeric plant immune receptor. *Science,* **344,** 299-303.

Winans, Katharine A & Hashimoto, Carl 1995. Ventralization of the *Drosophila* embryo by deletion of extracellular leucine-rich repeats in the Toll protein. *Molecular Biology of the Cell,* **6,** 587-596.

Wirthmueller, Lennart; Maqbool, Abbas & Banfield, Mark J 2013. On the front line: structural insights into plant-pathogen interactions. *Nature Reviews Microbiology,* **11,** 761-776.

Woloshuk, Charles P; Meulenhoff, Josien S; Sela-Buurlage, Marianne; van den Elzen, Peter JM & Cornelissen, Ben JC 1991. Pathogen-induced proteins with inhibitory activity toward *Phytophthora infestans*. *Plant Cell* **3,** 619-628.

Wubben, JP; Lawrence, CB & de Wit, PJGM 1996. Differential induction of chitinase and 1, 3-β-glucanase gene expression in tomato by *Cladosporium fulvum* and its race-specific elicitors. *Physiological and Molecular Plant Pathology,* **48,** 105-116.

Wulff, Brande BH; Chakrabarti, Apratim & Jones, David A 2009a. Recognitional specificity and evolution in the tomato-*Cladosporium fulvum* pathosystem. *Molecular Plant-Microbe Interactions,* **22,** 1191-1202.

Wulff, Brande BH; Heese, Antje; Tomlinson-Buhot, Laurence; Jones, David A; de la Peña, Marcos & Jones, Jonathan DG 2009b. The major specificity-determining amino acids of the tomato Cf-9 disease resistance protein are at hypervariable solvent-exposed positions in the central leucine-rich repeats. *Molecular Plant-Microbe Interactions,* **22,** 1203-1213.

Wulff, Brande BH; Kruijt, Marco; Collins, Peter L; Thomas, Colwyn M; Ludwig, Andrea A; de Wit, Pierre JGM & Jones, Jonathan DG 2004a. Gene shuffling-generated and natural variants of the tomato resistance gene *Cf-9* exhibit different auto-necrosis-inducing activities in *Nicotiana* species. *The Plant Journal,* **40,** 942-956.

Wulff, Brande BH; Thomas, Colwyn M; Parniske, Martin & Jones, Jonathan DG 2004b. Genetic variation at the tomato *Cf-4/Cf-9* locus induced by EMS mutagenesis and intralocus recombination. *Genetics,* **167,** 459-470.

Wulff, Brande BH; Thomas, Colwyn M; Smoker, Matthew; Grant, Murray & Jones, Jonathan DG 2001. Domain swapping and gene shuffling identify sequences required for induction of an Avr-dependent hypersensitive response by the tomato Cf-4 and Cf-9 proteins. *Plant Cell* **13,** 255-272.

Xu, Y; Chang, PFL; Liu, D; Narasimhan, ML; Raghothama, KG; Hasegawa, PM & Bressan, RA 1994. Plant defense genes are synergistically induced by ethylene and methyl jasmonate. *Plant Cell,* **6,** 1077-1085.

Yamamoto, Sumiko; Nakano, Toshitsugu; Suzuki, Kaoru & Shinshi, Hideaki 2004. Elicitor-induced activation of transcription via W box-related *cis*-acting elements from a basic chitinase gene by WRKY transcription factors in tobacco. *Biochimica et Biophysica Acta,* **1679,** 279.

Yanagisawa, Shuichi 2004. Dof domain proteins: plant-specific transcription factors associated with diverse phenomena unique to plants. *Plant and Cell Physiology,* **45,** 386-391.

Yang, Yinong; Li, Rugang & Qi, Min 2000. *In vivo* analysis of plant promoters and transcription factors by agroinfiltration of tobacco leaves. *The Plant Journal,* **22,** 543-551.

Yuan, Yinan; Haanstra, Jair; Lindhout, Pim & Bonnema, Guusje 2002. The *Cladosporium fulvum* resistance gene *Cf-ECP3* is part of the *Orion* cluster on the short arm of tomato Chromosome 1. *Molecular Breeding,* **10,** 45-50.

Zhang, Chu; Gutsche, Annie Tang & Shapiro, Allan D 2004. Feedback control of the *Arabidopsis* hypersensitive response. *Molecular Plant-Microbe Interactions,* **17,** 357-365.

Zhang, Lisha; Kars, Ilona; Essenstam, Bert; Liebrand, Thomas WH; Wagemakers, Lia; Elberse, Joyce; Tagkalaki, Panagiota; Tjoitang, Devlin; van den Ackerveken, Guido & van Kan, Jan AL 2014a. Fungal endopolygalacturonases are recognized as microbe-associated molecular patterns by the Arabidopsis receptor-like protein RESPONSIVENESS TO BOTRYTIS POLYGALACTURONASES1. *Plant Physiology,* **164,** 352-364.

Zhang, Shuqun & Klessig, Daniel F 1998. Resistance gene N-mediated de novo synthesis and activation of a tobacco mitogen-activated protein kinase by tobacco mosaic virus infection. *Proceedings of the National Academy of Sciences,* **95,** 7433-7438.

Zhang, Shuqun; Liu, Yidong & Klessig, Daniel F 2000. Multiple levels of tobacco WIPK activation during the induction of cell death by fungal elicitins. *The Plant Journal,* **23,** 339-347.

Zhang, Weiguo; Fraiture, Malou; Kolb, Dagmar; Löffelhardt, Birgit; Desaki, Yoshitake; Boutrot, Freddy FG; Tör, Mahmut; Zipfel, Cyril; Gust, Andrea A & Brunner, Frédéric 2013. Arabidopsis RECEPTOR-LIKE PROTEIN30 and Receptor-like kinase SUPPRESSOR OF BIR1-1/EVERSHED mediate innate immunity to necrotrophic fungi. *Plant Cell,* **25,** 4227-4241.

Zhang, Yaxi; Yang, Yuanai; Fang, Bin; Gannon, Patrick; Ding, Pingtao; Li, Xin & Zhang, Yuelin 2010. Arabidopsis *snc2-1D* activates receptor-like protein-mediated immunity transduced through WRKY70. *Plant Cell* **22,** 3153-3163.

Zhang, Yuelin; Goritschnig, Sandra; Dong, Xinnian & Li, Xin 2003. A gain-of-function mutation in a plant disease resistance gene leads to constitutive activation of downstream signal transduction pathways in *suppressor of npr1-1, constitutive 1*. *Plant Cell,* **15,** 2636-2646.

Zhang, Zhao; Song, Yin; Liu, Chun-Ming & Thomma, Bart PHJ 2014b. Mutational analysis of the Ve1 immune receptor that mediates *Verticillium* resistance in tomato. *PloS One,* **9,** e99511.

Zhang, Zhao & Thomma, Bart PHJ 2013. Structure-function aspects of extracellular leucine-rich repeat-containing cell surface receptors in plants. *Journal of Integrative Plant Biology,* **55,** 1212-1223.

Zhou, Dao-Xiu 1999. Regulatory mechanism of plant gene transcription by GT-elements and GT-factors. *Trends in Plant Science,* **4,** 210-214.

Zhou, Jun-Ma; Trifa, Youssef; Silva, Herman; Pontier, Dominique; Lam, Eric; Shah, Jyoti & Klessig, Daniel F 2000. NPR1 differentially interacts with members of the TGA/OBF family of transcription factors that bind an element of the *PR-1* gene required for induction by salicylic acid. *Molecular Plant-Microbe Interactions,* **13,** 191-202.

Zhu, Baolong; Chen, Tony HH & Li, Paul H 1995a. Activation of two osmotin-like protein genes by abiotic stimuli and fungal pathogen in transgenic potato plants. *Plant Physiology,* **108,** 929-937.

Zhu, Baolong; Chen, Tony HH & Li, Paul H 1995b. Expression of three osmotin-like protein genes in response to osmotic stress and fungal infection in potato. *Plant Molecular Biology,* **28,** 17-26.

Zipfel, Cyril; Kunze, Gernot; Chinchilla, Delphine; Caniard, Anne; Jones, Jonathan DG; Boller, Thomas & Felix, Georg 2006. Perception of the bacterial PAMP EF-Tu by the receptor EFR restricts *Agrobacterium*-mediated transformation. *Cell,* **125,** 749-760.

Appendix 1: Frequently used solutions and media

50x TAE	242 g/L Tris 5.71% (v/v) glacial acetic acid 50 mM Na_2EDTA
20x SSC	3 M NaCl 0.3 M Na_3 Citrate
LB medium	1% (w/v) NaCl 1% (w/v) Bactrotryptone 0.5% (w/v) yeast extract 1% (w/v) Bactoagar for solid medium
YEP medium	1% (w/v) Bactopeptone 1% (w/v) yeast extract 0.5% (w/v) NaCl
SOC medium	2% (w/v) Bactopeptone 0.5% (w/v) yeast extract 0.5% (w/v) NaCl 2.5 mM KCl 10 mM MgCl2 20 mM glucose

Appendix 2: Features of the pGREENII binary vector, the helper plasmid pSOUP and the pGREENII derivative pCBJ306

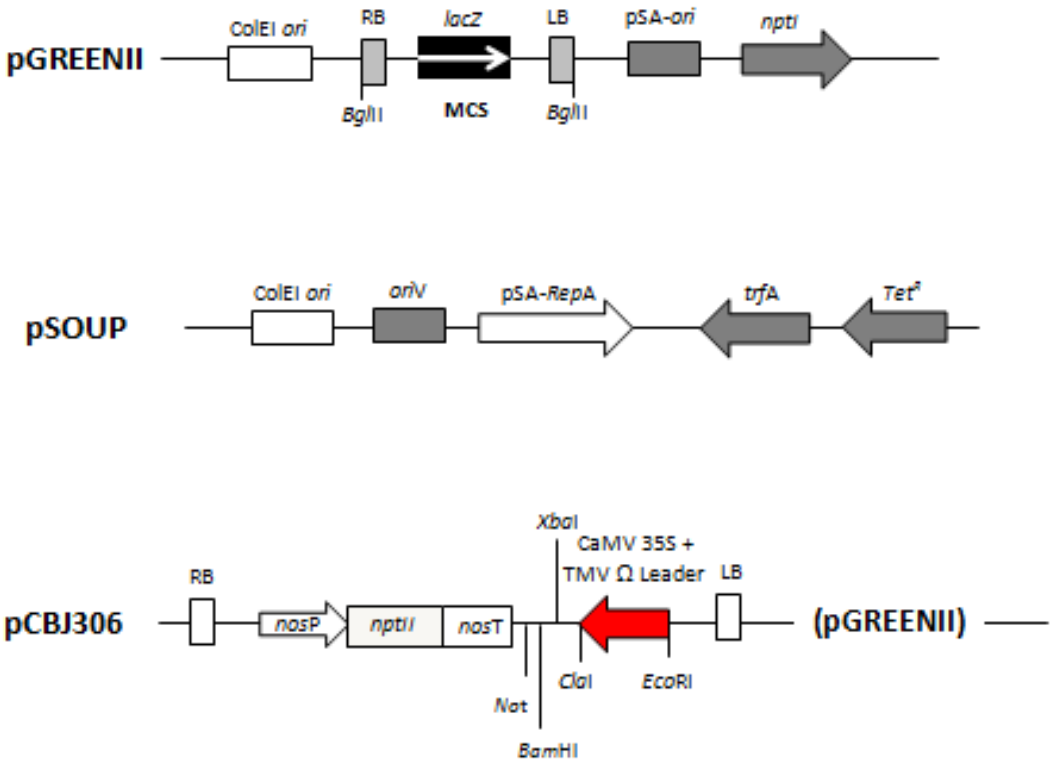

The pGREENII binary vector and pSOUP (Hellens *et al.*, 2000) are described at the pGREEN website (http://www.pgreen.ac.uk). The pCBJ306 plasmid is an empty vector derived from the pGREENII binary vector (Chakrabarti, 2005). This plasmid contains a CaMV 35S promoter and a neomycin phosphotransferase (*nptII*) cassette in the T-DNA region. ColEI *ori*: origin of replication in *E. coli*; pSa-*ori* and *ori*V: origin of replication in *A. tumefaciens*; pSa-*Rep*A: replication initiator for pSa-*ori*; *trf*A: replication initiator for *ori*V, Tet^R: tetracycline resistance gene; MCS: multiple cloning site from pBluescript II SK+; *lacZ*: β-galactosidase gene fragment, *nos*P and *nos*T: *nos* promoter and terminator sequence. The restriction sites of interest are shown. The drawings are not to scale.

Appendix 3: GUS activity induced by agroinfiltration of the defence activating constructs in transgenic pCYT-1 tobacco line 3B at 5 dpi

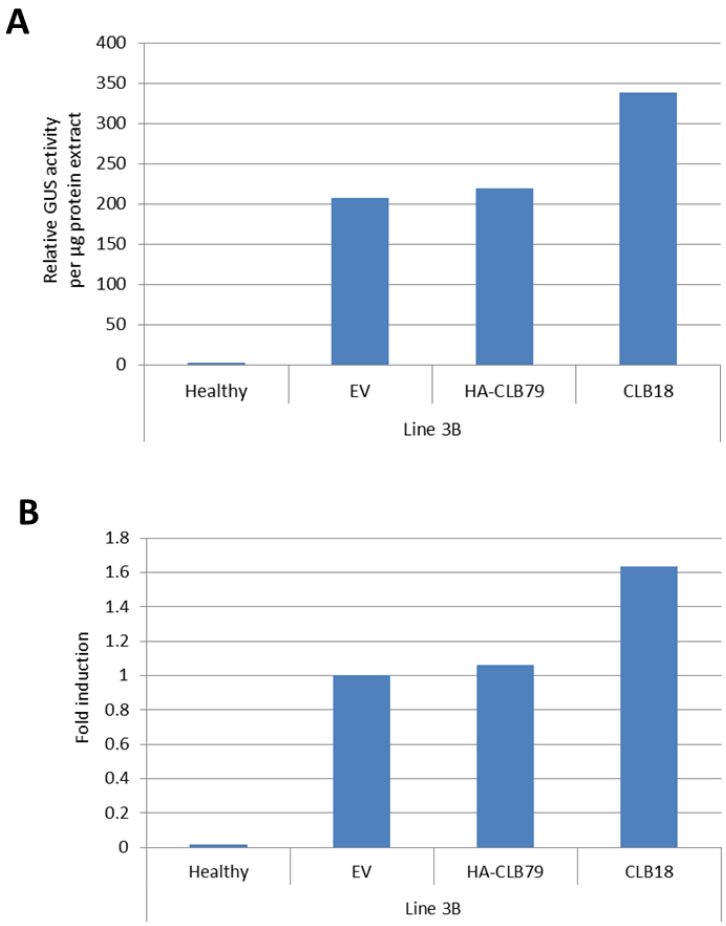

A) GUS activity in homogenates of five infiltrated leaf panels, one of each from five different plants for each construct measured by MUG assay. Empty vector (EV) control was included. HA-CLB79 and CLB18 are the defence activating constructs obtained from Anderson et al., (in preparation). Healthy: uninfiltrated leaf panels **B)** GUS activity normalized to that induced by the empty vector in each line as represented by fold of induction.

Appendix 4: GUS activity induced by agroinfiltration of the defence-activating constructs in transgenic *E22* promoter: *gusA* reporter (pCYT-1) tobacco line 16B, 20A, 20B, 30A and 30B at 7 days post-infiltration (dpi)

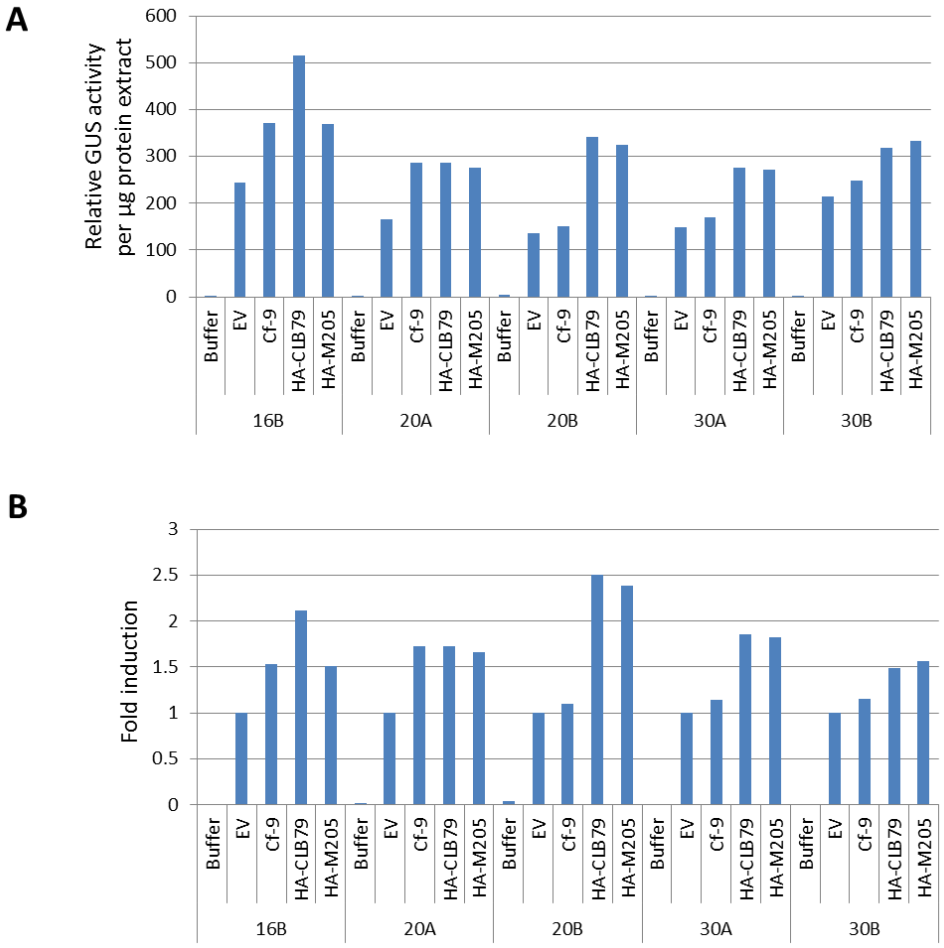

A) GUS activity determined by MUG assays in homogenates of five infiltrated leaf panels, one of each from five different plants for each construct. Empty vector (EV), Cf-9 and resuspension buffer controls were included. CLB79 and Hcr9-M205 were obtained from Anderson *et al.* (in preparation). **B)** GUS activity normalized to that induced by the empty vector in each line as represented by fold of induction.

Appendix 5: The *E22* gene (GenBank ID: X15224.1) promoter sequence

GAGCTCTTGGAAGTCATCAGCTTGTTATCCTGGTGTGTCATTTGATCTGTTGAGCGAGAGCCCT
TCCACACGGGACTCCCAAATCACTATGGTCAGCTTTAGTCTCTGTTCGACCAATATATGTGTTG
TATCGTTTGAGAAGTCATTTTTTTTTCTTTAAAGAAAATTGAATTATAATTTAAAAATTATTAT
AAGTAACCAAATTTTGAATAGTTTCTGATTATGAATTTCATTTAAAAAAATATCTAAGAAAATC
AATATTCAAATTCATACGTGAAACATATATATTCTCACTCTCCTGCATTTGAACCCTCTTTTGT
GATGGGAGGAACAATGAGCATTAGAATTAAAAGTTGTGTTTCAGTAATTAATATCTCTCCACAT
GAAAATATAAAAAGCAAATCTATATATTCAAACAATAATTTGTATACAAGTCACAGGCAAAGTG
GTATCAATGTTCATTCACTATATAGCTATGTCCAGCTAGTTTCAGGACCTCAATTCCCAAGCTC
AGAAAATTCAATTAGTGTCGGCTTGACTTGCAGGTCAAGAAGCAAGATTTTCCAGGAGAAGTAA
GAGCAAAAATTAGCACGCAAAAAGGACGTATTTAGGGCAAGGGATATGTGTTCACATGAACTCA
TGCTCCTTTCCCTAAATCATATATAACGTAATATTTTTTTAAAATTACTTAGATATATGTGTGT
GCACTCATGCTCAAAGACTCTTATGATGCAATATTAGTTATTGGGTGCACCTCTATAAGTGAAA
TTGACGGTTCAAATCCCACTCCGAACGGTCTTGTTTTAGGCACGAAGTATAAATATATAATTAT
ATATATTGAATCTATAATTTCAAAATGATAATGGGTTTATGGAAAGAGACTATAGTTAAATCCG
TCAAGTGTAAGTGCATCCATTCTCTTGAAATTGTGGATCCGCCAGTCTCTATTAGCGTGTTTGG
CACGAAATGGAAAAATGAGAGATGGAATTTATTGGCACATTAATAACAAGGACAAGAATATCAT
AATCTCTGAAATTTCAGAGCTTGTTACTTGATCAGCTATTTAAACCCATAGATAGTCTCCAAAT
AAACACATTCTCAAGTTTACAAAAAGAAAAAAAAA**ATG**

A 1048 bp sequence from -1051 to -4 (underlined) from the translation start site (ATG, +1 to +3, bold) of the *E22* promoter was PCR-amplified by the E22P-F and E22P-R primers listed in Table 3.1.